Summer 2014

Experimental and Computational Analysis of the Synucleins

Agatha Munyanyi
Old Dominion University

EXPERIMENTAL AND COMPUTATIONAL ANALYSIS OF THE SYNUCLEINS

by

Agatha Munyanyi
B.A. May 1978, Hampton Institute, USA
B.S. Medical Technology May 1980, Old Dominion University, USA
M.S. December 1981, Old Dominion University, USA

A Dissertation Submitted to the Faculty of Old Dominion University
in Partial Fulfillment of the Requirements for the Degree of

DOCTOR OF PHILOSOPHY

BIOMEDICAL SCIENCES

OLD DOMINION UNIVERSITY
August 2014

Approved by:

Lesley H. Greene (Director)

Christopher Osgood (Member)

Patricia Pleban (Member)

Jennifer Poutsma (Member)

ABSTRACT

EXPERIMENTAL AND COMPUTATIONAL ANLALYSIS OF THE SYNUCLEINS PROTEINS

Sr. Agatha Munyanyi
Old Dominion University
Director: Dr. Lesley Greene

The synuclein proteins α, β and γ which are located in the brain, have been a subject of intense research. Of particular interest is α-synuclein, which is found in misfolded forms in Lewy bodies that are associated with Parkinson's disease. Despite the efforts of researchers across the world, the physiological structure and function of the synucleins remains elusive. In recent years, highly controversial reports by some investigators indicate that in its natural form, α-synuclein exists as a tetramer instead of as an intrinsically unstructured monomer. This dissertation presents results of the experimental and computational analysis of the synucleins. First, we investigated methods of destroying protein fibrils from α-synuclein. We report that low temperature plasma can disrupt synuclein fibrils and proposed that neuronal macrophages can eliminate the resulting structures via phagocytosis. We also conducted inhibition studies to investigate the mechanism by which β-synuclein inhibits α-synuclein fibrillation. Using our experimental conditions, β-synuclein readily formed fibrils while α-synuclein inhibited β-synuclein fibrillation. We show, for the first time, that two fibril forming proteins when incubated together have an inhibitory effect on each other. This important information can be employed in the future development of inhibitors of formation. In order to determine the native structure of the synucleins, we expressed and isolated multimeric forms of the synuclein proteins. We found that expression of β-synuclein in

which we did not boil the bacterial lysate, yielded a high molecular weight multimeric β-synuclein form. This study has established the basis for further research with the ultimate aim of forming a well-diffracting crystal that will lead to solving a high resolution X-ray crystallographic structure of the native state. Finally, computational approaches involving bioinformatics and molecular modeling were employed to establish a superfamily for the synucleins. The hypothesis is based on the fact that the structure and function of the synucleins could be inferred from that of their related proteins, whose structure and function have been resolved. Our computational results indicated that the synucleins seem to be orphans in the animal kingdom but share sequence similarity with an endoglucanase enzyme from *Acetobacter pomorum* bacterium, a CRE-DUR-1 protein from a nematode, a cytochrome c protein from a spiral bacterium and a protein from the Tasmanian Devil. This study led to the development of a proposed evolutionary model for the synucleins, which hypothesized that β-synuclein, encoded by seven exons, is the oldest of the synucleins. α-Synuclein, encoded by 6 exons, evolved to contain amino acid sequences to prevent fibril formation such as the change from threonine 53 to alanine. Together, these results further our understanding of the synuclein proteins from a myriad of experimental and computational vantage points.

This thesis is dedicated to my parents. Regina and Paul Munyanyi
To the Sisters of the Child Jesus

ACKNOWLEDGMENTS

There are many people who have contributed to the completion of this dissertation. I extend my sincere gratitude to my mentor Dr. Lesley Greene for giving me the opportunity to conduct research both experimentally and computationally under her guidance. I thank all the members of Dr. Greene's research group.

I thank my dissertation committee members Dr. Christopher Osgood. Dr. Patricia Pleban and Dr. Jennifer Poutsma for their advice and guidance during my research and editing this dissertation.

I would like to thank my congregation, the Sisters of the Child Jesus for the opportunity to study here in the United States. I would like to thank the Bethlehem Fathers, Reverend Paul Patelli and Mr. and Mrs. Wüersch who made it possible for me to fly to the USA to commence my studies.

I am grateful to Professor Gary Pielak (UNC Chapel Hill, Department of Chemistry) for donating the α-synuclein clone and protocol for expressing the protein as well as forming fibrils and Professor Michael Goedert (University of Cambridge, Head of Neurobiology) for donating the β and γ-synuclein clones and protocol for expressing β-synuclein. I am grateful for the American Association of University Women Fellowship and for the Old Dominion University - Dominion Scholar Fellowship and travel awards from the College of Science.

NOMENCLATURE

2D	Two-dimensional
3D	Three-dimensional
AFM	Atomic force microscopy
ALP	Autophagosome-lysosome system
ATP	Adenosine tri-phosphate
BLAST	Basic Local Alignment Search Tool
DAT	Dopamine transporter
DOPA	Dihydroxyphenylalanine
CD	Circular dichroism
DAT	Dopamine transporter
DTT	Dithiothreitol
EDTA	Ethylenediaminetetraacetic acid
FASTA	FAST All
Hsp	Heat shock proteins
IPTG	Isopropyl β-D-1-thiogalactopyranoside
L-DOPA	Levo-dihydroxyphenylalanine
LGD	L-glutamic dehydrogenase
MUSCLE	Multiple Sequence Comparison by Log-Expectation
MW	Molecular weight
NCBI	National Center for Biotechnology Information
NMR	Nuclear Magnetic Resonance

OD	Optical density
PMSF	Phenylmethyl sulfonyl fluoride
PSI	Position-specific iterative
ROS	Reactive oxygen species
SDS-PAGE	Sodium dodecyl sulfate polyacrylamide gel electrophoresis
TEM	Transmission electron microscopy
TH	Tyrosine hydroxylase
ThT	Thioflavin T
UPS	Ubiquitin-proteasome system
UV	Ultra violet
WT	Wild-type
A	Alanine
C	Cysteine
D	Aspartate
E	Glutamate
F	Phenylalanine
G	Glycine
H	Histidine
I	Isoleucine
K	Lysine
L	Leucine
M	Methionine
N	Asparagine

P	Proline
Q	Glutamine
R	Arginine
S	Serine
T	Threonine
V	Valine
W	Tryptophan
Y	Tyrosine

TABLE OF CONTENTS

Page

LIST OF TABLES

LIST OF FIGURES

Page

Page

Page

CHAPTER I

INTRODUCTION

PROTEIN STRUCTURE

When amino acids are joined by covalent peptide bonds in a specific order, they produce a polypeptide. The specific amino acids, the order in which the amino acids are linked as well as the size of a chain are termed the primary structure of a polypeptide. The information for the correct folding of a particular polypeptide chain is contained in its sequence (Anfinsen, 1973). After a polypeptide chain is synthesized on the ribosomes, it forms secondary structures including α-helices and β-sheets, which are stabilized by hydrogen bonds between the carbonyl oxygen and the amide hydrogen of the polypeptide backbone. The α-helices, β-sheet structures and turns constitute the secondary structures of a protein.

It is a common view that for a protein to function, it must fold into a three-dimensional structure (3D) or tertiary structure. When the secondary structures of a polypeptide chain interact in space via noncovalent bonds including hydrogen bonds, van der Waal forces, non-polar hydrophobic interactions, acid/base ionic interactions and cysteine covalent disulfide bonds, a globular or tertiary structure is generated. Globular proteins are composed of either all α-helices, all β-sheets or mixed α/β secondary structures which interact in space to form a tertiary structure (Figure 1). A protein can be composed of one or more polypeptide chains. In the case of a multimeric

---

The journal for this dissertation is *Cell*

protein. different polypeptide chains associate through noncovalent bonds. disulfide bonds or cofactors to form a quaternary structure (Rodrigues et al.. 2012; Sanchez-Romero et al.. 2013).

Figure 1. Examples of globular monomeric protein structures based on class The rainbow color scheme indicates the flow of the polypeptide with the N-terminus in blue and the C-terminus of the polypeptide in red. The proteins from left to right are the all α-helical myoglobin protein (pdb code: 1a6n), the mixed α/β protein GB1 (pdb code: 1pgb) and the all β-sheet titin, (pdb code: 1tit). These structures are visualized with Rasmol (version 2.7.1).

In general, there are three types of fundamental protein forms: globular such as myoglobin, transmembrane such as bacteriorodopsin and fibrous structures such as collagen (Garrett and Grisham, 2013). The proteins in these three categories carry out the overwhelming majority of biological functions in an organism. from metabolism. to

cell structure, cell-cell adhesion, cell-cell communication, intracellular signaling, replication, transcription, translation and immunity. As the scientific community makes advances in protein research, it is now becoming understood that the traditional view of protein structure also extends to partially unfolded proteins (also known as intrinsically unstructured proteins) and protein fibrils (Soto, 2003; Tompa et al., 2005).

Intrinsically unstructured proteins

Contrary to conventional thinking that a defined 3D structure is necessary for protein function, experimental studies have shown that function can arise from unstructured proteins (Wiltzius et al., 2009). Their persistence in nature implies that they have a pivotal role to play in the biological activities of the cell. As a matter of fact, it has been proposed that over time, proteins have been evolving to lose their high degree of hydrophobic character in the core. The absence of a hydrophobic core has led the way for intrinsically unstructured proteins to evolve and come into existence (Mannige et al., 2012). For a protein to be described as intrinsically unstructured or unfolded, it must lack a hydrophobic core and have high densities of charged amino acids including lysine, glutamate and arginine (Nelson and Cox, 2013). The hormone amylin is a good example of an unstructured protein with metabolic function. Amylin, also known as islet amyloid polypeptide, is secreted in the beta-islet cells of the pancreas along with insulin (Westermark et al., 1987; Westermark et al., 2007). It regulates blood glucose levels in the body (Wiltzius et al., 2009) (Figure 2). As in the case of amylin, it appears at present that the majority of the functions of intrinsically unstructured proteins are involved in regulating cellular processes including transcription, translation, signal transduction and the cell cycle (Tompa, 2002). Apparently, the conformational flexibility of intrinsically

unstructured proteins allows them to interact with a wide range of different proteins (Wright and Dyson, 1999). Their unstructured state helps them to overcome steric hindrances and also enables them to make contact over a larger surface area of the substrate than could be achieved by a rigid structure (Figure 3) (Dunker et al., 2001).

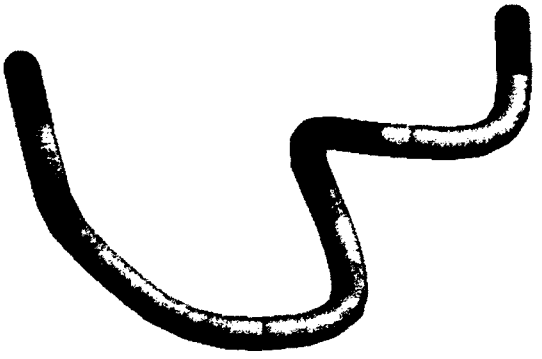

Figure 2. Model structure of amylin peptide hormone (pdb code: 1kuw)

The structure represented is conformer six in the ensemble which is the best representative of the peptide hormone in the pdb file. The model shows the peptide backbone of the amylin hormone. The black color indicates the N-terminus and the dark grey the C-terminus of the peptide. This structure is visualized with Rasmol (version 2.7.1).

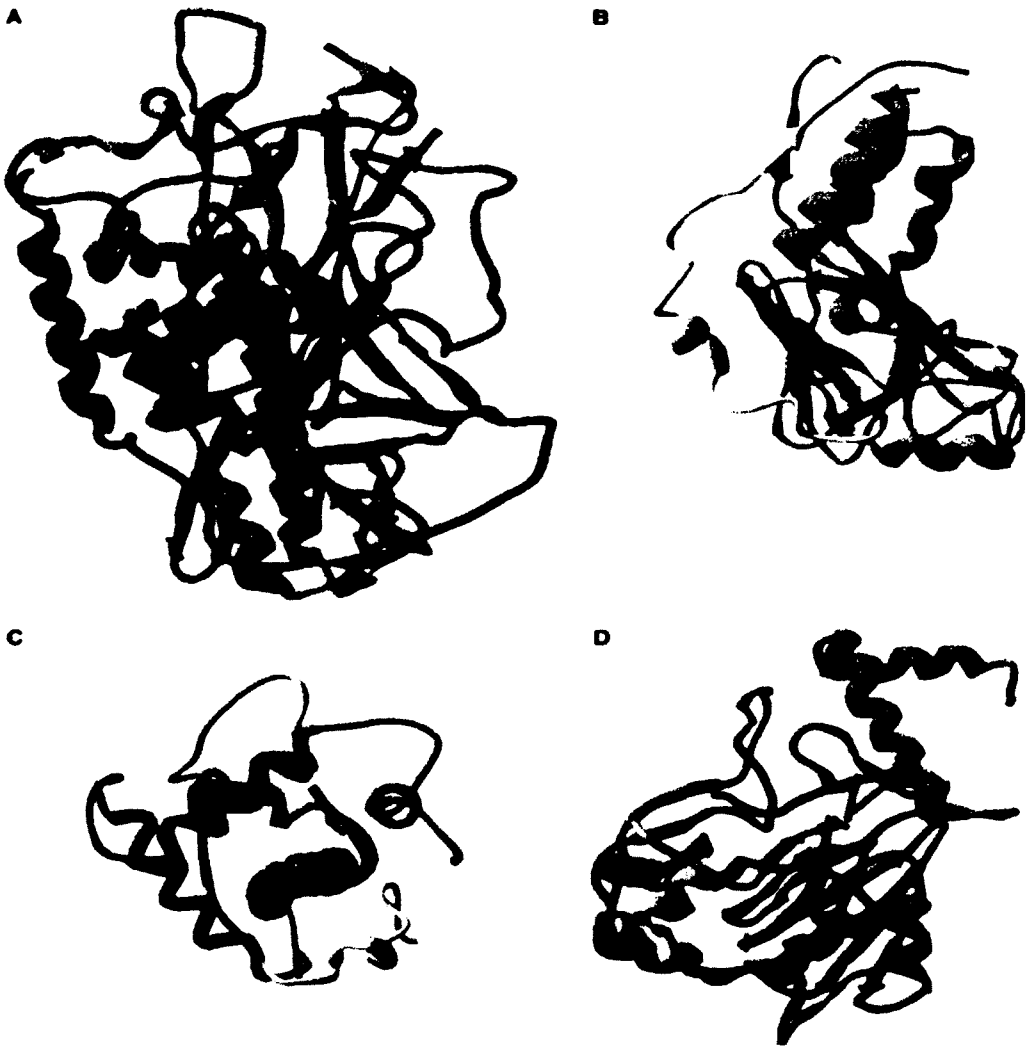

Figure 3. Intrinsically unstructured proteins interacting with globular proteins

Unstructured proteins depicted in red or yellow wrap around their respective protein substrates which are shown in blue (A-D). Their unfolded conformations allow them to cover a long stretch of their targets. Because intrinsically unstructured proteins contain more α-helix forming amino acid residues than β-sheet formers, they have a tendency to form α-helices (Tompa, 2005). Figure reproduced from Tompa (Tompa, 2005).

There must be a special feature in the amino acid sequence of intrinsically unstructured proteins that keeps them in the partially unfolded state at physiological conditions. Researchers observed that intrinsically unstructured proteins are rich in amino acids that have a high net charge and low hydrophobicity (Dunker et al., 2001; Williams et al., 2001; Tompa, 2002). Amino acids that keep the polypeptide in an extended or unstructured form include proline, arginine, glutamate, lysine, serine and glutamine (Malkov et al., 2009). The high net charge provided by lysine, glutamate and arginine promotes electrostatic repulsion which in turn prevents hydrophobic core formation (Kuznetsov and Rackovsky, 2003). The lack of cysteine residues avoids intra- or intermolecular disulfide bonds which otherwise are important stabilizing factors. The composition of amino acids in an intrinsically unstructured protein demonstrates that their structure has been evolutionarily selected (Tompa, 2002).

There are other factors that support the selection of a particular sequence by evolution. High net charge, low hydrophobicity and low β-sheet propensity help the intrinsically unstructured proteins to avoid β-aggregation (Linding et al., 2004). Some of the factors that enhance β-aggregation include a low net charge and the presence of amino acid residues including valine, isoleucine, tryptophan and phenylalanine which have side chains at the β-C position (Linding et al., 2003). In addition, high concentrations of proline and glutamine in an intrinsically unstructured protein prevent the polypeptide from forming β-strands because both residues do not promote β-sheet conformation which may result in fibril formation. The presence of many prolines at either the N- or the C-terminus of an intrinsically unstructured protein, results in the formation of polyproline II helices (Williamson, 1994; Adzhubei et al., 2013). The

polyproline II helices provide hydrophobic surfaces and carbonyl oxygens for protein-protein interactions between the intrinsically unstructured protein and its protein ligand (Williamson, 1994). Furthermore, the amino acid composition of intrinsically unstructured proteins is not as complex or variable as compared to that of a globular protein (Wootton, 1994). The low complexity is characterized by repeats of one or more amino acid residues, for example, the KTKEGV repeat sequences in the N-terminal regions of the synuclein proteins (Uversky et al., 2002).

Observations indicate that intrinsically unstructured proteins have a tendency to form local 1-4 hydrogen bonds leading to the formation of α-helices (Fuxreiter et al., 2004). Consequently, α-helical structures are observed more often than β-sheets since intrinsically unfolded proteins contain more α-helix forming amino acid residues than the β-sheet formers (Kuznetsov and Rackovsky, 2003).

Normally, unfolded proteins easily undergo protease digestion in the cell cytoplasm (Glickman and Ciechanover, 2002). However, there are mechanisms that protect disordered proteins from proteolytic enzymes. For example, some disordered segments are not accessible to proteases due to steric hindrance while other disordered segments lack protease susceptible amino acid residues (Dunker et al., 2002). In addition, some unfolded regions of proteins are protected by chaperones (Dunker et al., 2001). Also, association with another protein can protect the disordered region from protease digestion. However, when the protein substrate is removed, the disordered protein is susceptible to protease digestion (Dunker et al., 2002).

Experimental studies have shown that when intrinsically unstructured proteins were subjected to high temperatures, heat-induced secondary structures were formed

(Uversky et al., 2001a). For example, when the unfolded α-synuclein protein was heated, its circular dichroism spectrum changed from one of a random coil to that of a partially folded protein (Uversky et al., 2001a). In this case, heat induced the unstructured protein to partially fold. This finding is contrary to what would be expected in the case of a folded protein. It has been suggested that the partial folding upon heating may be due to increased hydrophobic interactions at higher temperatures (Uversky et al., 2001a). Similarly, at low pH, when the net charge was decreased, hydrophobic interactions also promoted α-synuclein protein to transition from a random coil to a partially folded conformation (Uversky et al., 1999; Uversky et al., 2001a).

When some unfolded proteins bind divalent or trivalent metal ions or lipids, they are transformed from a random coil to a conformation which contains secondary structures (Uversky et al., 2001b). The water soluble myelin basic protein (major component of myelin sheath), for example, has been reported to be transformed from a random coil to a partially folded conformation with secondary structures after binding lipids (Polverini et al., 1999). Ribosomal proteins involved in the assembly of the subunits 50S and 30S are unfolded in solution, but acquire a 3D structure after binding the ribosome subunits (Yusupov et al., 2001; Timsit et al., 2009).

During their protein-protein interaction, the unstructured proteins employ specific side chains to interact with the binding site or groove of the protein substrate (Rajamani et al., 2004). They bind their protein substrates with high specificity but with low affinity which enables them to dissociate easily from their substrates when the function is accomplished. The anchor side chains themselves are eventually buried in the groove after the formation of the complex. The segments of the unfolded protein which

are in an appropriate conformation for interacting with a protein substrate make the first contact. The recognition of binding sites on the substrate is followed by the organization of the flexible region and the stabilization of the protein-protein complex. Table 1 indicates several examples of intrinsically unstructured functional proteins. In solution, intrinsically unstructured proteins exist as a mixture of fluctuation conformational structures (Fuxreiter et al., 2004).

Protein fibrils

A protein fibril is a long and insoluble fibrous polymer which can arise from misfolded and normal monomeric protein molecules or peptides. The β-strands form β-sheets which then stack on each other to form a fibril and run perpendicular to the long axis of the fiber (Sunde and Blake, 1997) (Figures. 4-5). Generally protein fibrils are 10 nm in diameter but can vary in length. The distance between the β-strands is 0.48 nm while the β-sheet layers are 1.0 to 1.3 nm apart (Dobson, 1999; Serpell et al., 2000). The mechanism of protein fibrillation is not yet clearly understood. Interestingly, the protein fibril appears to be a unique protein fold that can be formed by all proteins under a specific set of conditions for a given protein (Collins and Greene, 2012). This hypothesis was proposed by Professor Christopher Dobson (University of Cambridge, UK) (Dobson, 1999). Details on protein fibrillation will be discussed in another section.

Table 1. Examples of functional intrinsically unstructured proteins

Protein	Function	Reference
Tau	Microtubule-binding, polymerization	(Uversky et al., 2000)
SRY	Assembly of transcription initiation complex	(Zhao and Koopman, 2012)
Prion protein	Copper binding	(Dunker et al., 2002)
Synaptobrevin	Protein-protein binding (membrane fusion)	(Fasshauer et al., 1997)
SNAP-25	Protein-lipid binding (membrane fusion)	(Fasshauer et al., 1997)
Topoisomerase I	Protein-protein and protein-DNA binding	(Stewart et al., 1996)
Topoisomerase II	Protein-protein binding, phosphorylation	(Shaiu et al., 1999)
Histone 5	Protein-DNA binding	(Ramakrishnan et al., 1993)
Histone 3	Protein-DNA binding	(Lambert et al., 1999)
Small heat shock chaperones	Protein-protein binding	(Kim et al., 1998)
50s ribosomal proteins	Protein-protein and protein-DNA binding	(Ban et al., 1999)
30s ribosomal proteins	Protein-protein and protein-DNA binding	(Ban et al., 1999)
Amylin peptide	Regulates blood glucose	(Wiltzius et al., 2009)

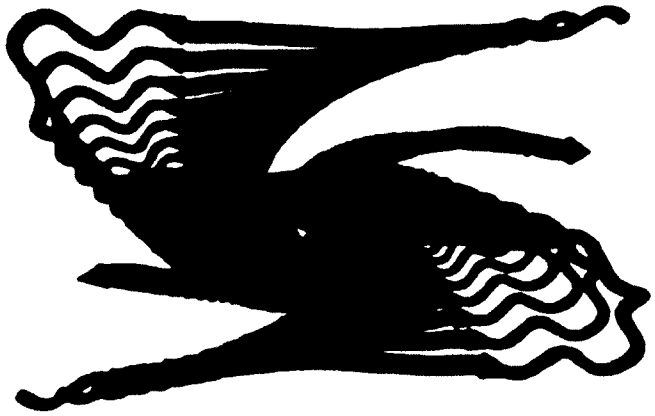

Figure 4. Early structural model of a fibril based on solid-state nuclear magnetic resonance spectroscopy

The structure shows a proposed model of the $A\beta_{1\text{-}40}$ protein fibril. The Aβ peptide contributes β-strands that form β-sheets (red and blue). The loops that link together the β-strands are indicated in green. Then the β-sheets stack on each other to form a fibril. Figure reproduced from Petkova (Petkova et al., 2006).

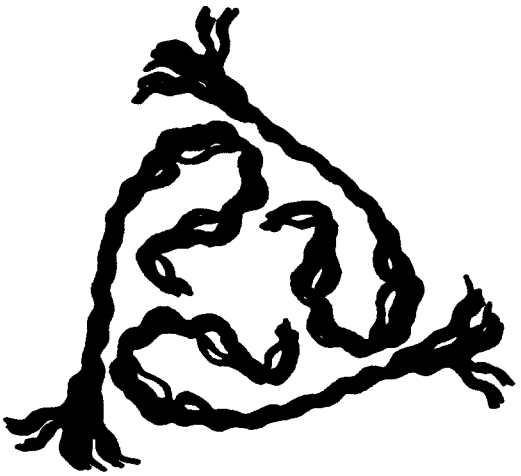

Figure 5. Most recent and accurate structure of the Aβ fibril based on solid-state nuclear magnetic resonance spectroscopy

The rainbow color scheme indicates the flow of the polypeptide with the N-terminus in blue and the C-terminus of the polypeptide in red. Several β-strands make a β-sheet. Then three β-sheets assemble to make a fibril. During the elongation of the fibril, triplet β-sheets stack on each other. Figure reproduced from Tycko (Tycko and Wickner, 2013).

BIOPHYSICAL TECHNIQUES TO STUDY THE STRUCTURE OF PROTEINS

Nuclear magnetic resonance (NMR) spectroscopy and X-ray crystallography are the two experimental methods presently in use to study protein structure (Clore and Gronenborn, 1998; Acharya and Lloyd, 2005). The solved structures of proteins are stored in the Protein Data Bank (PDB). In X-ray crystallography, the 3D structure of a protein is determined from a crystal of the protein. One of the challenges of the X-ray crystallographic technique is to find suitable conditions that enable the researcher to

grow single crystals of sufficient size to be used for determining structure (Smyth and Martin, 2000). The determination of the structure of a protein in its crystal form may not give an accurate evaluation of the true structure of a protein compared to what one would obtain when the protein is in solution. The NMR method has an advantage over X-ray crystallography in that the protein is analyzed in solution almost under physiological conditions but its applicability is limited by size unlike crystallography (Clore and Gronenborn, 1998).

Near- and far-ultraviolet circular dichroism

Circular dichroism (CD) is a biophysical technique employed to determine secondary and tertiary structure of a globular protein (Sreerama and Woody, 2004). The molecule under investigation must have a chiral center, or must be covalently linked to a chiral center or be in an asymmetric environment (Kelly and Price, 2000). An optically active molecule may absorb equal or unequal amounts of left- and right-circularly polarized light at a given wavelength. The difference in the absorption between the left- and right-circularly polarized light by the molecule is what is termed CD (Greenfield, 2006). When at a given wavelength, the chiral molecule absorbs equal left- and right-circularly polarized light, the resultant component is plane polarized light. However, when one of the components is absorbed more than the other, the result is an elliptically polarized light. The CD instrument displays dichroism either as the difference in absorption between the left- and right-circularly polarized light or as ellipticity in degrees (Kelly and Price, 2000).

In order for the polarized light to be absorbed, a protein must contain a chromophore which include the C=O of the peptide bond and the C=C bonds in the

aromatic rings tryptophan, tyrosine and phenylalanine (Kelly and Price, 2000). A chromophore is a group of atoms in a molecule that absorbs ultra-violet (UV) and visible radiation at specific wavelengths. The absorbed energy will cause either an n-σ^* or a π-π^* transition in the chromophore (Chen et al., 1972). In the case of a protein molecule, the far-UV CD signals are generated when the C=O chromophore of the peptide bond absorbs the radiation in the 240 nm -180 nm range. The chiral α-Cs of the amino acid residues provide an optically active environment for the C=O chromophores. In the near-UV, the CD signals are produced by the radiation absorbed by any one of the aromatic amino acid side chains depending on the asymmetry of their environments. These aromatic rings absorb radiation in the 260 nm - 320 nm range (Kelly and Price, 2000).

The far-UV CD provides the content of secondary structures in a natively folded or fibril protein structure, while the near-UV CD provides a signature of the tertiary structure. α-Helices show negative molar ellipticities at 208 nm and 222 nm and positive molar ellipticity 193 nm. Anti-parallel β-sheets show a negative molar ellipticity at 218 nm and a positive molar ellipticity at 195 nm. A random coil has a negative molar ellipticity at 195 nm. These basic patterns in ellipticities can be found in the work by Greenfield, Whitmore and Wallace (Greenfield, 2006; Whitmore and Wallace, 2008).

Bioinformatics

Bioinformatics, which is a combination of biology, biochemistry, computer science and mathematics, is increasingly being employed to complement the experimental methods used to investigate protein structure and function (Todd et al., 2001; Greene and Grant, 2012). Bioinformatics techniques use computer programs to

analyze protein or gene sequences in order to elucidate the relationship between them (Kinch and Grishin, 2002). One of the algorithms used to identify to which family or superfamily a protein belongs is the position-specific iterated basic local alignment search tool (PSI-BLAST) (Altschul et al., 1997). Proteins related to a common ancestor can be identified by a consensual sequence signature, a common 3D structure and may have a similar function (Greene and Higman, 2003). The structure and function of an uncharacterized protein can be inferred from that of its relatives (proteins which share sequence identity with the query protein) whose 3D structure and function have been determined. Despite the fact that there may be some sequence and structural changes over time as an ancestor protein evolves, those regions of the ancestral protein that are responsible for its structural stability and function remain largely preserved in the offspring protein (Kinch and Grishin, 2002; Alexander and Zhulin, 2007). This has great value when trying to understand the nature of a protein whose structure and function is not known. This is particularly important when it can take several years to solve the structure and function of a protein experimentally if at all as some proteins are not well behaved.

PROTEIN FOLDING

Protein folding is a process in which linear polypeptide chains are converted into their 3D structures that give proteins their functional properties. During the folding process, the polypeptide does not try out all possible conformations in order to find the native conformation. Instead, interactions between amino acid residues that lead to a stable native fold are chosen over those that lead to unstable conformations, thus, the process of folding is directed and nonrandom (Levinthal, 1968; Dinner et al., 2000).

The three most prominent mechanisms by which a polypeptide chain folds are: the hydrophobic collapse model, the framework model and the nucleation-condensation model. Early proposed protein folding pathways (Figure 6), include the framework and the hydrophobic collapse as well as the spontaneous refolding model, the nucleation growth model and the jigsaw model. In the framework model, some segments of the polypeptide chain may form helices and β-strand structures. The native conformation of the protein is then formed by diffusion and collision of the pre-formed secondary structures (Karplus and Weaver, 1994; Dinner et al., 2000). In the hydrophobic collapse model, nonpolar amino acid residues associate with each other and form a hydrophobic core in order to keep away from an aqueous environment. The remainder of the polypeptide chain folds around the hydrophobic core into a 3D structure (Cheung et al., 2002). Anfinsen proposed that a polypeptide chain can spontaneously fold (Anfinsen, 1973). The nucleation growth model suggests that a diffuse nucleus containing secondary structures is formed by specific amino acids, then the tertiary structure grows from this nucleus (Fersht, 2000; Vendruscolo et al., 2001). In the jigsaw model, individual polypeptide molecules can fold by any of the pathways into intermediates which then associate with one another to produce the native structure of the protein (Kim and Baldwin, 1982).

After the early protein folding models, another folding pathway, the nucleation-condensation model was proposed (Fersht, 2000; Vendruscolo et al., 2001) (Figure 7). In this model, the folding process begins via the formation of a nucleus which contains some secondary and tertiary structures (Daggett and Fersht, 2003). Then, the remainder of the polypeptide chain condenses around this nucleus. The formation of a fairly stable

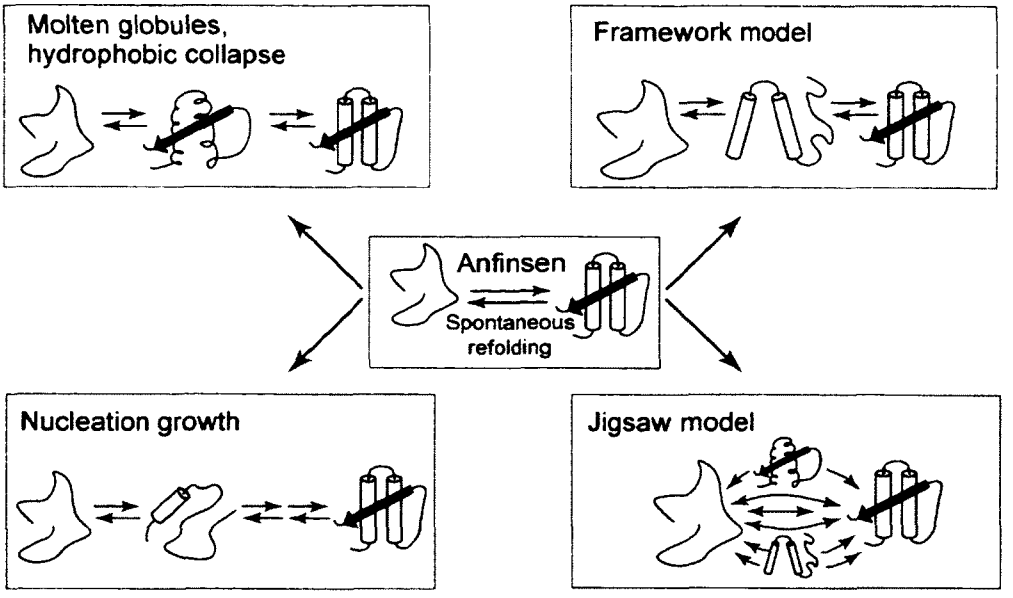

Figure 6. Early protein folding models

In the hydrophobic collapse model, hydrophobic side chains of amino acid residues associate to form a core in order to avoid the aqueous environment. The remainder of the polypeptide chain folds around the core into a 3D structure (Cheung et al., 2002). In the framework model, some segments of the polypeptide chain form secondary structures. The native fold is formed by diffusion and collision of the pre-formed secondary structures (Dobson, 2004). Anfinsen model suggests that the polypeptide chain can spontaneously fold (Anfinsen, 1973). The nucleation growth model proposes that specific amino acid residues associate to form a diffuse nucleus with secondary structure. Then, the tertiary structures develop from this nucleus to produce a 3D fold (Fersht, 2000; Vendruscolo et al., 2001). In the jigsaw model, individual polypeptide molecules may fold by any of the pathways into intermediates which then associate to form one 3D native structure of the protein (Kim and Baldwin, 1982). Figure reproduced from Radford (Radford, 2000).

nucleus limits the alternative pathways by which the polypeptide chain can fold (Fersht. 1995). Note, this model is different from the nucleation growth because its transition state contains some characteristics of the native state. The folding nucleus also termed the 'fold-determining core' by Greene et al. is proposed to be evolutionarily conserved (Greene et al., 2003).

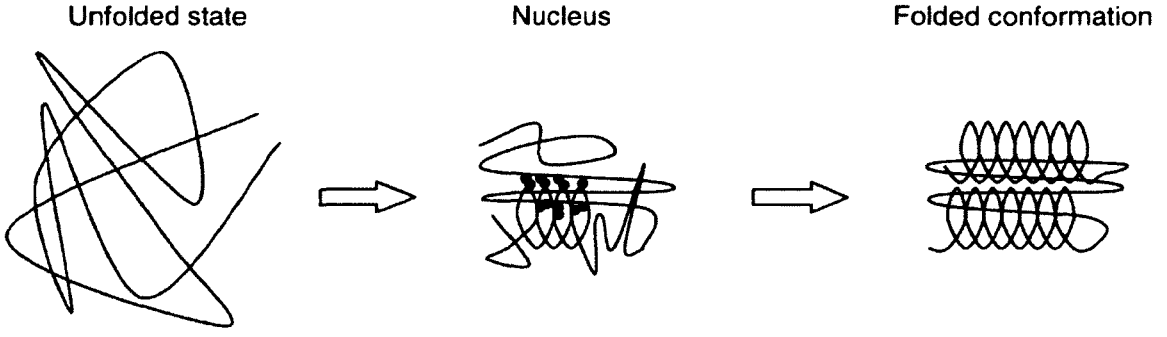

Figure 7. The nucleation-condensation protein folding model

The unfolded polypeptide chain first forms a nucleus which contains some secondary and tertiary structures. The remainder of the polypeptide chain folds around the nucleus to form the native conformation of the protein (Fersht, 1995). Figure reproduced from Nolting (Nolting and Andert, 2000).

Protein folding is now recognized to occur on a funnel shaped energy landscape; irrespective of the model (Figure 8) (Dill and Chan, 1997; Miao et al., 2014; Woodside and Block, 2014). The energy landscape describes the energy levels of different

conformations which a polypeptide can assume as it moves from a high energy level unfolded structure towards a low energy level native structure (Wolynes, 1997; Weinkam et al., 2010). Small proteins, such as chymotrypsin inhibitor 2 (64 residues), have one transition from the unfolded to the native state while large proteins (>100 residues) can involve intermediates (Jackson and Fersht, 1991; Walters et al., 2013). These intermediates may or may not contain structures similar to those in the native state of the protein (Brockwell et al., 2000). The polypeptide intermediates that contain native-like structures are said to be on the pathway while those with non-native-like

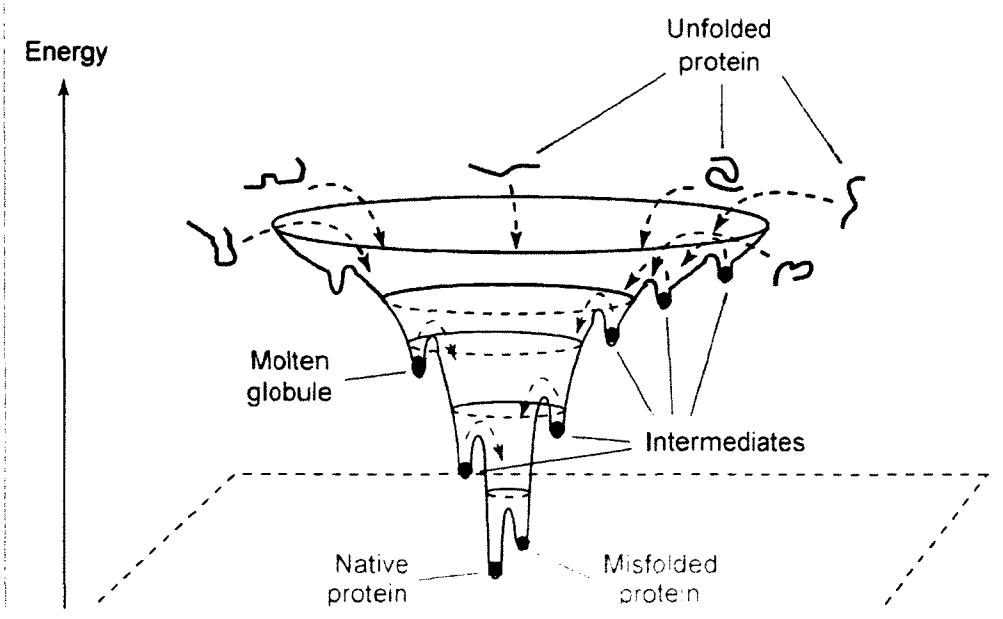

Figure 8. The protein folding funnel

Unfolded protein molecules at the top of the energy landscape fold to their native conformation using any of the folding models. Small proteins fold smoothly down the funnel to their native structure (Jackson, 1998). The folding of large proteins may involve few or many intermediates. The molten globule is one of the intermediates into

Figure 8 Continued

which a polypeptide can be trapped during the folding process (Schultz, 2000). Some protein molecules achieve their native fold at the bottom of the funnel while others fail to fold correctly and assume a misfolded conformation. Figure reproduced from Radford (Radford, 2000).

structures are described as off-pathway (Brockwell et al., 2000). Conformers on the off-pathway are trapped at certain energy levels of the folding funnel. Chaperones can assist the trapped intermediates to form native-like secondary structures which culminate in the native state (Radford, 2000; Kim et al., 2013).

Chaperones and *in vivo* folding

Under normal circumstances a cell employs molecular chaperones to deal with the problem of proteins that tend to misfold and/or aggregate. These chaperones maintain the normal levels and integrity of these proteins (Takalo et al., 2013). A molecular chaperone recognizes and binds the exposed hydrophobic segments of the newly synthesized polypeptide chains or misfolded proteins, assists them to fold correctly into their native conformations, prevents their aggregation and assists in the repair of damaged proteins (Hartl, 2011; Vabulas et al., 2010).

Chris Anfinsen used ribonuclease to show that a pure denatured protein can refold spontaneously *in vitro* to its functional native state when the denaturant is removed. This earned him a Nobel prize in 1972 (Anfinsen, 1973). However, the ideal conditions *in vitro* are different from those in the cell cytoplasm where there are many

other nascent polypeptide chains (Fink, 1999). A mechanism that prevents the newly synthesized polypeptides from interacting with each other is necessary. The exposed hydrophobic regions of linear polypeptide chains have the tendency to associate with each other resulting in flawed and premature folding (Srinivasan, 2012). In a folded protein, such hydrophobic patches are buried in the core of the protein or in the lipid bilayers in the case of membrane proteins (Bross, 2011). Chaperones are able to identify and bind these hydrophobic segments of the polypeptide chains and prevent inappropriate interactions within the chain or between the chains (Chaudhuri and Gupta, 2005). Chaperones do not determine how a protein will fold to its native conformation, but prevent ineffective intra- and intermolecular contacts and assist the linear polypeptide chain to reach its 3D structure determined by its amino acid sequence (Hartl and Martin, 1995; Dahiya and Chaudhuri, 2014). Some polypeptide chains do not require chaperones and fold as they emerge from the ribosomes or fold after they are released into the cytoplasm (Figure 9) or into the lumen of the endoplasmic reticulum (Hardesty et al., 1999).

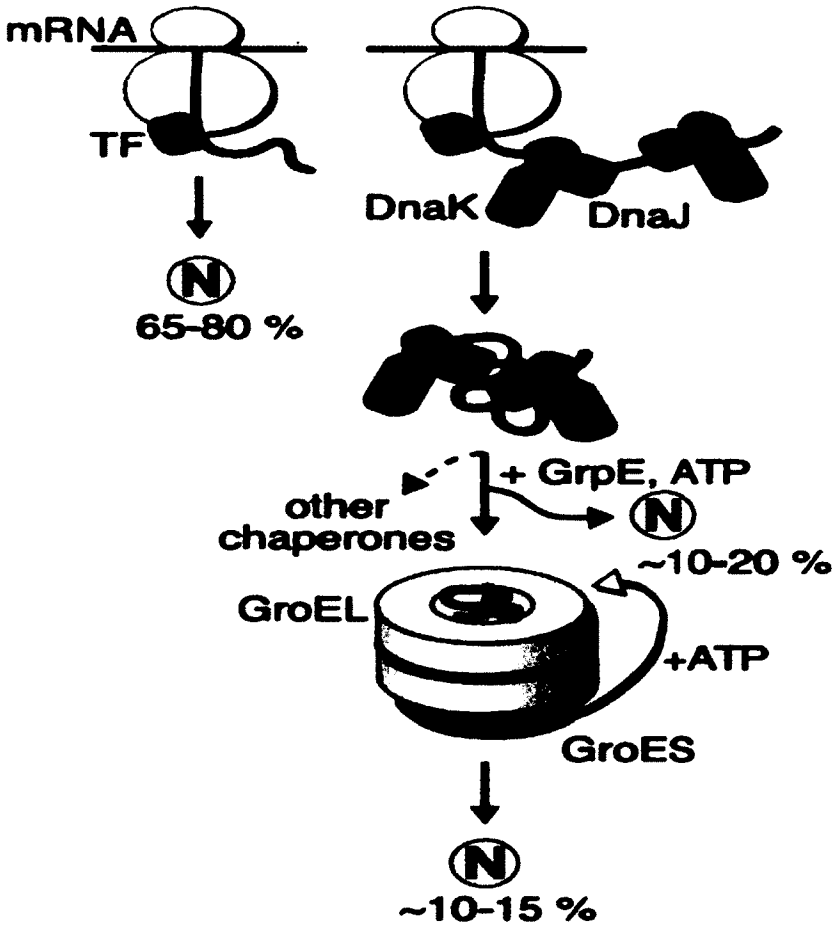

Figure 9. Chaperones assist the newly synthesized polypeptide chains to fold

The figure depicts the folding process in a prokaryotic cell. Approximately seventy percent of small polypeptide chains fold spontaneously to their native structure with the help of the trigger factor (TF). About twenty percent of larger polypeptides require the assistance of Hsp70 (DnaK) and Hsp40 (DnaJ) chaperones to fold correctly as they emerge from the ribosomes. Ten percent of the larger polypeptide chains will enter the GroeEL-GroES complex where they will fold and then be released into the cytoplasm (Hartl and Hayer-Hartl, 2002; Vabulas et al., 2010; Dahiya and Chaudhuri, 2014). Figure reproduced from Hartl.

The molecular chaperones found in eukaryotic cells include heat shock proteins (Hsp) Hsp40, Hsp60, Hsp70 and Hsp90 (Hartl and Hayer-Hartl, 2002). The Hsp are synthesized when a cell experiences stress due to environmental changes including increased temperatures above the physiological level (Schlesinger et al., 1997). The heat shock proteins are able to distinguish between native and non-native conformations of proteins (McClellan and Frydman, 2001). The activities of the Hsp60 and Hsp70 are regulated by the binding and hydrolysis of ATP. The Hsp60 chaperones, which are GroEL-like proteins, have a central cavity. In a prokaryotic cell, the GroEL and its cochaperone the GroES isolate a nascent or a misfolded protein from the cytoplasm and allow it to fold in a protected environment and then release it again into the cytoplasm after it has folded correctly (Hartl, 2011). The Hsp70 chaperones do not only assist the newly synthesized polypeptides to fold but also protect the hydrophobic patches of the polypeptide chains as they translocate from the cytoplasm into the endoplasmic reticulum (Fink, 1999). Another group of chaperones are the small heat shock proteins which are not ATP regulated. These chaperones form spherical structures to which unfolded proteins can bind during unfavorable conditions until chaperones that assist the proteins to fold are available (Bross, 2011).

PROTEIN MISFOLDING

When a polypeptide folds into a conformation which is different from the native state, it is considered to be misfolded. Often misfolded proteins can refold properly with the help of chaperones (Hartl, 2011; De Los Rios and Barducci, 2014). Misfolded proteins that cannot be rescued by molecular chaperones are destroyed by the cell through mechanisms discussed in the next section. However, a small group of proteins

can misfold into an alternative, stable conformation that eventually leads to fibrils. As mentioned previously, most fibrils are stacked β-sheets which elongate into an insoluble polymer. Some peptides naturally form β-sheet polymers, for example, the conversion of fibrinogen to fibrin during the formation of a blood clot. Studies have shown that proteins and peptides associated with neurodegenerative diseases including Huntington's, Parkinson's, Alzheimer's and Dementia with Lewy bodies are misfolded and have a β-sheet conformation, which is prone to aggregation and fibrillation (Soto, 2003; Ross and Poirier, 2004; Suzuki, 2014; Valastyan and Lindquist, 2014). The fate of a newly synthesized polypeptide chain is determined by the physiological conditions in the cell cytoplasm which may enhance or prevent it from folding to its native conformation implying that disease states have different cell cytoplasm conditions (Figure 10).

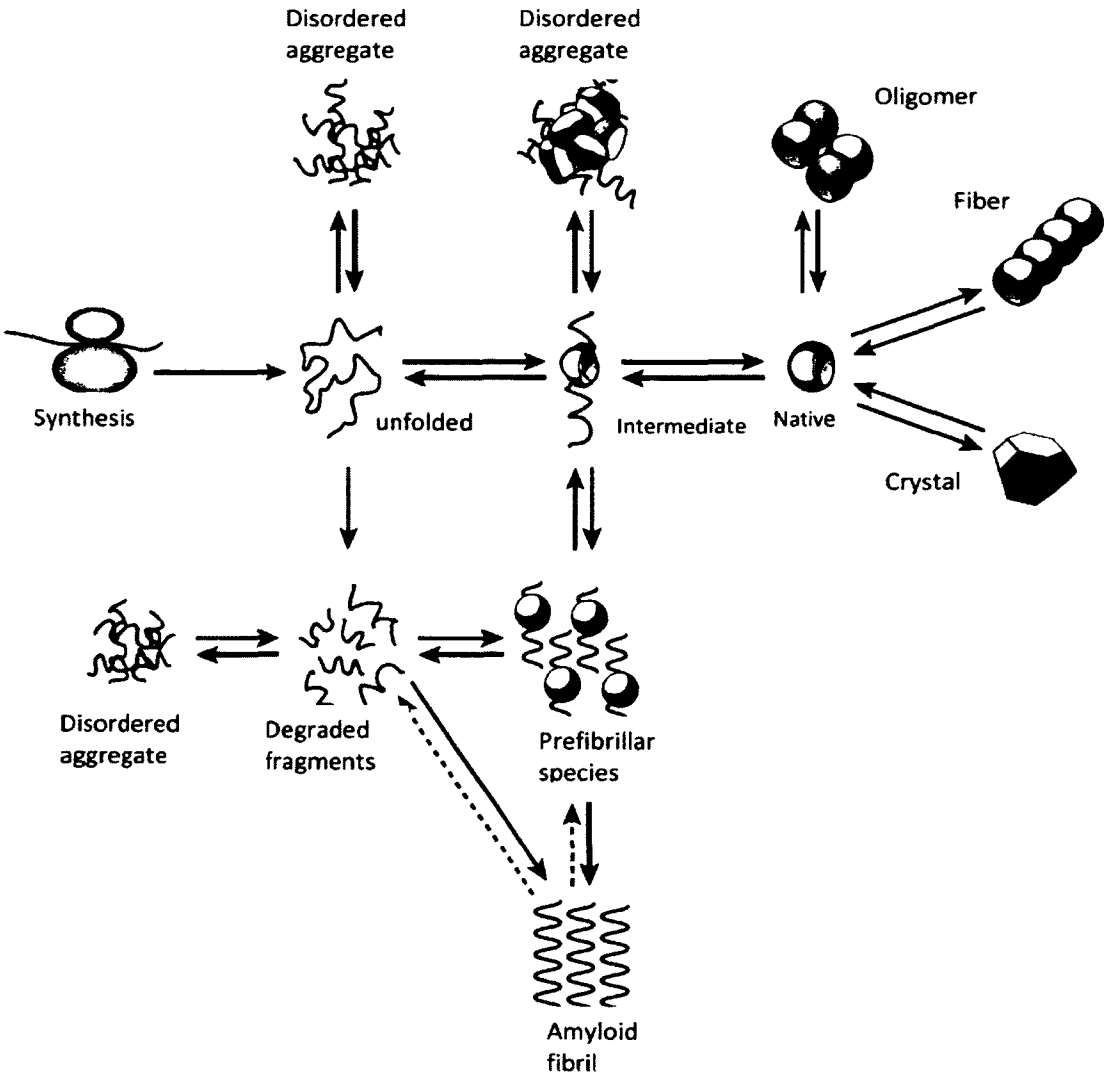

Figure 10. The fate of a polypeptide chain coming off the ribosome

The nascent polypeptide chain can, through an intermediate, fold to a monomeric native structure, or form a protein fiber, a functional oligomer or a crystal *in vitro*. The polypeptide intermediate can form disordered aggregates or prefibrillar species which assemble into amyloid fibrils. The unfolded polypeptide chain can also form disordered aggregates and/or amyloid fibrils or it can be degraded into fragments. The degraded fragments can assemble into disordered aggregates or amyloid fibrils (Dobson, 2003). Figure reproduced from Dobson.

Certain conditions, such as inflammation, oxidative stress and aging have a tendency to enhance protein oxidation, phosphorylation, nitration and protease truncation (Haigis and Yankner, 2010; Tarawneh and Galvin, 2010). These can result in protein misfolding and aggregation. Reactive oxygen species (ROS) including superoxide anion (O_2^-), hydrogen peroxide (H_2O_2) and peroxynitrite ($ONOO^-$) are produced during cell respiration and by the oxidative burst of macrophages during inflammation (Sultana et al., 2006; Slauch, 2011). The reactive species can generate free radicals which react with and damage nucleic acids, lipids and proteins. The resulting oxidation at the cysteine and methionine residues increases protein susceptibility to aggregation (Slauch, 2011). In individuals with Alzheimer's disease, hyperphosphorylation of the tau protein enhances tau aggregation (Mandelkow and Mandelkow, 2012). Furthermore, increased cleavage of the Aβ precursor protein by β- and γ-secretase enzymes increases the levels of β-amyloid peptide resulting in its accumulation and aggregation (Haass et al., 2012).

Other examples of unfavorable conditions in a cell that trigger protein conformational changes include high concentrations of free fatty acids due to obesity (Boden, 2008) and the presence of numerous unfolded newly synthesized polypeptide chains (Goldberg, 2003). The hydrophobic regions of fatty acids act as micelles which denature proteins by binding their hydrophobic regions. Denatured proteins whose hydrophobic cores are exposed to the aqueous solvent have the propensity to aggregate before they are destroyed by the proteasome system (Sherman and Goldberg, 2001).

Another cause of protein misfolding problems is from mutations in the sequence that are prone to form β-sheets and fibrils (Bross, 2011). The mutations either impair

correct folding or decrease the stability of the native conformation (Valentini, 2013). Thus, energy of the folding funnel is affected such that misfolded proteins have a greater chance of forming.

Neurodegenerative diseases are generally related to a combination of aging and mutations (Migliore and Coppede, 2009). During aging, the protein quality control system declines and fails to efficiently sustain protein homeostasis (Haigis and Yankner, 2010). Increased accumulation of misfolded and aggregated proteins may overwhelm the protein quality control and the clearance systems (Cuervo et al., 2010).

Protein misfolding and degradation

A cell has two mechanisms by which it maintains protein quality (Bross, 2011). The first mechanism, already discussed, involves chaperones which assist in folding and refolding nascent polypeptides and denatured proteins, respectively (Hartl, 2011). In the case of proteins beyond rescue, chaperones will interact with the ubiquitination system to mark them for degradation by the ubiquitin-proteasome system (UPS) or by the autophagosome-lysosome pathway (ALP) (Ciechanover et al., 2000; Dikic et al., 2009; Amm et al., 2014). The UPS involves the 26S proteasome system (Figure 11) which eliminates proteins no longer required by the cell and those incapable of folding to their native structure. The 26S protease complex consists of a central 20S cavity and a regulatory 19S particle at both ends of the cavity (Voges et al., 1999; Glickman and Ciechanover, 2002). Most cell proteins are degraded by the 26S proteasome (Glickman and Ciechanover, 2002). The ubiquitinated proteins enter the proteasome system through the 19S regulatory particle, which contains ATPases that bind the proteins and use ATP hydrolysis to unfold them and then transfer the linear polypeptides to the 20S particle

(Benaroudj et al., 2003). The 19S particle also contains enzymes which dissociate ubiquitin molecules from the proteins (Glickman and Ciechanover, 2002). The peptidases of the 20S particle digest the polypeptides into small peptides (Kisselev et al., 1999). The peptides released into the cytoplasm are rapidly broken down to amino acids by cytosolic endopeptidases and aminopeptidases (Saric et al., 2004).

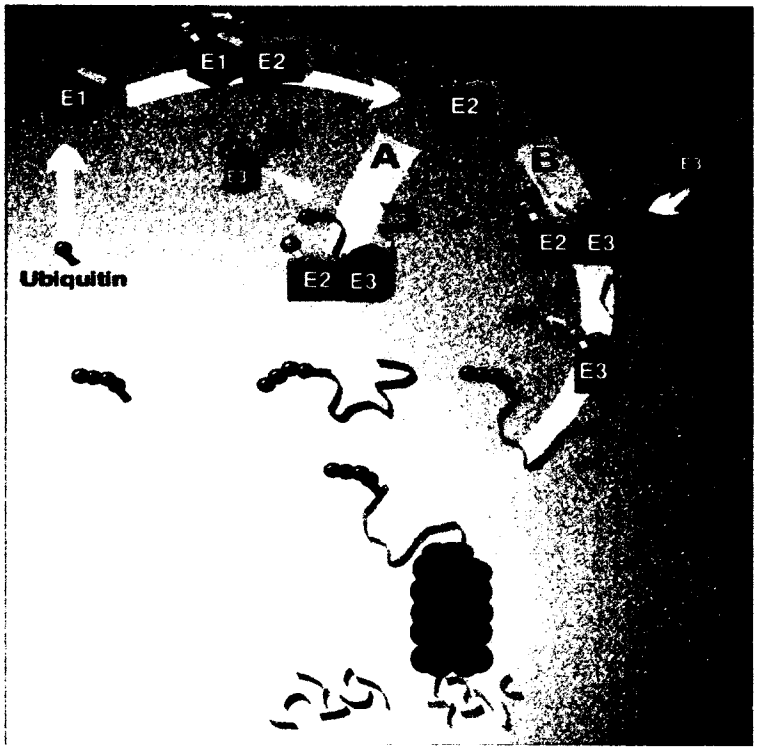

Figure 11. The ubiquitin-proteasome system

Three ligase enzymes E1, E2 and E3; the ubiquitin protein and the barrel shaped 26S proteasome complex make up the ubiquitin-proteasome system. Enzyme E1 activates the ubiquitin molecule. The activated ubiquitin molecule is transferred to E2 (the ubiquitin conjugating enzyme).The ubiquitin can either be transferred to a protein substrate already bound to E3 enzyme or it is transferred first to an E3 enzyme and

Figure 11 Continued

then transferred to the E3 bound substrate. In a similar manner, additional molecules of ubiquitin are successively added to the already conjugated ubiquitin strand. The protein substrate enters the 26S proteasome complex where it is broken down to small peptides. The deubiquitination enzymes free the ubiquitin strand from the protein substrate for reuse. Figure reproduced from Ciechanover (Ciechanover and Brundin, 2003).

The second pathway for protein degradation involves the ALP. A constitutively expressed cytoplasm Hsp70 chaperone directs proteins intended for degradation to the surface of lysosomes (Pan et al., 2008). The proteins are then transferred into the lysosomes and are degraded (Mijaljica et al., 2010). When a misfolded protein fails to refold and is not degraded by either the UPS or ALP, it is isolated in a specific location in the cell, where it forms an intracellular inclusion body (Kopito, 2000; Olzmann et al., 2008). Inclusion bodies in the surviving neurons, are believed to be a defense scheme by the cell against misfolded proteins and aggregates (Kopito, 2000). The sequestration of misfolded proteins into inclusions reduces the accumulation of misfolded proteins and toxic species and prevents them from interacting with other proteins and cell organelles (Chen et al., 2011). Protein folding, refolding, degradation and isolation into inclusion bodies all require the action of different types of chaperones (Takalo et al., 2013).

Protein misfolding and fibril formation

Under certain unfavorable conditions, a natively folded protein may unfold partially or completely and expose its hydrophobic patches, which are normally buried

in the protein core, to the aqueous environment. These hydrophobic segments of a polypeptide have the tendency to associate with one another and form soluble oligomers that are stabilized by β-sheet structures (Hilbich et al., 1992). The soluble oligomers can be formed by a few or several residues of the polypeptide chain (Chamberlain et al., 2000). These oligomers can act as a nucleus and incorporate additional monomers to form larger polymers called protofibrils, which are the precursors of protein fibrils (Walsh et al., 1997; Walsh et al., 1999; Alexander and Zhulin, 2007). The fibrils are characterized by an interior cross β-sheet structure which resists protease digestion, binds to Congo red and thioflavin T dyes and appears as rod-like structures under transmission electron microscopy and atomic force microscopy (Soto, 2003).

Protein fibrils can arise from proteins with a folded native state and from intrinsically unstructured proteins. The ability to form fibrils is not restricted to proteins associated with diseases and is an intrinsic property of polypeptide chains (Chiti et al., 1999). In fact the general overall basic morphology is similar for large and small proteins as well as peptides (Lopez De La Paz et al., 2002). The core of the fibril is held together by hydrogen bonds involving the polypeptide backbone (Dobson, 2004). Since the polypeptide backbone is common to all proteins; it explains why protein fibrils formed by proteins of different native conformations have certain common morphological features. However, each protein and even the same proteins forming fibrils under different conditions have unique structural characteristics (Collins and Greene, 2014).

In a folded protein, the polypeptide backbone is buried in the interior of the protein. The polypeptide backbone must be exposed before fibrillation process can take

place. Consequently, globular proteins must fully or partially unfold before they refold into fibrils (Kelly, 1998). Protein fibrillation *in vitro* has a lag phase that is followed by a rapid growth of fibrils (Harper and Lansbury, 1997). The lag phase is the period when the fibril nucleus is formed and the rapid growth or elongation period occurs when the nucleus incorporates monomers or oligomers. The nucleation phase can be by passed by adding preformed exogenous fibrils or oligomers to fresh protein solution (Harper and Lansbury, 1997).

The mechanism of protein fibrillation is not yet fully understood. One proposed pathway for amyloid fibril formation suggests that a natively folded protein is destabilized and unfolds (Figure 12). Then the misfolded intermediates aggregate into soluble oligomers which are stabilized by a cross β-sheet structure (Soto, 2003). These soluble oligomers then incorporate additional misfolded monomers to form protofibrils. The protofibrils then stack up to form mature, insoluble fibrils. The fibrils can also serve as nuclei to which monomers, soluble oligomers and protofibrils are incorporated. Factors including pH, temperature, ionic strength, protein concentration and agitation have an effect on the length of the lag phase *in vitro*. Each protein has its own unique conditions under which it unfolds and then forms fibrils (Soto, 2003). The factors *in vivo* are more elusive and can involve concentration, mutation and presence of certain metals for example.

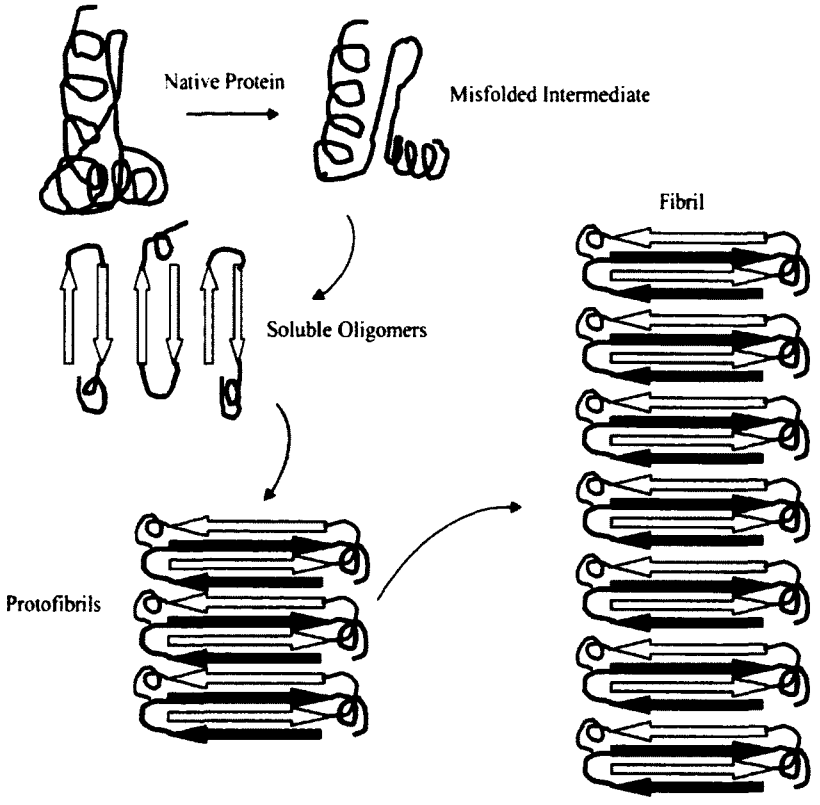

Figure 12. Model of protein fibril formation

The native protein is destabilized and unfolds, the misfolded intermediates form soluble oligomers which incorporate more misfolded intermediates to form protofibrils. Protofibrils interact through hydrogen bonds to form fibrils. The β-strands are perpendicular to the long axis of the fibril. Figure adapted from Soto (Soto, 2003).

Protein misfolding and potential disease states

Neurodegenerative disorders including Alzheimer's, Parkinson's, Huntington's, Amyotrophic Lateral Sclerosis and Dementia with Lewy bodies are characterized by a gradual loss of neurons in certain regions of the brain resulting in abnormal synapses and clinical symptoms (Martin, 1999). In addition, intracellular or extracellular protein

fibrils are found in the affected regions of the brain (Dobson, 2001). The cytoplasmic inclusions that are detected in surviving neurons contain ubiquitin tagged misfolded proteins that have transformed into an amyloidogenic or fibril conformation (Soto, 2003; Ross and Pickart, 2004). The loss of neurons occurs by programmed cell death (Mattson, 2000; Simon et al., 2012). Cell death can occur because the function of a specific protein associated with the disease has been lost due to the protein having a misfolded or fibril conformation. The regions of the brain and the type of neurons affected by the protein fibrils determine the clinical symptoms associated with each disease (Soto, 2003).

Protein fibrils, particularly those deposited outside the cell may interact with surface receptors and activate signal transduction pathways leading to apoptosis (Bamberger et al., 2003). When protein aggregates bind transcription factors and chaperones, they interfere with the production of mRNA and the protein folding process respectively (Soto, 2003). Soluble protein oligomers may form ion channels which are large and nonselective (Lashuel et al., 2002). These channels disrupt membrane potential and allow an influx of calcium ions which initiates apoptosis (Lin et al., 1997). Protein aggregates may also stimulate oxidative stress by producing ROS resulting in protein and lipid oxidation. For example, when α-synuclein located at the inner mitochondrial membrane aggregates, it potentially inhibits complex I which can disrupt the electron transport chain system (Schapira, 2007, 2008). Consequently ATP production is reduced. An acidic cytosolic environment created by the ROS activates cytochrome c and an apoptotic pathway can then be initiated resulting in cell death. (Mounsey and Teismann, 2010).

Additionally, brain inflammation may be triggered by the accumulation of protein aggregates or by signals from injured neurons. A large number of activated microglia and astrocytes are usually found in the areas around protein deposits (Zhang et al., 2005). Activated microglia cells produce superoxide anions resulting in oxidative stress in the affected neurons (Colton et al., 1989).

Two types of fibrils are observed for those with Alzheimer's disease. The amyloid plaques are deposited outside the cell and the main component of the plaque is a 40 or 42 residue Aβ peptide fibril (Glenner and Wong, 1984). However, these plaques do not necessarily correlate with the severity of the disease. The fibrillar tangles (tau protein fibrils), whose main constituent is tau protein, are deposited in the cytoplasm (Grundke-Iqbal et al., 1986) and are potentially one of the contributing factors in this disease. It is presently under intensive investigation. In Alzheimer's disease the loss of hippocampus and neocortex neurons result in dementia.

Patients with Parkinson's disease have inclusions called Lewy bodies and Lewy neurites in the cytoplasm of the substantia nigra neurons. The major protein in the Lewy body and Lewy neurite inclusions is α-synuclein fibrils (Spillantini et al., 1997). Rigidity and tremor in Parkinson's are caused by the lack of the neurotransmitter dopamine due to the death of the dopamine producing neurons in the substantia nigra region (Wu, 2011). The presence of Lewy bodies is not directly linked as a cause to these motor problems.

Huntington's disease is characterized by the aggregated huntingtin protein which is deposited in the nucleus of the cell (Kaltenbach et al., 2007). Depleted levels of huntingtin protein (an anti-apoptotic protein) due to its aggregation result in the death of

the striatum and cortex neurons (Cattaneo et al., 2001). The loss of brain cells of the cerebral cortex and striatum in Huntington's disease results in uncontrolled movements and dementia.

Individuals with Amyotrophic Lateral Sclerosis have aggregates composed of superoxide dismutase which are deposited in the cell bodies and axons of motor neurons (Turner et al., 2005). The enzyme superoxide dismutase, which catalyzes the conversion of superoxide anions to hydrogen peroxide, is depleted by misfolding and aggregation (Murakami et al., 2011). The loss of superoxide dismutase activity results in the accumulation of superoxide anions which initiate lipid peroxidation. Lipid peroxidation causes neuronal membrane damage which results in cell death (Mattson, 2000; Wang et al., 2012). In this disease, neuronal cell death occurs in the spinal cord, the brain stem and the motor cortex causing progressive paralysis (Soto, 2003).

Functional protein fibrils

Although protein fibrils are more often associated with select neurodegenerative diseases, functional fibrils have been identified in bacteria, fungi, insects, invertebrates and humans. The fibril structure is now described as a quaternary structure formed by hydrogen bonded β-sheets (Chiti and Dobson, 2006). *E. coli* and *Salmonella* species employ curli fibrils (from protein curli) to attach themselves to surfaces to form colonies and invade host cells (Cherny et al., 2005; Gebbink et al., 2005; Fowler and Kelly, 2012). Insects and fish use chorion protein fibrils as a structural component and for protection of their eggshells (Hamodrakas et al., 2004). The electron micrographs of α-synuclein and chorion protein fibrils are shown in Figure 13. There appears to be no significant difference in structure between functional and disease state fibrils.

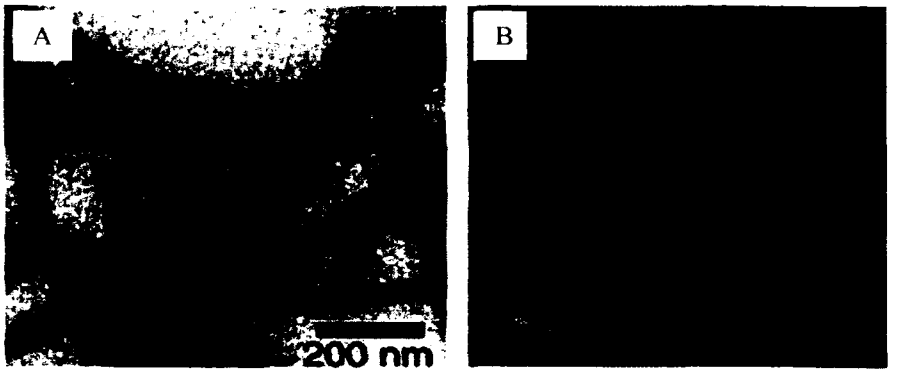

Figure 13. Fibril structures of α-synuclein and silkmoth chorion proteins

(A) Transmission electron microscopy micrograph of α-synuclein fibrils.

(B) Transmission electron microscopy micrograph of silkmoth protein fibrils.

Figures reproduced from Bousset, Panel A (Bousset et al., 2013) and Hamodrakas, Panel B (Hamodrakas et al., 2004).

Fibrin fibrils are also employed in clot formation. Factor XII initiates the cleavage of fibrinogen into fibrin. The fibrin polymerizes and contributes to the formation of a blood clot (Kranenburg et al., 2002; Allan et al., 2012). Human Pmel17 protein forms fibrils which function as sites at which melanin is synthesized from tyrosine in the melanosomes (Figure 14). The Pmel17 fibrils also bind reactive melanin precursors which are toxic to the melanocytes (Fowler et al., 2007).

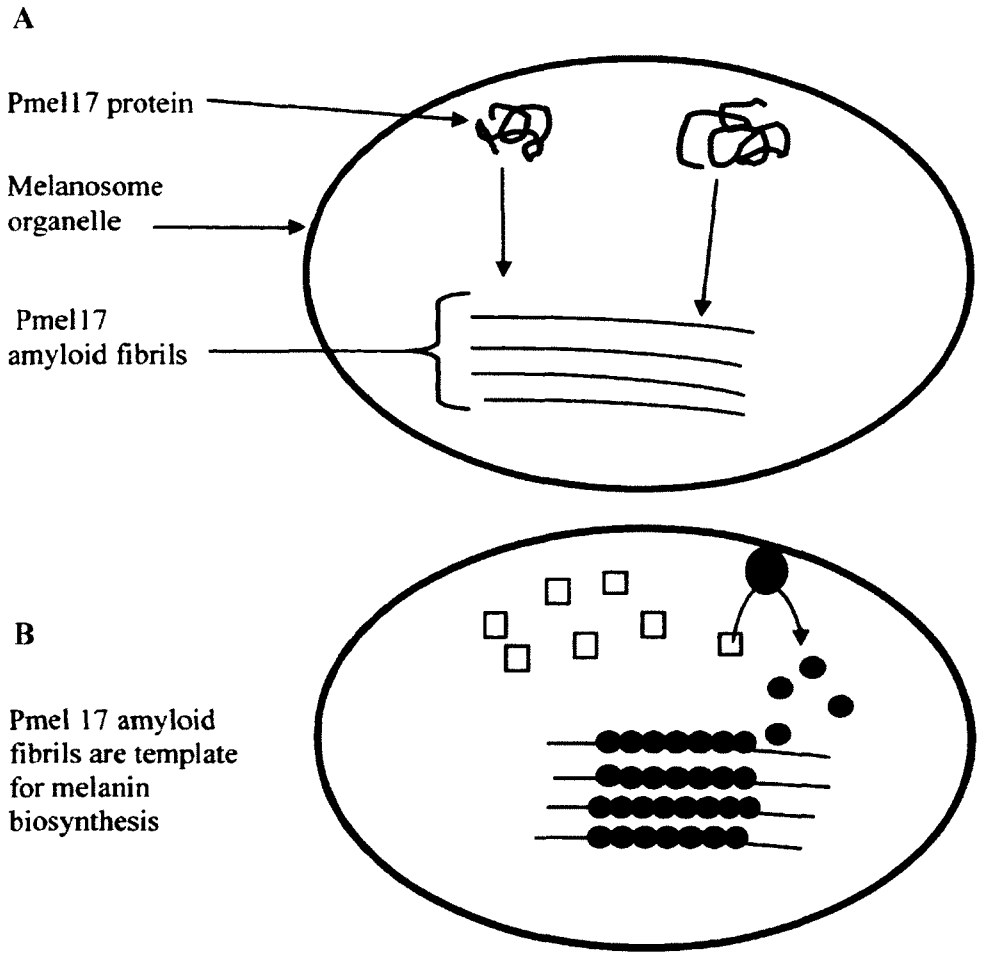

Figure 14. Biosynthesis of melanin from tyrosine on human Pmel17 fibrils

(A) Human Pmel17 protein forms fibrils in the melanosome of a melanocyte.

(B) Pmel17 fibrils are scaffold for melanin biosynthesis (Fowler et al., 2007). This schematic is modified from Fowler et al. The symbols shown correlates to the following: □ = tyrosine; ● = reactive melanin precursor; ● = tyrosinase; ●●● = melanin polymer.

THE SYNUCLEIN FAMILY

The synuclein family consists of small and soluble proteins: α, β and γ which are primarily expressed in the brain cells of vertebrates (George, 2002). The size of human

synucleins ranges from 127 to 140 amino acid residues (Yoshida et al., 2006). α- and β-Synucleins are expressed predominantly in the presynaptic axon terminals of the central nervous neurons including the dopamine producing neurons of the substantia nigra while γ-synuclein is expressed in the peripheral nervous system neurons. The three proteins are encoded by three specific α-, β-, and γ-synuclein genes. In humans, α-, β-, and γ-genes are located in chromosomes 4, 5 and 10, respectively (Chen et al., 1995; Spillantini et al., 1995; Lavedan, 1998). α-Synuclein shares 60% and 78% identity with γ- and β-synuclein, respectively. β-Synuclein differs from α-synuclein by the deletion of a cluster of eleven amino acids in its central region (Uversky et al., 2002; Sung and Eliezer, 2006).

The synuclein polypeptide chain is divided into three regions: the N-terminus, the central region and the C-terminus (Figure 15). The region of highest homology among the synuclein proteins is the N-terminal region which contains several degenerate eleven amino acid repeats with a KTK(E/Q)GV conserved sequence (Sung and Eliezer, 2007). Their C-terminal domains are diverse. α-and γ-Synucleins contain seven repeat domains while β-synuclein has five. The sixth and seventh repeat sequences in β-synuclein are incomplete because of the deletion of the eleven amino acid residues in the central region (Lavedan, 1998). There is a variation in the KTK(E/Q)GV sequence among the three human synucleins, however, the third hexameric sequence is highly conserved. Several experimental studies have shown that the synuclein monomers are random coils in solution but adopt an α-helical conformation when associated with phospholipids (Perrin et al., 2001; Uversky et al., 2002; Sung and Eliezer, 2006; Israeli and Sharon, 2009).

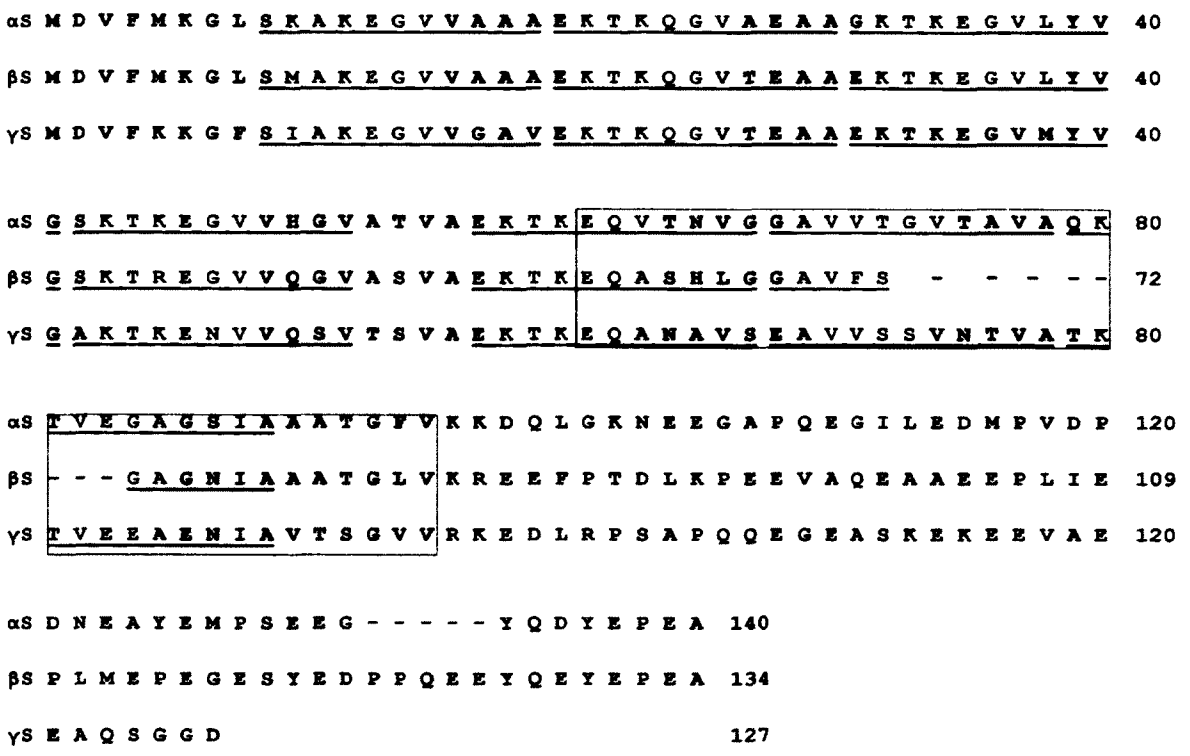

Figure 15. Sequence alignment of the human synuclein family

The number of amino acid residues in α-, β- and γ-synuclein proteins are 140, 130 and 127, respectively. The synuclein polypeptides are divided into three regions: the N-terminal (blue); the central (boxed area) and the C-terminal (yellow). In the N-terminal region there are degenerate 11 amino acid repeats (underlined) with conserved KTK(E/Q)GV sequences (red). The sixth and seventh repeats lack the KTK(E/Q)GV conservation (Uversky et al., 2002).

α-Synuclein

Human α-Synuclein is a 140 amino acid protein encoded by the α-synuclein gene consisting of six exons (Maroteaux et al., 1988; McLean et al., 2012). Alternative splicing in which exon 3 or 5 or both are omitted yields 126, 112 and 98 α-synuclein

variants, respectively (McLean et al., 2012). There are conflicting reports about the native structure of α-synuclein. Some researchers insist that the protein exists *in vivo* predominantly as an unstructured monomer (Fauvet et al., 2012) while others maintain that α-synuclein can form a helical tetramer which resists fibril formation under physiological conditions (Bartels et al., 2011; Wang et al., 2011).

Gurry and coworkers, using simulation approaches, recently reported that though a larger fraction of α-synuclein protein exists *in vivo* as a monomer, a small fraction forms helical trimers and tetramers (Gurry et al., 2013). The researchers suggest that the formation of the helical tetrameric conformation is a mechanism for storing high concentrations of non-membrane bound monomeric α-synuclein in order to prevent it from aggregating (Gurry et al., 2013).

Another group of researchers have reported that after cross linking α-synuclein in the primary neurons and neuroblastoma cells in cell culture, a large fraction of the protein exists as a helical 60 kDa tetramer with a small fraction of 80 and 100 kDa species and variable amounts of the monomer (Dettmer et al., 2013). β-synuclein was also shown to exist in the same conformations. This folded form of α- and β-synuclein may be their natural structure in the brain tissue.

The N-terminal region of α-synuclein forms α-helices when associated with lipid membranes. The middle region of the protein, which is between residues 65 to 95 is prone to aggregation. A portion of the C-terminus (residues 120 to 140) of α-synuclein has a net negative charge of 8, which is contributed by aspartate and glutamate residues (Uversky et al., 2002). The central region encompassing residues 65 to 95, has a positive charge of 3, which is contributed by lysine residues (Uversky et al., 2002). Between the

C-terminus and the central region the electrostatic interactions may prevent the central regions of α-synuclein molecules from associating with each other and forming fibrils (Bertoncini et al., 2005). A decrease in the negative net charge increases the propensity of α-synuclein to fibrillate (Uversky et al., 2001b).

The results of some experimental studies suggest that the role of the conserved KTK(E/Q)GV repeat sequence is to maintain α-synuclein in its unfolded state when in solution and to interact with membrane phospholipids (Sode et al., 2007). When α-synuclein is associated with a micelle, it forms a hairpin structure (Figure 16) (Ulmer et al., 2005). One helix covers a stretch that includes residues 3-37 and the other is composed of residues between 45 and 92. The loop that joins the two helices encompasses residues 38-44.

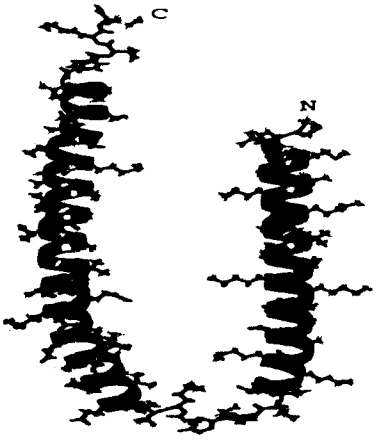

Figure 16. Micelle-bound α-synuclein based on solution NMR

Under physiological conditions in a neuron, a fraction of α-synuclein is associated with lipid membranes and assumes a hairpin structure. Figure reproduced from Ulmer (Ulmer et al., 2005).

It is proposed that α-synuclein may first form an α-helical intermediate before converting into fibrils (Uversky et al.. 2001a). The degenerate KTK(E/Q)GV sequences resist the formation of the partially folded α-synuclein. Mutants of α-synuclein are more prone to fibrillation than the unmutated form (Li et al.. 2001). The three point mutations A30P. E46K and A53T in the N-terminal region of α-synuclein disrupt some of the repeat sequences (Sode et al.. 2007). These mutations are believed to enhance the formation of α-helical intermediates leading to fibril formation (Harada et al.. 2009).

Polymeropoulos and coworkers discovered an A53T point mutation in α-synuclein which was associated with early-onset of familial Parkinson's disease (Polymeropoulos et al., 1997). A second A30P mutation was reported in 1998 (Kruger et al., 1998) and a third E46K α-synuclein mutant was also reported in 2004 (Zarranz et al., 2004). Recently, two new mutations H50Q and G51D which are also associated with early-onset Parkinson's disease were reported (Lesage et al., 2013). The five point mutations are all in the N-terminal region. It should be noted that early-onset familial Parkinson's disease is actually a rare medical condition.

The physiological function of α-synuclein in the brain tissue is not clearly understood but a number of possible functions have been proposed. Several experimental studies seem to indicate that α-synuclein is involved in the biosynthesis and storage of the neurotransmitter dopamine (Peng et al., 2005). In addition, α-synuclein may be involved in dopamine release and reuptake at the presynaptic terminals (Sung and Eliezer, 2007). Dopamine biosynthesis involves the conversion of tyrosine to levo-dihydroxyphenylalanine (L-DOPA) in a reaction that is catalyzed by a phosphorylated tyrosine hydroxylase (TH) (Sidhu et al., 2004b). The enzyme DOPA

decarboxylase catalyzes the conversion of L-DOPA to dopamine. A chaperone protein 14-3-3 binds the phosphorylated TH and stabilizes its phosphorylated conformation and prevents its dephosphorylation (Kleppe et al., 2001; Obsilova et al., 2008). α-Synuclein can either directly bind the dephosphorylated TH and prevent the phosphorylation of TH at serines 19 and 40, rendering the TH inactive (Leal et al., 2002; Perez et al., 2002), or activate a protein phosphatase 2A that dephosphorylates the TH enzyme (Lou et al., 2010). However, when α-synuclein itself is phosphorylated at serine 129, it cannot activate the phosphatase 2A, which in turn will not dephosphorylate the TH enzyme. Phosphorylation and dephosphorylation of TH regulates dopamine synthesis. After dopamine is synthesized, it is immediately stored in synaptic vesicles (Perez et al., 2002). Low levels of α-synuclein in the nerve terminals due to low expression or aggregation, results in increased activity of TH with subsequent increase in the production of dopamine. If dopamine levels exceed the ability of the cell to clear the neurotransmitter from the cytoplasm, the accumulated dopamine forms dopamine quinones and other reactive species including hydrogen peroxide, superoxide anion and hydroxyl radicals (Hasegawa, 2010). These ROS can extract electrons from double bonds in lipids, proteins and nucleic acids leading to cell damage.

Another possible function for α-synuclein is regulation of the formation of synaptic vesicles. A transmembrane enzyme phospholipase D2 is essential for synaptic vesicle formation. The enzyme hydrolyzes phospholipids in order to generate phosphatidic acid, which is one of the building components for the synaptic vesicles (Sidhu et al., 2004a). When α-synuclein binds phospholipase D2, the enzyme is inactivated (Jenco et al., 1998). On the other hand when α-synuclein is phosphorylated at

position 129 (phospho-Ser 129), it loses its ability to interact with phospholipase D2 and allows vesicles to be built (Pronin et al., 2000; Ellis et al., 2001). Thus the binding and release of phospholipase D2 by α-synuclein regulates formation of the synaptic vesicles.

α-Synuclein may also be involved in the reuptake of dopamine from the synaptic cleft by the protein dopamine transporter (DAT) (Chadchankar et al., 2011). The rate of reuptake of dopamine must not exceed the rate at which it is repackaged into vesicles. α-Synuclein binds to the dopamine transporter with its middle region encompassing residues 58 to107 (Wersinger et al., 2003). This protein-protein interaction controls the amount of free DAT available for the reuptake of dopamine. The regulation of the amount of free DAT prevents an excess of free dopamine in the cytoplasm of the terminal axon. The acidic pH of the storage vesicles prevents a spontaneous oxidation of dopamine (Sidhu et al., 2004a). At physiological pH in the cytoplasm and in the presence of molecular oxygen, dopamine is oxidized and generates reactive quinones, superoxide and hydrogen peroxide (Sidhu et al., 2004a). The DAT protein has been identified in the intracellular Lewy bodies together with α-synuclein (Bellucci et al., 2008). As a result of this retention, dopamine transporter levels in the cell are depleted. The rate of reuptake of the dopamine from the synaptic cleft is adversely affected.

In order for the synaptic vesicles to release dopamine into the synaptic cleft, they must fuse with the presynaptic membrane. α-Synuclein bound to the vesicle SNARE protein synaptobrevin-2 seems to promote the formation of the complex between the v-SNARE proteins in the vesicle membrane and the t-SNARE proteins in the membrane of the pre-synaptic terminal. The fusion of the two membranes facilitates the release of the neurotransmitter into the synaptic cleft (Burre et al., 2010). The absence of the three

synucleins in experimental animals showed a marked decrease in the fusion between the v-SNAREs (integral membrane proteins of the vesicle) and the t-SNAREs (the integral membrane proteins of the presynaptic terminal).

PARKINSON'S DISEASE

Parkinson's disease is a movement disorder that affects about six million individuals world-wide who are over 50 years of age (Bellucci et al., 2012). At the age of 40-50, those affected generally have early-onset Parkinson's disease due in part to select mutations already discussed in the previous section. The areas of the brain affected by the disease include the substantia nigra also known as substantia nigra pars compacta (Arias-Carrion et al., 2010) and the striatum (Wersinger et al., 2004). The disease is characterized by a progressive loss of dopamine producing neurons of the substantia nigra (Figure 17) and the presence of Lewy bodies and Lewy neurites in the terminal axon cytoplasm (Wu, 2011). Depleted levels of dopamine due to the loss of the dopamine producing neurons, produces the Parkinson's disease clinical symptoms. The surviving neurons contain Lewy bodies and Lewy neurites inclusions.

Although α-synuclein is the major component in the Lewy bodies, there are also several other proteins which are associated with Parkinson's disease and it appears to be a multifactorial problem. The proteins include PINKI, Parkin, DJ-1, leucine-rich repeat kinase 2 and Fbxo7 (Bonifati et al., 2003; Darios et al., 2003; Valente et al., 2004; Zimprich et al., 2004; Burchell et al., 2013). Each of the five proteins plays a role in the normal function of the mitochondria. Mutations in any one of them disrupts the mitochondrial function, including the electron transport chain, resulting in the generation of ROS (Murphy, 2009).

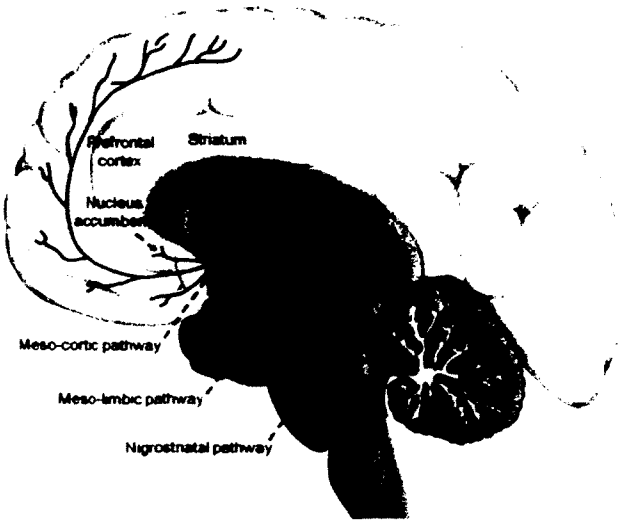

Figure 17. A cross section of the brain showing the substantia nigra pars compacta (SNc)

The areas of the brain mainly affected by Parkinson's disease are the striatum and the substantia nigra pars compacta (Wersinger et al., 2004). Axons of the substantia nigra neurons (red) extend into the striatum region (Arias-Carrion et al., 2010). Figure reproduced from Arias-Carrion.

The mechanism or therapy by which Parkinson's disease progression can be completely stopped has not yet been discovered. Current treatment of the disease is the administration of the dopamine precursor levo-dihydroxyphenylalanine (L-DOPA). Once L-DOPA has crossed the blood-brain barrier, it is converted to dopamine in a reaction catalyzed by DOPA decarboxylase (Perez et al., 2002). However, the drug L-DOPA loses its effect in alleviating the symptoms as the disease progresses. There are three other drugs that inhibit α-synuclein fibril formation and they include selegiline, entacapone and tolcapone (Braga et al., 2011). Unfortunately, these drugs have serious

side effects including nausea, hypertension and liver toxicity (Simola et al., 2010). None of the drugs that inhibit α-synuclein fibrillation or ameliorate Parkinson's disease symptoms can stop the progression of the disease, which further indicates the multifactorial nature of the problem.

Another alternative therapy for combating the disease is the direct replacement of dopamine producing neurons using human embryonic stem cells (Wakeman et al., 2011). However, dopamine producing neurons derived from embryonic stem cells have been shown to develop Lewy bodies after eleven to sixteen years (Kordower et al., 2008). Other compounds which can disrupt α-synuclein aggregation in a concentration-dependent manner are being tested to assess their effect. Experimental studies have shown that rifampicin, an antibiotic used to treat bacterial infection, can inhibit α-synuclein aggregation *in vitro* in a concentration-dependent manner (Li et al., 2004) and also dissolve α-synuclein mature fibrils. Flavonoid baicalein from a Chinese herb *Scutellaria baicalensis* was shown to inhibit α-synuclein fibrillation and to disaggregate its mature fibrils into non-toxic soluble oligomers both *in vitro* and *in vivo* (Li et al., 2004; Ma et al., 2014). Other compounds that inhibit α-synuclein fibrillation include curcumin, polyphenols, nicotine and hydroquinone (Braga et al., 2011).

When misfolded and aggregated α-synuclein cannot be cleared from the cytoplasm either by the UPS or the ALP systems, it is isolated into inclusions called Lewy bodies. The location of the Lewy bodies depends on the type of the disease (Davies et al., 2011). For example, in Parkinson's disease the Lewy bodies are found in the substantia nigra while in Dementia with Lewy bodies they are present in the neocortex and the brain stem (Kruger et al., 1998). When Lewy bodies in the affected

neurons are stained with hematoxylin and eosin. they appear spherical with a dense core surrounded by a halo of granular matter (Figure 18).

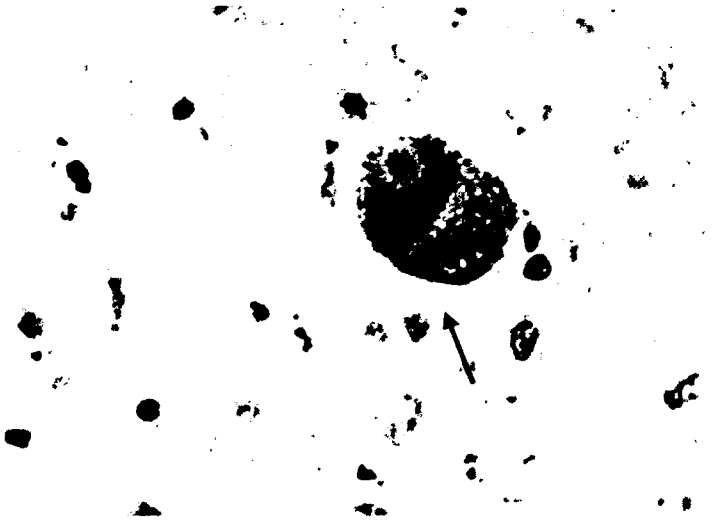

Figure 18. A Lewy body stained by hematoxylin and eosin stain

A section of the substantia nigra region stained with hematoxylin and eosin stain shows a Lewy body. The Lewy body appears spherical and has a dense core surrounded by granular material. Figure reproduced from Spillantini (Spillantini et al., 1997).

α-Synuclein and disease implications

The scientific community believes that α-synuclein may play a role in Parkinson's disease. Its mutants (A30P, E46K , H50Q, G51D and A53T) are associated with early-onset Parkinson's disease (Schulz-Schaeffer, 2010). The cause of α-synuclein accumulation in the presynaptic terminals has not yet been elucidated. Epidemiological studies show that Parkinson's disease is a multifaceted disorder caused by various

factors both in the body and from the environment (Elbaz and Moisan, 2008). Nonetheless, α-synuclein aggregation is potentially a step in the development of Parkinson's disease in select patients.

An experimental study involving mice showed that the expression of α-synuclein in the substantia nigra decreases with advance in age (Mak et al., 2009). In another study involving monkeys and humans, the results indicated an increase in α-synuclein expression with increase in age (Chu and Kordower, 2007). Chu and coworkers hypothesized that an increased accumulation of α-synuclein in the human substantia nigra may trigger the onset of Parkinson's disease. Perhaps the accumulation of the protein is due to age associated inefficiency of the ubiquitin-proteasome system to remove unwanted α-synuclein protein molecules from the cell. It may not necessarily be an overexpression of the protein in old age.

α-Synuclein is most commonly found in the brain and cerebrospinal fluid (CSF) but the protein has also been recently found in red blood cells (Tokuda et al., 2006; Fauvet et al., 2012) and recent attempts to quantitatively and reliably determine if it is in blood plasma have been made (Tinsley et al., 2010). Conflicting results on the levels of α-synuclein in individuals with Parkinson's and in those without the disease have been reported. One group of researchers, using cerebrospinal fluid, observed that α-synuclein levels in individuals with Parkinson's disease was lower than in non-Parkinson disease CSF (Kasuga et al., 2010). Borghi and coworkers reported no significant difference in the CSF α-synuclein levels between patients with Parkinson's disease and control subjects (Borghi et al., 2000). Tokuda and coworkers have also reported elevated CSF α-synuclein levels in individuals with Parkinson's disease compared to control subjects

(Tokuda et al., 2010). The variability may lie in the different methods used to determine the α-synuclein concentration.

Different oligomers have been identified that can lead to fibril formation. Fibrillar oligomers are soluble filaments with a β-sheet structure and develop into protofibrils (Apetri et al., 2006; Hong et al., 2011). Protofibrils are β-strands arranged in parallel with the side chains on the surface of the β-sheets (Breydo et al., 2012). Recently, a group of researchers has identified a ring shaped α-synuclein oligomer. This form is capable of adversely interacting with artificial cell vesicles *in vitro* and causing nonspecific ion transport. They can also assemble into fibrils (Giehm et al., 2011).

In cell cultures some oligomers appear to be able to move from one cell to another, though the new cells degrade the oligomers in the lysosome (Lee et al., 2011). Within neuronal *in vitro* cell cultures, α-synuclein aggregates can be transmitted from cell-to-cell under extreme nonphysiological conditions (Desplats et al., 2009). In addition, experimental studies involving neuronal cell cultures have shown that specific forms of exogenous oligomers generated in the presence of $FeCl_3$ can induce intracellular α-synuclein aggregation (Danzer et al., 2009).

α-Synuclein oligomers bind to lipid membranes and can potentially make channels in the bilayer membrane thereby creating nonselective membrane channels (van Rooijen et al., 2010). These oligomers, and not mature fibrils, could be a more responsible factor in Parkinson's disease. For example, cell death *in vitro* takes place before α-synuclein fibrils are detected (Gosavi et al., 2002). In one experiment when human α-synuclein was expressed in rat substantia nigra, the death of dopaminergic neurons occurred before Lewy bodies were formed (Lo Bianco et al., 2002).

Consequently, a correlation between fibril accumulation and cell death is now questionable, suggesting that oligomers are potentially a toxic species or the soluble oligomers interact with unknown cofactors. Dopaminergic neurons containing Lewy bodies do not necessarily undergo apoptosis faster than the normal population of neurons (Schulz-Schaeffer, 2010). However, the presence of α-synuclein oligomers in the dopaminergic neurons compromises the integrity of the cells.

Protein modification, which can occur during protein translation or after translation, is a mechanism that regulates the activity, binding affinity and stability of a protein (Schonichen et al., 2013). α-Synuclein undergoes posttranslational modifications including phosphorylation, oxidation, nitration and protein cleavage. Some modifications stabilize the protein while others cause it to misfold and form fibrils (Oueslati et al., 2010). Phosphorylation of the serines at positions 87 and 125 protects α-synuclein from misfolding and fibrillation (Paleologou et al., 2010; Oueslati et al., 2012). However, phosphorylation of serine 129 in the C-terminus of α-synuclein increases the propensity of the protein to form fibrils (Fujiwara et al., 2002). α-Synuclein in Lewy bodies and Lewy neurites is highly phosphorylated at serine 129 (Fujiwara et al., 2002; McCormack et al., 2012).

All four methionine residues of α-synuclein are prone to oxidation to sulfoxides (Met-S-O) *in vitro* (Glaser et al., 2005). Experimental studies have shown that the more methionines oxidized the higher the resistance of α-synuclein to fibrillation. Interestingly, a methionine-oxidized α-synuclein inhibits the fibrillation of other non-modified α-synuclein molecules (Zhou et al., 2010). On the other hand, when metal ions bind at the sulfoxide moieties of the methionine-oxidized α-synuclein, they promote its

fibrillation (Glaser et al., 2005). Zn^{2+}, Al^{3+} and Pb^{2+} ions overcome the resistance of methionine-oxidized α-synuclein to form fibrils (Yamin et al., 2003).

Tyrosine nitration promotes fibril formation (Giasson et al., 2001). The 20S proteasome system is unable to break down α-synuclein molecules that have a nitrated tyrosine at position 39 (Hodara et al., 2004). The failure to clear abnormal α-synuclein from the brain tissue results in its accumulation, aggregation and formation of Lewy bodies. Experimental studies have shown that incomplete degradation of α-synuclein generates synuclein fragments which are more prone to aggregation *in vitro* than the full length α-synuclein (Liu et al., 2005). It appears that modifications in different regions of the α-synuclein protein have different effects on its structure. Dopamine and other positively charged molecules interact with the C-terminal region and induce the protein to aggregate (Norris et al., 2005).

Lewy bodies have been reported to contain an abundant amount of C-terminally cleaved α-synuclein (Liu et al., 2005; Lewis et al., 2010). Cleavage sites lie between residues 115 and 135. The C-terminus is cleaved by the protease enzyme calpain-1 (Dufty et al., 2007). Studies have shown that a C-terminally truncated α-synuclein has a high tendency to fibrillate both *in vivo* and *in vitro* (Li et al., 2005; Kim et al., 2010).

Metals and α-synuclein aggregation

Most of α-synuclein protein is copper bound *in vivo* (Breydo et al., 2012). The imidazole of histidine at position 50 is the anchoring point for copper. α-Synuclein in solution binds copper ions with methionine 1, aspartate 2 and histidine 50 (Dudzik et al., 2013). When α-synuclein is membrane bound, the histidine is spatially unavailable and therefore copper is bound by only methionine 1 and aspartate 2 (Dudzik et al., 2013).

Copper-bound α-synuclein has ferrireductase enzyme activity that catalyzes the reduction of Fe^{3+} to Fe^{2+} (Davies et al., 2011).

Epidemiological studies conducted in Quebec, Detroit and Michigan indicated that heavy metals were a risk factor for Parkinson's disease (Uversky et al., 2001b). Occupational exposure to manganese, iron, and copper seemed to increase the incidence of Parkinson's disease (Gorell et al., 1999). Postmortem of tissues from Parkinson's disease brains showed higher levels of iron, zinc and aluminum in the substantia nigra compared with brain tissue unexposed to the metals (Uversky et al., 2001b). Interaction between metals and α-synuclein causes changes in the conformation of the protein (Uversky et al., 2001b; Santner and Uversky, 2010). When α-synuclein is incubated with Al^{3+} ions, there are changes in the far-UV CD, the UV absorbance and the intrinsic fluorescence spectra which are attributed to a partially folded species (Santner and Uversky, 2010). Changes in the structure of α-synuclein eventually lead to fibril formation.

The relationship between calcium and α-synuclein appears to be complex. Investigators have observed that α-synuclein regulates the channels by which Ca^{2+} ions enter the cell (Mosharov et al., 2009). However, the interactions between α-synuclein, dopamine and Ca^{2+} ions can cause the death of substantia nigra neurons (Mosharov et al., 2009). In addition, Ca^{2+} ions can interact with the last fifteen amino acid residues of the C-terminus of α-synuclein and induce the protein to form the previously mentioned ring-shaped oligomers, which can form pores in the cell membrane (Lowe et al., 2004). High concentrations of Ca^{2+} ions in the cytoplasm cause α-synuclein to bind to lipid

membrane with both the N- and the C-termini leading to aggregation of the protein and eventual perforation of the membrane (Pountney et al., 2005).

Iron has been implicated in Parkinson's disease (Mounsey and Teismann, 2012). Postmortem analysis of Parkinson's disease brain tissue has shown iron accumulation in the substantia nigra (Gorell et al., 1999; Ayton and Lei, 2014). The elevated levels of iron are accompanied by an increase in the concentration of ferritin protein, which binds Fe^{3+} ions (Davies et al., 2011). In addition, since Fe^{2+} is a cofactor of tyrosine hydroxylase, the lower concentration of Fe^{2+} ions decreases the rate of dopamine synthesis (Davies et al., 2011). The copper-bound α-synuclein maintains a supply of Fe^{2+} ions by reducing Fe^{3+}through its interaction with the ferrireductase. The loss of α-synuclein through aggregation reduces its ferrireductase activity. Consequently Fe^{3+} ions accumulate resulting in the generation of ROS.

Lead exposure has been shown to increase α-synuclein expression and induce the formation of inclusion bodies (Zuo et al., 2009). Pb^{2+} ions can even overcome the resistance of methionine-oxidized α-synuclein to fibril formation (Yamin et al., 2003). The concentration of magnesium has been known to decrease in the cerebral spinal fluid as Parkinson's disease progresses (Bocca et al., 2006). A study using mice revealed that magnesium intake between 1-4 mM concentration was sufficient to protect α-synuclein against fibrillation (Oyanagi et al., 2006). At concentrations greater than 10 mM, Mg^{2+} ions induced α-synuclein fibrillation (Oyanagi et al., 2006). Furthermore, 1-4 mM magnesium concentration was shown to protect dopaminergic neurons from 1-methyl-4-phenylpyridinium (MPP^+), a neuron toxin (Hashimoto et al., 2008). The interaction

between magnesium and α-synuclein seems to play a protective role by inhibiting aggregation of the protein.

Manganese toxicity produces symptoms that are similar to Parkinson's disease. The clinical symptoms include fixed gaze, slowness of movement, postural difficulties and tremor (Lucchini et al., 2009). However, there are no Lewy bodies present in manganese induced Parkinsonism and the neurons of the substantia nigra region are not involved (Bleecker, 1988) When a manganese transporter protein PARK9 is omitted in *in vitro* studies, there is an increase in α-synuclein aggregation and toxicity (Gitler et al., 2009). Manganese ions can oxidize α-synuclein resulting in the formation of di-tyrosine cross-links both intra- and intermolecular (Uversky et al., 2001b; Santner and Uversky, 2010). This modification makes α-synuclein more prone to aggregation.

Although higher levels of zinc have been observed in Parkinsonian substantia nigra tissue compared with control tissue, the correlation between zinc exposure and disease progression is questionable (Forte et al., 2005). However, *in vitro* studies have indicated that zinc can accelerate α-synuclein fibril formation (Uversky et al., 2001b).

On the whole there are two types of interactions between metals and α-synuclein. One type involves electrostatic interaction between metal ions and the negatively charged side chains of α-synuclein in the C-terminal region. The second type of interaction between metals and α-synuclein is facilitated by methionine 1, aspartate 2 and histidine 50 in the N-terminal region of the protein (Dudzik et al., 2013). Cu (II) binds with high affinity to the N-terminal region of α-synuclein specifically the ^{1}MDVFMKGLS^{9} and ^{48}VVHGV^{52} sites and histidine 50 is the anchoring residue. Other

divalent metal ions have a preference to bind the ^{119}DPDNEA^{124} site in the C-terminal region and aspartate 121 is the anchoring residue (Binolfi et al., 2006).

Many metals stimulate partial folding of α-synuclein (Uversky et al., 2001b). The partially folded conformation is prone to aggregation. Iron, aluminum, cobalt and manganese and high levels of copper ions are the most effective at inducing α-synuclein partial folding with subsequent aggregation (Uversky et al., 2001b).

APPROACHES TO STUDY PROTEIN FIBRILS *IN VITRO*

Transmission electron microscopy

Examination of a specimen under a transmission electron microscope (TEM) gives information about the surface features, size and shape of an object on a nanometer to micrometer scale. A modern TEM consists of an electron source, a specimen stage, an objective lens system, the magnification lens system and data collection system. The magnified electron image is projected onto a fluorescent viewing screen or the image can be captured by a charge coupled device camera and displayed on a computer screen (Wang, 2000).

A beam of electrons generated in a high vacuum by an electron gun is accelerated towards the specimen and it interacts with the atoms of the specimen. The interactions and effects on the electron beam are detected and converted into an image.(Wang, 2000) Thinner areas of the specimen allow more unscattered electrons to be transmitted and these areas appear light. Areas of the specimen that are thicker allow fewer unscattered electrons to be transmitted and appear dark (Wang, 2000). However, a beam of high energy electrons is not compatible with molecules such as proteins. Such molecules would easily dry up and their structure would collapse. In addition, the

molecules do not have the ability to scatter the electrons (Ohi et al., 2004). Negative staining, for example, the use of uranyl acetate, has been introduced to insert the specimen in a layer of dried heavy metal solution. The heavy metal upholds the structure of the specimen. In addition, the heavy metal can withstand the radiation from electrons and is capable of scattering the electrons more efficiently than the delicate protein specimen.

Atomic force microscopy

As the name implies, atomic force microscopy (AFM) characterizes the nature of surfaces at atomic scale. The atomic force microscope generates very high resolution 2D and 3D images by using a very small probe tip at the end of a cantilever (Meyer, 1992). Atomic force microscopy is employed to erase nanoscale electronic structures, measure surface structures of biological substances, visualize objects from living cells and to conduct drug crystallization studies (Jensen, 2013) The main components of an AFM are a cantilever with a sharp tip at one end, a source of laser beam and a photo detector. Interactions between the tip of the cantilever and the sample surface are regulated by different types of forces including van der Waals forces, adhesive forces, capillary forces and electrostatic forces (Meyer, 1992). The van der Waals forces are the most commonly associated with AFM.

When the cantilever tip is a few angstroms from the surface of the sample, repulsive van der Waals forces have an effect on the tip. But when the tip is several angstroms from the sample surface it experiences attractive van der Waals forces (Meyer, 1992; Hayton et al., 2010; Jensen, 2013). The van der Waals forces between the

tip and sample surface generate electrical signals which are converted into topographic images.

The tapping mode AFM is most commonly used for soft and biological samples. In the tapping mode atomic force microscopy, the tip oscillates vertically, makes contact with the surface and lifts off. The oscillation distance ranges from 20 nm to 100 nm. When the tip comes too close to the sample surface, van der Waals forces, dipole-dipole interactions and electrostatic forces act on the cantilever and cause a decrease in the amplitude of oscillation (Jensen, 2013). As the cantilever tip scans the sample surface, the oscillation amplitude changes with varying contours of the surface. The changes in the amplitude cause the cantilever to reflect the incident laser beam at different angles. The photo detector records the changes in amplitude and these signals are converted by the computer into images of the sample (Jensen, 2013).

Thioflavin T fluorescence

The fluorescence of a benzothiazole dye thioflavin T is an established test for detecting and monitoring amyloid fibril formation. Thioflavin T dye is composed of a hydrophobic dimethylamino group attached to a benzene ring which is linked to a polar benzothiazole containing a polar nitrogen and sulfur (Khurana et al., 2005) (Figure 19). When a free thioflavin T molecule absorbs a photon of light, the angle of rotation between the rings rises to 90°. The dimethylamino benzene ring becomes positively charged while the benzothiazole ring is slightly negative (Wolfe et al., 2010). The fluorescence of the dye at this conformation is weak. When the dye is trapped between β-sheets of amyloid fibrils and is irradiated, the angle of rotation is reduced to 65°, the

positive charge on the dimethylaminobenzene ring decreases and fluorescence of the dye is enhanced.

In a polar solvent, the thioflavin dye peak absorption is at 340 nm and its maximum emission is at 445 nm (Wolfe et al., 2010). However, when the dye molecule is trapped between β-sheets of protein fibrils that has more of a nonpolar environment, there is a shift in its absorption and emission peaks to 440 nm and 480 nm respectively (Wolfe et al., 2010; Hsu et al., 2013). Besides limiting the rotation between the thioflavin rings, the protein fibrils also reduce the quenching effects of the environment of the dye thereby enhancing its fluorescence (Hsu et al., 2013).

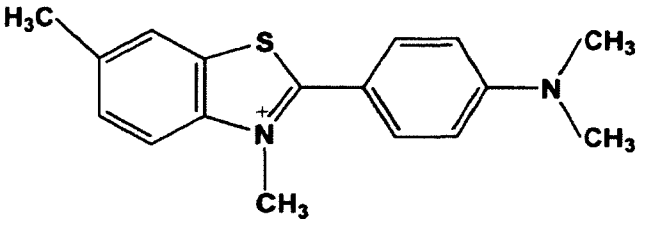

Figure 19. Structure of a thioflavin T molecule

The benzothiazole ring on the left is linked to the dimethylaminobenzene ring on the right. The dimethylaminobenzene is the hydrophobic portion of the molecule while the benzothiazole is the polar portion .There is an angle of rotation between the rings. When the molecule is trapped between β-sheets of the protein fibrils, the rotation between the two rings is restricted causing the bound molecule to fluoresce more than the free molecule and there is also no quenching effect.

SPECIFIC AIMS OF THE RESEARCH PROJECT

The purpose of my research project was to contribute to the further understanding of the synuclein proteins and investigate potential treatments for the synucleinopathies. Experimental and computational approaches were employed to conduct the study. The first aim was to investigate potential methods of destroying protein fibrils with the hope that these methods could be employed to facilitate medical treatment of fibril related diseases. The second aim was to explore the mechanism by which β-synuclein inhibits α-synuclein fibril formation. In the future, synthetic protein molecules mimicking β-synuclein could be employed to arrest α-synuclein fibrillation. My third aim was to express and isolate a multimeric β-synuclein from which well diffracting crystals could be produced for X-ray crystallographic studies in order to elucidate its physiological structure. The fourth aim was to use bioinformatics techniques to construct a superfamily for the synucleins in order to identify ancestral relatives which may shed light on their native structure and function in the brain.

CHAPTER II

MATERIALS AND METHODS

MATERIALS

All reagents were of analytical grade. Thioflavin T, phenylmethyl sulfonyl fluoride (PMSF) and sodium chloride were purchased from EMD Chemicals Inc. (Gibbstown, NJ). Hepes free acid buffer was purchased from AMRESCO (Solon, Ohio) and the n-octyl-β-D-glucopyranoside was from Indofine Chemical Company (ICC) (Hillsborough, N.J). Carbenicillin disodium salt, sodium dodecyl sulfate (SDS) running buffer and tryptone medium were obtained from Teknova (Hollister, CA.). G-75 Sephadex medium size and Q-Sepharose Fast Flow anion exchange resins were from GE Healthcare (Pittsburgh, PA). Isopropyl-β-D-thiogalactoside was purchased from IBI Scientific (Peosta, IA). Tris Base and ethylenediaminetetraacetic acid (EDTA) were purchased from T.J Baker (Pillipsburg, NJ). Ammonium sulfate was obtained from Mallinckrodt (St. Louis, MO). Streptomycin sulfate was from Calbiochem (La Jolla, CA). Dithiothreitol (DTT) was purchased from MP Biomedicals, LLC (Solon, OH). Competent *Escherichia coli* BL 21 (DE3) cells were purchased from Aligent Technologies Stratagene (Santa Clara, CA).Yeast extract was purchased from Research Organic (Cleveland, OH). Buffers were prepared and filtered through a 450 nm or 220 nm filter purchased from Pall Life Sciences (Ann Arbor, MI). Molecular porous membrane for dialysis was obtained from Spectrum Laboratories (Rancho Dominguez, CA). Copper grids of formvar carbon support 400 mesh, uranyl acetate and round grid

mats were purchased from Electron Microscopy Sciences (Hatfield, CA). Ultrapure water was used to prepare all the solutions. Gycerol was purchased from Fisher Scientific (Fair Lawn, NJ). Rosetta 2(DE3) cells were purchased from EMD Chemicals (San Diego, CA).

METHODS FOR THE PROTEIN CHEMISTRY AND BIOPHYSICAL ANALYSIS OF THE SYNUCLEINS

Transformation

Transformation is a process of introducing foreign plasmid DNA into a competent bacterial cell. A frozen aliquot (50 µl) of competent *E. coli* cells was thawed on ice for 30 minutes. Then 1-3 µl of recombinant DNA were added to the cells and the reaction mixture was incubated for 30 minutes on ice. The cells were heat shocked in a water bath at 42°C for 30 seconds and then placed on ice for 2 minutes. The cells were heat shocked again for 15 seconds and placed on ice.

An aliquot of 950 µl of SOC nutrient media was added to the bacterial cells and the cells were incubated at 37°C in an incubator shaking at 150 rpm for 1 hour. Bacterial cells were then centrifuged at 300 rpm for 5 minutes. 900 µl of the media were removed and discarded. Transformants were selected by plating the bacterial cells on agar plates containing carbenicillin (100 µg/ml) and incubating the plates at 37°C overnight. Bacterial cells that grew on the agar had the recombinant DNA since the plasmid conferred resistance against the carbenicillin antibiotic. Refer also to IBC rDNA/biosafety protocol #12-006.

Protein Expression

Expression and purification of α- and β-synuclein were performed according to the protocol of Conway and coworkers with a few modifications (Conway et al., 1998). Human wild type recombinant α-synuclein was expressed in *Escherichia coli* BL21(DE3) cells using a pT7-7 human wild-type α-synuclein plasmid. Similarly human wild-type recombinant β-synuclein was also expressed in *Escherichia coli* BL21(DE3) cells using a pRK172 human β-synuclein plasmid.

Following induction with 1 mM isopropyl-β-D-thiogalactoside (triggers transcription and expression of the protein) for 4 hours, bacterial cells were harvested by centrifuging at 7000 rpm for 30 minutes at 4°C. Cells were lysed (20 mM Tris Base, pH 8.5, 1 mM EDTA and 1 mM PMSF) by sonication in a lysis buffer. The lysate was boiled in a water bath at 100°C for 30 minutes and then centrifuged at 9000 rpm at 4°C for 1 hour. Streptomycin sulfate at a 10 mg/ml concentration was used to precipitate the nucleic acids. After centrifugation, ammonium sulfate was added to the supernatant at 361 mg/ml to precipitate α- or β-synuclein.

Protein purification procedure

The α-synuclein pellet was dissolved in 20 mM Tris Base buffer (pH 8.5) and loaded onto a Q-Sepharose Fast Flow anion exchange column equilibrated with the same buffer and eluted in a gradient of 0-0.6 M NaCl. Protein solution from the column was collected in 5 ml fractions. Fractions containing α-synuclein were verified by Coomassie-stained SDS-PAGE, then the protein was dialyzed against ultrapure water and lyophilized. A Q-Sepharose Fast Flow anion exchange column for β-synuclein was equilibrated with 25 mM Tris base buffer containing 1 mM EDTA, 0.1 mM DTT and

0.1 mM PMSF at pH 7.4. The protein was eluted with a gradient of 0-0.5 M NaCl. Fractions containing β-synuclein were verified by Coomassie-stained SDS-PAGE, dialyzed against ultrapure water and lyophilized. Protein concentration was determined by dividing the absorbance of the protein solution at 280 nm by the molar extinction coefficient of the monomeric α- and β-synuclein (0.3541 and 0.3583), respectively.

The second step in the purification process involved gel filtration. Lyophilized α-synuclein protein (14.0 kDa) was dissolved in 20 mM Tris base buffer, pH 8.5 and loaded onto a Sephadex G-75 gel filtration size exclusion column and eluted with 0.3M NaCl in 20 mM Tris Base at pH 8.5. α-Synuclein fractions were pooled together, dialyzed against ultrapure water, lyophilized and stored at -80° C. β-Synuclein was also loaded onto a Sephadex G-75 gel filtration size exclusion column and eluted with 50 mM NaCl in 50 mM Tris base containing 0.1 mM DTT and 0.1 mM PMSF at pH 8.3. Purified protein was dialyzed against ultrapure water, lyophilized and stored at -85°C.

Calibration of G-75 size exclusion column

The G-75 size exclusion column was standardized with protein standards from Sigma-Aldrich: blue dextran, chymotrypsinogen A, ovalbumin, albumin and ribonuclease. They were donated to us by Professor Ellis Bell (Richmond University, Virginia). The blue dextran standard was run on its own by injecting the column 3mls of the protein at 1 mg/ml concentration. The second run was a combination of albumin and chymotrypsinogen. 10 mg of each protein was dissolved in 3 ml of ultra-pure water and the protein solution was injected the column. Similarly a combination of ribonuclease and ovalbumin were dissolved in 3 ml of ultrapure water and injected into the column. The resulting G-75 chromatogram is shown in the appendix (Figure A).

Isolation of multimeric β-synuclein

The same protocol for the expression of monomeric β-synuclein was used. However, the Rosetta 2(DE3) cells instead of the BL21(DE3) cells were used to express the protein. Hepes buffer (100 mM Hepes, 1 mM EDTA, 1 mM PMSF, pH 7.4) was used in place of Tris Base. Hepes buffer offers a more conducive environment to the tetramer than the Tris Base buffer. After sonication, the lysate was not boiled (to preserve multimeric forms) but centrifuged at 4000 rpm at 4°C to separate soluble and insoluble fractions. The supernatant was loaded onto a Q-Sepharose Fast Flow anion exchange column equilibrated with Hepes buffer (100 mM Hepes, 10% glycerol, 0.1% n-octyl-β-D-glucopyranoside, 0.1 mM EDTA, 0.1 mM PMSF). The β-synuclein was eluted at 2 ml/min in a gradient of 0-0.5 M NaCl in Hepes buffer (100 mM Hepes, 10% glycerol, 0.1% n-octyl-β-D-glucopyranoside, 0.1 mM EDTA, 0.1 mM PMSF). The multimeric complex was concentrated by centrifuging at 4000 rpm at 4°C at intervals of one hour until the desired volume of the protein solution was achieved.

The second step in isolating the multimeric complex involved gel-filtration. The concentrated multimeric β-synuclein solution was injected into a Sephadex G75 size exclusion column equilibrated with Hepes buffer (100 mM Hepes, 10% glycerol, 0.1% n-octyl-β-D-glucopyranoside, pH 7.4). The multimeric β-synuclein protein was eluted with 0.15 M NaCl in Hepes buffer at 1ml/min and stored in 1 ml aliquot solutions at -80°C.

Synuclein fibril formation

A modified method of Hoyer and coworkers was developed for α-and β-synuclein fibrillation (Hoyer et al., 2002). Using sealed sterile eppendorf tubes, proteins

were dissolved in 20 mM Tris base buffer containing 0.2 M NaCl. pH 7.5 and incubated at 37° C with agitation at 190 rpm in a New Brunswick Scientific Incubator Shaker Model 25 for up to 14 days.

Monitoring fibril formation

Fibril formation was monitored by thioflavin T (ThT) fluorescence using a black and flat bottom 96 well microtiter plate and microplate reader Synergy HT (BioTek Inc., VT). 15 µl of fibril solution were added to 3 ml of 50 µM thioflavin T solution (Nilsson, 2004). The excitation and emission wavelengths were 440 nm and 485 nm, respectively. All samples were run in triplicates.

Secondary structures of β-synuclein fibrils determined by circular dichroism

In order to determine the secondary structures of β-synuclein fibrils, fibril solutions were diluted to a final concentration of 0.2 mg/ml for far-UV CD. The concentration was determined by absorption at 280 nm on a Varian Cary UV spectrophotometer (Varian Inc., NC). Using a MOS 450 (Bio-logic, France), the monomeric and fibril samples were analyzed in the 200-250 nm far-UV range in a 1 mm path length quartz CD cuvette. Slit widths were set to 1 mm. Spectra were repeated 30 times. The machine signal was converted to molar ellipticity which takes into account the concentration of the protein being measured. The average was graphed and analyzed using Sigma Plot (version 10).

Secondary structure of the multimeric β-synuclein

CD was used to determine the secondary structures of the multimeric β-synuclein protein. The protein was measured at 0.2 mg/ml in the far-UV CD range (200-250 nm) on a MOS 450 (Bio-logic, France) using a 1 mm path length quartz CD cuvette. Slit

widths were set to 1 mm. The machine signal was converted to molar ellipticity which takes into account the concentration of the protein being measured. The average was graphed and analyzed using SigmaPlot (version 10).

Atomic force microscopy imaging of fibrils

In our experimental studies, AFM was used to examine α- and β-synuclein fibrils. The fibril samples were diluted to 2 mg/ml for imaging on a Veeco DI Nanoscope 3D Atomic Force Microscope using the tapping force mode (Veeco Inst., NY). From each sample, 2 μl of the dilute fibrils were placed onto a mica grid and spread evenly. The sample was allowed to air dry and then washed 4-5 times with 20 μl of ultrapure water and allowed to stand for 1-2 minutes before removing the excess solution. The dried sample was then examined for fibrils. These studies were conducted with the assistance of Mr. Jason Collins (Old Dominion University, Greene Group).

Transmission electron microscopy imaging of fibrils

To prepare samples for TEM, a 5μl aliquot of α-synuclein fibril solution was adsorbed onto a film of 400 mesh formvar carbon coated copper grid. After 60 seconds of adsorption, excess fibril solution was blotted and the grid was washed several times with ultrapure water. The grid was air dried. Then the fibrils were stained with 10 μls of 2% uranyl acetate for 25 seconds before final blotting. The grid was washed by dipping it several times in ultrapure water and then drying it in air. The grids were examined for fibrils under a JEOL TEM at the Applied Research Center (Newport News, VA).

Destruction of α-synuclein fibrils by low temperature plasma jet

Plasma is a neutral medium composed of positively and negatively charged gas molecules. The 'plasma pencil' generated the room temperature (or cold) plasma which

was employed to break α-synuclein fibrils into smaller fragments. A sample of the α-synuclein fibril solution (6 mg/ml) was placed in a small tube (0.2 ml) and exposed to the plasma for varying lengths of time up to 10 minutes under the following conditions: high voltage pulse 7.5 kV; frequency 5 kHz; pulse width 1 μs; operating gas helium flow rate 5 L/min. The distance between the nozzle of the pen and the samples was 2 cm. These plasma studies were conducted with Dr. Erdinc Karakas (Old Dominion University, Laroussi Group). After exposure, the fibrils were fixed onto 400 mesh formvar coated copper grids for analysis by TEM.

Chemical and biosafety

Wet lab experiments were conducted under Biosafety level 2 conditions. The Greene lab is a designated BSL-2 laboratory. The Basic Biosafety and NIH Recombinant DNA CITI training was successfully completed and is on file with the Office of Research. Biohazard waste was disposed of in accordance with the Old Dominion University 'Regulated Medical Waste Management Guidelines', through the Biological Sciences Support Facility and the Office of Environmental Health and Safety. Hazardous chemical waste was disposed of through the Office of Environmental Health and Safety. Standard Biosafety Operating Procedures and Material Safety Data Sheets are maintained for reference in the Greene laboratory. Safety education included training in proper experimental procedures, good laboratory practice, hygiene, the proper wear of personal protective equipment (ie. lab coats, goggles, disposable gloves), hazards, decontamination, disposal and emergency procedures. Refer also to IBC recombinant DNA/biosafety protocol #12-006.

METHODS FOR THE COMPUTATIONAL ANALYSIS OF THE SYNUCLEINS

In order to trace the origins of the synuclein proteins as well as assist in better understanding their structure and function we used bioinformatics approaches. This included searching for related proteins, aligning sequences, searching for related protein structures and functional sites. A flow chart indicates how the synuclein ancestral relatives were retrieved from databases (Figure 20). The program FASTA (Lipman and Pearson, 1985) retrieved protein sequences in an appropriate format from the NCBI (National Center for Biotechnology Information) protein database. The position-specific iterative basic local alignment search tool (PSI-BLAST) (Altschul et al., 1997) at the NCBI used α-, β- or γ-synuclein sequences as probes to search the database for proteins with similar sequences. The identified related proteins were each aligned with several α-, β- and γ-synucleins from various species. The program, Multiple Sequence Comparison by Log-Expectation (MUSCLE) (Edgar, 2004), was used to create the multiple sequence alignment of proteins in order to determine positions of identity. Identity or similarity between sequences was considered significant when the statistical e-value was less than 5×10^{-3}. The structures of the synucleins, endoglucanase, CRE-DUR-1, Tasmanian Devil protein and cytochrome c were constructed using the program, SWISS-MODEL (Biasini et al., 2014). The structure modelling was conducted with the assistance of Ms. Nardos Sori (Old Dominion University, Greene Group).

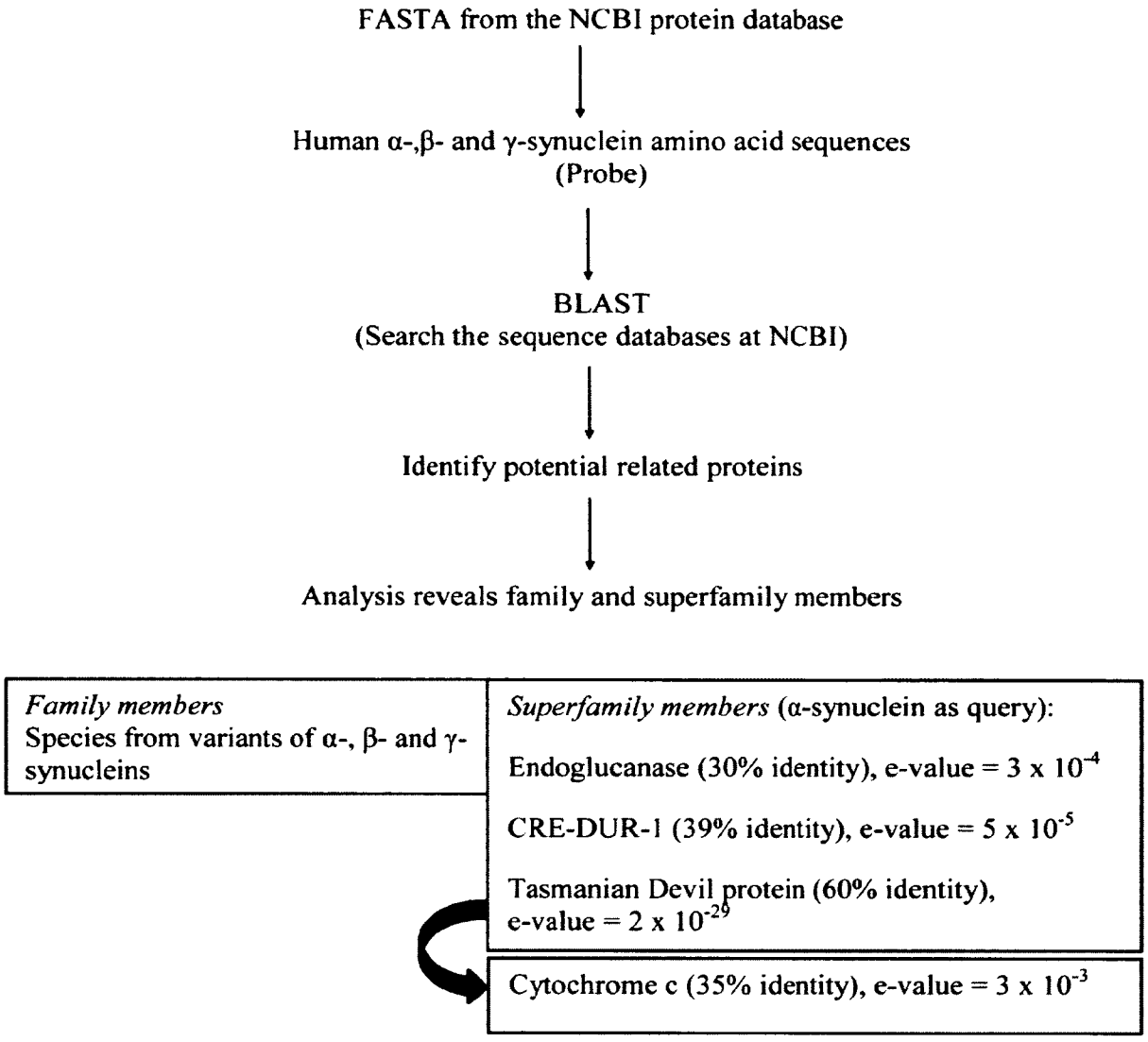

Figure 20. The flow chart showing the construction of the synuclein superfamily

FASTA retrieved protein sequences from NCBI protein database. PSI-BLAST was run against the protein database to identify sequences similar to synuclein proteins.

To further confirm the evolutionary relationship between the synucleins and the retrieved proteins other algorithms, the scan prosite and the scan motif, were employed. ProSite is a database for domains, functional sites and amino acid patterns (Falquet et al., 2002). The scan prosite algorithm searches for functional sites or amino acid patterns that match those of the query sequence. The human synucleins and their related proteins were used as query sequences in order to identify functional sites at conserved locations (Appendix B).

The phylogenetic tree of the synucleins and the disparate proteins

The Phylogeny.fr computer program was used to construct a phylogenetic tree from the human synucleins and disparate protein sequences. The Phylogenetic.fr (program reconstructs and analyzes the evolutionary relationship between protein sequences (Dereeper et al., 2008).

Websites for the bioinformatics computer programs

PSI-BLST	http://www.ebi.ac.uk/Tools/sss/psiblast/
MUSCLE	http://www.ebi.ac.uk/Tools/msa/muscle/
Scan prosite	http://prosite.expasy.org/scanprosite/
Motif scan	http://myhits.isb-sib.ch/cgi-bin/motif_scan
Phylogeny.fr	http://www.phylogeny.fr/
Swiss-Model	http://swissmodel.expasy.org
K2D3	http://k2d3.ogic.ca/

CHAPTER III

DESTRUCTION OF α-SYNUCLEIN BASED AMYLOID FIBRILS BY LOW TEMPERATURE PLASMA JET

INTRODUCTION

Plasma is considered the fourth state of matter (Heinlin et al., 2010), consisting of neutral molecules, excited atoms, electrons, and positive and negative ions (Niemira, 2012). In low temperature (or cold) plasma, the temperature of the electrons is higher than that of the ions and neutral molecules. Such plasmas are classified as non-equilibrium because of the difference between the energies of the electrons and of the heavier particles (Heinlin et al., 2010). Heat, electricity or laser radiation are the sources of energy that ionizes gas molecules into plasma (Niemira, 2012).

The biomedical application of low temperature or cold plasma is emerging as a field of great interest to physicists, engineers, chemists, and medical researchers. Various groups have shown that non-equilibrium plasmas can inactivate bacteria, help the proliferation of human fibroblasts and coagulate blood (Laroussi, 2009; Brun et al., 2012). Low temperature plasma technology is also finding application in the food industry. Microbial organisms on fruits, vegetables and meats can be inactivated by reactive species in the plasma (O_2^+, O_2^-, O_3, O,O^+,O^-, N_2, N_2^-, ionized ozone and free electrons) making the food products safe for consumption (Niemira, 2012). The investigators did not observe any adverse effects of the plasma on the quality of the food products. Cold plasma has been successful in sterilizing packaging materials (Misra et

al., 2014; Pankaj et al., 2014). Also, *E. coli* suspensions in liquid media in a sealed package have been completely inactivated by cold plasma (Ziuzina et al., 2013). In the future, food products can be disinfected after they are packaged.

The treatment of chronic wounds by cold atmospheric argon plasma decreases the bacterial load of the wounds and promotes healing (Isbary et al., 2010). It appears bacterial cells resistant to antibiotics succumb to cold plasma. Both *in vitro* and *in vivo*, cold plasma activates the human dermal fibroblast genes. The products of these genes are essential for wound healing and repair (Arndt et al., 2013). In addition, cold plasma was shown to eradicate cancer cells both *in vitro* and *in vivo* (Keidar et al., 2013). Laroussi and coworkers, also demonstrated that *in vitro*, low temperature plasma can kill leukemia cells in a dose-dependent manner (Barekzi and Laroussi, 2012). These important findings indicate that plasma has a potential role in sterilization, decontamination, wound healing and cancer therapy.

The plasma jet/plume used in our study was generated by a device (the plasma pencil) capable of emitting a long cold plasma plume in ambient air (Laroussi and Lu, 2005) (Figure 21). The plasma pencil is driven by short (nanoseconds to microseconds in width) high voltage pulses and uses helium as a carrier gas. Other gas mixtures can also be used (such as helium/oxygen mixtures, argon/oxygen mixtures, air). The plasma plume which appears as a continuous plasma jet is in fact a train of small packets of plasma (generally known as "plasma bullets") traveling at supersonic velocities (Shi et al., 2008; Mericam-Bourdet et al., 2009) (Figure 22). These plasma bullets are vehicles whereby chemically reactive species can be delivered to biological matter such as proteins or cells.

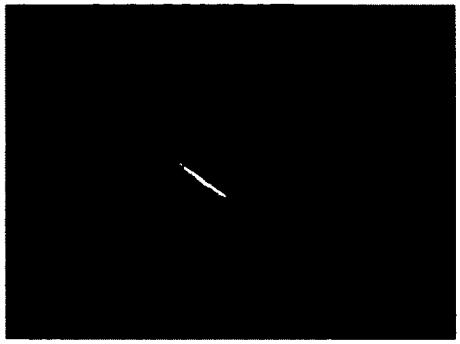

Figure 21. Photograph of the plasma pencil

The pen is indicated in red and the purple color is the plasma issuing from the pen. Figure reproduced from Karakas (Karakas et al., 2010).

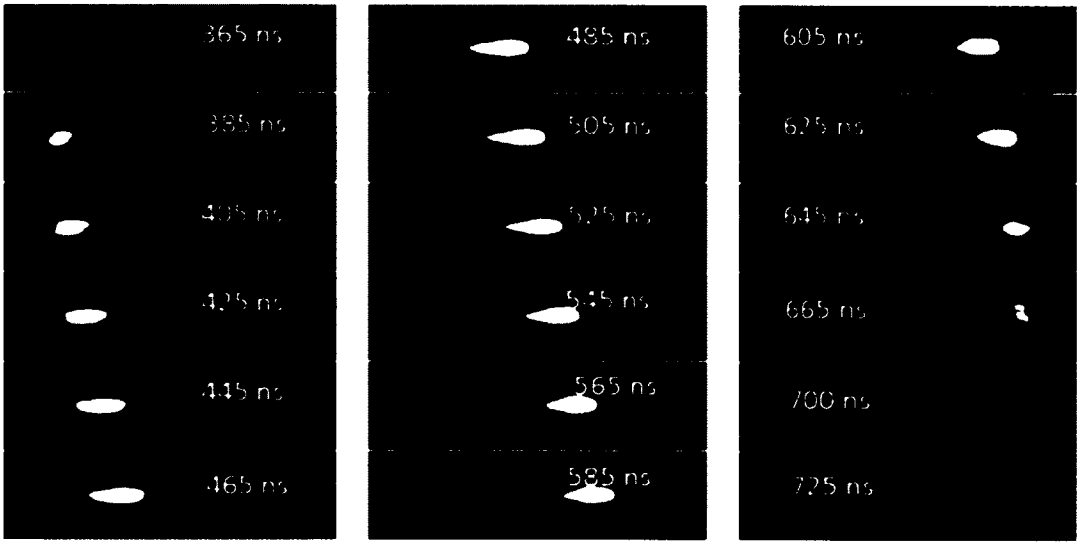

Figure 22. Image of plasma packets or bullets

High-speed camera images show that the plasma plume, in fact, consists of a series of packet structures called plasma bullets. These bullets propagate in the surrounding air with supersonic velocities in order of 10^4-10^5 m/s without any external electric field. The exposure time of the camera is 20 nanoseconds. Figure reproduced from Karakas (Karakas et al., 2010).

The aim of this study was to explore potential methods in which the use of cold plasma could destroy α-synuclein fibrils *in vitro*. Potentially, this method could also be applied to the destruction of fibrils in the joint spaces that are formed by β2-microglobulin in patients undergoing prolonged renal dialysis and amylin fibrils that can form in the pancreas of patients with diabetes for example. Additionally, prion proteins could be destroyed, which would have value in decontamination processes in the meat industry.

The human protein α-synuclein was selected as the initial model system. In this experiment, the plasma pencil generated the plasma bullets that were applied directly to the prepared α-synuclein fibril samples. The operating conditions of the plasma were the following: voltage pulse magnitude = 7.5 kV; pulse width = 500 ns; frequency = 5 kHz, helium flow rate = 5 L/min. In Figure 23, the intensity of the chemical species is on the Y-axis and the distance between the plasma pen and sample is on the X-axis. This information enables the researcher to determine the distance between the plasma pencil and the biological samples downstream of the plasma jet.

The synuclein fibrils in solution were placed into small tubes (0.2 ml), after an initial trial on glass slides was not effective, and exposed to the plasma pencil for varying lengths of time (up to 10 minutes). The distance between the nozzle of the device and the samples was 2 cm. After exposure the fibrils were immediately fixed onto 400 mesh formvar coated copper grids for analysis by electron transmission microscopy.

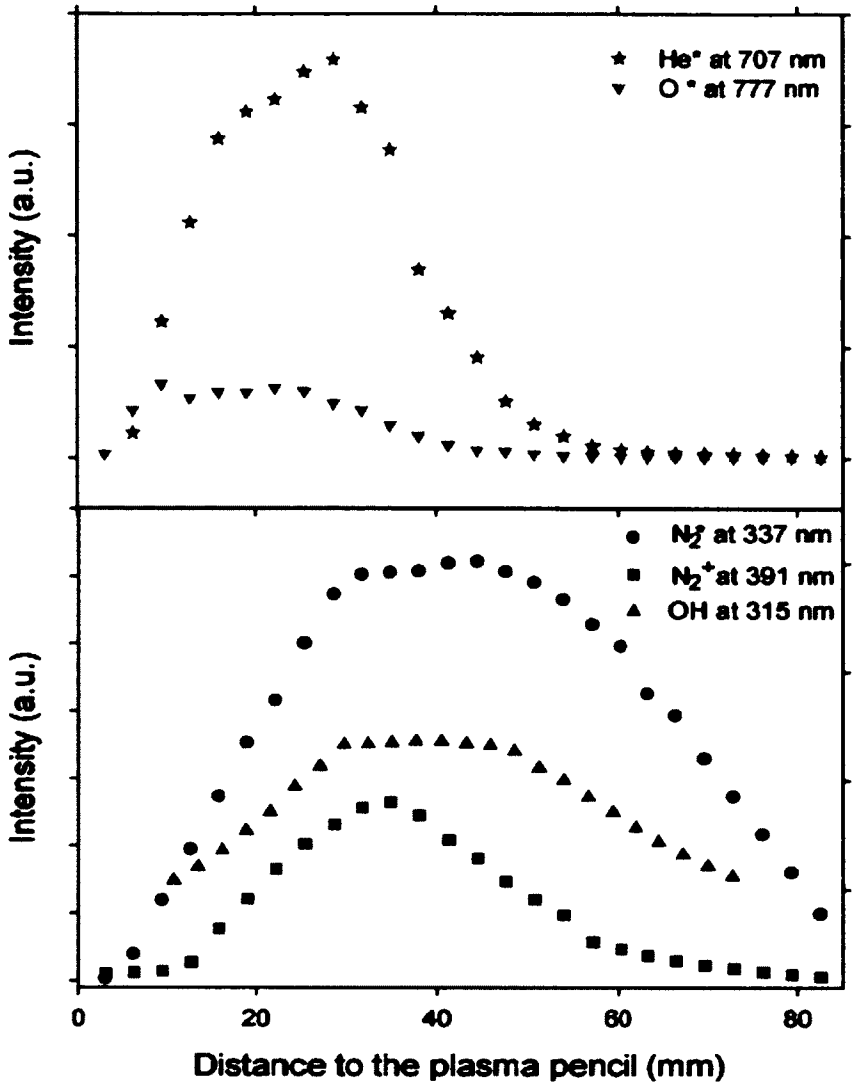

Figure 23. Intensities of He^*, N_2^*, N_2^+, OH and O^* as a function of distance from nozzle

The intensities of the excited He^*, N_2^*, N_2^+, OH and O^* species emitted by the plasma pencil vary with distance from the plasma pencil. Experimental conditions were as follows: voltage pulse magnitude, 7.5 kV; pulse repetition frequency, 5 kHz; helium gas flow rate, 5 L/min; pulse width, 500 ns; fibril solution placement, 20 mm from pencil. Figure reproduced from Karakas (Karakas et al., 2010).

RESULTS

Aliquots were taken from the original tubes used to form the fibrils as described in the methods chapter. The fibril solutions were exposed to plasma for varying lengths of time (2, 4, 6 and 10 minutes). Each tube was exposed to one time frame. 10 μl samples from each tube, was placed onto 400 mesh formvar carbon coated grids and stained with 2% uranyl acetate to fix the fibrils. The grids were then analyzed by TEM at the Applied Research Center (Newport News, VA).

The experimental results show that the plasma bullets emitted by the plasma pencil and delivered to a solution of α-synuclein fibrils can break these fibrils into smaller units. Protein fibrils are otherwise very stable and difficult to destroy. The results (Figure 24 A and B) clearly show that a six minute exposure to the plasma caused major damage to the fibrils, resulting in extensive breakage. Evidence of breakage started showing up after only two minutes exposure to the plasma.

DISCUSSION

Although preliminary, these are extremely important results as this methodology provides a facile mechanism whereby protein fibrils can be easily destroyed. This work is also very timely as quite recently, three other methods have also been shown to break fibrils. These are laser beam irradiation, ultrasonication (Chatani et al., 2009; Ozawa et al., 2009; Yagi et al., 2010) and mechanical breakage by stirring at 1000 rpm (Xue et al., 2009). However, unlike these methods which rely on physical mechanisms, the cold plasma method is based on the chemical species of the plasma. Non-equilibrium plasmas such as the one generated by the plasma pencil are sources of ROS and reactive nitrogen species, which are known to chemically denature cellular lipids and proteins. We

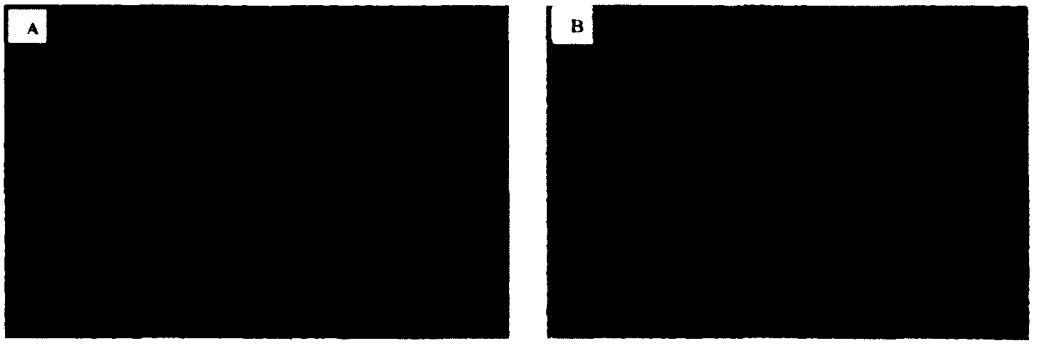

Figure 24. Cold plasma breaks α-synuclein fibrils

(A) TEM image of mature intact α-synuclein fibrils.

(B) TEM image of the fibrils after six minutes exposure to the plasma plume, showing clear evidence of extensive breakage. Experimental conditions were as follows: voltage pulse amplitude, 7.5 kV; pulse repetition frequency, 5 kHz; helium gas flow rate, 5 L/min; pulse width, 500 ns. Figure reproduced from (Karakas et al., 2010).

expect that under plasma exposure the fibrils undergo chemical reactions that compromise their structural as well as chemical integrity.

Microglial cells, which are the macrophages of the central nervous system, are known to engulf and destroy Aβ fibrils (Gaikwad et al., 2009). Thus, these cells may take up and destroy the broken α-synuclein fibrils generated by the plasma. While this hypothesis was a driving force behind the cold plasma experiments, the microglial experiment has yet to be undertaken.

The fact that protein fibrils are associated with debilitating medical conditions such as Parkinson's and possibly Alzheimer's disease makes these results of even greater relevance. However, what remains to be tested is the cytotoxicity of plasma with

regard to neurons/neuronal cells. Although studies on other types of eukaryotic cells have shown that low power doses of cold plasma do not cause the cells irreversible damage. (Kong et al.. 2009; Laroussi. 2009) to date there are no known tests on neuronal type cells.

CHAPTER IV

INHIBITION OF β-SYNUCLEIN FIBRIL FORMATION IN VITRO BY α-SYNUCLEIN

INTRODUCTION

α- and β-synuclein colocalize in the presynaptic axon terminals of the central nervous system including the dopamine producing neurons of the substantia nigra. A number of previous studies, both *in vitro* and *in vivo*, have indicated that soluble, monomeric β-synuclein can inhibit the fibrillation or aggregation of α-synuclein (Shaltiel-Karyo et al., 2010; Vigneswara et al., 2013). This discovery led to the suggestion that β-synuclein plays a protective chaperone role *in vivo*. Inhibition studies by Uversky and coworkers, for example, demonstrated that a 1:1 (α:β) molar ratio significantly reduced the rate of α-synuclein fibrillation and increased the lag period before fibrils were observed *in vitro* (Uversky et al., 2002). The 1:2 molar ratio further increased inhibition and the 1:4 molar ratio resulted in almost complete inhibition even after an incubation period of several weeks (Uversky et al., 2002). Interestingly, one study indicated that in patients with Parkinson's disease, the expression of β-synuclein was down regulated and α-synuclein up-regulated (Beyer et al., 2011). Based on these findings, β-synuclein's physiological role may be the prevention of α-synuclein fibrillation and suggests that it may have therapeutic value (Park and Lansbury, 2003; Hashimoto et al., 2004).

While α-synuclein rapidly and easily forms fibrils *in vitro*, it appears as if

formation of β-synuclein fibrils *in vitro* is neither facile nor rapid (Serpell et al., 2000; Uversky et al., 2002; Park and Lansbury, 2003). However, Yamin and coworkers demonstrated that the inclusion of certain additives such as divalent metal, Cu^{2+}, Zn^{2+} and Pb^{2+} as well as select pesticides could induce the protein to rapidly form fibrils (Yamin et al., 2005). The aim for conducting inhibition studies in the present dissertation research was to elucidate the mechanism for β-synuclein inhibition of α-synuclein fibrils.

Although α- and β-synuclein fibrils have been produced in various laboratories, conditions for fibril formation seem to differ from one lab to another. Therefore conditions for α- and β-synuclein fibril formation had to be established for our lab. Fibrils formed when the synuclein proteins were each dissolved in 20 mM Tris Base containing 0.2 M NaCl, pH 7.5, and incubated at 37°C in a shaking incubator at 190 rpm for 14 days (see methods for more details). In order to study the inhibitory effect of synuclein fibrillation, two studies were conducted. In the first experiment, 3.5 mg of α-synuclein and 7 mg of β-synuclein were combined to give an approximate 1:2 ratio and incubated under the physiological conditions mentioned above to form fibrils. In the second study, a 1:4 ratio was used (α:β, 4 mg:16 mg). Fibril formation was monitored by thioflavin T fluorescence under physiological conditions in triplicates.

Circular dichroism and atomic force microscopy studies were conducted to confirm the presence and character of β-synuclein fibrils. In order to assess the secondary structure content of the β-synuclein fibrils, the fibril solution was diluted to 0.2 mg/ml for far-UV CD and then analyzed in the 200-250 nm far-UV range. Samples for atomic force microscopy imaging were diluted to 2 mg/ml. Then a 2 μl aliquot of the

dilute fibrils was air dried onto a grid and then the sample was examined for fibrils using the tapping mode atomic force microscope.

RESULTS

Several *in vitro* trials were conducted until conditions that were conducive to produce α- and β-synuclein fibrils were successfully determined. The formation of fibrils was monitored by fluorescence spectroscopy and thioflavin T dye over time (Figures 25-26). In the analysis of the fibril formation of α-synuclein (Figure 25), there was a lag period between day 0 and day 1 which is the period when the fibril nuclei may form. A sharp rise in fluorescence occurred after day 1 indicating growth of protein fibrils. After five days of incubation, the thioflavin T fluorescence reached its maximum peak when soluble, monomeric α-synuclein was possibly all used. The slight dip in fluorescence at day 8 is due to inadequate amount of fibrils drawn into the pipet when sampling the fibril solution, possibly due to matting. Thus the fewer fibrils there were to interact with the dye and the lower the fluorescence intensity.

In the analysis of the fibril formation of β-synuclein (Figure 26), the lag period for the β-synuclein was about three days. Thioflavin T fluorescence levels off at about day seven when possibly all soluble, monomeric β-synuclein protein solution is used to form fibrils. The sharp drop in fluorescence at day eleven is a problem of sampling the fibrils. As the fibrils grow, they tend to form a mat which makes it difficult to draw them into the micropipet tip. Fewer fibrils interacting with the thioflavin T dye can result in lower fluorescence intensity.

In both of the inhibition experiments of the 1:2 and 1:4 ratios, it appears that β-synuclein fibrillation is inhibited by α-synuclein (Figures. 27-28). This conclusion is

based on the mixture of α- and β-synuclein showing reduced rate of fibril formation in comparison to β-synuclein alone. In the 1:4 ratio inhibition experiment the α-synuclein control does not appear to be forming fibrils. The insert in figure 28 shows that the 4 mg α-synuclein control may be forming a small amount of fibrils. The fluorescence intensity for the α-synuclein fibrils appears lower than that of the β-synuclein.

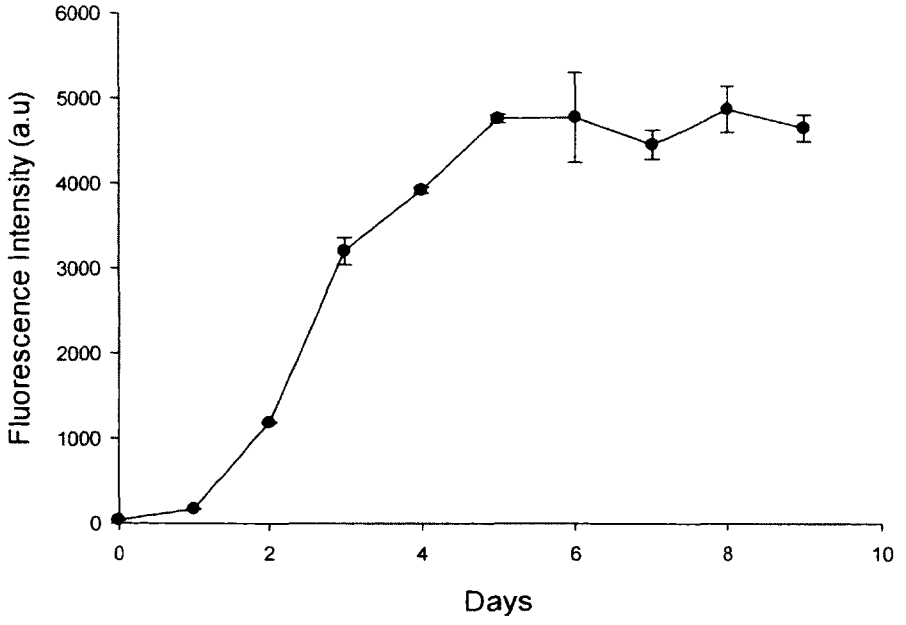

Figure 25. α-Synuclein time course of fibril formation

6 mg/ml of α-synuclein in Tris Base buffer, pH 7.5, was incubated at 37°C with agitation at 190 rpm in sealed sterile eppendorf tubes. α-Synuclein fibrillation was monitored by thioflavin T fluorescence. 15 µl of synuclein fibril solution was added to 3 mls of 50 mM Thioflavin T solution. The excitation and emission wavelengths were 440 nm and 485 nm, respectively. A graph was constructed using the scientific graphing program, SigmaPlot (version 11). Error bars were derived from calculated standard deviations among replicates (n=3).

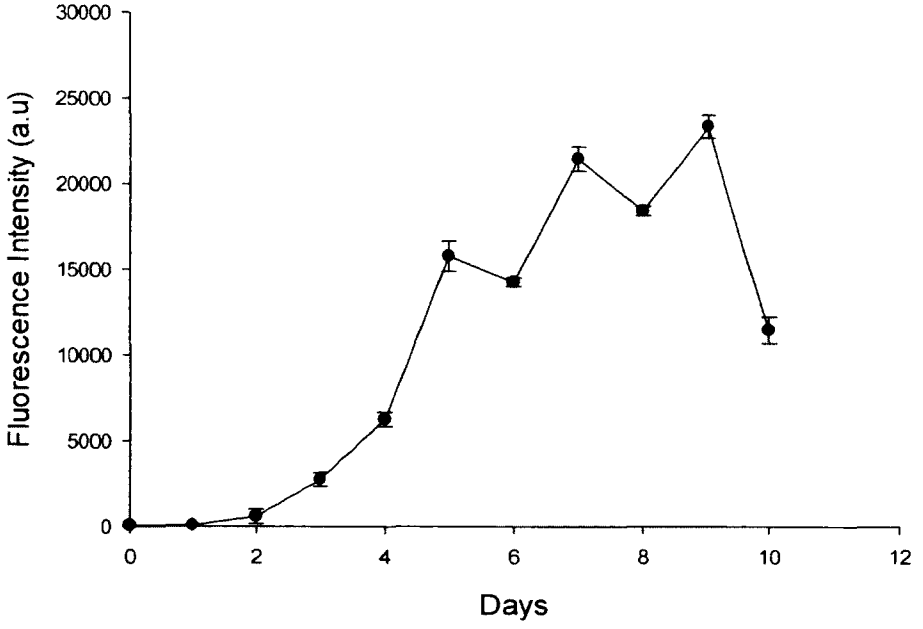

Figure 26. β-Synuclein time course of fibril formation

7 mg/ml of β-synuclein in Tris Base buffer, pH 7.5, was incubated at 37°C with agitation at 190 rpm in sealed sterile eppendorf tubes. β-Synuclein fibrillation was monitored by thioflavin T fluorescence. 15 µls of synuclein fibril solution was added to 3 mls of 50 mM Thioflavin T solution. The excitation and emission wavelengths were 440 nm and 485 nm, respectively. The graph was constructed using the scientific graphing program, Sigma Plot (version 11). Error bars were derived from the standard deviations among replicates (n=3).

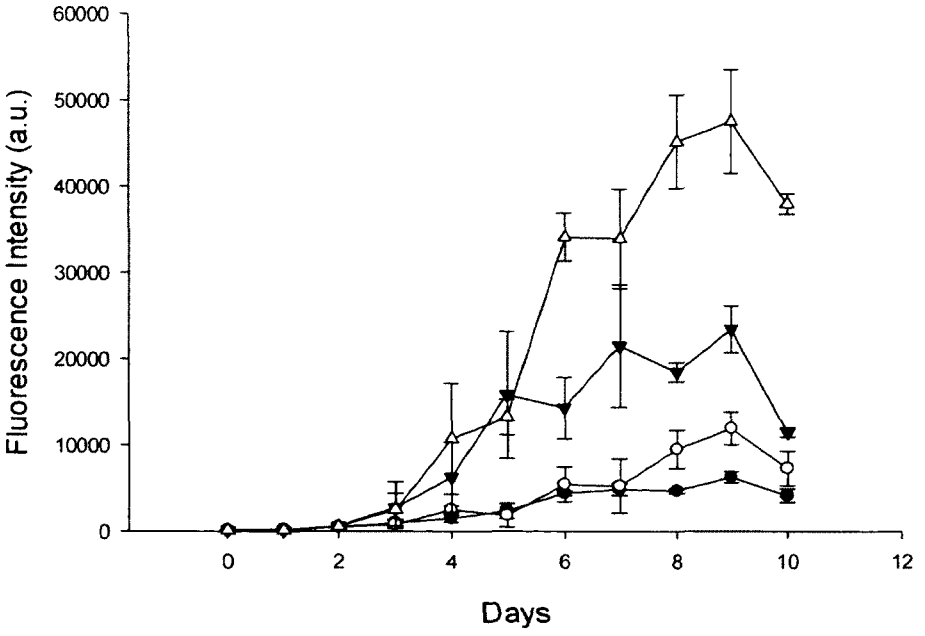

Figure 27. Inhibition studies of an approximate 1:2 ratio

Open triangle = β-synuclein control (16 mg/ml); filled/inverted triangle = β-synuclein control (7 mg/ml); open circle = (α:β; 3.5 mg:7 mg); filled circle = α-synuclein control (3.5 mg/ml). α- and β-Synuclein were incubated in Tris Base buffer, pH 7.5 at 37°C with agitation at 190 rpm in sealed sterile eppendorf tubes. Fibril formation was monitored by thioflavin T fluorescence by adding 15 μls of synuclein fibril solution to 3 mls of 50 μM Thioflavin T solution. The excitation and emission wavelengths were 440 nm and 485 nm, respectively. The graph was constructed using the scientific graphing program, Sigma Plot (version 11). Error bars were derived from the standard deviations among replicates (n=3). β-Synuclein fibril growth in the mixture appears to be inhibited by the presence of α-synuclein.

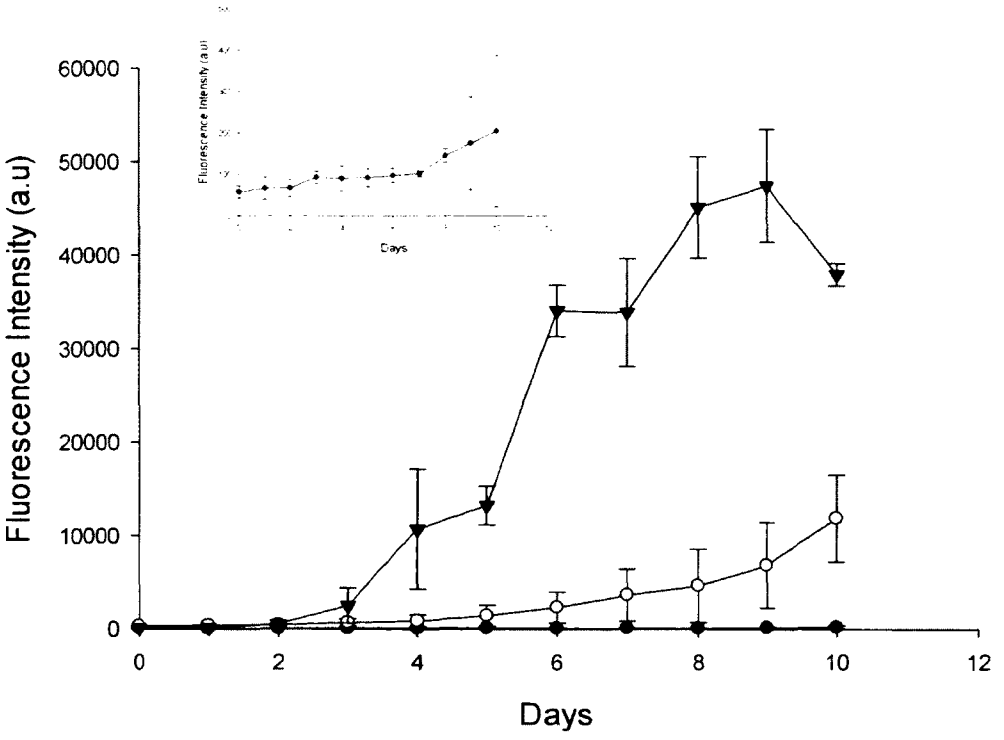

Figure 28. Inhibition studies of an approximate 1:4 ratio

Filled/inverted triangles = β-synuclein control (16 mg/ml); open circles = (α:β; 4 mg:16 mg); filled circles = α-synuclein control (4 mg/ml). α- and β-Synuclein were solubilized in Tris Base buffer, pH 7.5, and incubated at 37°C with agitation at 190 rpm. Fibril formation was monitored by thioflavin T fluorescence after adding 15 µls of synuclein fibril solution to 3 mls of 50 µM Thioflavin T solution. The excitation and emission wavelengths were 440 nm and 485 nm, respectively. Error bars are derived from calculated standard deviations among replicates (n=3). The insert is an expanded view of the fibrillation of the α-synuclein control 4 mg/ml. The β-synuclein fibrillation appears to be inhibited by α-synuclein.

Results of the far-UV circular dichroism analysis indicated that monomeric β-synuclein is intrinsically unstructured in solution. The negative molar ellipticity at around 200 nm wavelength is characteristic of a random coil conformation (Figure 29) (Whitmore and Wallace. 2008). After incubating the protein at 37°C. with agitation. the β-synuclein fibrils appears to have a β-sheet secondary structure content as seemingly evidenced by the beta-ellipticity with a single minimum at approximately 216 nm (Kelly et al.. 2005).

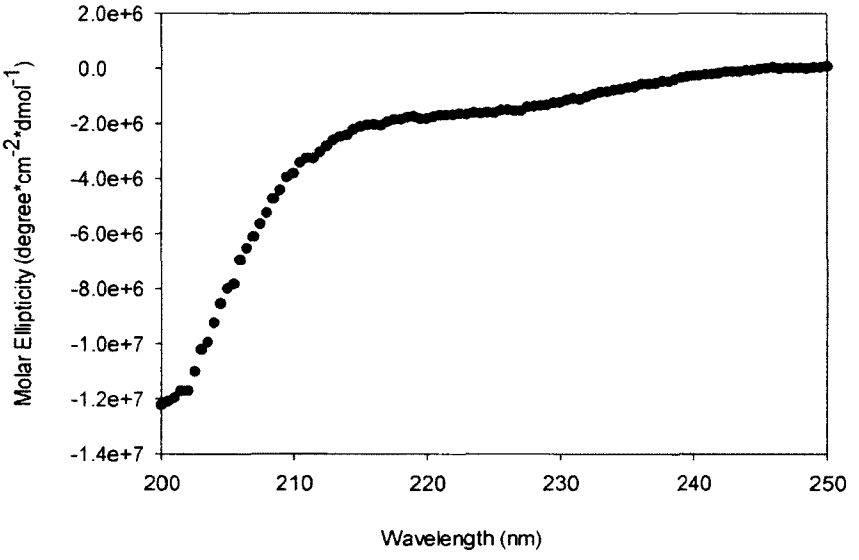

Figure 29. Far-UV circular dichroism analysis of monomeric β-synuclein

Monomeric β-synuclein at concentration 0.2 mg/ml in Tris base buffer, pH 7.5 was scanned been 200 nm and 250 nm. The machine signal was converted to molar ellipticity which takes into account the concentration of the protein being measured. Spectra were repeated 30 times and the average was graphed and analyzed using Sigma Plot (version 10). The plot shows a typical random coil signature.

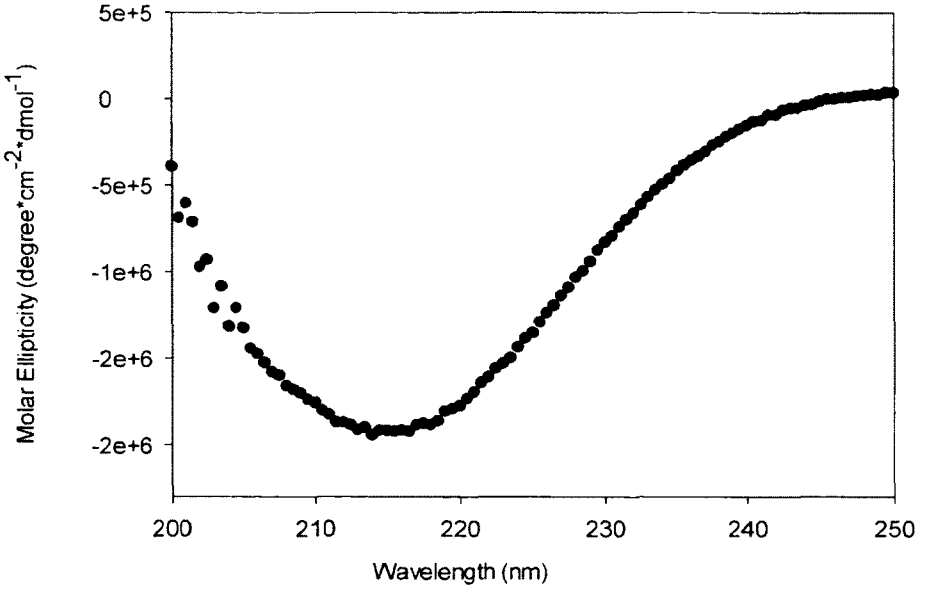

Figure 30. Far-UV circular dichroism analysis of β-synuclein fibrils

β-synuclein fibril solution at concentration 0.2 mg/ml in Tris Base buffer, pH 7.5 was scanned between 200 nm and 250 nm. The machine signal was converted to molar ellipticity which takes into account the concentration of the protein being measured. The spectra were repeated 30 times and the average was graphed and analyzed using Sigma Plot (version 10). The presence of β-sheet structure is indicated by the signature beta-ellipticity with a single minimum at approximately 216 nm in comparison to the random coil signature.

AFM studies were conducted to visually confirm the presence of fibular structures. Subjectively, the AFM images of α-synuclein fibrils (Figure 31 A and B) are shorter and more dispersed in comparison to what is seen in the literature. which tend to be elongated filaments (Conway et al., 2000; Sweers et al., 2012). This result may be

due to the nature of using AFM versus TEM and the variability in making fibrils in general. In addition, the scales vary between studies (Bisaglia et al., 2009). Conversely, β-synuclein has many long entangled fibrils (Figure 32 A and B) which is similar to reports of α-synuclein fibrils (Conway et al., 2000; Lemkau et al., 2013). β-Synuclein forms long entangled fibrils in the presence of sodium dodecyl sulfate (Rivers et al., 2008). Size analysis indicates a possible "matting effect" or oligomerization of single fibril strands of β-synuclein. The original concentrations of the proteins that made the 1:2 molar ratio (α:β) were 3.5 mg for α-synuclein and 7 mg for β-synuclein. The α/ β synuclein amyloid fibril solution at 2 mg/ml concentration was used for microscopic imaging. Subjectively, the mixed fibrils (1:2 ratio) appear to have a thicker morphology more similar to the β-synuclein fibrils (Figure 33 A and B).

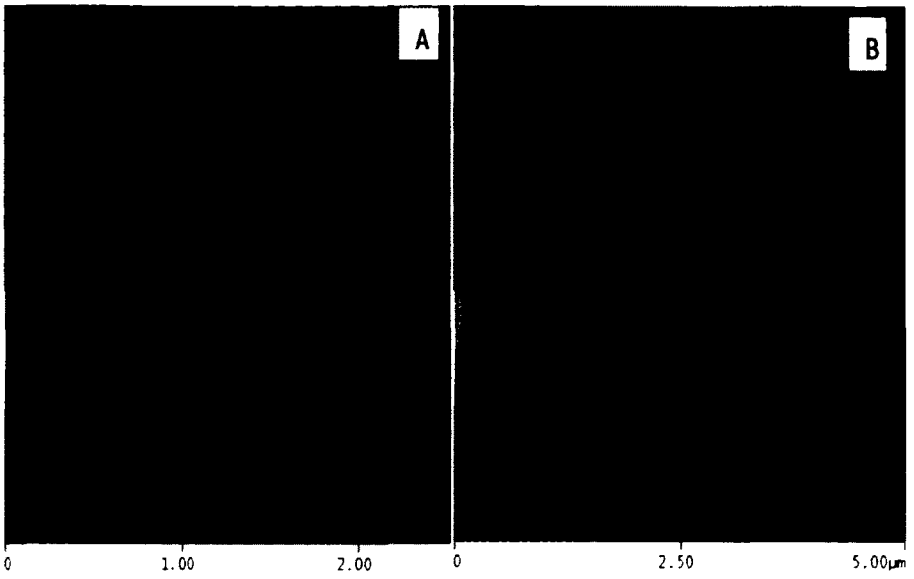

Figure 31. Tapping mode atomic force microscopy of α-synuclein fibrils

(A) 2D image of α-synuclein fibrils is shown at high magnification. 2 µl of a 2 mg/ml solution was imaged.

(B) 2D image of α-synuclein fibrils is shown at low magnification. 2 µl of a 2 mg/ml solution was imaged.

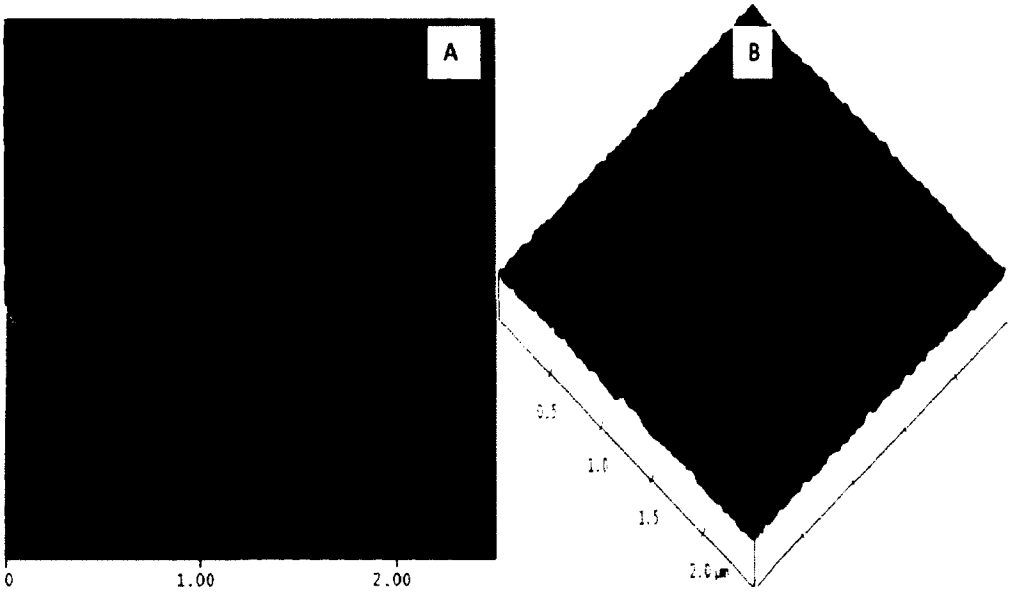

Figure 32. Tapping mode atomic force microscopy of β-synuclein fibrils

(A) 2D image of β-synuclein fibrils is shown at high magnification. 2 μl of a 2 mg/ml solution was imaged.

(B) 3D image of β-synuclein fibrils is shown at high magnification. 2 μl of a 2 mg/ml solution was imaged.

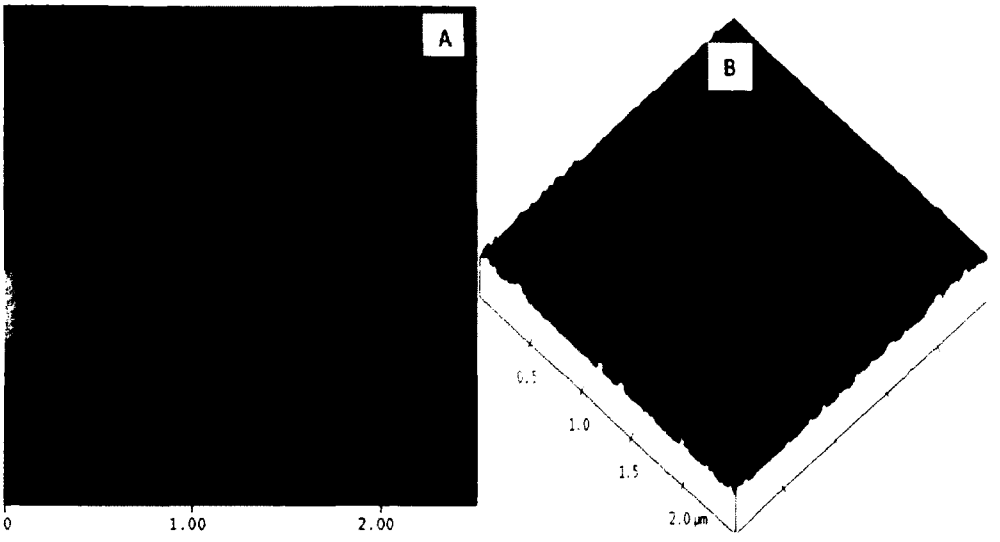

Figure 33. Tapping mode atomic force microscopy of α/β-synuclein fibrils

(A) 2-D image of the α/β-synuclein fibrils is shown at high magnification. 2 µl of a 2 mg/ml solution was imaged.

(B) 3D image of α/β-synuclein fibrils is shown at high magnification. 2 µl of a 2 mg/ml solution was imaged.

DISCUSSION

Interestingly, under the experimental conditions of our study, we observe that β-synuclein can form fibrils rapidly under the same conditions as α-synuclein. β-synuclein fibrils have higher fluorescence intensity when they bind thioflavin T dye compared with those of α-synuclein. In the literature, β-synuclein forms fibrils rapidly in the presence of sodium dodecyl sulfate (mimics lipid micelles) and metal ions (Yamin et al., 2005; Rivers et al., 2008). To the best of our knowledge this is the first study of a co-incubation of two fibril forming proteins under fibrillation promoting conditions, which may be the reason this observation has not been previously reported. Further, we

observe that α-synuclein can inhibit the formation of β-synuclein fibrils when incubated together. In the two trials, the β-synuclein fibrils formed at a similar rate irrespective of concentration. One or a combination of the different forms of α-synuclein including the monomer, protofibril or mature fibrils inhibited β-synuclein fibrillation. Considering the putative chaperone activity of the synucleins, it is possible that the monomeric α-synuclein decelerated the aggregation of the β-synuclein by binding it to form a soluble high molecular weight (MW) complex. Rekas and coworkers have reported that the full length α-synuclein and the α-synuclein (61-140 residues) fragment can prevent a heat stressed catalase enzyme from aggregating *in vitro* (Rekas et al., 2012). They also observed that the fibrillated full length α-synuclein had better chaperone activity than the soluble monomer. Their results appear to suggest that the chaperone activity of α-synuclein is in the amyloidogenic region (61-95). The C-terminus solubilizes the high molecular complex of the synuclein and its substrate thereby preventing its precipitation or aggregation (Park et al., 2002; Rekas et al., 2012). It appears that the β-sheet conformation enhances α-synuclein's protein-protein interaction with its substrates. Our studies also indicate that β-synuclein fibrils can form reasonably rapidly under the same conditions *in vitro* as α-synuclein, with β-synuclein showing a short lag phase of approximately 2-3 days (Figure 26). In our study, a form(s) of α-synuclein was capable of inhibiting β-synuclein fibrillation, which at the time the study was conducted was a very novel finding.

Also, most importantly the results of this research suggest that when two proteins capable of forming fibrils under the same conditions are incubated together, an inhibitory effect can occur. Our results suggest that two different fibril forming proteins

can exert an inhibitory effect on each other *in vivo*. although in nature. fibril associated proteins each occupy distinct niches within or outside various tissues in the body. These findings may provide new lines of investigation regarding the design of inhibitors as well as facilitate our general understanding of the mechanism of fibril formation. The outcome of this study has not yet answered the initial goal to understand the mechanism of inhibition. Further experimental studies are necessary to identify the species that prevent fibrillation.

CHAPTER V

INITIAL INVESTIGATION TO ISOLATE SYNUCLEIN TETRAMERS

INTRODUCTION

Since their isolation from the brains of vertebrates, the synuclein proteins have been believed to exist only in an unstructured conformation (Lavedan, 1998; Uversky et al., 2002). This assumption may have arisen from the fact that the protocols used in the standard purification process involves a step in which the bacterial lysate is boiled in a water bath at 100°C for thirty minutes (Conway et al., 1998). As a result, any multimeric species of the proteins may have been dissociated and denatured by the heat.

Researchers have been able to determine structures of full-length and segments of α-synuclein. Some examples of such structures include micelle-bound full length α-synuclein (pdb code: 1xq8), full length α-synuclein bound to detergent sodium lauroyl sarcosinate (pdb code: 2kkw), N-terminally acetylated α-synuclein peptide complexed with calmodulin (pdb code: 2m55) (Figure 34) (Ulmer et al., 2005; Rao et al., 2010; Gruschus et al., 2013)(Ulmer et al., 2005; Rao et al., 2010; Gruschus et al., 2013). NMR structures of fragments of α-synuclein bound to maltose-binding protein have been determined including segments 1-19 residues (pdb code: 3q25), segment 9-42 residues (pdb code: 3q26), segment 32-57 residues (pdb code: 3q27) and segment 58-79 residues (pdb code:3q28) (Zhao et al., 2011).

Figure 34. Model structure of N-terminally acetylated α-synuclein peptide (cyan) complexed with calmodulin protein (blue) (pdb code: 2m55)

The unbound peptide (yellow) forms a helical conformation (cyan) when complexed with the calmodulin protein (Gruschus et al.. 2013). The acetyl (CH_3-CO) group is attached to methionine 1(M^1) of α-synuclein (Kang et al., 2012). This structure is visualized with Rasmol (version 2.7.1).

In spite of conflicting reports from various groups at Harvard University, Stanford University and Ecole Polytechnique Fédérale de Lausanne in Switzerland about the native structure of the synucleins, a growing body of information suggests that a multimeric form of the proteins may exist in equilibrium with its monomeric fraction (Wang et al., 2011). Protocols in which denaturing conditions, such as boiling the lysate were omitted during the purification process, yielded a helical tetrameric α-synuclein (Bartels et al., 2011; Wang et al., 2011; Dettmer et al., 2013). The investigators suggest that the tetramer is composed of helices (Figure 35).

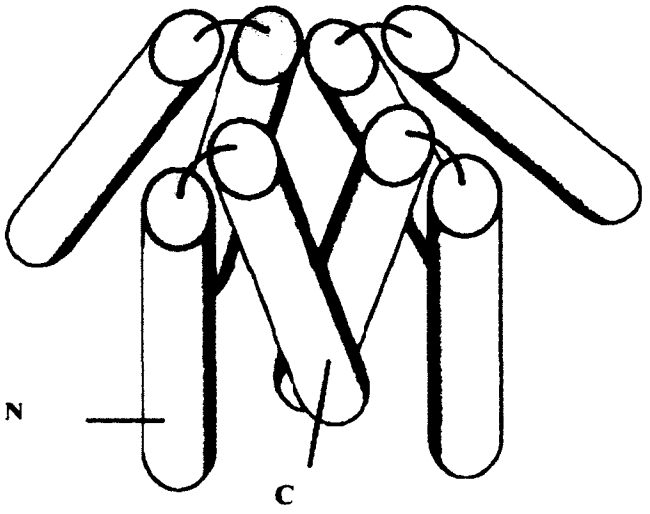

Figure 35. A model structure of the helical tetrameric α-synuclein

The helices are represented by the cylinders. Each pair of cylinders is an α-helix with an N-and C-terminus. The portion of the α-synuclein that makes α-helix includes residues 1-103 which is the N-terminal region of the synuclein. 'N' indicates the N-terminus and 'C' indicates the C-terminus. This figure is reproduced from Wang (Wang et al., 2011).

All of these findings are still at their infant stage and need further investigation. In our attempt to isolate the multimeric form of β-synuclein, recombinant β-synuclein was expressed in Rosetta 2(DE3) cells. Hepes buffer which offers a more conducive environment for the multimeric forms than the Tris Base was used. After breaking open the cells by sonication, the lysate was not boiled in order to preserve the multimeric forms of β-synuclein. In addition, we added to the Hepes buffer glycerol and n-octyl-β-D-glucopyranoside which were meant to stabilize the multimeric forms of the protein. The final step in isolating the multimeric β-synuclein involved gel-filtration. The multimeric β-synuclein was eluted with 0.15 M NaCl in Hepes buffer and stored in 1 ml

aliquots at -80°C. The details of the first and final steps in the purification process are described in the Materials and Methods section. Far-UV studies were conducted to determine the secondary structure content of the β-synuclein.

RESULTS

The expression of recombinant human β-synuclein in which we did not boil the bacterial lysate, yielded a high MW β-synuclein. A protein standard, glutamic dehydrogenase initially believed to have a MW of 55.6 kDa was run through the same Sephadex G-75 gel filtration size exclusion showed a similar elution profile (Figures 36-37) as the β-synuclein complex. A MW of 55.6 kDa which is almost 4 times the MW of monomeric β-synuclein (14 kDa) implies the presence of a tetramer.

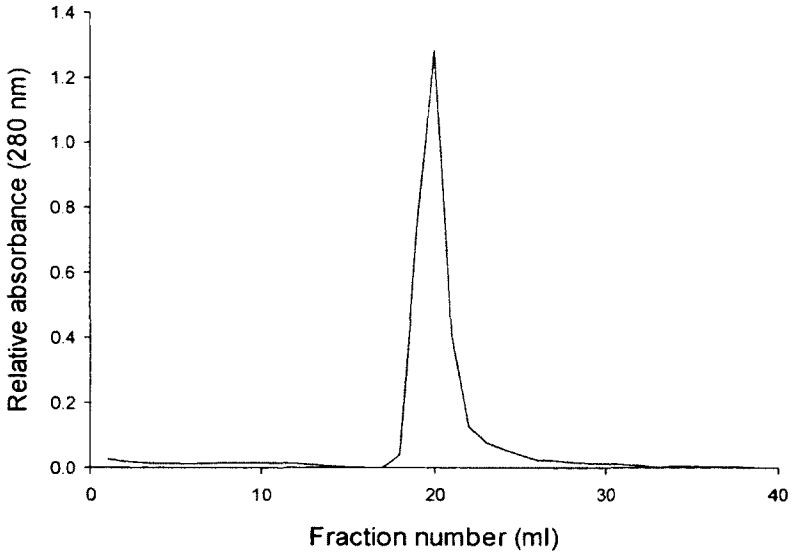

Figure 36. G-75 size exclusion chromatography elution profile of a high molecular weight β-synuclein

The high MW β-synuclein eluted with a sharp peak at fraction 20. Each fraction is 5 ml. The absorbance of protein in each fraction was determined at 280 nm using a UV-Vis spectrophotometer by hand. The graph was constructed by plotting absorbance against fraction number in Microsoft Excel (version 2010).

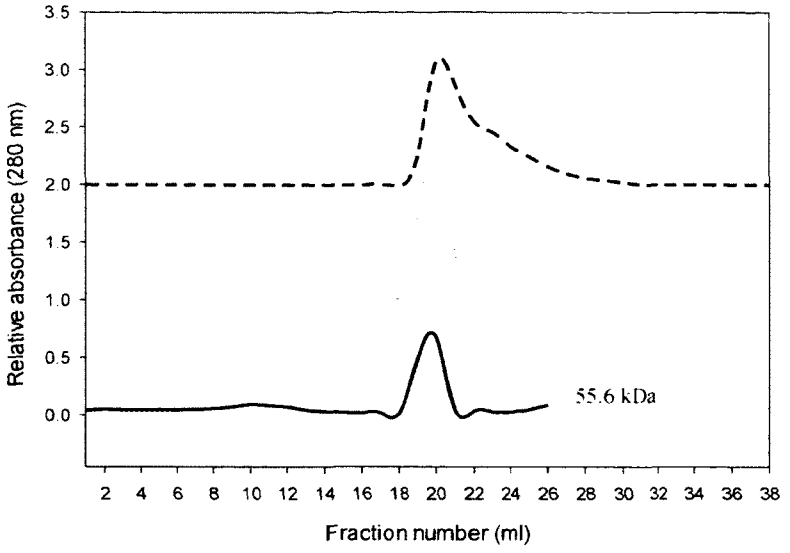

Figure 37. G-75 size exclusion chromatography elution profiles of β- and α-synuclein and glutamic dehydrogenase

β-synuclein complex (dashed line), α-synuclein complex (dotted line) and glutamic dehydrogenase (solid line) are all eluting at fraction 20. Each protein was run separately. The absorbance of the protein in each fraction was determined at 280 nm using a UV-Vis spectrophotometer by hand. The graph of each protein was constructed by plotting absorbance against fraction number in Microsoft Excel (version 2010). The molecular weight of glutamic dehydrogenase is annotated on the graph according to the weight listed on the bottle purchased from Sigma-Aldrich.

A computer program K2D3 (Louis-Jeune et al., 2011) used the far-UV circular dichroism spectra to estimate that the β-synuclein complex was 68% α-helical, 6.7% β-sheet and 25.2% random coil (Figure 38). The computer program compares the CD spectrum of the protein under investigation to a reference set of CD spectra of proteins

whose structures have been resolved. The program then predicts or estimates the secondary structure content of the query protein.

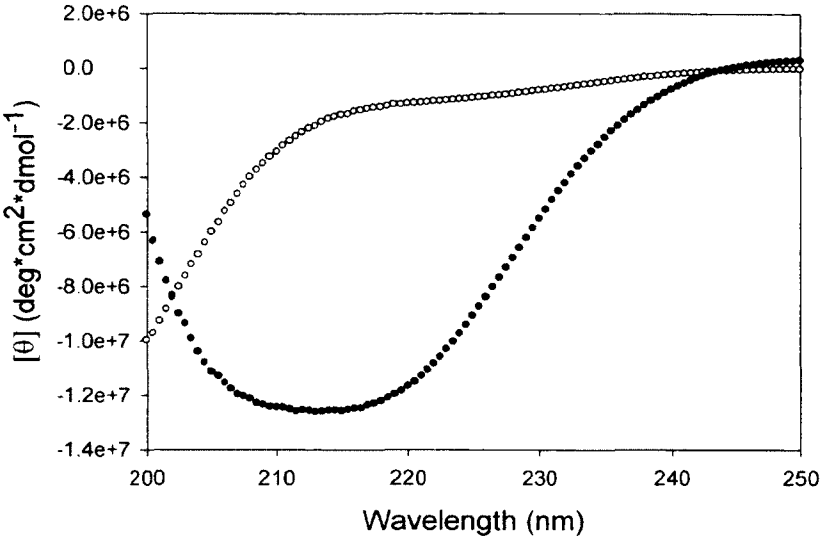

Figure 38. Far-UV circular dichroism spectra for β-synuclein random coil (empty circles) and high molecular weight β-synuclein (filled circles)

According to the K2D3 program prediction of secondary structure, the high MW β-synuclein is 68% helical, 6.7% βand 25.2% random coil and the random coil is 4% α-helical, 34.9% β-sheet and 61.1% random coil.

DISCUSSION

The groups of researchers who attempted to isolate the multimeric form of α-synuclein reported a range of molecular weights for the complex: 56 kDa, 58 kDa and 60 kDa (Bartels et al., 2011; Wang et al., 2011; Dettmer et al., 2013). Our β-synuclein

complex under non-denaturing conditions is about 56 kDa or larger. (We discuss how to ascertain the absolute size in future work.) A small fraction of the expressed β-synuclein was a multimeric complex (0.5 mg/L of Luria broth culture). The remainder of the protein was the monomeric form. One group that successfully isolated a tetrameric α-synuclein reported a yield of 1 mg/L of Luria broth culture (Wang et al., 2011). From the disproportionately small yield of multimeric protein versus the monomeric protein, it is possible that the multimeric form of the synucleins does not normally exist in the cytoplasm but may exist when bound to the cell membrane. Reports in the literature indicate that the synucleins acquire secondary structure when bound to the cell membrane (Jain et al., 2013; Wietek et al., 2013). Therefore, when recombinant synucleins are expressed in bacteria, the multimeric forms are likely to fall apart in the cytoplasm of the bacterial cells.

The acetylation of the α-synuclein in the neuronal cells has been shown to enhance and stabilize the helical structure of the membrane bound protein (Trexler and Rhoades, 2012; Dikiy and Eliezer, 2014). In addition, an acetylated N-terminus of α-synuclein has been shown to decelerate fibrillation (Kang et al., 2012; Kang et al., 2013). When the synuclein proteins are expressed in bacterial cells, the acetylation modification does not take place. The expression of the synuclein in bacterial cells deprives the protein of the essential acetylation modification, which appears to be critical for helical formation. However, one cannot base the formation of multimeric complex of the synucleins on N-terminus acetylation alone. Other factors in the cell, yet to be elucidated, may also be critical for the formation and stabilization of the multimeric synucleins.

Additionally, in our experiment, glutamic dehydrogenase was selected based on looking for a protein that would serve as an ideal MW marker for the gel-filtration column. The choice was based on studying the available protein and their reported molecular weights in the Sigma-Aldrich catalogue. However, subsequently, after the studies were conducted and in discussion with Professor Ellis Bell (Richmond University, Virginia), he indicated that at neutral pH this protein is a hexamer (Sakamoto et al., 1975; Norouzi et al., 2010). Therefore, at pH 7.4, the eluted glutamic dehydrogenase was possibly a hexamer which is six times the size of the monomer (55.6 kDa). The G-75 size exclusion column cannot optimally separate proteins greater than 60 kDa. All proteins that are equal or greater than 55.6 kDa can elute to the same location. Thus, the β-synuclein eluted may either be a higher MW species than originally thought or be the desired tetramer but was not well separated in the column and came out in the void volume. The methodology to further test the size and confirm that the eluted species is actually a tetramer is discussed in Future Work.

CHAPTER VI

COMPUTATIONAL ANALYSIS OF THE SYNUCLEINS

INTRODUCTION

New protein sequences continue to be added to those already stored in the protein and nucleic acid databases at the National Center of Biotechnology Information (NCBI) in Maryland. Their corresponding protein structures are being determined at a slower rate and are deposited in the Research Collaboratory for Structural Bioinformatics Protein Data Bank (RCSB-PDB) at Rutgers University (New Jersey). Computational approaches are now complementing experimental methods to accelerate the process of determining the structure and biological function of proteins.

The structure and function of an uncharacterized protein may be elucidated from its ancestral relatives whose native structure and function have been resolved. Ancestral relatives are identified by certain features that persist in a superfamily from one generation to the next. Despite structural modifications as the protein evolves over time, evolution tends to conserve those motifs of the sequence that are responsible for structure stability and function (Redfern et al., 2009).

In order to trace the origins of proteins, researchers use bioinformatics approaches which include searching for related protein sequences, searching for related protein structures and analyzing the nature of the relationship. Bioinformatics algorithms which include PSI-BLAST (Altschul et al., 1997), MUSCLE (Edgar, 2004) and scan

ProSite (Falquet et al., 2002) are employed to construct evolutionary families and superfamilies of proteins.

A protein family is composed of proteins that originate from a common ancestor and generally share a common structure and function and significant sequence identity. The work of Todd, Orengo and Thornton and other research groups led to the conclusion that proteins which are >40% similar in their sequences have a specific conserved function (Todd et al., 2001). However, there are instances when the same gene can encode a protein with a dual function or multiple functions. For example, in a duck (*Anas platyrhynchos*), the ε-crystallin structural protein in the eye lens can also serve as an enolase and lactate dehydrogenase (Wistow et al., 1987; Wistow et al., 1988). Such proteins with multiple functions are now referred to as moonlighting proteins (Huberts and van der Klei, 2010). A superfamily is composed of proteins that have a common ancestor, a common 3D structure and conserved features for folding but little or no significant sequence similarity (Figure 39) (Greene and Higman, 2003).

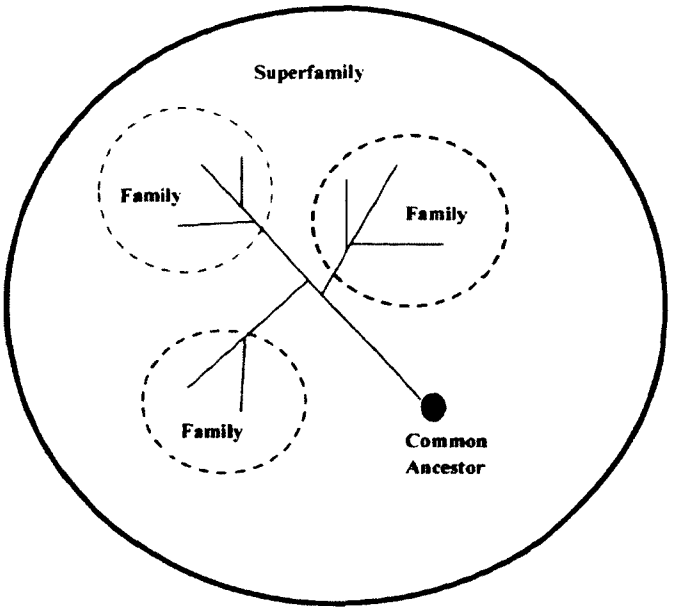

Figure 39. Hypothetical schematic of a protein family and superfamily

Each blue dashed circle is a family of proteins. The green circle contains all the families of proteins that make a superfamily. Proteins in the superfamily are related by a common ancestor (solid purple circle). They can be identified by a consensual sequence signature, common 3D structure and may have a similar function. Segments of a protein that are responsible for structural stability and function are conserved as the protein evolves in order to adapt to its environment.

A number of factors which cause changes in the structure and function of a protein as it evolves include gene deletion, gene insertion, point mutation, gene duplication and oligomerization (Garrett and Grisham, 2013). In gene deletion and insertion, one or more base pairs are removed from or added to a gene, respectively. The deletion or insertion can cause a frame shift resulting in inappropriate incorporation of the next amino acid residues in the protein encoded by the gene. Alterations in the amino

acid sequence may lead to a change in the conformation and/or the function of the protein. Point mutations where a single nucleotide is replaced by another may result in a change in the coded amino acid residue. Gene duplication can result in a change of function when one of the copies undergoes mutation (Magadum et al., 2013). Variation of structure and function may result from oligomerization when multiple domains, either homo- or heterodimers, trimers or tetramers, are formed (Zhang, 2003; Kottyan et al., 2012).

Researchers across the world employ both experimental and computational methods to determine the native structure and function of the synuclein family yet both remain elusive and controversial. The results published in recent Nature and Proceeding of the National Academy of Science journals indicate that α-synuclein forms a helical tetramer (Bartels et al., 2011; Wang et al., 2011; Dettmer et al., 2013). This folded form of α-synuclein may be its natural structure in brain tissue but remains highly controversial. We employed bioinformatics algorithms including PSI-BLAST, MUSCLE, scan prosite and scan motif to construct a superfamily in order to further our understanding of the structure and as yet unresolved native function of the α-, β- and γ-synucleins. Our hypothesis proposed that identifying synuclein relatives, whose 3D structure and function have been resolved, would facilitate the elucidation of the physiological structure and function of the synucleins and illuminate their evolutionary history. Understanding the structure and function of the synucleins would facilitate an understanding of the mechanisms of protein folding and misfolding, and potentially assist in finding an effective therapy for protein misfolding related diseases including Parkinson's disease.

Human α-, β- and γ-synucleins were the probe sequences used to identify similar sequences in protein databases. The similarity was considered significant when the statistical e-value was less than 5×10^{-3}. Then, the identified proteins were aligned to the synucleins from various species in order to establish positions of identity and similarity in the sequences. A phylogenetic tree was also constructed from the human synucleins and the identified related proteins in order to determine their ancestor.

Unlike humans who succumb to neurodegenerative diseases as they age, animals such as the giant tortoise can live for 255 years. A further analysis of the synuclein alignments was made in order to identify any differences between humans and other animals, particularly for those that live longer than humans. Neurodegenerative diseases have been observed in domestic animals including horses, dogs and cats (Siso et al., 2006).

RESULTS

Among the α-synuclein proteins, interestingly there is variation in size. The sizes range from 121 to 151 amino acid residues. In the case of the house mouse α-synuclein, an extra eleven amino acid residues have been added to the N-terminal of the protein. The minke whale α-synuclein protein lacks the first four residues at the N-terminal and the last 12 residues at the C-terminal (Figure 40).

The PSI-BLAST search with human α-, β- and γ-synuclein probe sequences identified an endoglucanase enzyme from the bacterium *Acetobacter pomorum,* the CRE-DUR-1 protein from a nematode and the Tasmanian Devil protein. The Tasmanian Devil protein identified cytochrome c protein from the spiral bacterium *Thiomicrospira crunogena*. The percentage similarity between the synucleins and their related proteins,

the e-values and the portion of the synucleins (% coverage) similar to the related proteins are summarized in Tables 2-4.

Table 2. Similarity between α-synuclein and the three disparate proteins

Protein	% α-synuclein coverage	% Similarity	E-value
Endoglucanase	65	35	1×10^{-3}
CRE-DUR-1	77	36	1×10^{-5}
Tasmanian Devil	71	65	1×10^{-28}

Table 3. Similarity between β-synuclein and the three disparate proteins

Protein	% β-synuclein coverage	% Similarity	E-value
Endoglucanase	95	20	2×10^{-3}
CRE-DUR-1	76	32	2×10^{-6}
Tasmanian Devil	77	55	2×10^{-27}

Table 4. Similarity between γ-synuclein and the three disparate proteins

Protein	% γ-synuclein coverage	% Similarity	E-value
Endoglucanase	81	27	1×10^{-5}
CRE-DUR-1	96	36	4×10^{-10}
Tasmanian Devil	95	80	2×10^{-54}

Endoglucanase enzyme

The three human synucleins share 20-35% identity with the endoglucanase. The putative (predicted from its nucleotide sequence) endoglucanase protein contains several conserved KTKEGV sequences. A multiple sequence alignment of endoglucanase with α-synuclein proteins from 14 different species was constructed (Figure 40). The blue color represents positions of identity; the purple are positions with hydrophobic character; the red are positions of hydrophilic character and the green indicates positions where a given amino acid residue is highly prevalent. The endoglucanase enzyme is composed of 218 amino acid residues and the portion which is significantly similar to the N-terminal region of the synucleins is between amino acid residues 61 and 177. The first 60 residues have no relationship with the α-synuclein proteins and do not contain the KTKEGV sequences. The second, fourth and fifth KTKEGV motifs of the α-synucleins are highly identical to those of the endoglucanase enzyme. The most conserved residues between the synucleins and the endoglucanase enzyme are highlighted in the human α-synuclein helices with the same color code as in the alignment (Figure 41).

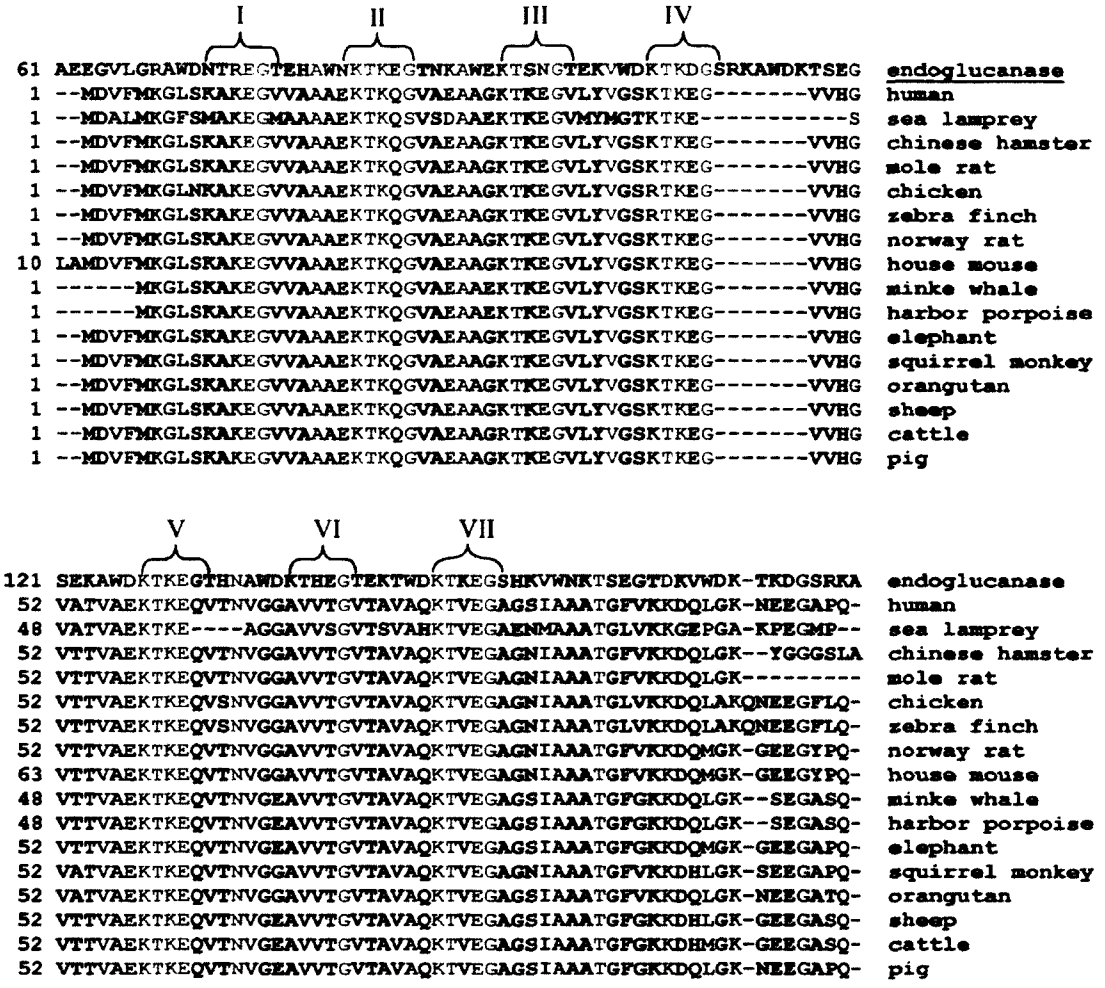

Figure 40. Sequence alignment of 16 variant α-synucleins with endoglucanase

The portion of the protein that is similar to the α-synucleins is between residues 61 and 177. The first 60 amino acid residues of the endoglucanase do not contain the KTK(E/Q)GV sequences. The portion of the α-synucleins that is similar to the endoglucanase lies between residues 1 and 109. The KTK(E/)GV repeats are marked I-VII. In the sixth sequence, the KTKE residues have been substituted. Color scheme: blue (sequence identity); red (conserved hydrophilic character); purple (conserved hydrophobic character); green indicates positions where a residue is highly prevalent. The alignment was constructed with MUSCLE (Edgar, 2004; McWilliam et al., 2013).

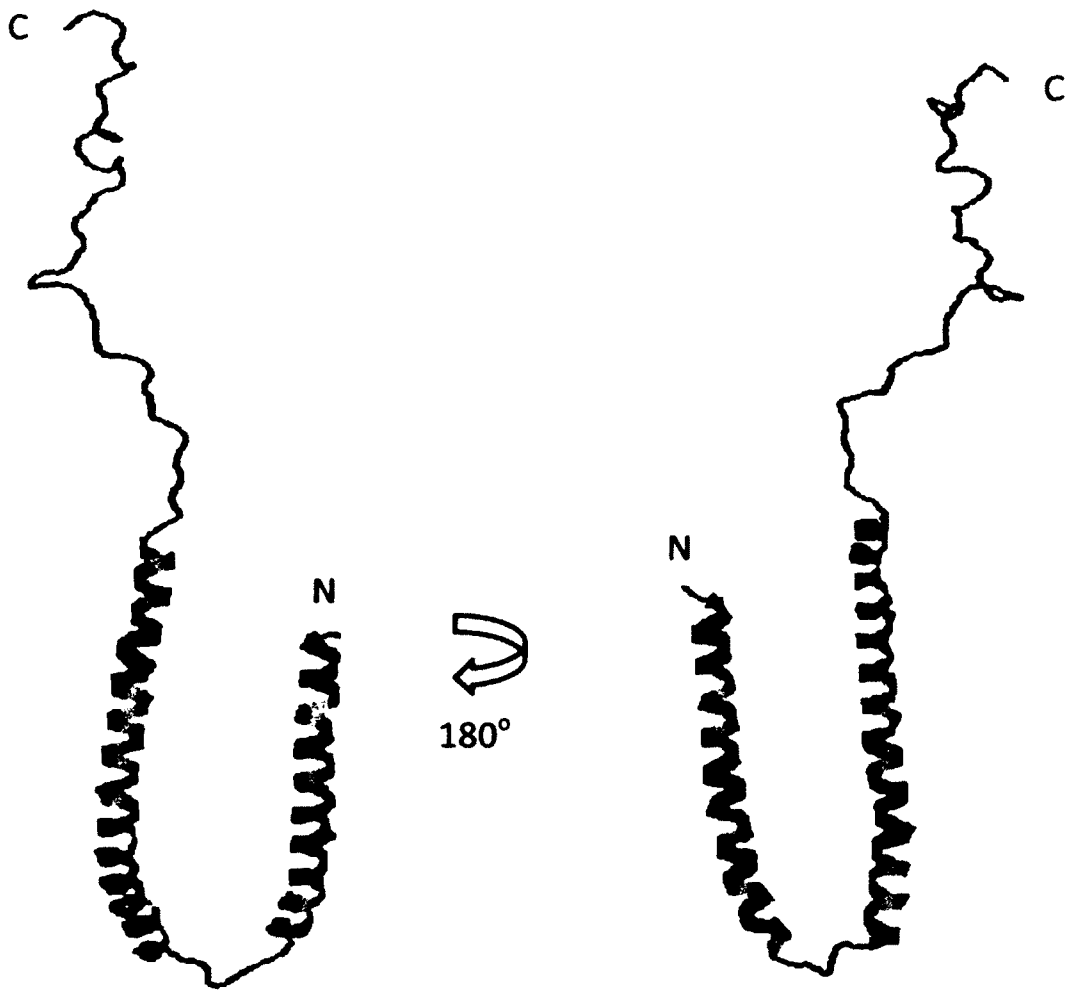

Figure 41. Regions of human α-synuclein (pdb code: 1xq8) similar to the endoglucanase

The color coding in the figure indicates the regions of the human α-synuclein that are similar to the endoglucanase enzyme. The figure was rotated 180 degrees. Color scheme: blue (sequence identity); red (conserved hydrophilic character); purple (conserved hydrophobic character); green indicates positions where a residue is highly prevalent. The letter 'N' designates the N-terminus and 'C' designates the C-terminus of the protein. These structures are visualized with Rasmol (version 2.7.1).

The portion of the endoglucanase that shares identity with the β-synucleins is between amino acid residues 48 and 163 (Figure 42). The shift from the 61-177 residue α-synuclein alignment is a result of the long β-synuclein from the naked mole rat. The protein is composed of 210 amino acid residues, with a 76 amino acid peptide added to the N-terminus. The second repeat sequence of the β-synucleins has the highest degree of identity with the endoglucanase.

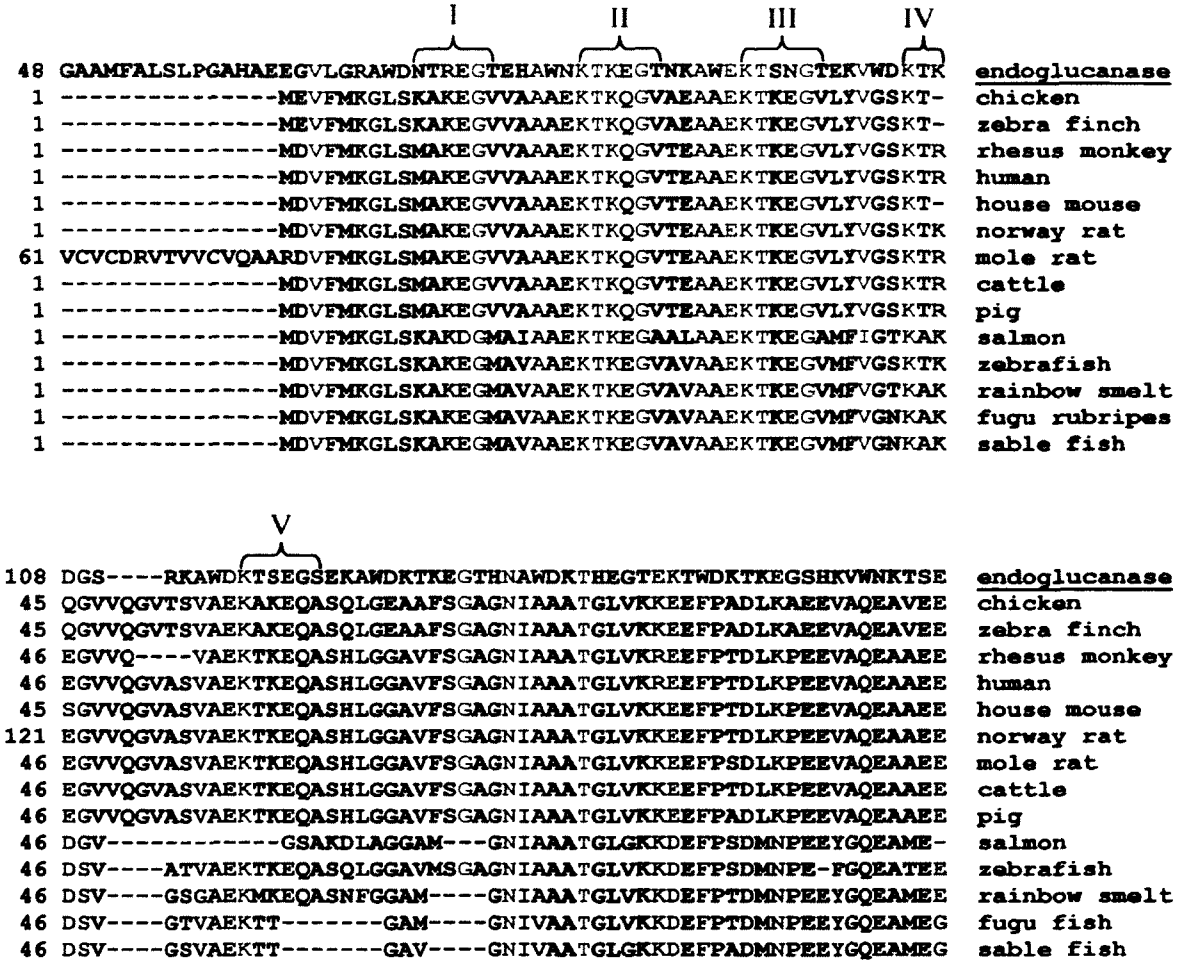

Figure 42. Sequence alignment of 14 variant β-synucleins with endoglucanase

The portion of the endoglucanase that shares significant similarity with the β-synucleins is between residues 48 and 163. Among the β-synucleins, there is variability in the repeat sequences except in the third. Color scheme: blue (sequence identity); red (conserved hydrophilic character); purple (conserved hydrophobic character); green indicates positions where a residue is highly prevalent. The alignment was constructed with MUSCLE (Edgar, 2004; McWilliam et al., 2013).

The alignment between the endoglucanase and the γ-synucleins from 16 species indicates that the fifth repeat sequence of the synuclein proteins is highly identical to the endoglucanase (Figure 43). A multiple sequence alignment between the endoglucanase and the α-, β- and γ-synucleins altogether shows that the second and fifth repeat sequences of the synucleins share the highest identity with those of the endoglucanase enzyme (Figure 44).

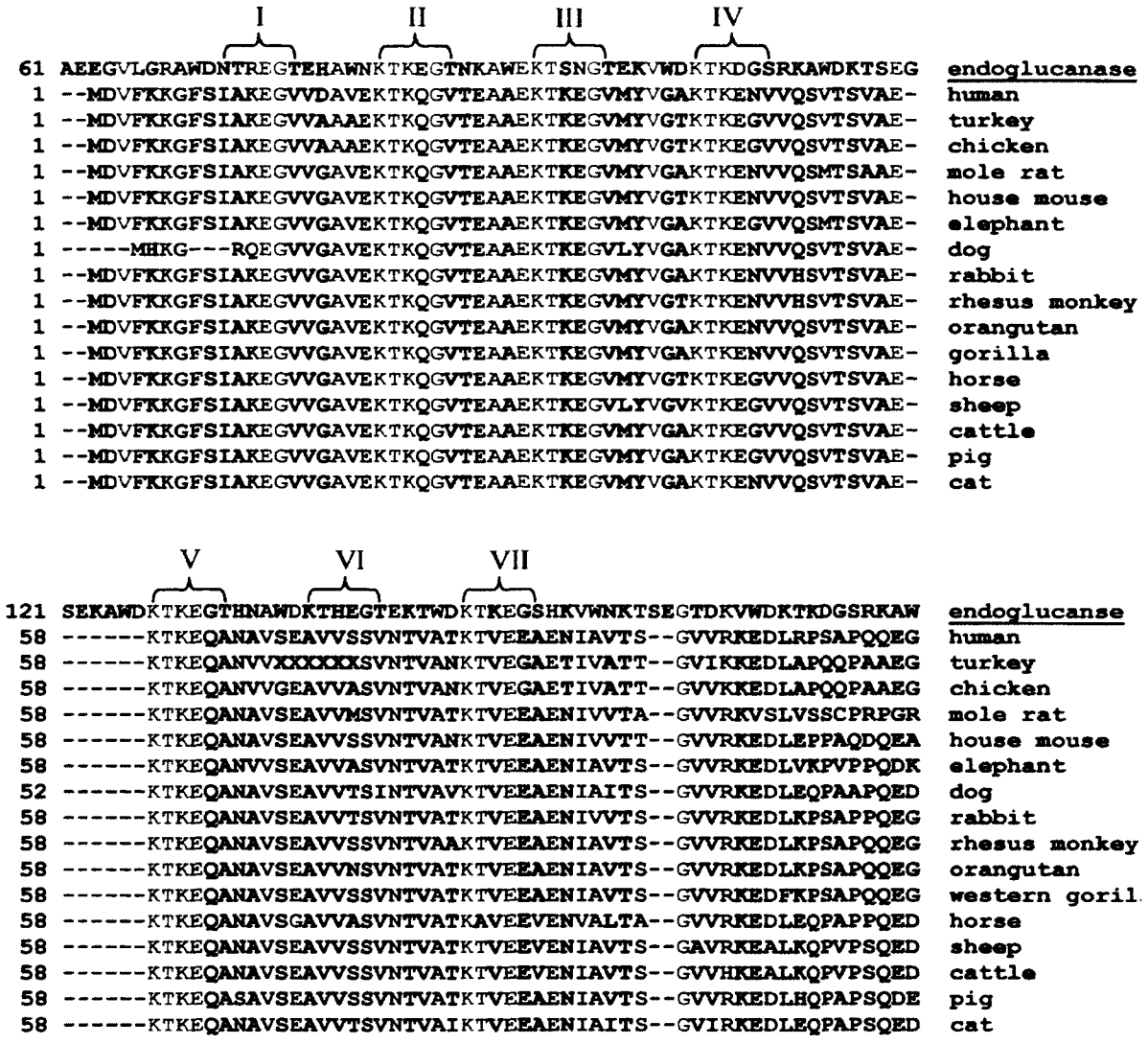

Figure 43. Sequence alignment of 16 variant γ-synucleins with endoglucanase

The portion of the endoglucanase that shares significant identity with the γ-synucleins lies between residues 61 and 171. The fifth repeat sequence of the γ-synucleins shares the highest identity with the endoglucanase. Color scheme: blue (sequence identity); red (conserved hydrophilic character); purple (conserved hydrophobic character); green indicates positions where a residue is highly prevalent. The alignment was constructed with MUSCLE (Edgar, 2004; McWilliam et al., 2013).

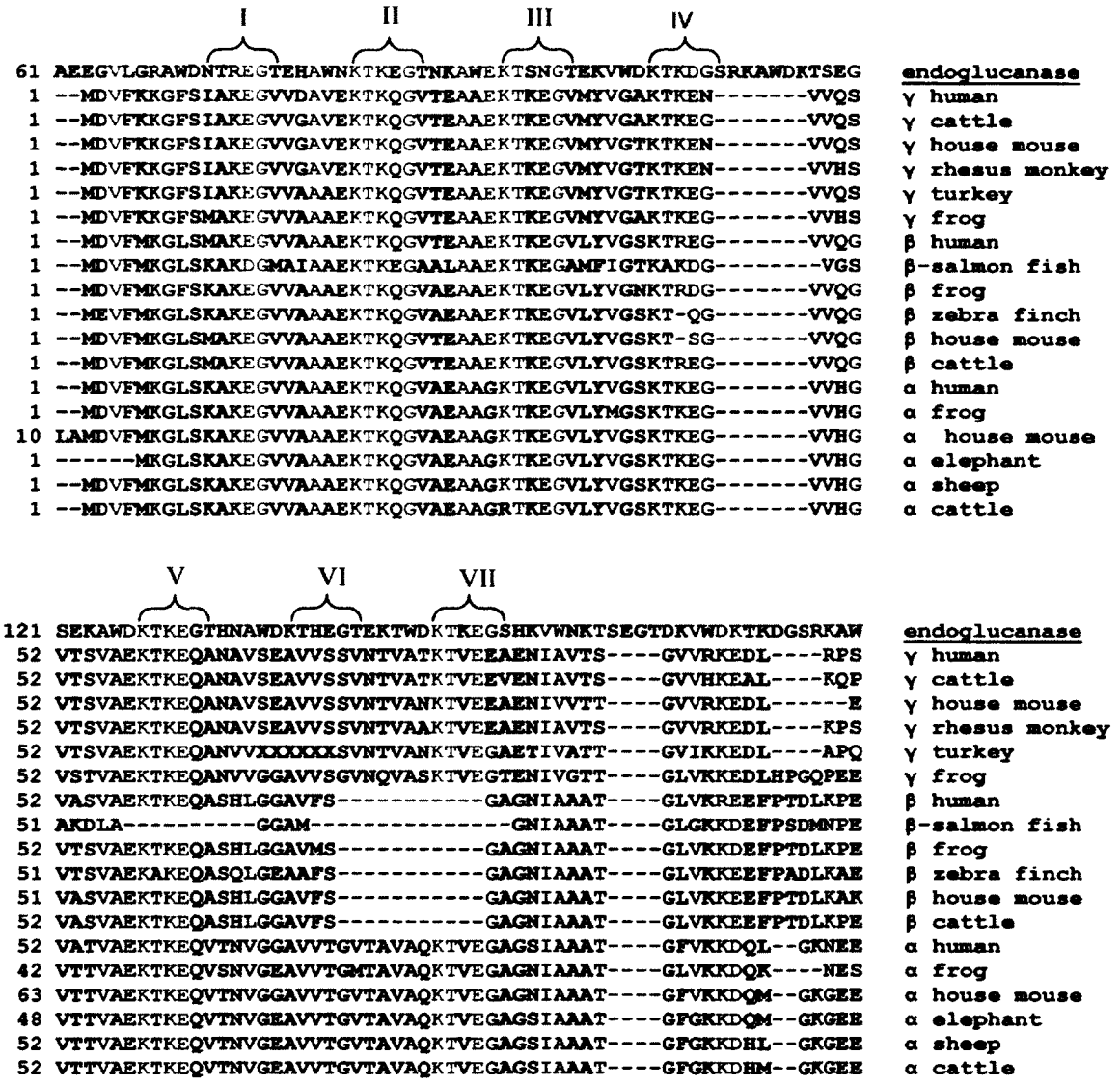

Figure 44. Summary sequence alignment of endoglucanase with 18 species variants of α-, β- and γ-synucleins

It appears the endoglucanase matches with the N-terminal region of the synuclein protein. The KTK(E/Q)GV sequence is the element of similarity between the endoglucanase and the synucleins. Color scheme: blue (sequence identity); red (conserved hydrophilic character); purple (conserved hydrophobic character); green indicates positions where a residue is highly prevalent. The alignment was constructed with MUSCLE (Edgar, 2004; McWilliam et al., 2013).

CRE-DUR-1 protein

The PSI-BLAST search with the human α-, β- and γ-synuclein probe sequences also identified a putative CRE-DUR-1 protein from a nematode. The CRE-DUR-1 protein is composed of 524 amino acid residues. The CRE-DUR-1 shares 32%-36% identity with human synucleins in the overlapping region. The sequence alignment between the CRE-DUR-1 and α-synucleins from various species indicates that the first 356 amino acid residues of the protein share no identity with the synucleins (Figure 45). The regions of the human α-synuclein that are similar to the CRE-DUR-1 protein are marked on the helical structure of the α-synuclein in Figure 46. The CRE-DUR-1 alignment with α-, β- and γ-synucleins is shown in Figure 47.

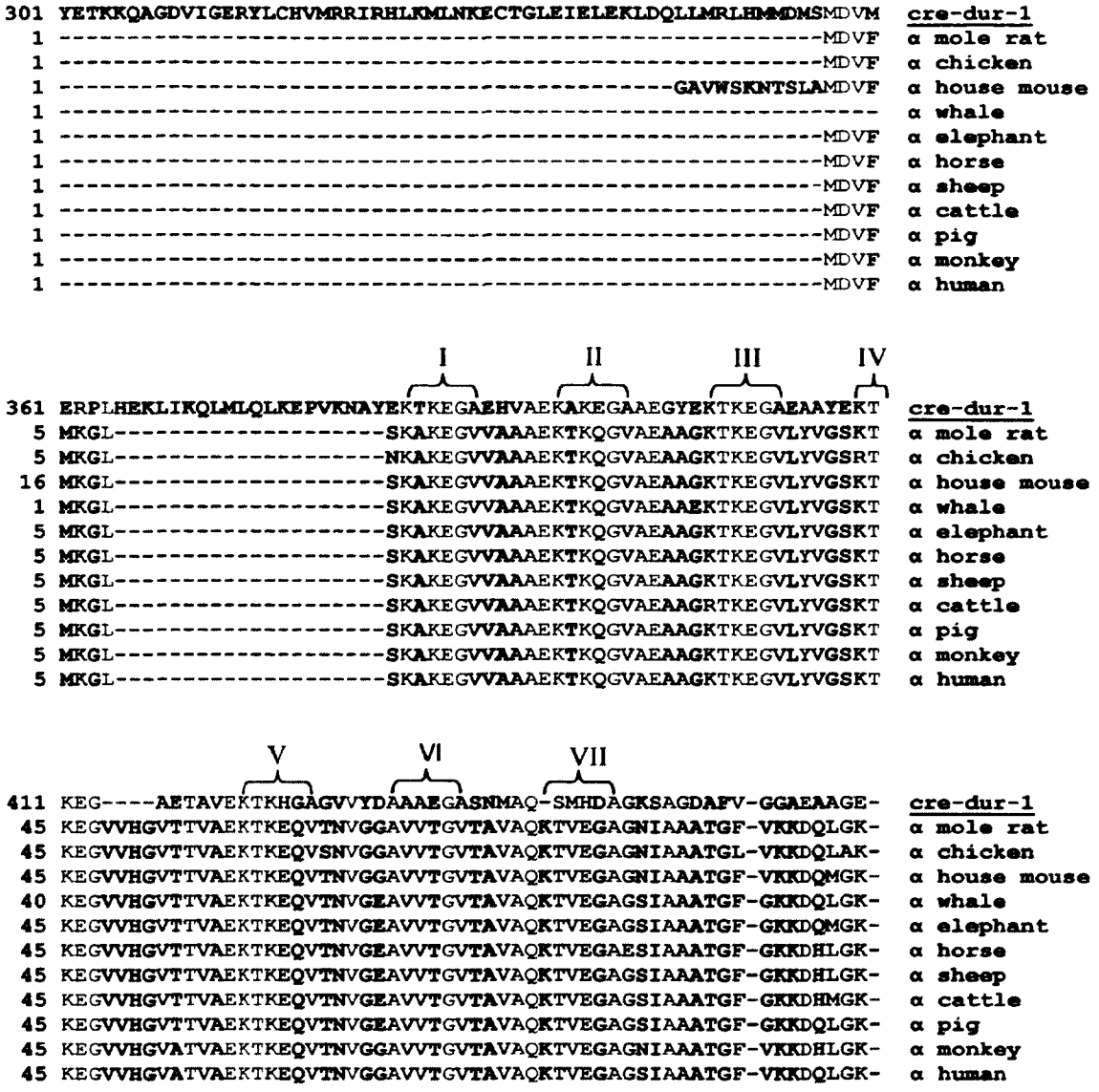


```
301 YETKKQAGDVIGERYLCHVMRRIRHLKMLNKECTGLEIELEKLDQLLMRLHMMDMSMDVM  cre-dur-1
  1 ------------------------------------------------------MDVF  α mole rat
  1 ------------------------------------------------------MDVF  α chicken
  1 ------------------------------------------GAVWSKNTSLAMDVF  α house mouse
  1 ------------------------------------------------------      α whale
  1 ------------------------------------------------------MDVF  α elephant
  1 ------------------------------------------------------MDVF  α horse
  1 ------------------------------------------------------MDVF  α sheep
  1 ------------------------------------------------------MDVF  α cattle
  1 ------------------------------------------------------MDVF  α pig
  1 ------------------------------------------------------MDVF  α monkey
  1 ------------------------------------------------------MDVF  α human

361 ERPLHEKLIKQLMLQLKEPVKNAYEKTKEGAEHVAEKAKEGAAEGYEKTKEGAEAAYEKT  cre-dur-1
  5 MKGL--------------------SKAKEGVVAAAEKTKQGVAEAAGKTKEGVLYVGSKT  α mole rat
  5 MKGL--------------------NKAKEGVVAAAEKTKQGVAEAAGKTKEGVLYVGSRT  α chicken
 16 MKGL--------------------SKAKEGVVAAAEKTKQGVAEAAGKTKEGVLYVGSKT  α house mouse
  1 MKGL--------------------SKAKEGVVAAAEKTKQGVAEAAEKTKEGVLYVGSKT  α whale
  5 MKGL--------------------SKAKEGVVAAAEKTKQGVAEAAGKTKEGVLYVGSKT  α elephant
  5 MKGL--------------------SKAKEGVVAAAEKTKQGVAEAAGKTKEGVLYVGSKT  α horse
  5 MKGL--------------------SKAKEGVVAAAEKTKQGVAEAAGKTKEGVLYVGSKT  α sheep
  5 MKGL--------------------SKAKEGVVAAAEKTKQGVAEAAGRTKEGVLYVGSKT  α cattle
  5 MKGL--------------------SKAKEGVVAAAEKTKQGVAEAAGKTKEGVLYVGSKT  α pig
  5 MKGL--------------------SKAKEGVVAAAEKTKQGVAEAAGKTKEGVLYVGSKT  α monkey
  5 MKGL--------------------SKAKEGVVAAAEKTKQGVAEAAGKTKEGVLYVGSKT  α human

411 KEG----AETAVEKTKHGAGVVYDAAAEGASNMAQ-SMHDAGKSAGDAFV-GGAEAAGE-  cre-dur-1
 45 KEGVVHGVTTVAEKTKEQVTNVGGAVVTGVTAVAQKTVEGAGNIAAATGF-VKKDQLGK-  α mole rat
 45 KEGVVHGVTTVAEKTKEQVSNVGGAVVTGVTAVAQKTVEGAGNIAAATGL-VKKDQLAK-  α chicken
 45 KEGVVHGVTTVAEKTKEQVTNVGGAVVTGVTAVAQKTVEGAGNIAAATGF-VKKDQMGK-  α house mouse
 40 KEGVVHGVTTVAEKTKEQVTNVGEAVVTGVTAVAQKTVEGAGSIAAATGF-GKKDQLGK-  α whale
 45 KEGVVHGVTTVAEKTKEQVTNVGEAVVTGVTAVAQKTVEGAGSIAAATGF-GKKDQMGK-  α elephant
 45 KEGVVHGVTTVAEKTKEQVTNVGEAVVTGVTAVAQKTVEGAESIAAATGF-GKKDHLGK-  α horse
 45 KEGVVHGVTTVAEKTKEQVTNVGEAVVTGVTAVAQKTVEGAGSIAAATGF-GKKDHLGK-  α sheep
 45 KEGVVHGVTTVAEKTKEQVTNVGEAVVTGVTAVAQKTVEGAGSIAAATGF-GKKDHMGK-  α cattle
 45 KEGVVHGVTTVAEKTKEQVTNVGEAVVTGVTAVAQKTVEGAGSIAAATGF-GKKDQLGK-  α pig
 45 KEGVVHGVATVAEKTKEQVTNVGGAVVTGVTAVAQKTVEGAGNIAAATGF-VKKDHLGK-  α monkey
 45 KEGVVHGVATVAEKTKEQVTNVGGAVVTGVTAVAQKTVEGAGSIAAATGF-VKKDQLGK-  α human
```

Figure 45. Sequence alignment of CRE-DUR-1 protein with 11 variant α-synucleins

The portion of the protein sequence related to the synucleins lies between residues 356 and 463. When the CRE-DUR-1 was used as a sequence probe, the greater part of the α-synucleins were identified as being similar. The conserved repeat KTKEG sequences I-V of the synucleins are also contained in the CRE-DUR-1 protein. Color scheme: blue (sequence identity); red (conserved hydrophilic character); purple (conserved hydrophobic character); green indicates positions where a residue is highly prevalent. The alignment was constructed with MUSCLE (Edgar, 2004; McWilliam et al., 2013).

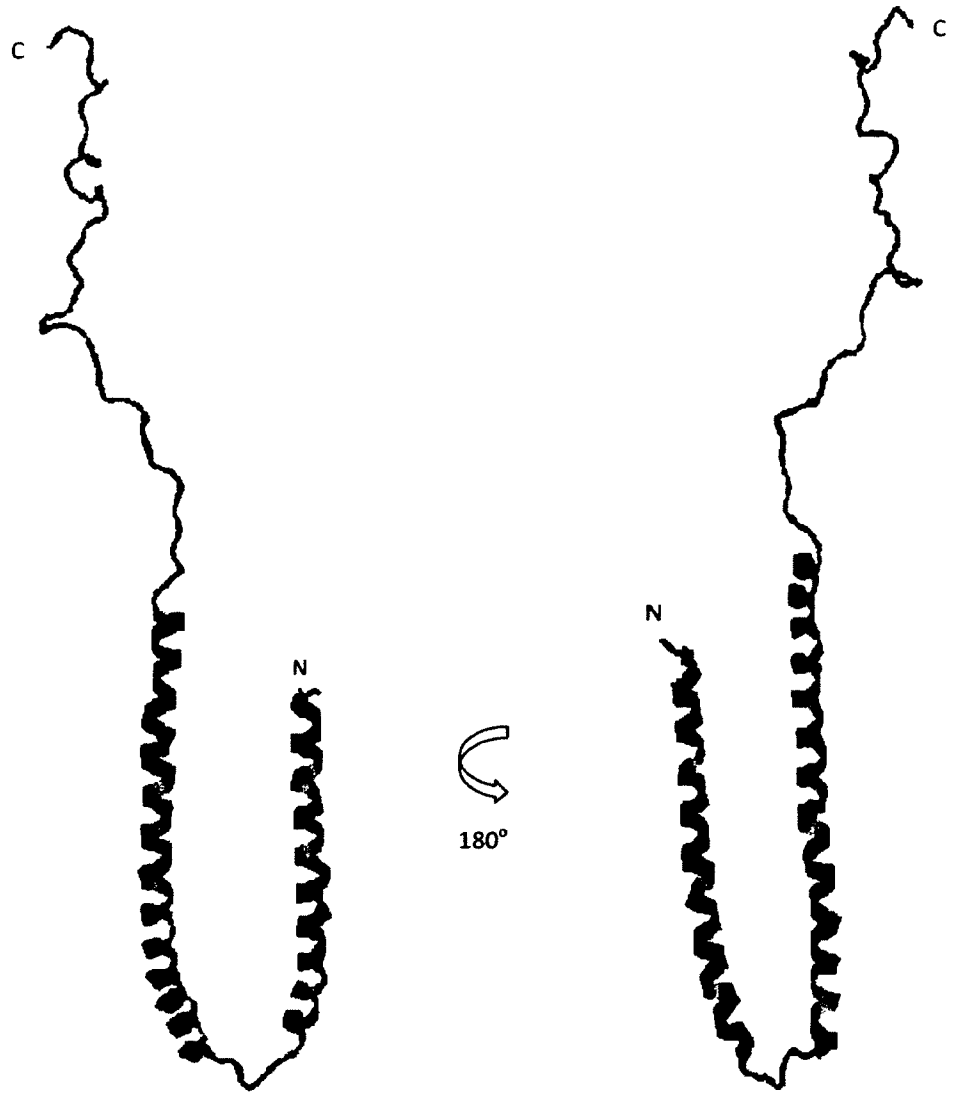

Figure 46. Regions of human α-synuclein similar to CRE-DUR-1 protein

The colors in the figure indicate the regions within human α-synuclein that are similar to the CRE-DUR-1 protein (pdb code: 1xq8). The figure was rotated 180 degrees. Color scheme: blue (sequence identity); red (conserved hydrophilic character); purple conserved hydrophobic character); green indicates positions where a residue is highly prevalent. The letter 'N' designates the N-terminus and 'C' designates the C-terminus of the protein. These structures are visualized with Rasmol (version 2.7.1).

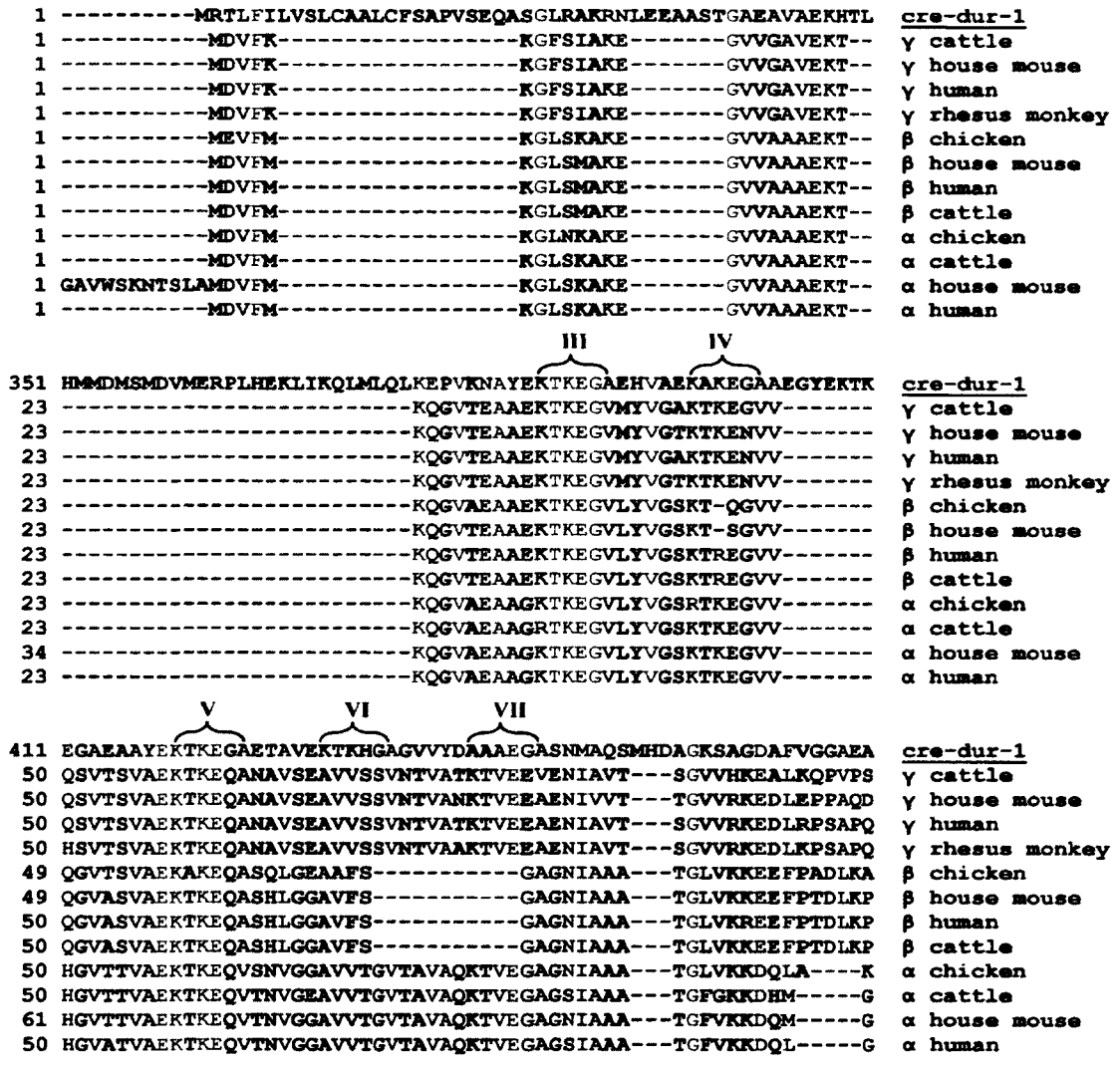

Figure 47. Sequence alignment of CRE-DUR-1 with 12 species variants of α-, β- and γ-synucleins

The KTK(E/Q)GV sequence is the element of similarity between the CRE-DUR-1 and the synucleins. Color scheme: blue (sequence identity); red (conserved hydrophilic character); purple (conserved hydrophobic character); green indicates positions where a residue is highly prevalent. The alignment was constructed with MUSCLE (Edgar, 2004; McWilliam et al., 2013).

The Tasmanian Devil protein

The marsupial protein shares 65%, 55% and 80% identity with α-, β- and γ-synucleins, respectively in the overlapping regions. The sequence alignment between the Tasmanian Devil protein and human synucleins indicates that the N-terminal region of the protein is almost identical to the N-terminal regions of the α-synucleins (Figure 48). The remainder of the protein appears unrelated to synucleins. The regions of the human α-synuclein that are similar to the Tasmanian Devil protein are shown in Figure. 49. Also, most of the sequence identity is in the α-helices.

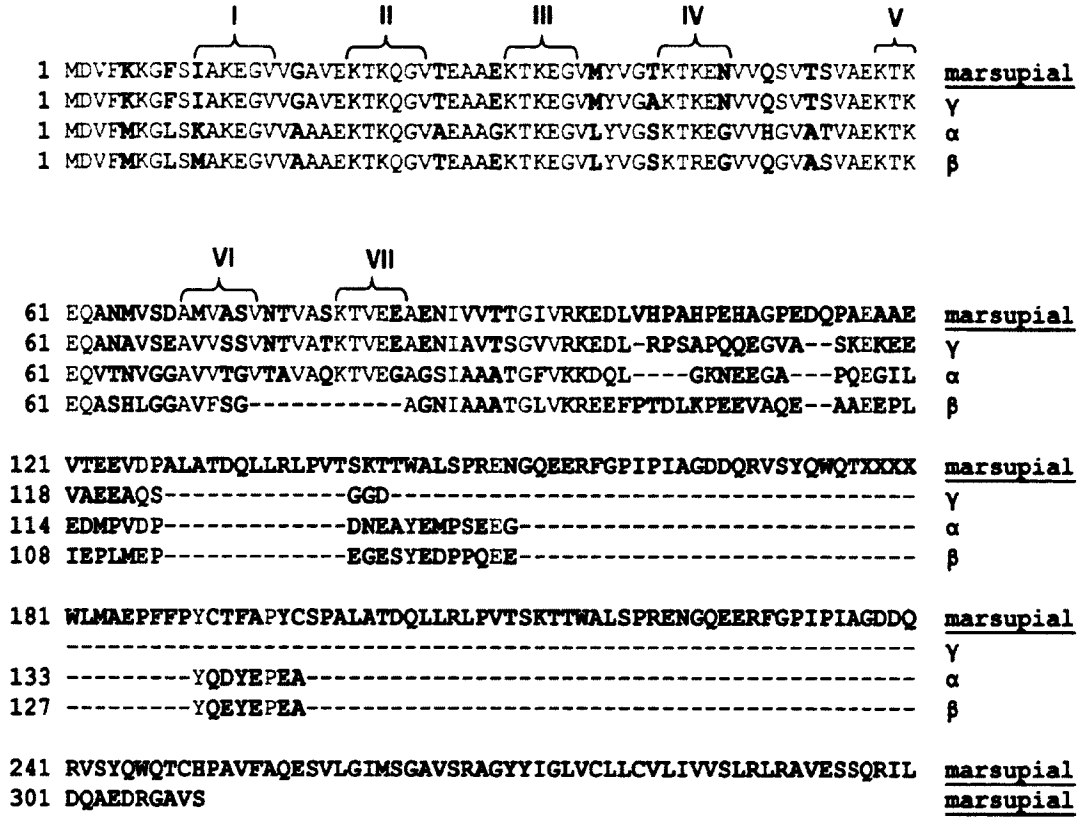

Figure 48. Sequence alignment of the putative Tasmanian Devil protein and the human α-, β- and γ-synucleins

The first 100 amino acid residues of the Tasmanian Devil are almost identical to the N-terminal regions of the synucleins The remainder of the protein is unrelated to the synucleins. Color scheme: blue (sequence identity); red (conserved hydrophilic character); purple (conserved hydrophobic character); green indicates positions where a residue is highly prevalent. The alignment was constructed with MUSCLE (Edgar, 2004; McWilliam et al., 2013).

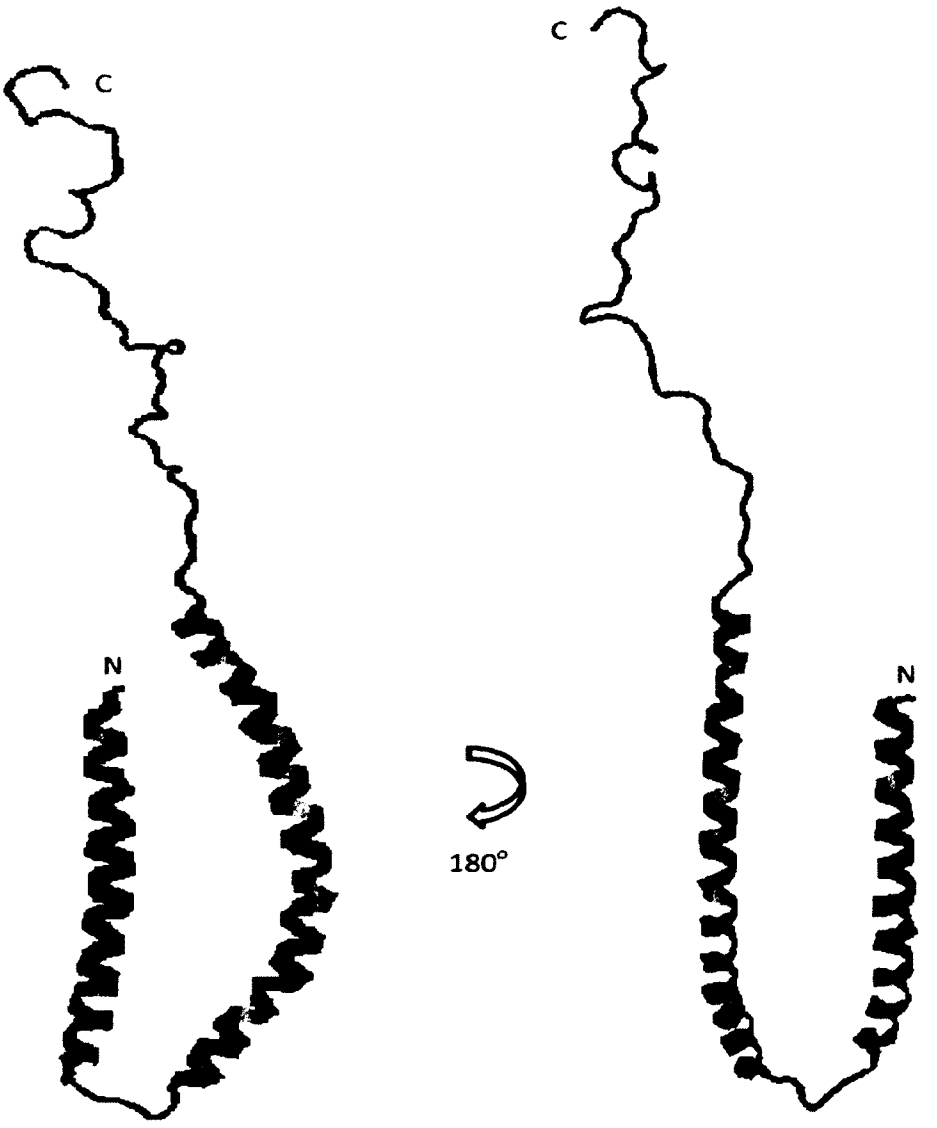

Figure 49. Regions of the human α-synuclein similar to the Tasmanian Devil protein

The colors in the figure indicate the regions within human α-synuclein that are similar to the Tasmanian Devil protein (pdb code: 1xq8). The figure was rotated 180 degrees. Color scheme: blue (sequence identity); red (conserved hydrophilic character); purple (conserved hydrophobic character); green indicates positions where a residue is highly prevalent. The letter 'N' designates the N-terminus and 'C' designates the C-terminus of the protein. These structures are visualized the Rasmol (version 2.7.1).

Cytochrome c

The Tasmanian Devil protein identified in the protein database cytochrome c from the bacterium *Thiomicrospira crunogena.* It shares 35% identity with cytochrome c in the overlapping region and the e-value is 4×10^{-3}. The synucleins were thus linked to cytochrome c through linkage with the Tasmanian Devil protein. The alignment between the synucleins and cytochrome c is shown in Figure 50. The regions of the human α-synuclein that are similar to the cytochrome c are highlighted on the helical structure of α-synuclein protein in Figure 51. The cytochrome c class I identified by the Tasmania Devil protein consists of 192 amino acid residues. The portion of the protein which is similar to the N-terminus of the synucleins is between residues 15 and 120 and the similarity lies in the conserved repeat sequences II-V. The cytochrome c protein which transports electrons between complex III and IV in the electron transport chain is a member of the class I cytochromes (Battistuzzi et al., 2001). The alignment between the synucleins and the disparate proteins is shown in Figure 52.

```
                                                                II          III
  1 -MHLNRWKLNPLVLSLTVMMGGALLAACSDDSQQKAAEAVEDVKQSTSEAYEEAKETTQE cytochrome c
  1 ---------------MDVFKKGFSIA------KEGVVGAVEKTKQGVTEAAEKTKEGVMY γ human
  1 ---------------MDVFKKGFSMA------KEGVVAAAEKTKQGVTEAAEKTKEGVMY γ frog
  1 ---------------MDVFKKGFSIA------KEGVVAAAEKTKQGVTEAAEKTKEGVMY γ turkey
  1 ---------------MDVFKKGFSIA------KEGVVGAVEKTKQGVTEAAEKTKEGVMY γ cattle
  1 ---------------MDVFKKGFSIA------KEGVVGAVEKTKQGVTEAAEKTKEGVMY γ pig
  1 ---------------MDVFKKGFSIA------KEGVVGAVEKTKQGVTEAAEKTKEGVMY γ house mouse
  1 ---------------MDVFKKGFSIA------REGVVGAVEKTKQGVTEAAEKTKEGVMY γ norway rat
  1 ---------------MDVFKKGFSIA------KEGVVGAVEKTKQGVTEAAEKTKEGVMY γ rhesus monkey
  1 ---------------MDVFMKGLSMA------KEGVVAAAEKTKQGVTEAAEKTKEGVLY β human
  1 ---------------MDVFMKGLSMA------KEGVVAAAEKTKQGVTEAAEKTKEGVLY β norway rat
  1 ---------------MDVFMKGLSMA------KEGVVAAAEKTKQGVTEAAEKTKEGVLY β house mouse
  1 ---------------MDVFMKGLSMA------KEGVVAAAEKTKQGVTEAAEKTKEGVLY β rhesus monkey
  1 ---------------MDVFMKGLSMA------KEGVVAAAEKTKQGVTEAAEKTKEGVLY β gorilla
 61 VCVCDRVTVVCVQAARDVFMKGLSMA------KEGVVAAAEKTKQGVTEAAEKTKEGVLY β mole rat
  1 ---------------MDVFMKGLSMA------KEGVVAAAEKTKQGVTEAAEKTKEGVLY β cattle
  1 ---------------MDVFMKGLSMA------KEGVVAAAEKTKQGVTEAAEKTKEGVLY β pig
  1 ---------------MDVFMKGLSKA------KEGVVAAAEKTKQGVAEAAGKTKEGVLY α human
  1 ---------------MDVFMKGLSKA------KEGVVAAAEKTKQGVAEAAGKTKEGVLY α mole rat
  1 ---------------MDVFMKGLNKA------KEGVVAAAEKTKQGVAEAAGKTKEGVLY α chicken
  1 ---------------MDVFMKGLSKA------KEGVVAAAEKTKQGVAEAAGKTKEGVLY α elephant
  1 ---------------MDVFMKGLSKA------KEGVVAAAEKTKQGVAEAAGRTKEGVLY α cattle
  1 ---------------MDVFMKGLSKA------KEGVVAAAEKTKQGVAEAAGKTKEGVLY α monkey
  1 ---------------MDVFMKGLSKA------KEGVVAAAEKTKQGVAEAAGKTKEGVLY α norway rat
  1 ----GAVWSKNTSLAMDVFMKGLSKA------KEGVVAAAEKTKQGVAEAAGKTKEGVLY α house mouse

        IV                  V                  VI          VII
 60 VMDETQEAVSDSVDSVEEATESAGEAVSDMTESANETTKDAINEAAEEVDEAVTTASVSG cytochrome c.
 40 VGAKTKENVVQSVTSVAEKTK---EQANAVSEAVVSSVNTVATKTVEEAENIAVTSGVVR γ human
 40 VGAKTKEGVVHSVNTVAEKTK---EQANVVGGAVVSGVNQVSSKTVEGTENVVSSTGLVK γ frog
 40 VGTKTKEGVVQSVTSVAEKTK---EQANVVXXXXXXSVNTVANKTVEGAETIVATTGVIK γ turkey
 40 VGAKTKEGVVQSVTSVAEKTK---EQANAVSEAVVSSVNTVATKTVEEVENIAVTSGVVH γ cattle
 40 VGAKTKEGVVQSVTSVAEKTK---EQASAVSEAVVSSVNTVATKTVEEAENIAVTSGVVR γ pig
 40 VGTKTKENVVQSVTSVAEKTK---EQANAVSEAVVSSVNTVANKTVEEAENIVVTTGVVR γ house mouse
 40 VGTKTKENVVQSVTSVAEKTK---EQANAVSEAVVSSVNTVATKTVEEAENIVVTTGVVR γ norway rat
 40 VGTKTKENVVHSVTSVAEKTK---EQANAVSEAVVSSVNTVAAKTVEEAENIAVTSGVVR γ rhesus monkey
 40 VGSKTREGVVQGVASVAEKTK---EQASHLGGAVFS-----------GAGNIAAATGLVK β human
 40 VGSKTKEGVVQGVASVAEKTK---EQASHLGGAVFS-----------GAGNIAAATGLVK β norway rat
 40 VGSKT-SGVVQGVASVAEKTK---EQASHLGGAVFS-----------GAGNIAAATGLVK β house mouse
 40 VGSKTREGVVQ----VAEKTK---EQASHLGGAVFS-----------GAGNIAAATGLVK β rhesus monkey
 40 V--------------VAEKTK---EQASHLGGAVFS-----------GAGNIAAATGLVK β gorilla
115 VGSKTREGVVQGVASVAEKTK---EQASHLGGAVFS-----------GAGNIAAATGLVK β mole rat
 40 VGSKTREGVVQGVASVAEKTK---EQASHLGGAVFS-----------GAGNIAAATGLVK β cattle
 40 VGSKTREGVVQGVASVAEKTK---EQASHLGGAVFS-----------GAGNIAAATGLVK β pig
 40 VGSKTKEGVVHGVATVAEKTK---EQVTNVGGAVVTGVTAVAQKTVEGAGSIAAATGFVK α human
 40 VGSKTKEGVVHGVTTVAEKTK---EQVTNVGGAVVTGVTAVAQKTVEGAGNIAAATGFVK α mole rat
 40 VGSRTKEGVVHGVTTVAEKTK---EQVSNVGGAVVTGVTAVAQKTVEGAGNIAAATGLVK α chicken
 40 VGSKTKEGVVHGVTTVAEKTK---EQVTNVGEAVVTGVTAVAQKTVEGAGSIAAATGFGK α elephant
 40 VGSKTKEGVVHGVTTVAEKTK---EQVTNVGEAVVTGVTAVAQKTVEGAGSIAAATGFGK α cattle
 40 VGSKTKEGVVHGVATVAEKTK---EQVTNVGGAVVTGVTAVAQKTVEGAGNIAAATGFVK α monkey
 40 VGSKTKEGVVHGVTTVAEKTK---EQVTNVGGAVVTGVTAVAQKTVEGAGNIAAATGFVK α norway rat
 51 VGSKTKEGVVHGVTTVAEKTK---EQVTNVGGAVVTGVTAVAQKTVEGAGNIAAATGFVK α house mouse
```

Figure 50. Sequence alignment of the predicted cytochrome c and 18 synucleins (α, β and γ) from various species

The portion of the protein similar to the synucleins is between residues 15 and 119. The region of similarity involves the repeat sequences II, III, IV and V. Color scheme: blue (sequence identity); red (conserved hydrophilic character); purple (conserved hydrophobic character); green indicates positions where a residue is highly prevalent. The alignment was constructed with MUSCLE. (Edgar, 2004; McWilliam et al., 2013).

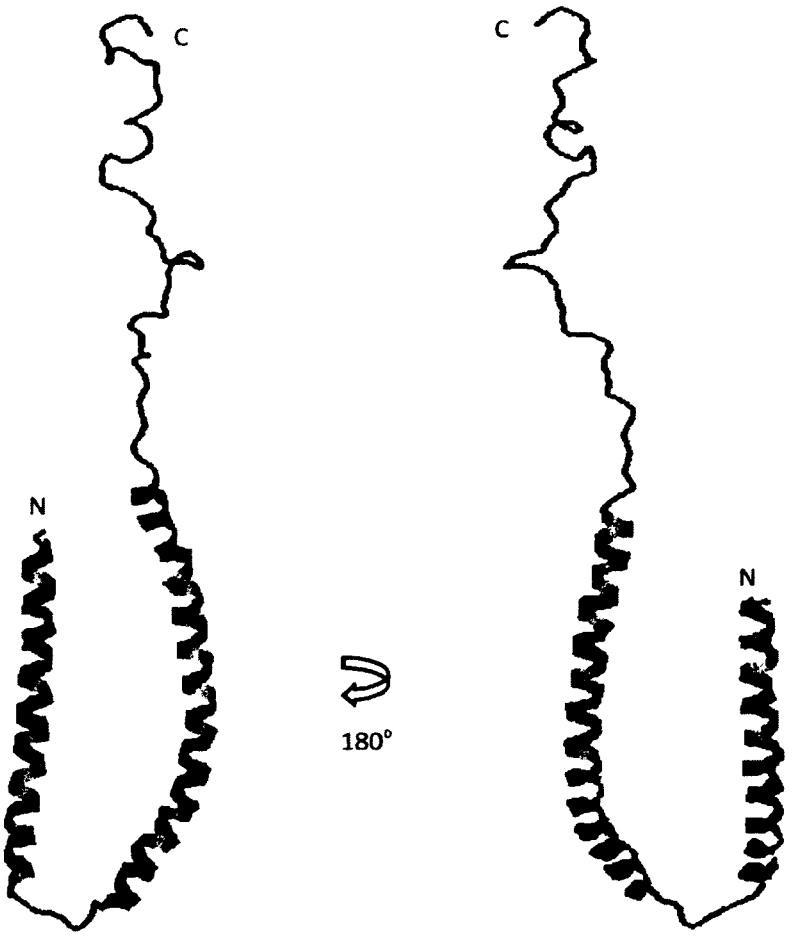

Figure 51. Regions of the human α-synuclein similar to cytochrome c

The colors in the figure indicate the regions within human α-synuclein that are similar to the cytochrome c class I protein (pdb code: 1xq8). The figure was rotated 180 degrees. Color scheme: blue (sequence identity); red (conserved hydrophilic character); purple (conserved hydrophobic character); green indicates positions where a residue is highly prevalent. These structures are visualized with Rasmol (version 2.7.1). The letter 'N' designates the N-terminus and 'C' designates the C-terminus of the protein. These structures are visualized with Rasmol (version 2.7.1).

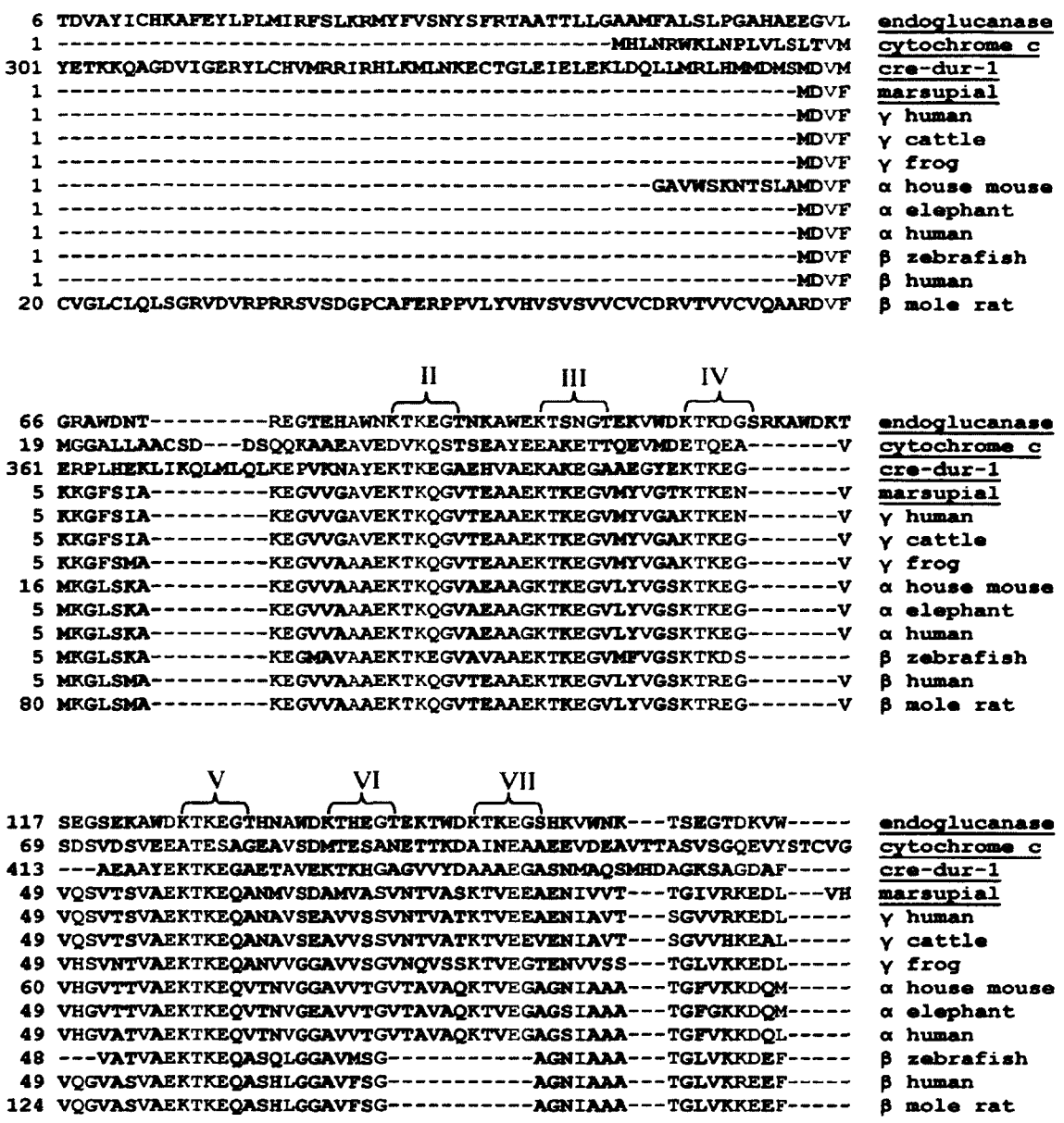

Figure 52. Sequence alignment of variant synucleins with disparate proteins

The seemingly disparate proteins contain the synuclein N-terminal domain. Color scheme: blue (sequence identity); red (conserved hydrophilic character); purple (conserved hydrophobic character); green indicates positions where a residue is highly prevalent. The alignment was constructed with MUSCLE (Edgar, 2004; McWilliam et al., 2013).

Modification sites

The scan prosite algorithm identified sites where a myristic fatty acid and phosphate moieties are predicted to be added to the human synucleins and the disparate sequences. The glycine residues, to which the fatty acid molecules are added by the N-myristoyltransferase, were identified in conserved locations. The threonine/serine and tyrosine residues to which phosphate groups are added by the enzymes casein kinase II and tyrosine kinase respectively, were also identified (Figure 53). The modification sites are highlighted on the helical structure of human α-synuclein (Figure 54).

```
 67 GR--------------------AW------DNTREGTEHAWNKTKEGTNKAWEKTSNGTE  endoglucanase
361 ERPLHEKLIKQLMLQLKEPVKNAY------EKTKEGAEHVAEKAKEGAAEGYEKTKEGAE  cre-dur-1
 19 MG--------------------GALLAACSDDSQQKAAEAVEDVKQSTSEAYEEAKETTQ  cytochrome c
  5 KK--------------------GF------SIAKEGVVGAVEKTKQGVTEAAEKTKEGVM  marsupial
  5 KK--------------------GF------SIAKEGVVGAVEKTKQGVTEAAEKTKEGVM  γ-mouse
  5 KK--------------------GF------SIAKEGVVGAVEKTKQGVTEAAEKTKEGVM  γ-cow
  5 KK--------------------GF------SIAKEGVVGAVEKTKQGVTEAAEKTKEGVM  γ-mulata
  5 KK--------------------GF------SIAKEGVVGAVEKTKQGVTEAAEKTKEGVM  γ-human
  5 KK--------------------GF------SIAKEGVVGAVEKTKQGVTEAAEKTKEGVM  γ-pongo abeli
  5 MK--------------------GF------SKAKDGVVAAAEKTKQGVTGAAEMTKDGVM  α-rubripes
  5 MK--------------------GL------NKAKEGVVAAAEKTKQGVAEAAGKTKEGVL  α-chicken
  5 MK--------------------GL------SKAKEGVVAAAEKTKQGVAEAAGRTKEGVL  α-cow
 16 MK--------------------GL------SKAKEGVVAAAEKTKQGVAEAAGKTKEGVL  α-mouse
  5 MK--------------------GL------SKAKEGVVAAAEKTKQGVAEAAGKTKEGVL  α-human
  5 MK--------------------GL------SMAKEGVVAAAEKTKQGVTEAAEKTKEGVL  β-mouse
  5 MK--------------------GL------SMAKEGVVAAAEKTKQGVTEAAEKTKEGVL  β-human
  5 MK--------------------GL------SMAKEGVVAAAEKTKQGVTEAAEKTKEGVL  β-cow
  5 MK--------------------GL------SKAKEGMAVAAEKTKEGVAVAAEKTKEGVM  β-rubripes
  5 MK--------------------GL------SKAKEGMAVAAEKTKEGVAVAAEKTKEGVM  β-danario

101 KVWDKTKDGSRKAWDKTSEGSEKAWDKTK---EGTHNAWDKTHEGTEKTWDKTKEGSHKV  endoglucanase
415 AAYEKTKEG----AETAVE-------KTK---HGAGVVYDAAAE-----------GASNM  cre-dur-1
 59 EVMDETQEAVSDSVDSVEE-------ATESAGEAVSDMTESANETTKDAINEAAEEVDEA  cytochrome c
 39 YVGTKTKENVVQSVTSVAE-------KTK---EQANMVSDAMVASVNTVASKTVEEAENI  marsupial
 39 YVGTKTKENVVQSVTSVAE-------KTK---EQANAVSEAVVSSVNTVANKTVEEAENI  γ-mouse
 39 YVGAKTKEGVVQSVTSVAE-------KTK---EQANAVSEAVVSSVNTVATKTVEEVENI  γ-cow
 39 YVGTKTKENVVHSVTSVAE-------KTK---EQANAVSEAVVSSVNTVAAKTVEEAENI  γ-mulata
 39 YVGAKTKENVVQSVTSVAE-------KTK---EQANAVSEAVVSSVNTVATKTVEEAENI  γ-human
 39 YVGAKTKENVVQSVTSVAE-------KTK---EQANAVSEAVVNSVNTVATKTVEEAENI  γ-pongo abeli
 39 FVGTKTKDG----VTVVAG-------KTV---SGVSQVGGAMVTGVTAVAQKTVESAGSI  α-rubripes
 39 YVGSRTKEGVVHGVTTVAE-------KTK---EQVSNVGGAVVTGVTAVAQKTVEGAGNI  α-chicken
 39 YVGSKTKEGVVHGVTTVAE-------KTK---EQVTNVGEAVVTGVTAVAQKTVEGAGSI  α-cow
 50 YVGSKTKEGVVHGVTTVAE-------KTK---EQVTNVGGAVVTGVTAVAQKTVEGAGNI  α-mouse
 39 YVGSKTKEGVVHGVATVAE-------KTK---EQVTNVGGAVVTGVTAVAQKTVEGAGSI  α-human
 39 YVGSKT-SGVVQGVASVAE-------KTK---EQASHLGGAVFS-----------GAGNI  β-mouse
 39 YVGSKTREGVVQGVASVAE-------KTK---EQASHLGGAVFS-----------GAGNI  β-human
 39 YVGSKTREGVVQGVASVAE-------KTK---EQASHLGGAVFS-----------GAGNI  β-cow
 39 FVGNKAKDS----VGTVAE-------KTT----------GAM---------------GNI  β-rubripes
 39 FVGSKTKDS----VATVAE-------KTK---EQASQLGGAVMS-----------GAGNI  β-danario
```

Figure 53. Sites for myristoylation and phosphorylation in the synuclein and disparate proteins

The blue color indicates the sites where myristic acid is predicted to be added to the proteins by the enzyme N-myristoyltransferase; the red color indicates sites predicted for phosphorylation by casein kinase II; and the green color indicates sites predicted for phosphorylation by the tyrosine kinase enzyme. The disparate proteins and the synucleins are myristoylated at N-terminal glycines (G) that are in conserved locations. The phosphorylation by casein kinase II occurs at either a threonine (T) or serine residue (S) also in a conserved location. Phosphorylation by tyrosine kinase occurs at tyrosine (Y) residues in a conserved location. The alignment was constructed with MUSCLE (Edgar, 2004; McWilliam et al., 2013).

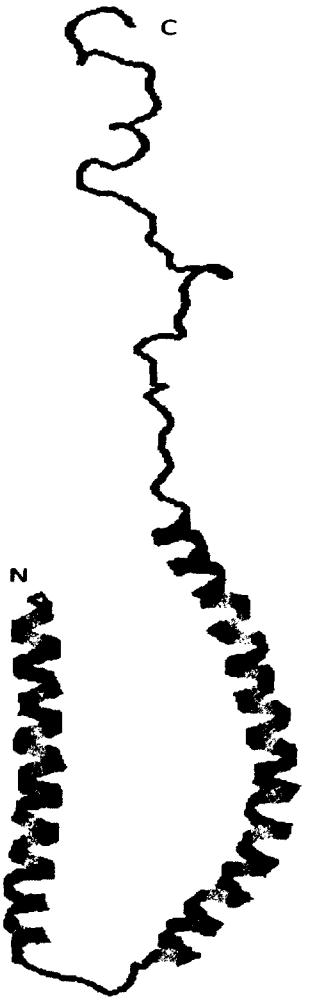

Figure 54. Sites for myristoylation and phosphorylation in the α-synuclein

The blue regions are sites of myristoylation of N-terminal glycines by the N-myristoyltransferase, the green region is the site for phosphorylation of specific tyrosine residues by tyrosine kinase enzyme and the red is the region for phosphorylation of specific threonine/serine residues by the enzyme casein kinase II. The letter 'N' designates the N-terminus and 'C' designates the C-terminus of the protein. This structure is visualized with Rasmol (pdb code: 1xq8) (version 2.7.1).

Protein size, coverage and sequence similarity

The sizes of the human synucleins and their related proteins are summarized in Table 5. The sequence similarity and overlap between each human synuclein and the four disparate proteins according to our results are summarized in Tables 6-8. The percentage similarity between synucleins and the related proteins was obtained as follows: the number of residues of the related protein that were identical or similar to the synuclein was divided by the total length of the related protein and then multiplied by 100. The percentage synuclein coverage was obtained as follows: the length of the synuclein containing regions which were similar to the related protein was divided by the total length of the synuclein and then multiplied by 100. The percent related protein coverage was obtained as follows: the length of the related protein containing regions similar to the synuclein was divided by the total length of the related protein and then multiplied by 100.

Table 5. Sizes of the synucleins and the disparate proteins

Protein	Size of protein (amino acids)
α-Synuclein	140
β-Synuclein	134
γ-Synuclein	127
CRE-DUR-1	524
Endoglucanase	218
Tasmanian Devil	310
Cytochrome c class I	192

Table 6. Similarity between α-synuclein and the four disparate proteins

Protein	% Similarity	[a]Length of α-synuclein	% α-Synuclein coverage	[b]Length of related protein	% Related protein coverage
Endoglucanase	24	109 (1-109)	78	120 (61-180)	55
CRE-DUR-1	9	100 (1-100)	71	108 (357-464)	21
Marsupial	27	113 (1-113)	81	120 (1-120)	39
Cytochrome c	23	96 (1-96)	69	106 (15-120)	55

[a]Length (residues) of α-synuclein containing regions similar to the related protein.
[b]Length (residues) of the related protein containing regions similar to α-synuclein.

Table 7. Similarity between β-synuclein and the four disparate proteins

Protein	%Similarity	[a]Length of β-synuclei	% β-synuclein coverage	[b]Length of related proten	% Related Protein coverage
Endoglucanase	21	105 (1-105)	78	116 (48-163)	53
CRE-DUR-1	7	89 (1-89)	66	108 (357-464)	21
Marsupial	25	107 (1-107)	79	120 (1-120)	39
Cytochrome c	22	85 (1-85)	63	106 (15-120)	55

[a]Length (residues) of β-synuclein containing regions similar to the related protein.
[b]Length (residues) of the related protein containing regions similar to the β-synuclein.

Table 8. Similarity between γ-synuclein and the four disparate proteins

Protein	% Similarity	[a]Length of γ-synuclein	% γ-Synuclein coverage	[b]Length of related protein	% Related protein coverage
Endoglucanase	22	109 (1-109)	85	120 (61-180)	55
CRE-DUR-1	9	100 (1-100)	79	108 (357-464)	21
Marsupial	27	117 (1-117)	92	120 (1-120)	39
Cytochrome c	24	96 (1-96)	76	106 (15-120)	55

[a]Length (residues) of γ-synuclein containing regions similar to the related protein.
[b]Length (residues) of the related protein containing regions similar to γ-synuclein.

The organisms in which the four disparate proteins related to the synucleins are found range from a bacterium to a vertebrate (Figure 55). In this figure are shown images or illustrations of the *Caenorhabditis remanei* nematode, the gram negative bacilli *Acetobacter pomorum*, the gram negative spiral shaped *Thiomicrospira crunogena* and the Tasmanian Devil. A phylogenetics analysis was conducted using the synucleins and the protein sequences identified from these organisms. From the phylogenetic tree constructed the CRE-DUR-1, endoglucanase and β-synuclein proteins seems to be the closest to the ancestor protein and the furthest from the ancestor are γ-synuclein and cytochrome c (Figure 56). The relative distances of the proteins from the ancestor are summarized in Table 9.

A

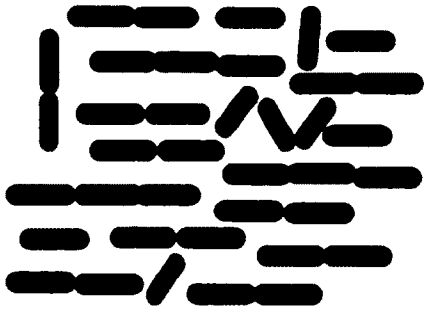

B

C

D

Figure 55. Organisms in which proteins related to the synucleins are found

(A) The protein CRE-DUR-1 is from *Caenorhabditis remanei* nematode. The figure is reproduced from Timmermeyer (Timmermeyer et al., 2010).

(B) Endoglucanase enzyme is from a gram negative bacillus (Sokollek et al., 1998).

(C) Cytochrome c class I is from a motile gram negative spiral shaped bacterium *Thiomicrospira crunogena*. This figure is reproduced from (Jannasch et al., 1985).

(D) The Tasmanian Devil protein is from the Tasmanian Devil. The figure is reproduced from the website: www.devilsatcradle.com.

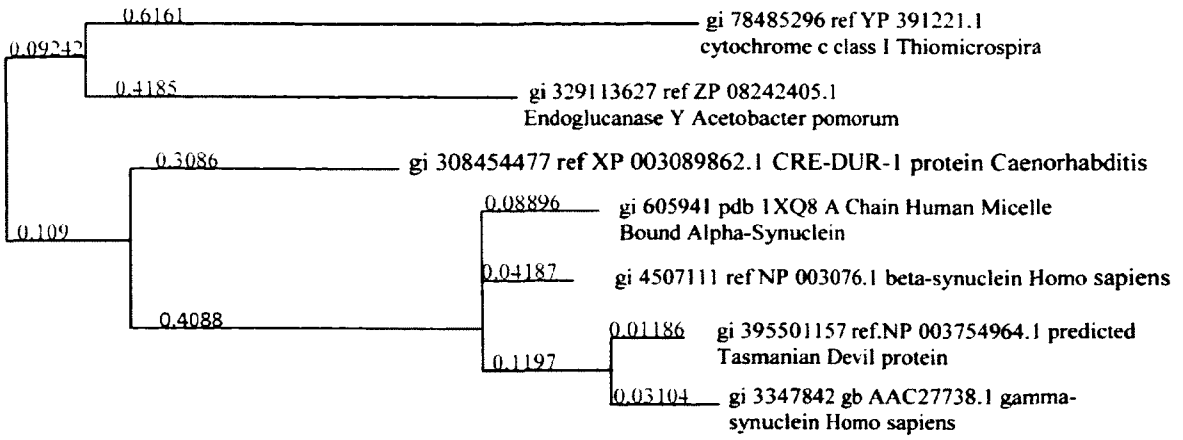

Figure 56. The phylogenetic tree constructed from the human synucleins and the four related proteins

The numbers in red indicate the relative distances between the ancestor and the individual proteins.

Table 9. Relative distances of the proteins from the ancestor

Protein	Relative distance from ancestor
CRE-DUR-1 (0.109 + 0.3086)	0.4176
Endoglucanase (0.09242 + 0.4185)	0.51092
β-synuclein (0.109 + 0.4088 + 0.04187)	0.55967
α-Synuclein (0.109+ 0.4088+ 0.08896)	0.60676
Marsupial (0.109 + 0.4088 + 0.1197 + 0.01186)	0.64936
Cytochrome c (0.09242 + 0.6161)	0.70852
γ-Synuclein (0.109 + 0.4088 + 0.1197 +0.03104)	0.66854

Modeling the protein structures

Interestingly, the model structures of the four disparate proteins show helical and

hairpin structures similar to the micelle bound α-synuclein in Figure 16. Models of the four disparate proteins and the three synuclein proteins are shown in Figures 57 and 58, respectively.

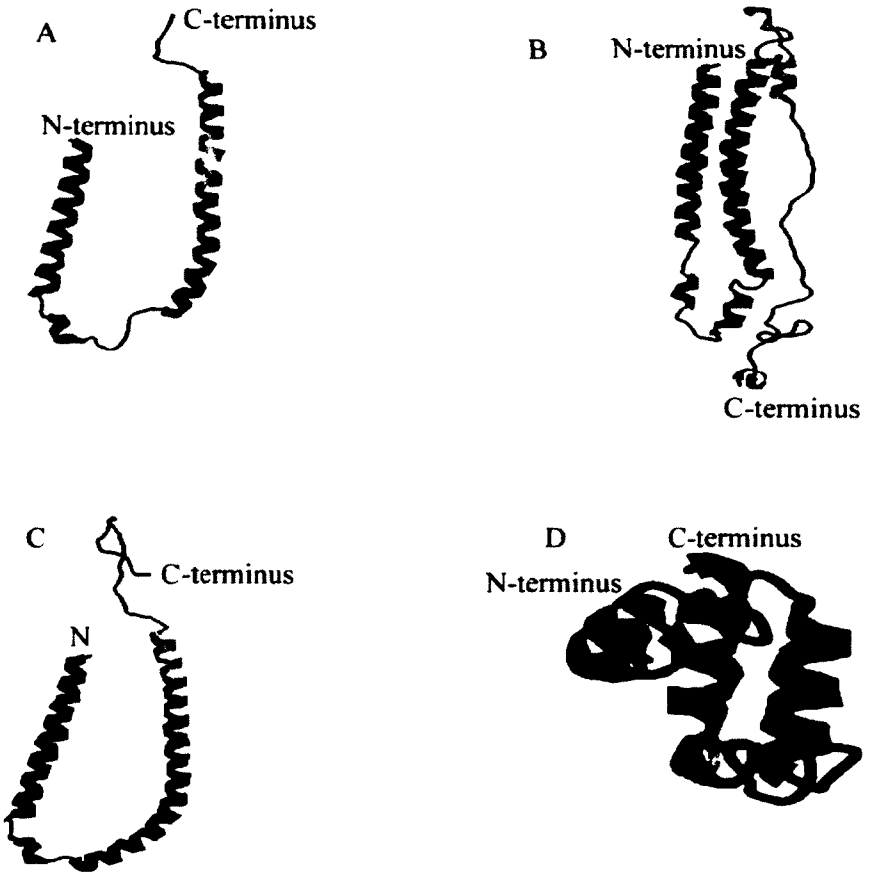

Figure 57. The predicted three-dimensional structure of the disparate proteins related to the synucleins using Swiss-Model

(A) Endoglucanase from a gram negative bacillus *Acetobacter pomorum.*

(B) CRE-DRU-1 protein from the *Caenorhabditis remanei* nematode.

(C) Tasmanian Devil protein from the Tasmanian Devil mammal.

(D) Cytochrome c from a gram negative spiral bacterium *Thiomicrospira crunogena.*

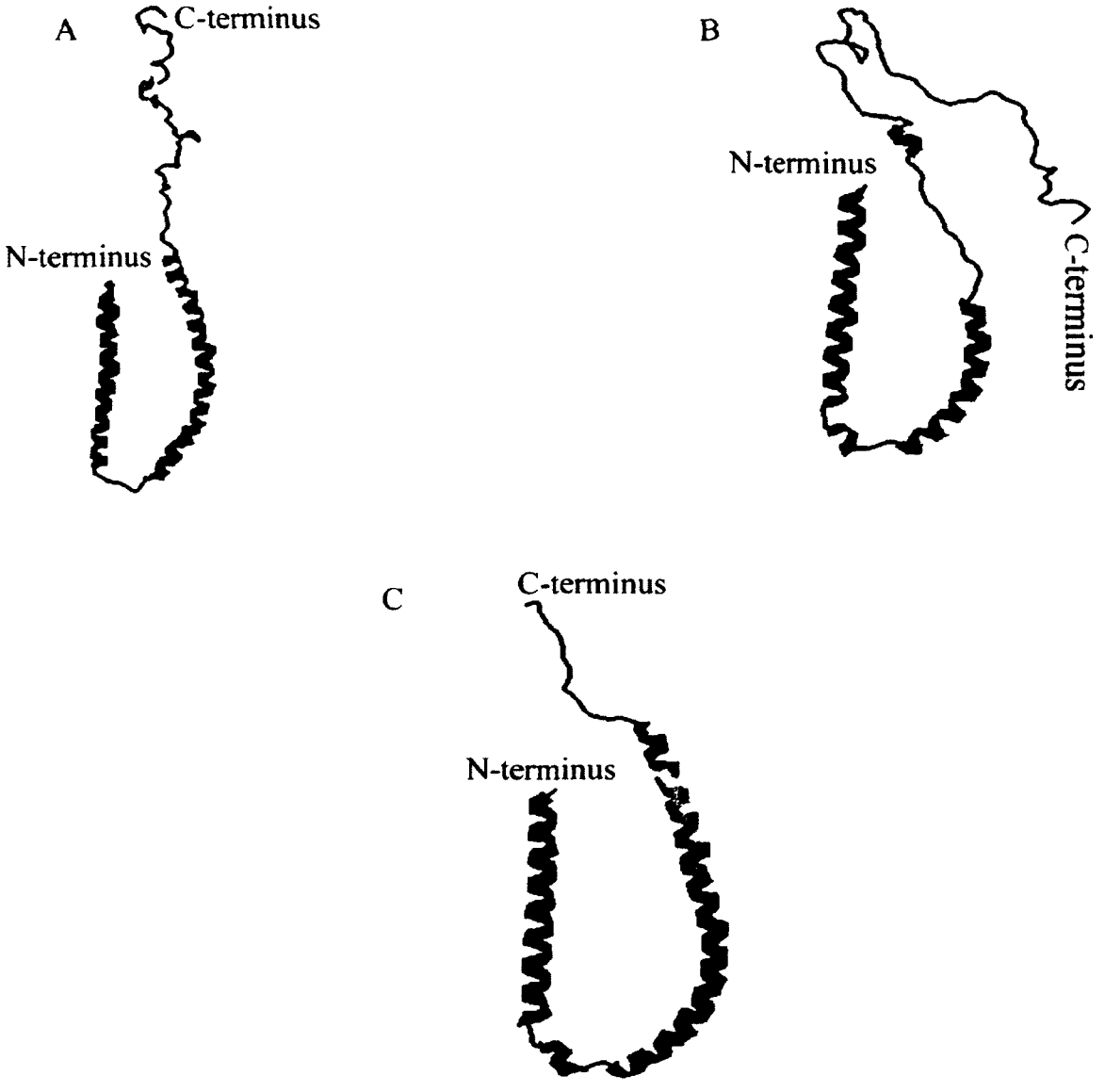

Figure 58. The predicted three-dimensional structure of the synucleins using Swiss-Model

(A) Human α-synuclein.

(B) Human β-synculein.

(C) Human γ-synuclein.

Point mutations and exon locations

An investigation to distinguish any differences between human synucleins and those of other animals, particularly in connection with the A30P, E46K, H50Q, G51D and A53T point mutations was conducted. All of these point mutations are associated with early-onset Parkinson's disease in humans. The mutations from one amino acid to another are caused by one base change either in the first or second position of the triplet codon. The codons and base mutations of the amino acids are shown in Table 10. The color red highlights the point mutations and the green is the normal base present.

Table 10. Codons of amino acid mutations associated with early-onset Parkinson's Disease

Codon	Amino acid	Codon	Amino acid
GCU		CAU	
GCC		CAC	Histidine
GCA		CAA	
GCG	Alanine	CAG	Glutamine
ACU		GGU	
ACC		GGC	Glycine
ACA		GAU	
ACG	Threonine	GAC	Aspartate
CCU		GAA	
CCC		GAG	Glutamate
CCA		AAA	
CCG	Proline	AAG	Lysine

In the A30P and the A53T mutations, the guanine (green) base in the alanine codon is substituted with an adenine (red) and cytosine (red) to generate a threonine and a proline residue respectively. The change of the uracil or cytosine base in the third position (green) in the histidine codon to adenine or guanine results in a glutamine residue in the H50Q mutation. When the guanine base (green) in the second position of the glycine codon is replaced by an adenine (red) the result is an aspartate residue in the G51D mutation. Finally, in the E46K mutation, the guanine base (green) in position one of the glutamate codon is substituted with an adenine (red) and a lysine is produced.

The life spans of humans and other animals whose synucleins were used to study the differences in the synuclein mutations are shown in Table 11. They come from a wide variety of animals ranging from mammals to amphibians, reptiles and birds for example. The ages differ from 4 years for the mouse to 255 for the giant tortoise.

Table 11. The life span of various animals including humans

Animals	Life span (years)
Giant tortoise	150-255
Human	68-112
Crocodile	50-75
Catfish	80
Elephant	60-70
Chimpanzee	53
Sturgeon fish	100
Pygymy chimpanzee	40
Minke whale	50
Gorilla	40-50
Orangutan	50
Crab eating monkey	37
Spider monkey	33
Horse	25-33
Woolly monkey	30
Bear	40
Rhesus monkey	29
Squirrel monkey	21
Cattle	18-25
Pig	15-20
Mouse	4
Zebra finch (bird)	14
Rabbit	9
Dog	22
Cat	25
Gerbil (dessert rat)	5

The source of this information comes from the following: Rowe, (1996); Larsen et al., (2009) and http://sonic.net/-petdoc/lifespan.htm

An alignment of human and other primate α-synucleins was constructed (Figure 59). The green color indicates locations where the mutations A30P, E46K, H50Q, G51D and A53T can occur in humans. The purple color indicates regions in the synucleins that are prone to aggregation (Kumar et al., 2009). The red color indicates amino acid residues different from those of the human α-synuclein at the same location. The α-synucleins of the spider and the woolly monkeys have the mutant A53T while the rest of the primates have the conserved alanine (A), glutamate (E), histidine (H), glycine (G) and alanine (A) at locations 30, 46, 50, 51 and 53 respectively. Simulations studies have

also shown that the ^{36}GVLYVG^{41} sequence forms the loop between the two helices of α-synuclein associated with lipid membrane, while the sequence ^{68}GAVVTGVTAVA^{78} is in the second helix (Kumar et al., 2009) (Figure 60). Both sequences are conserved in the primates compared to α-synuclein.

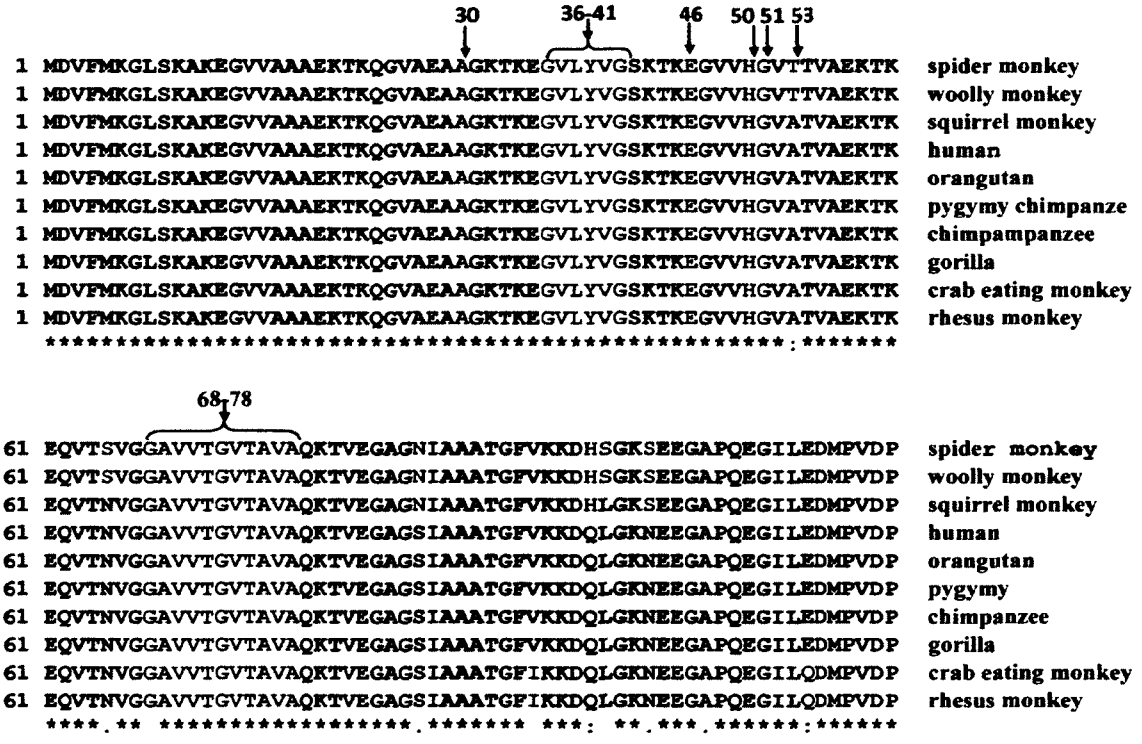

Figure 59. Sequence alignment of human and other primate α-synucleins

The green color indicates the locations where mutations A30P, E46K, H50Q, G51D and A53T can occur. The red color indicates amino acids different from human α-synuclein. The purple regions are prone to aggregation (Kumar et al., 2009). The spider and woolly monkey have a threonine (T) instead of an alanine in location 53. The star symbol indicates identical residues; two dots, very similar; one dot, moderately similar. The alignment was constructed with MUSCLE (Edgar, 2004; McWilliam et al., 2013).

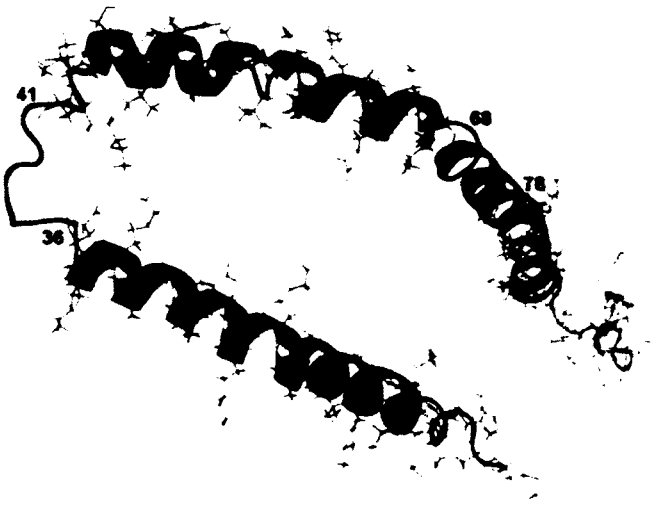

Figure 60. Amyloidogenic regions (blue) of human α-synuclein

This structure was generated by molecular dynamics simulations (Kumar et al., 2009). The figure is reproduced from Kumar (Kumar et al., 2009).

A comparison between human α-synuclein and α-synucleins from wild animals other than primates and from domestic animals showed that all the animals have a threonine residue (T) at location 53 instead of the alanine (A) (Figure 61). The birds including the zebra finch, canary, duck and turkey differ significantly from the human α-synuclein in the sequence stretch between residues 113 and 120. The advantage of this difference from other animals is not yet known.

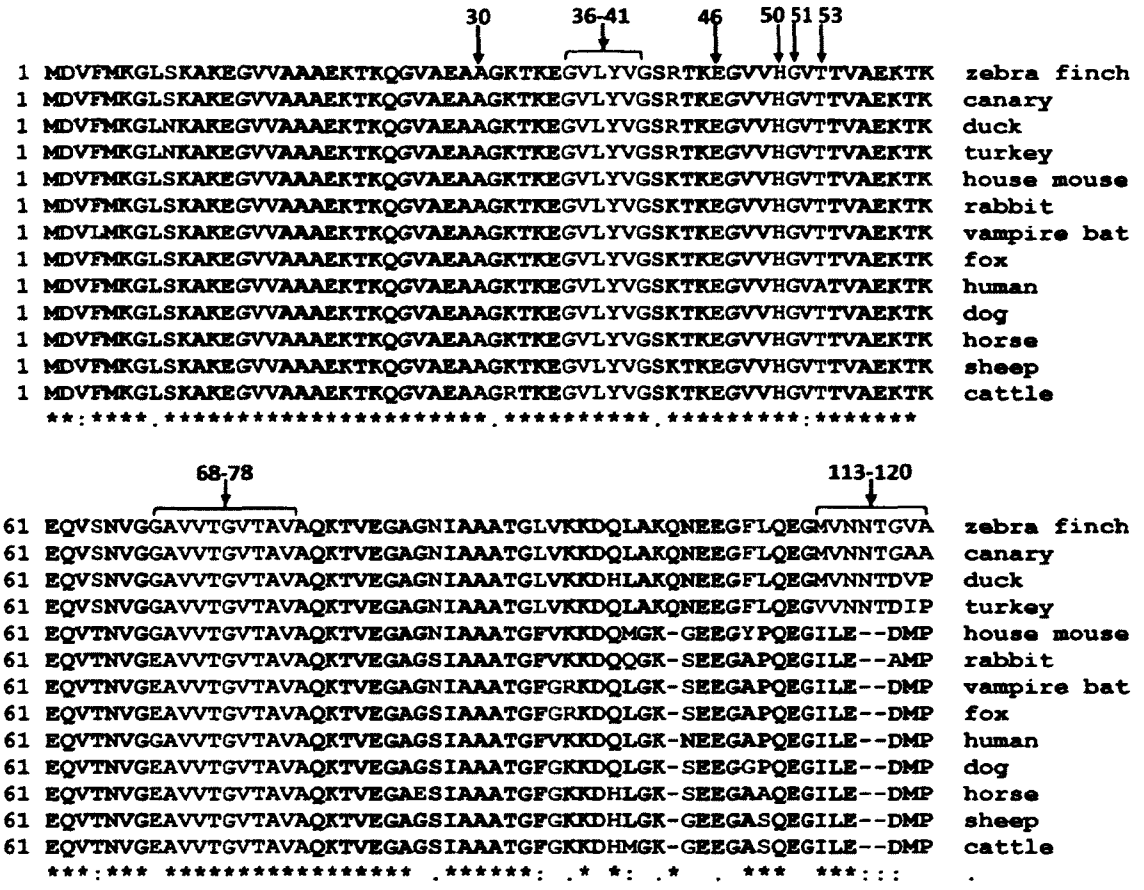

Figure 61. Sequence alignment of human, domestic and wild animal α-synucleins

All the animals have the A53T mutation. The α-synucleins of the birds differ significantly from the human α-synuclein between residues 113 and 120. The purple amyloidogenic regions are intact except for glutamate (E) substitutions for the glycine (G) at position 68 of the 68-78 residue sequence. Color code: green are locations of mutations; purple are the amyloidogenic regions; and red are amino acid residues that are different from those of the human α-synucleins at a given location. In the alignment: the star symbol indicates identical residues; the two dots, very similar; one dot, moderately similar. The alignment was constructed with MUSCLE (Edgar, 2004; McWilliam et al., 2013).

The α-synucleins of long-lived animals have threonine (T) at location 53 (Figure 62). The alignment also indicates truncations of the long-lived animal synucleins at both the N- and the C-termini. The long-lived animals lack the ^{1}MDVF^{4} and the ^{130}EEGYQDYEPEA^{140}sequences that are present in the human α-synuclein. The truncations result in shorter α-synucleins ranging from 124-125 amino acids in length. Interestingly, this is not observed in other animals (Figure 62).

The β-synuclein alignment indicates that some animals have a substitution at the glutamate (E) location (46). The observed substitutions are aspartate (D), glutamine (Q) or serine (S) (Figure 63). Also, some animals have threonine (T) or glycine (G) instead of the alanine (A) at position 53. The salmon, zebra, rainbow smelt fish and the African clawed frog have several substitutions in the 36-41 amyloidogenic sequence. Both humans and animals have extensive substitutions in the 68-78 amyloidogenic sequence. Interestingly, both humans and other animals have glutamine (Q) at location 50 instead of a histidine (H) as was observed for α-synucleins.

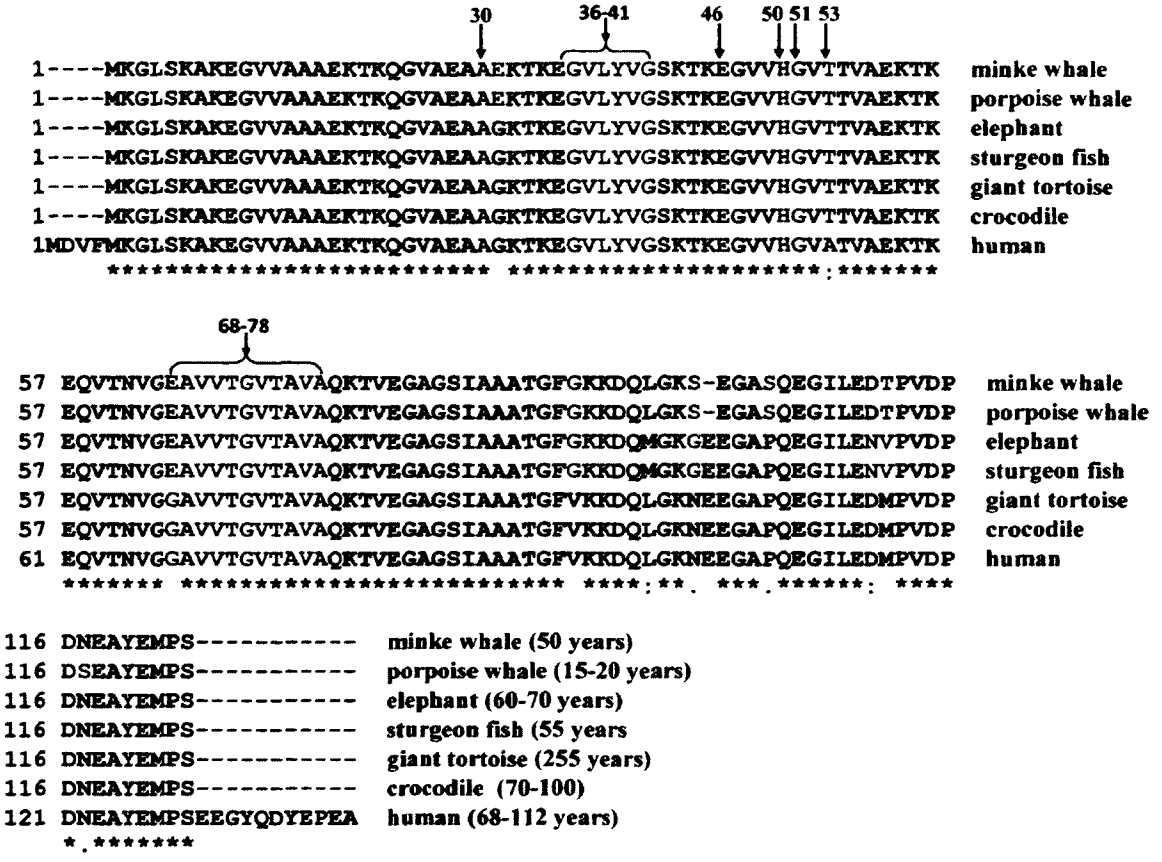

Figure 62. Sequence alignment of human and long-lived animal α-synucleins

The animals have shorter α-synucleins ranging from 124 to125 amino acid residues. There are truncations at the N- and the C-terminus. There is a threonine residue (T) at location 53 in all the animals. Color code: green are locations of possible mutations; purple are the amyloidogenic regions; and red are amino acid residues different from those of the human α-synucleins at a given location. The alignment was constructed with MUSCLE (Edgar, 2004; McWilliam et al., 2013).

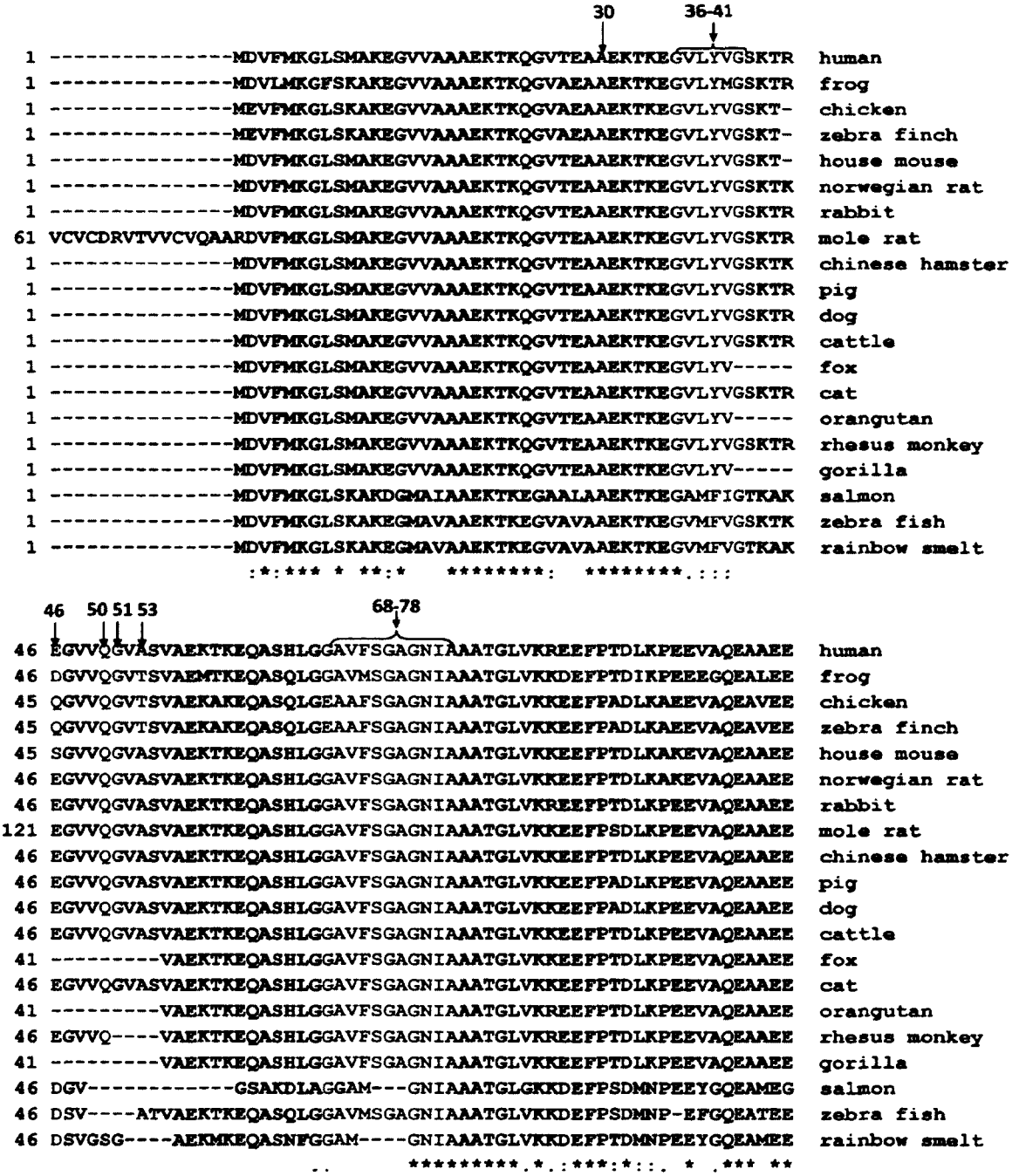
30
36-41
1 ----------MDVFMKGLSMAKEGVVAAAEKTKQGVTEAAEKTKEGVLYVGSKTR human
1 ----------MDVLMKGFSKAKEGVVAAAEKTKQGVAEAAEKTKEGVLYMGSKTR frog
1 ----------MEVFMKGLSKAKEGVVAAAEKTKQGVAEAAEKTKEGVLYVGSKT- chicken
1 ----------MEVFMKGLSKAKEGVVAAAEKTKQGVAEAAEKTKEGVLYVGSKT- zebra finch
1 ----------MDVFMKGLSMAKEGVVAAAEKTKQGVTEAAEKTKEGVLYVGSKT- house mouse
1 ----------MDVFMKGLSMAKEGVVAAAEKTKQGVTEAAEKTKEGVLYVGSKTK norwegian rat
1 ----------MDVFMKGLSMAKEGVVAAAEKTKQGVTEAAEKTKEGVLYVGSKTR rabbit
61 VCVCDRVTVVCVQAARDVFMKGLSMAKEGVVAAAEKTKQGVTEAAEKTKEGVLYVGSKTR mole rat
1 ----------MDVFMKGLSMAKEGVVAAAEKTKQGVTEAAEKTKEGVLYVGSKTK chinese hamster
1 ----------MDVFMKGLSMAKEGVVAAAEKTKQGVTEAAEKTKEGVLYVGSKTR pig
1 ----------MDVFMKGLSMAKEGVVAAAEKTKQGVTEAAEKTKEGVLYVGSKTR dog
1 ----------MDVFMKGLSMAKEGVVAAAEKTKQGVTEAAEKTKEGVLYVGSKTR cattle
1 ----------MDVFMKGLSMAKEGVVAAAEKTKQGVTEAAEKTKEGVLYV----- fox
1 ----------MDVFMKGLSMAKEGVVAAAEKTKQGVTEAAEKTKEGVLYVGSKTR cat
1 ----------MDVFMKGLSMAKEGVVAAAEKTKQGVTEAAEKTKEGVLYV----- orangutan
1 ----------MDVFMKGLSMAKEGVVAAAEKTKQGVTEAAEKTKEGVLYVGSKTR rhesus monkey
1 ----------MDVFMKGLSMAKEGVVAAAEKTKQGVTEAAEKTKEGVLYV----- gorilla
1 ----------MDVFMKGLSKAKDGMAIAAEKTKEGAALAAEKTKEGAMFIGTKAK salmon
1 ----------MDVFMKGLSKAKEGMAVAAEKTKEGVAVAAEKTKEGVMFVGSKTK zebra fish
1 ----------MDVFMKGLSKAKEGMAVAAEKTKEGVAVAAEKTKEGVMFVGTKAK rainbow smelt
:*:*** * **:* ******** ********.:::
46 50 51 53
68-78
46 EGVVQGVASVAEKTKEQASHLGGAVFSGAGNIAAATGLVKREEFPTDLKPEEVAQEAAEE human
46 DGVVQGVTSVAEMTKEQASQLGGAVMSGAGNIAAATGLVKKDEFPTDIKPEEEGQEALEE frog
45 QGVVQGVTSVAEKAKEQASQLGEAAFSGAGNIAAATGLVKKEEFPADLKAEEVAQEAVEE chicken
45 QGVVQGVTSVAEKAKEQASQLGEAAFSGAGNIAAATGLVKKEEFPADLKAEEVAQEAVEE zebra finch
45 SGVVQGVASVAEKTKEQASHLGGAVFSGAGNIAAATGLVKKEEFPTDLKAKEVAQEAAEE house mouse
46 EGVVQGVASVAEKTKEQASHLGGAVFSGAGNIAAATGLVKKEEFPTDLKAKEVAQEAAEE norwegian rat
46 EGVVQGVASVAEKTKEQASHLGGAVFSGAGNIAAATGLVKREEFPTDLKPEEVAQEAAEE rabbit
121 EGVVQGVASVAEKTKEQASHLGGAVFSGAGNIAAATGLVKKEEFPSDLKPEEVAQEAAEE mole rat
46 EGVVQGVASVAEKTKEQASHLGGAVFSGAGNIAAATGLVKKEEFPTDLKPEEVAQEAAEE chinese hamster
46 EGVVQGVASVAEKTKEQASHLGGAVFSGAGNIAAATGLVKKEEFPADLKPEEVAQEAAEE pig
46 EGVVQGVASVAEKTKEQASHLGGAVFSGAGNIAAATGLVKKEEFPADLKPEEVAQEAAEE dog
46 EGVVQGVASVAEKTKEQASHLGGAVFSGAGNIAAATGLVKKEEFPTDLKPEEVAQEAAEE cattle
41 ---------VAEKTKEQASHLGGAVFSGAGNIAAATGLVKKEEFPTDLKPEEVAQEAAEE fox
46 EGVVQGVASVAEKTKEQASHLGGAVFSGAGNIAAATGLVKKEEFPTDLKPEEVAQEAAEE cat
41 ---------VAEKTKEQASHLGGAVFSGAGNIAAATGLVKREEFPTDLKPEEVAQEAAEE orangutan
46 EGVVQ----VAEKTKEQASHLGGAVFSGAGNIAAATGLVKREEFPTDLKPEEVAQEAAEE rhesus monkey
41 ---------VAEKTKEQASHLGGAVFSGAGNIAAATGLVKKEEFPTDLKPEEVAQEAAEE gorilla
46 DGV----------GSAKDLAGGAM---GNIAAATGLGKKDEFPSDMNPEEYGQEAMEG salmon
46 DSV----ATVAEKTKEQASQLGGAVMSGAGNIAAATGLVKKDEFPSDMNP-EFGQEATEE zebra fish
46 DSVGSG----AEKMKEQASNFGGAM----GNIAAATGLVKKDEFPTDMNPEEYGQEAMEE rainbow smelt
.. ********.*.:***:*:. * .*** **

Figure 63. Sequence alignment of human and other animal β-synucleins

Color code: green are locations of possible mutations: purple are the amyloidogenic regions; red are amino acid residues different from those of the human α-synucleins at a given location. In the alignment: the star symbol indicates identical residues; the two dots, very similar ones; and one dot, moderately similar ones. The alignment was constructed with MUSCLE (Edgar, 2004; McWilliam et al., 2013).

γ-Synucleins in both humans and animals have the threonine (T) at location 53 (Fig. 64). Fish and frog have asparagine (N) instead of threonine at this position. The leucine (L) in the 36-41 amyloidogenic sequence is substituted with either isoleucine (I) or methionine (M). The 68-78 amyloidogenic sequence is extensively substituted. The alanine (A) in position 30 and the glutamate (E) in position 46 are conserved in both humans and animals. γ-Synuclein in humans and the majority of animals have glutamine (Q) instead of histidine (H) in location 50, serine (S) instead of glycine (G) at location 51 and threonine (T) instead of alanine (A) at location 53.

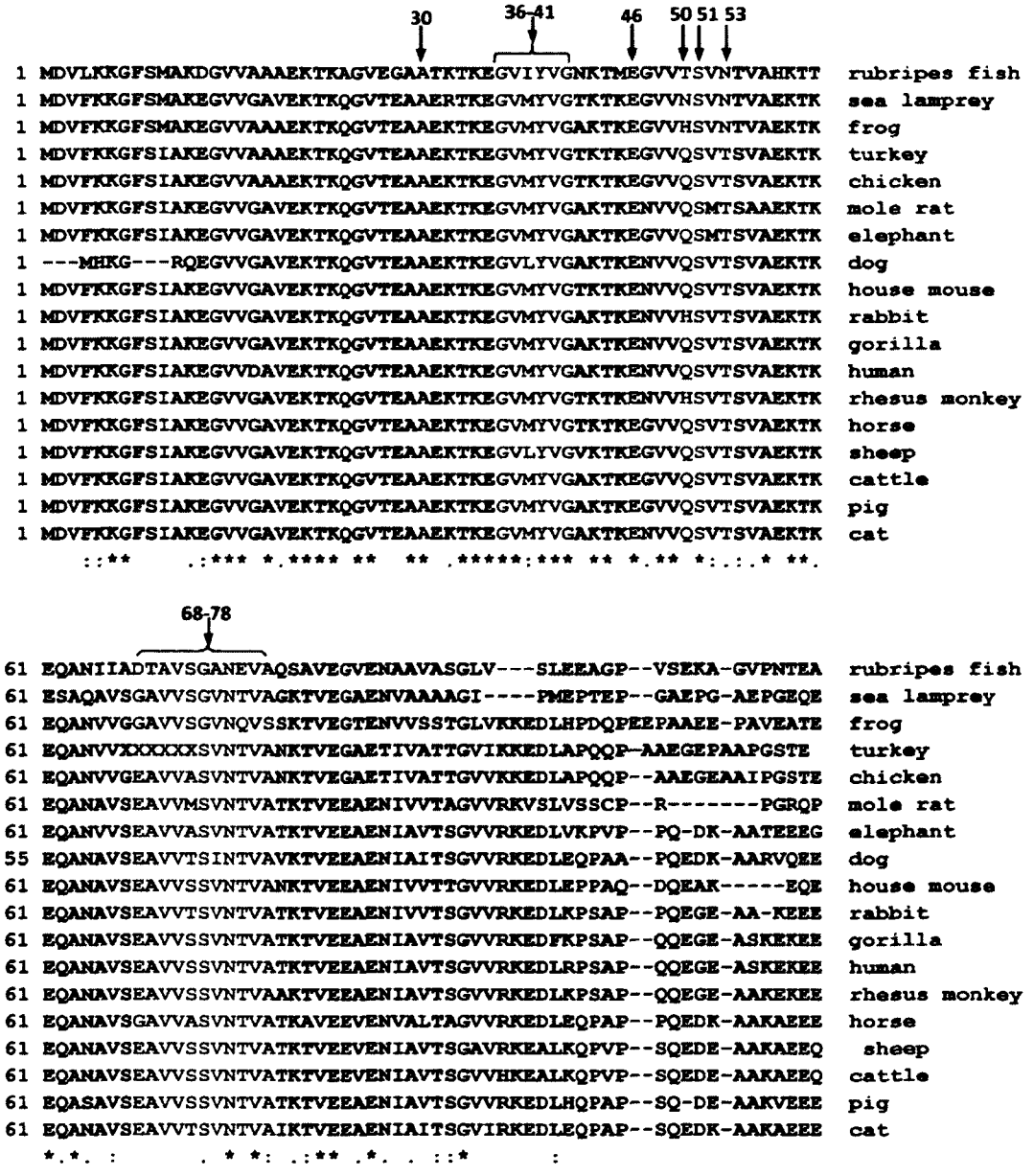
30
36-41
46
50 51 53
1 MDVLKKGFSMAKDGVVAAAEKTKAGVEGAATKTKEGVIYVGNKTMEGVVTSVNTVAHKTT rubripes fish
1 MDVFKKGFSMAKEGVVGAVEKTKQGVTEAAERTKEGVMYVGTKTKEGVVNSVNTVAEKTK sea lamprey
1 MDVFKKGFSMAKEGVVAAAEKTKQGVTEAAEKTKEGVMYVGAKTKEGVVHSVNTVAEKTK frog
1 MDVFKKGFSIAKEGVVAAAEKTKQGVTEAAEKTKEGVMYVGTKTKEGVVQSVTSVAEKTK turkey
1 MDVFKKGFSIAKEGVVAAAEKTKQGVTEAAEKTKEGVMYVGTKTKEGVVQSVTSVAEKTK chicken
1 MDVFKKGFSIAKEGVVGAVEKTKQGVTEAAEKTKEGVMYVGAKTKENVVQSMTSAAEKTK mole rat
1 MDVFKKGFSIAKEGVVGAVEKTKQGVTEAAEKTKEGVMYVGAKTKEGVVQSMTSVAEKTK elephant
1 ---MHKG---RQEGVVGAVEKTKQGVTEAAEKTKEGVLYVGAKTKENVVQSVTSVAEKTK dog
1 MDVFKKGFSIAKEGVVGAVEKTKQGVTEAAEKTKEGVMYVGTKTKENVVQSVTSVAEKTK house mouse
1 MDVFKKGFSIAKEGVVGAVEKTKQGVTEAAEKTKEGVMYVGAKTKENVVHSVTSVAEKTK rabbit
1 MDVFKKGFSIAKEGVVGAVEKTKQGVTEAAEKTKEGVMYVGAKTKENVVQSVTSVAEKTK gorilla
1 MDVFKKGFSIAKEGVVDAVEKTKQGVTEAAEKTKEGVMYVGAKTKENVVQSVTSVAEKTK human
1 MDVFKKGFSIAKEGVVGAVEKTKQGVTEAAEKTKEGVMYVGTKTKENVVHSVTSVAEKTK rhesus monkey
1 MDVFKKGFSIAKEGVVGAVEKTKQGVTEAAEKTKEGVMYVGTKTKEGVVQSVTSVAEKTK horse
1 MDVFKKGFSIAKEGVVGAVEKTKQGVTEAAEKTKEGVLYVGVKTKEGVVQSVTSVAEKTK sheep
1 MDVFKKGFSIAKEGVVGAVEKTKQGVTEAAEKTKEGVMYVGAKTKEGVVQSVTSVAEKTK cattle
1 MDVFKKGFSIAKEGVVGAVEKTKQGVTEAAEKTKEGVMYVGAKTKEGVVQSVTSVAEKTK pig
1 MDVFKKGFSIAKEGVVGAVEKTKQGVTEAAEKTKEGVMYVGAKTKENVVQSVTSVAEKTK cat
::** .:*** *.**** ** ** .*****:*** ** *.** *:.:.* **.
68-78
61 EQANIIADTAVSGANEVAQSAVEGVENAAVASGLV---SLEEAGP--VSEKA-GVPNTEA rubripes fish
61 ESAQAVSGAVVSGVNTVAGKTVEGAENVAAAAGI----PMEPTEP--GAEPG-AEPGEQE sea lamprey
61 EQANVVGGAVVSGVNQVSSKTVEGTENVVSSTGLVKKEDLHPDQPEEPAAEE-PAVEATE frog
61 EQANVVXXXXXXSVNTVANKTVEGAETIVATTGVIKKEDLAPQQP--AAEGEPAAPGSTE turkey
61 EQANVVGEAVVASVNTVANKTVEGAETIVATTGVVKKEDLAPQQP--AAEGEAAIPGSTE chicken
61 EQANAVSEAVVMSVNTVATKTVEEAENIVVTAGVVRKVSLVSSCP--R-------PGRQP mole rat
61 EQANVVSEAVVASVNTVATKTVEEAENIAVTSGVVRKEDLVKPVP--PQ-DK-AATEEEG elephant
55 EQANAVSEAVVTSINTVAVKTVEEAENIAITSGVVRKEDLEQPAA--PQEDK-AARVQEE dog
61 EQANAVSEAVVSSVNTVANKTVEEAENIVVTTGVVRKEDLEPPAQ--DQEAK-----EQE house mouse
61 EQANAVSEAVVTSVNTVATKTVEEAENIVVTSGVVRKEDLKPSAP--PQEGE-AA-KEEE rabbit
61 EQANAVSEAVVSSVNTVATKTVEEAENIAVTSGVVRKEDFKPSAP--QQEGE-ASKEKEE gorilla
61 EQANAVSEAVVSSVNTVATKTVEEAENIAVTSGVVRKEDLRPSAP--QQEGE-ASKEKEE human
61 EQANAVSEAVVSSVNTVAAKTVEEAENIAVTSGVVRKEDLKPSAP--QQEGE-AAKEKEE rhesus monkey
61 EQANAVSGAVVASVNTVATKAVEEVENVALTAGVVRKEDLEQPAP--PQEDK-AAKAEEE horse
61 EQANAVSEAVVSSVNTVATKTVEEVENIAVTSGAVRKEALKQPVP--SQEDE-AAKAEEQ sheep
61 EQANAVSEAVVSSVNTVATKTVEEVENIAVTSGVVHKEALKQPVP--SQEDE-AAKAEEQ cattle
61 EQASAVSEAVVSSVNTVATKTVEEAENIAVTSGVVRKEDLHQPAP--SQ-DE-AAKVEEE pig
61 EQANAVSEAVVTSVNTVAIKTVEEAENIAITSGVIRKEDLEQPAP--SQEDK-AAKAEEE cat
.. : . * *: .:** .*. . ::* :

Figure 64. Sequence alignment of human and other animal γ-synucleins

γ-Synucleins of frog, rabbit and rhesus monkey have histidine (H) in location 50 while the other animals including humans have glutamine (Q). γ-Synucleins of both humans and animals have a serine (S) in location 51 instead of a glycine (G) as is the case in α- and β-synuclein (Figures 61 and 63). In addition, in location 53, some animals have an asparagine (N) instead of threonine (T). Color code: green are locations of possible mutations; purple are the amyloidogenic regions; and red are amino acid residues different from those of the human α-synuclein at a given location. In the alignment: the star symbol indicates identical residues: the two dots, very similar ones; and one dot, moderately similar ones. The alignment was constructed with MUSCLE (Edgar, 2004; McWilliam et al., 2013).

The observations made of the synuclein mutations in humans and other animals are summarized in Table 12. Among the primates. the woolly and spider monkey α-synucleins have a threonine at location 53 instead of an alanine residue. Long-lived and other animal α-synucleins also have a threonine at location 53. β-synucleins have a glutamate. aspartate or glutamine residue at location 46. They also have a glutamine at location 50 instead of a histidine. At location 53. they have either an alanine or a threonine residue. γ-Synucleins have substitutions at locations 50, 51 and 53.

The segments of the α-, β- and γ-synuclein genes that translate into the degenerate repeat sequences were identified. The repeat sequences are indicated by the purple color and are underlined (Tables 13-15). For α-synuclein, exon two contains the first, second and third degenerate repeat sequences. The third exon contains the fourth, while the fourth exon contains the fifth, sixth and seventh repeat sequences (Table 13). For β-synuclein, the first, second and third repeat sequences are in exon three The fourth repeat sequence is in exon four. The fifth and the truncated sixth and seventh repeat sequences are in exon three (Table 15).

Table 12. Point mutations in the synucleins

Protein	**[a]Locations of select key mutations**				
	A30P	E46K	H50Q	G51D	A53T
Primate α-synucleins	A	E	H	G	A
Woolly and spider monkey α-synucleins	A	E	H	G	T
Long-lived animal α-synucleins	A	E	H	G	T
Other animal α-synucleins	A	E	H	G	T
β-synucleins	A	E/D/Q	Q	G	A/T
γ-synucleins	A	E	T/Q/H	S	N/T

[a]Alanine (A); Glutamate (E); Histidine (H); Lysine (K); Asparagine (N); Proline (P); Glutamine (Q); Serine (S); Threonine (T)

Table 13. α-Synuclein exons that encode the degenerate repeat sequences

Exon	DNA sequence	Amino acid
Exon 2	atg gat gta ttc atg aaa gga ctt tca aag gcc aag gag gga gtt gtg gct gct gct gag aaa acc aaa cag ggt gtg gca gaa gca gca gga aag aca aaa gag ggt gtt ctc tat gta	1 MDVFMKGL SKAKEGVVAAA EKTKQGVAEAA GKTKEGVLYV
Exon 3	ggc tcc aaa acc aag gag gga gtg gtg cat ggt gtg gca aca gtg gct	41 G SKTKEGVVHGV ATVA
Exon4	gag aag acc aaa gag caa gtg aca aat gtt gga gga gca gtg gtg acg ggt gtg aca gca gta gcc cag aag aca gtg gag gga gca ggg agc att gca gca gcc act ggc ttt gtc aaa aag gac cag ttg ggc aag	57 EKTKEQVTNVG GAVVTGVTAVA QKTVEGAGSIA AATGFVKKDQLGK

Table 14. β-Synuclein exons that encode the degenerate repeat sequences

Exon	DNA sequence	Amino acid sequence
Exon 3	atg gac gtg ttc atg aag ggc ctg tcc atg gcc aag gag ggc gtt gtg gca gcc gcg gag aaa acc aag cag ggg gtc acc gag gcg gcg gag aag acc aag gag ggc gtc ctc tac gtc	1 MDVFMKGL SMAKEGVVAAA EKTKQGVTEAA EKTKEGVLYV
Exon 4	gga agc aag acc cga gaa ggt gtg gta caa ggt gtg gct tca gtg gct	41 G SKTREGVVQGV ASVA
Exon 5	gag aag acc aaa gag caa gtg aca aat gtt gga gga gca gtg gtg acg ggt gtg aca gca gta gcc cag aag aca gtg gag gga gca ggg agc att gca gca gcc act ggc ttt gtc aaa aag gac cag ttg ggc aag	57 EKTKEQASHLG GAVFS GAGNIA AATGLVKREEFPTDLK

Table 15. γ-Synuclein exons that encode the degenerate repeat sequences		
Exon	**DNA sequence**	**Amino acid sequence**
Exon 1	atg gat gtc ttc aag aag ggc ttc tcc atc gcc aag gag ggc gtg gtg ggt gcg gtg gaa aag acc aag cag ggg gtg acg gaa gca gct gag aag acc aag gag ggg gtc atg tat gtg	1 MDVFKKGF SIAKEGVVGAV EKTKQGVTEAA EKTKEGVMYV
Exon 2	gga gcc aag acc aag gag aat gtt gta cag agc gtg acc tca gtg gcc	41 G AKTKENVVQSV TSVA
Exon 3	gag aag acc aag gag cag gcc aac gcc gtg agc gag gct gtg gtg agc agc gtc aac act gtg gcc acc aag acc gtg gag gag gcg gag aac atc gcg gtc acc tcc ggg gtg gtg cgc aag	57 EKTKEQANAVS EAVVSSVNTVA TKTVEEAENIA VTSGVVRK

DISCUSSION

Among the synucleins, there is variability in size with some proteins containing 121 residues (mole rat α-synuclein), while others are composed of 210 residues (mole rat β-synuclein). For the long synucleins, the extra residues are added at the N-terminus, (Figures 40 and 42). There are also truncations at either the N- or C-terminus or both, as is the case for α-synucleins in long-lived animals (Figure 62). The histidine residue at location 50 is only seen for the α-synucleins. This histidine in α-synucleins is necessary for binding copper. As already discussed in a previous section, α-synucleins have a copper-dependent ferrireductase enzyme activity (Davies et al., 2011). Further, α- and β-synuclein have an alanine at position 53 while γ-synuclein has a threonine which is interesting, as a mutation in α-synuclein to threonine is found in some patients with early-onset Parkinson's. Lastly, all three synucleins vary in the number of exons with β-synuclein having 7, and α- and γ-synuclein having 6 and 5, respectively which suggests deletion was involved in the evolution of the latter two.

The synucleins and their related proteins

Our bioinformatics results indicate that the synucleins do not appear to belong to a superfamily in animals. However, they share a marginal relationship to four disparate proteins which include an endoglucanase enzyme, a CRE-DUR-1 protein, a marsupial (Tasmanian Devil) protein and cytochrome c. The similarity between the synucleins and the endoglucanase, the CRE-DUR-1 and the cytochrome c proteins is based on the presence of the hexameric KTK(E/Q)GV motif in their polypeptide sequences. The N-terminus of the marsupial protein is almost identical to that of the synucleins (Figure 48).

The endoglucanase enzyme from bacterium *Acetobacter pomorum* shares 20-35% similarity with the human synucleins as indicated in Tables 2-4. The protein belongs to a group of enzymes in bacteria and fungi which are responsible for wood decay by breaking the β-1,4-glycosidic bonds in cellulose to generate smaller saccharides. A characterized endoglucanase (218 amino acids) from a fungus is composed of two β-sheet sandwiches and one α-helix (Sandgren et al., 2001), while another from bacterium *Thermotoga maritime* contains α-helices and β-sheets arranged into a barrel shape (Pereira et al., 2010). The synucleins are heat stable at 100°C. Interestingly, some endoglucanase enzymes are also thermophiles that are stable at 70°C, such as an endoglucanase from the fungus *Daldinia eschscholziii* (Karnchanatat et al., 2008). The endoglucanase from the bacterium *Acetobacter pomorum* has not yet been characterized. It is possible that the synuclein-like repeats are interacting with the cellulose.

The second relative of the synucleins retrieved from the database was the protein from the Tasmanian Devil which shares 80%, 65% and 55% similarity with human γ-,α- and β-synuclein respectively (Tables 2-4). The protein is composed of 310 amino acid residues. The marsupial polypeptide sequence has an alanine (A) at location 30 a glutamate (E) at location 46, a glutamine (Q) at location 50, a serine (S) at location 51 and a threonine (T) at location 53. This pattern is similar to the one observed in the γ-synucleins (Figure 64). The N-terminus domain of the marsupial protein may have a function similar to that of the N-terminus of γ-synucleins.

The CRE-DUR-1 is a large protein composed of 524 amino acid residues. The segment of the polypeptide that is similar to the synucleins is the stretch between residues 356 and 463 and begins with MDV (methionine, aspartate and valine, respectively) which is similar to the synucleins (Figure 45). The CRE-DUR-1 protein shares 36% similarity with α- and γ synucleins, and 32% with the β-synuclein (Tables 2-4). The phylogenetic tree (Figure 56) appears to indicate that the CRE-DUR-1 protein is the one closest to the ancestor and is also closer to the synucleins than the endoglucanase and cytochrome c. The 108 amino acid section of similar residues of CRE-DUR-1 appears to correspond to the synuclein N-terminal domain. The CRE-DUR-1 has not been characterized and its function in the nematode is not known. However, the CRE-DUR-1 shares 27% (e-value $=7 \times 10^{-9}$) sequence identity with the late embryogenesis abundant (LEA) proteins. LEA proteins in a nematode *Aphelenchus avenae* have a chaperone-like function (Goyal et al., 2005). They protect other proteins in the worm from aggregation induced by desiccation. The proteins are described as

greatly hydrophilic and unstructured in solution (Goyal et al., 2005). The CRE-DUR-1 may have a similar function as the LEA-1 proteins.

The fourth protein related to the synucleins is cytochrome c class I from the bacterium *Thiomicrospira crunogena*. Cytochrome c which transports electrons between complex III and complex IV of the electron transport chain in both prokaryotes and eukaryotes, belongs to class I cytochromes (Battistuzzi et al., 2001). The cytochrome c from the *Thiomicrospira crunogena* bacterium is composed of 192 residues and shares 23%, 22% and 24% sequence similarity with α-, β- and γ-synucleins respectively (Tables 6-8). The segment of the protein that is similar to the synuclein N-terminus is between residues 15 and 119 (Figure 50). Incidentally, both human cytochrome c and α-synuclein associate with the inner membrane of the mitochondria (Parihar et al., 2008). Interestingly, the aggregated mutant A53T of α-synuclein causes the release of cytochrome c into the cytoplasm at the human mitochondria membrane. This release initiates apoptosis, resulting in the death of the cell (Parihar et al., 2008). There is no significant sequence identity between α-synuclein and the human mitochondrial cytochrome c. It appears that mitochondrial cytochrome c and α-synuclein are related to the cytochrome c from the *Thiomicrospira crunogena* which does not have mitochondria.

Role of the conserved KTKEGV sequence

The function of the repeat KTK(E/Q)GV sequences in the synuclein proteins is not clear. However, mutation of the least conserved sixth AVVTGV and the seventh KTVEGA repeat sequences of the human α-synuclein (Figure 40) to the conserved KTKEGV motif showed a decrease in the tendency of the protein to form fibrils (Sode

et al., 2007). According to these researchers, the conserved KTKEGV sequences seem to maintain the unfolded native state of the synuclein proteins and also make them soluble in aqueous solution. The mutation A30P is in the second repeat motif while E46K, H50Q and the G51D mutations are in the fourth. The A53T mutation is between the fourth and fifth repeat sequences (Figure 65). The presence of the mutations in these regions, have been shown to enhance the fibrillation of α-synuclein (Narkiewicz et al., 2014).

The fact that the region containing the repeat sequences is conserved, implies that this domain in both the synucleins and their four relatives has a critical role in the function of the proteins. My hypothesis is that the synucleins in the vertebrates were once functional domains of larger ancient proteins. Over time, this N-terminal functional region (in higher organisms) became stable enough to exist in the cells independent of the precursor proteins. Because the synucleins have only been identified in vertebrates so far, they may not be ancient proteins. In addition, it appears that the main function of the N-terminus of the synucleins is to provide a binding surface to facilitate protein-protein and protein-membrane interactions.

Curiously, the N-terminus of β-synuclein from mole rat (residues 20-76) contains several cysteine residues which normally form stabilizing disulfide bonds in globular proteins, but may not happen in this protein (Figure 42). Also, this β-synuclein contains in its N-terminus the KTKEGV motifs that maintain it in a unstructured confirmation.

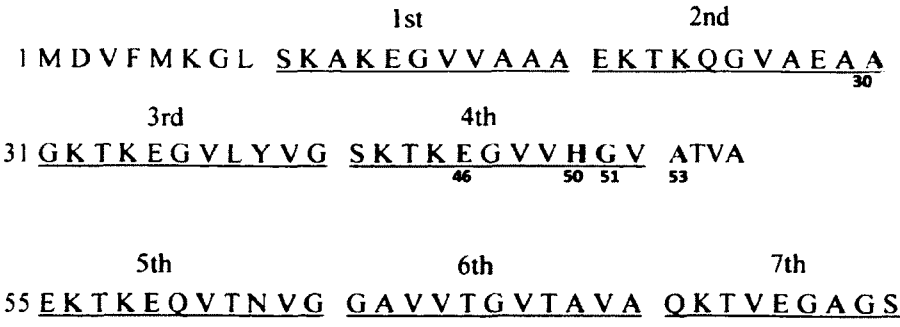

Figure 65. A schematic indicating locations of point mutations in α-synuclein

The underlined residues are the degenerate eleven amino acid repeat sequences. The green color are: A (alanine), E (glutamate), H (histidine) and G (glycine) which can undergo point mutations to A30P, E46K, H50Q, G51D and A53T. These point mutations are in the second, fourth and between fourth and fifth repeat sequences.

Sites of protein modification

The scan prosite and scan motif algorithms further confirmed the evolutionary relationship between the synucleins and the four disparate proteins by identifying functional sites at conserved locations. The algorithms identified sites for phosphorylation and N-terminal myristoylation. The N-terminal glycine (G) residues to which the myristic fatty acid ($CH_3(CH_2)_{12}COOH$) is added by the enzyme N-myristoyltransferase are in conserved locations (Figure 53). The addition of a myristic acid moiety to the N-terminal glycines of a protein increases the hydrophobicity of the protein. In the case of synuclein proteins that associate with cell membranes, myristoylation would enable them to efficiently bind to cell membranes (Wright et al., 2010).

Similarly, the site for phosphorylation by the enzymes casein kinase II and tyrosine kinase were identified. Phosphorylation of a protein occurs when a phosphate group (PO_3^{3-}) is covalently bound to a tyrosine, threonine or serine via an ester bond. Phosphorylation is a mechanism by which the function of a protein is regulated as it moves between the phosphorylated form and the unphosphorylated form (Pearlman et al., 2011). One of the forms is active while the other inactivate. Our results indicate that the casein kinase II phosphorylates at the threonine or serine residues in conserved locations while phosphorylation by tyrosine kinase is at conserved tyrosine (Y) residues (Figure 53). In α-synuclein, depending on the location of the serine or threonine residue phosphorylated, the modification can either inhibit aggregation or enhance it. For example, phosphorylation at serine 129 enhances α-synuclein fibrillation (Lou et al., 2010; Sato et al., 2011) while phosphorylation at serine 87 and 125 inhibits fibrillation (Paleologou et al., 2010; Oueslati et al., 2012).

The synuclein phylogenetic tree

The phylogenetic tree suggests that the proteins cytochrome c and γ-synuclein are the furthest from the ancestor and β-synuclein is the most ancient (Figure 56). The marsupial protein is closer to the γ-synuclein and both appear to be more distant from the ancestor than the α- and β-synucleins. The protein CRE-DUR-1 is the closest to the ancestor. A recent publication reports that γ-synuclein could be the ancestor of the α- and β-synucleins (Yuan and Zhao, 2013). Other phylogenetic algorithms need to be employed in order to achieve conclusive results. Interestingly, our results suggest the order of evolution is, β-, α- and γ-synuclein. Based on the number of exons, β-synuclein

has seven. α-synuclein has six and γ-synuclein has five. Thus gene duplication and deletion may have led to the formation of the α- and γ-synucleins.

Analysis of human and other animal synucleins

When human beings advance in age, they may succumb to various neurodegenerative diseases including Parkinson's. The focus of the analysis was on the point mutations A30P, E46K, H50Q, G51D and A53T which cause early-onset Parkinson's disease in humans (Narkiewicz et al., 2014). In the sequence alignment of primates, the α-synuclein proteins are the same except for the woolly and spider monkeys that have threonine (T) instead of alanine at position 53 and a few substitutions at some other locations (Figure 59). The alanine (A) in position 30 and the glutamate (E) in position 46 are conserved. Among the mutations, A53T has the highest propensity to cause aggregation. Investigators observed that the presence of threonine (T) at location 53 favors the formation of a β-sheet structure which may result in fibrillation (Choubey et al., 2011).

Domestic and wild animal α-synucleins have a threonine residue (T) at location 53 instead of alanine (A) (Figure 61). The two amyloidogenic sequences 36-41 and 68-78 are intact except for a few glutamate (E) substitutions for glycine (G) at position 68 in some animals (Figure 61). The birds, zebra finch, canary, duck and turkey differ significantly from humans at a stretch between residues 113 and 120 (Figure. 61). The α-synucleins of the long-lived animals have a threonine (T) at location 53 and truncations at both the N- and the C-termini, resulting in short α-synucleins (124-125 residues) (Figure 62). The two amyloidogenic sequences (the purple regions), and the

A30, E46, H50 and G51 residues are unchanged except for a few substitutions at position 68 (Figure 62).

The β-synucleins of wild and domestic animals have the conserved alanine (A) at position 30 (Figure 63). Some animals have alanine (A) at location 53, while others have threonine (T) or glycine (G). At location 46 some animals have the conserved glutamate (Q) while others have aspartate (D) or serine (S). The salmon, zebra and rainbow smelt fish have some substitutions in the 36-41 amyloidogenic sequence. The substitutions may reduce the tendency of the region to aggregate. Both humans and animals have extensive substitutions in the 68-78 amyloidogenic sequence compared to α-synuclein (Figure 63). However, some substitutions, for example, phenylalanine (F) and isoleucine (I) do not diminish the hydrophobicity of the region (Figure 63). Interestingly, β-synucleins have a glutamine residue (Q) at location 50 instead of a histidine (H) (Figure 63). A group of researchers discovered two mutations in β-synuclein that may be associated with Dementia with Lewy bodies. (Ohtake et al., 2004; Fujita et al., 2010). The mutations are valine 70 to methionine (V70M) and proline 123 to histidine (P123H). These two mutations make the β-synuclein protein more susceptible to fibrillation and also render the synuclein incapable of preventing α-synuclein fibrillation (Fujita et al., 2010). The mutations in β-synuclein are hypothesized to predispose an individual to Dementia with Lewy bodies (Ohtake et al., 2004). In transgenic mice, the P123H β-synuclein induced a neurodegeneration whose symptoms were axonal swelling and memory disorder (Fujita et al., 2010).

γ-Synucleins in both humans and animals have a threonine (T) in location 53 instead of an alanine (A) (Fig. 64). In addition, the proteins have a glutamine (Q) instead

of a histidine (H) in location 50 and a serine (S) instead of a glycine (G) in location 51. The leucine (L) residue in the 36-41 amyloidogenic sequence is replaced by either isoleucine (I) or methionine (M) residue. The 68-78 sequence is extensively substituted by polar residues including asparagine (N), serine (S) and threonine (T) thereby reducing protein's hydrophobicity and propensity to aggregate (Figure 63). The disrupted amyloidogenic sequences may explain why γ-synuclein proteins do not readily aggregate and form fibrils despite the threonine at location 53.

The presence of a threonine (T) in non-primates seems to suggest that originally the synucleins had the threonine residue in that position. Our computational results appear to suggest that among the three proteins, β-synuclein is the oldest and evolved to contain amino acid sequences to prevent fibril formation, such as the change from threonine at location 53 to alanine. α-Synuclein also does not have a threonine at position 53. However, interestingly, γ-synuclein does have a threonine, but this protein is not prone to fibril formation.

Of the three human synucleins, α-synuclein is the largest, leading to an increase in the number of charged residues including glutamate (E) and aspartate (D) in its C-terminus. The VI repeat sequence in α-synuclein is prone to aggregation (Figure 62) (Kumar et al., 2009). Perhaps its C-terminus has an increased number of charged amino acid residues in order to counteract the propensity of the amyloidogenic VI sequence to aggregate when the protein is in the cytoplasm. This sequence was most likely maintained because α-synuclein needs the VI (^{68}GAVVTGVTAVA^{78}) repeat region for associating with lipid membranes and perhaps to facilitate the assembly of multimeric forms of the protein.

Taken altogether, the synuclein proteins appear to have no bona fide superfamily relatives in animals, but share significant sequence similarity with endoglucanase, CRE-DUR-1, cytochrome c and the Tasmanian Devil proteins. Each one of the related proteins contains KTK(E/Q)GV repeats which are a unique characteristic of the N-termini of the synucleins. The identical sites of protein modifications in both the synuclein and the disparate proteins further suggest an evolutionary relationship between the synucleins and the disparate proteins. The analysis of the synucleins indicated that almost all primates avoided the A30P, E46K, H50Q, G51D and A53T substitutions. However, all other animal α-synucleins have the A53T substitution. β-synucleins have the H50Q substitution. Almost all γ-synucleins have the H50Q/T, G51S and A53T/N substitutions. In conclusion, we also speculate based on conversations with other scientists (Ellis and Jessica Bell) that the N-and C-termini of the synucleins actually came from two different proteins and at an earlier point fused together to form β-synuclein.

CHAPTER VII

CONCLUSIONS AND FUTURE WORK

CONCLUSIONS

This research project presents original results and theories based on the experimental and computational analysis of the synuclein proteins. In our laboratory we were able to express and purify α-and β-synuclein and also establish conditions which induce them to form fibrils *in vitro*.

In Chapter III, in collaboration with engineers, we were able to show for the first time that low temperature plasma bullets or plume emitted by a plasma pencil can break protein fibrils into small fragments which we propose will facilitate their elimination. α-Synuclein was used as the protein model. Fragmentation of the synuclein fibrils began to show up at two minutes and the maximum time to achieve extensive breakage was six minutes. Other methods including ultrasonication, laser beam irradiation and mechanical shaking have been employed to break protein fibrils. However, unlike these methods which rely on physical mechanisms, our method is based on the reactive species of the low temperature plasma. We expect that under plasma exposure the fibrils undergo chemical reactions that compromise their structural as well as chemical integrity.

In Chapter IV, we conducted synuclein inhibition studies in which a 1:2 and 1:4 ratio of α-synuclein to β-synuclein were employed. Under the experimental conditions of the study, our results indicated that some form(s) of α-synuclein can inhibit fibril formation of β-synuclein which is quite surprising. Furthermore, our studies indicated

that β-synuclein fibrils can form reasonably rapidly under the same conditions as α-synuclein *in vitro*. Most importantly the results suggested that when two proteins capable of forming fibrils are incubated together under the same conditions, an inhibitory effect can occur. To the best of our knowledge, this is the first study of a co-incubation of two fibril forming proteins under fibrillation promoting conditions. Because investigators in the past did not conduct a study similar to ours, they did not observe this phenomenon. Two different fibril forming proteins *in vivo* could perhaps cancel each other out, although in nature each fibril associated protein occupies distinct niches within or outside various tissues in the body. These findings may provide new lines of investigation regarding the design of inhibitors, as well as facilitate our general understanding of the mechanism of fibril formation.

In Chapter V, we isolated a high MW form of the human β-synuclein protein, which is an important step in addressing the controversy over the true native, physiological state of the synucleins. A computer program K2D3 estimated from the far-UV circular dichroism spectra that the β-synuclein complex was 68% α-helical, 6.7% β-sheet and 25.2% random coil. This prediction suggests that our β-synuclein complex is predominantly helical in structure as we would predict.

In Chapter VI, a PSI-BLAST search tool retrieved from the database four disparate protein sequences that we propose are related to the synucleins: endoglucanase enzyme from bacterium *Acetobacter pomorum*, a CRE-DUR-1protein from a nematode, a putative protein from the Tasmanian Devil and cytochrome c from the bacterium *Thiomicrospira crunogena*, all of which had significant sequence similarity to the synucleins. Each one of the retrieved sequences contained KTK(E/Q)GV repeats which

are a unique characteristic of the N-terminal regions of the synucleins. Surprisingly the synucleins seem to be orphan proteins in the vertebrate line. Two other bioinformatics search engines, the scan prosite and scan motif, identified sites of myristoylation and phosphorylation in the synucleins. These sites are similar to those found for related proteins as well. The myristoylation is expected to occur at specific glycine residues in the N-terminal regions of the synucleins. Phosphorylation was at specific tyrosine, threonine and serine residues which are also in the N-terminal region. An alignment of the synucleins with their related proteins indicated that the glycines and serine/threonine residues involved in the protein modification were in conserved locations. The conserved sites of protein modification further suggest an evolutionary relationship between the synucleins and the four disparate proteins.

A phylogenetic tree generated from the three human synucleins and the four proteins indicated that the CRE-DUR-1 protein is more closely related to the synucleins than the endoglucanase and cytochrome c. The Tasmanian Devil protein shares the same ancestor with γ-synuclein. The link between the CRE-DUR-1 protein and the ancestor protein is the shortest while the longest link is for cytochrome c and γ-synuclein. According to these links, α- and β-synuclein, which have six and seven exons respectively, appear to be evolutionarily older than the γ-synuclein, which has five exons.

We identified the exons of the synucleins that contain the degenerate repeat sequences. In α-synuclein, the first three degenerate repeats are in exon two, the fourth is in exon three, the fifth, sixth and seventh are in exon four. The first three degenerate repeats in β-synuclein are in exon three, the fourth is in exon four, the fifth and the small

segments of the sixth and seventh repeats are in exon five. In γ-synuclein, the first three repeats are in exon one, the fourth is in exon two, the fifth, sixth and seventh are in exon three. Taken altogether it means that exon two of α-synuclein is similar to exon three of β-synuclein and exon one of γ-synuclein. Exon three of α-synuclein is similar to exons four and two of β- and γ-synuclein respectively. Similarly, exon four of α-synuclein is similar to exons five and three of β- and γ-synuclein respectively.

When α-synucleins of primates were aligned, we observed that the protein sequences are the same except for the woolly and spider monkey, which have a threonine residue at location 53 instead of alanine. The α-synucleins of domestic and other wild animals, have a threonine residue at location 53. In addition, long-lived animals have truncations at both the N- and the C-terminus resulting in α-synucleins ranging between 124 and 125 residues. In addition, the alanine at location 30, glutamate at location 46, histidine at location 50 and glycine at location 51 are conserved. β-synucleins of some animals have the conserved alanine at location 53, while others have a threonine, aspartate or glycine residue. Both human and animal β-synucleins have extensive substitutions in the ^{68}GAVVTGVTAVA^{78} amyloidogenic sequence. The alanine at location 30, and the glycine at location 51 are conserved. β-synucleins of some animals have an aspartate or serine residue instead of the glutamate at location 46. In addition, β-synucleins of some animals have a glutamine residue at location 50 instead of a histidine, while others have neither a histidine nor a glutamine. Interestingly, γ-synucleins in both humans and animals carry the A53T mutation. The 68-78 sequence is heavily disrupted by substitutions. In humans, the α-synuclein A53T mutation is associated with early-onset Parkinson's disease (Wan and Chung, 2012; Oaks et al.,

2013). γ-synucleins, the alanine in location 30 and the glutamate in location 46 are conserved, while at location 50, a histidine is substituted with a glutamine and at location 51, a glycine is substituted with a serine. Seemingly, human γ-synucleins carry the H50Q and the A53T 'mutations' which have not been reported to be associated with Parkinson's disease. These sequences appear to suggest that primates are longer lived without the mutations but as these mutations are present in most animals they may be functionally less advantageous to primates.

FUTURE WORK

Application of low temperature plasma on protein fibrils

Although we were successful in breaking protein fibrils into smaller units, the nature of the damage needs further investigation. Tests need to be conducted to determine whether the glial cells can clear the fibril fragments via phagocytosis. It will also be of interest to determine if the broken fibrils can be eliminated by the ALP or UPS systems. Further investigations are additionally necessary to determine whether or not the broken fibrils will reassemble, seed the soluble protein molecules to enhance fibrillation, or become cytotoxic. Also, the cytotoxicity of the plasma itself with regard to neurons and neuronal cells needs to be examined. The outcome of such investigations will determine the viability of employment of cold plasma as a therapy against diseases associated with plaques.

Inhibitory effects of α-synuclein on β-synuclein fibrillation

The species and the mechanism by which α-synuclein inhibits β-synuclein fibrillation needs further investigation. In addition, the nature of the complex formed between α- and β-synuclein during the inhibition process needs to be determined. Future

investigations may include finding another protein that forms fibrils under the same conditions as α-and β-synuclein and then incubate the protein with α-and β-synuclein in a 1:1 and 1:4 ratio to further test the hypothesis that two different fibril forming proteins will inhibit each other.

Isolation of a multimeric β- and γ-synuclein

A repeat of the expression and isolation of the β-synuclein folded multimeric protein is necessary in order to determine its biophysical properties including its stability at different pH, concentrations and temperature ranges. A well calibrated gel-filtration column using commercially available gel-filtration protein standards will be necessary in order to obtain an accurate estimate of the size of the multimeric form of the β-synuclein. The resin should be changed from G-75 to G-100 and G-200. A G-100 or 200 column can, for example, separate a 2000 kDa protein molecule from a 56 kDa one, while the G-75 elutes both molecules around the same fraction. Thus, the putative β-synuclein tetramer (56 kDa) and the putative glutamic dehydrogenase hexamer (333.6 kDa) would elute to the same location when a G-75 column is used. Also, a monomeric protein standard with a true 56 kDa MW will be critical for estimating the size of the multimeric form of the β-synuclein.

For protein expression, other cell lines can also be used such as Chinese Hamster ovary cells and Baculovirus insect cells which may provide a more conducive environment close to that of a neuron, for forming and stabilizing the tetramer. Substances including glycerol and n-octyl-β-D-glucopyranoside may be used to stabilize the tetramer. A higher temperature (30°C) during anion exchange and gel-filtration purification process may increase the hydrophobic effect. Future work also includes the

formation of well-diffracting crystals of the β-synuclein complex for X-ray crystallography studies to determine its 3D structure. In order to make a complete study of the synucleins, it is necessary to express, isolate and characterize the folded multimeric form of γ-synuclein. It will also be necessary to see if hetero-complexes can be formed between the synucleins.

Previous experiments have shown that α-and β-synuclein interact with polyunsaturated fatty acids *in vitro* (Israeli and Sharon, 2009). Molecular modelling techniques can be employed to investigate the regions by which, for example, α-synuclein binds its protein ligands. The polyunsaturated fatty acids including docosahexaenoic acid and arachidonic acid, which are abundant in neuronal membranes, can be used as model ligands for the synuclein (Rapoport, 2008; De Franceschi et al., 2011). Besides being associated with amyloidogenesis, the other possible roles of the ^{36}GVLYVG^{41}and ^{68}GAVVTGVTAVA^{78} regions need further investigation using molecular modelling techniques. These regions may play a role in bringing together monomers to form the natural multimeric forms of the synucleins, which may confer the normal physiological function.

Analysis of the genes of centenarians and supercentenarians

Analysis of the genes of individuals who live to be 100 years and beyond will shed light on what keeps them healthy, while others may succumb to neurodegenerative diseases. From our studies, we have identified that exon two of human α-synuclein contains the repeat sequences where the mutations A30P, E46K, H50Q, G51D and A53T can occur. One could examine and compare exons two and three of a supercentenarian (a person who lives over 110 years of age) with that of an individual with Parkinson's

disease, since these mutations occur in those regions of the γ-synuclein gene. It will also be interesting to compare the sequences of chaperones and protein clearance systems between patients with Parkinson's and supercentenarians as further examples.

REFERENCES

Acharya, K.R., and Lloyd, M.D. (2005). The advantages and limitations of protein crystal structures. Trends Pharmacol. Sci. *26*, 10-14.

Adzhubei, A.A., Sternberg, M.J., and Makarov, A.A. (2013). Polyproline-II helix in proteins: structure and function. J. Mol. Biol. *425*, 2100-2132.

Alexander, R.P., and Zhulin, I.B. (2007). Evolutionary genomics reveals conserved structural determinants of signaling and adaptation in microbial chemoreceptors. Proc. Natl. Acad. Sci. USA *104*, 2885-2890.

Allan, P., Uitte de Willige, S., Abou-Saleh, R.H., Connell, S.D., and Ariens, R.A. (2012). Evidence that fibrinogen gamma' directly interferes with protofibril growth: implications for fibrin structure and clot stiffness. J. Thromb. Haemost. *10*, 1072-1080.

Altschul, S.F., Madden, T.L., Schaffer, A.A., Zhang, J., Zhang, Z., Miller, W., and Lipman, D.J. (1997). Gapped BLAST and PSI-BLAST: a new generation of protein database search programs. Nucleic Acids Res. *25*, 3389-3402.

Amm, I., Sommer, T., and Wolf, D.H. (2014). Protein quality control and elimination of protein waste: the role of the ubiquitin-proteasome system. Biochim. Biophys. Acta *1843*, 182-196.

Anfinsen, C.B. (1973). Principles that govern the folding of protein chains. Science *181*, 223-230.

Apetri, M.M., Maiti, N.C., Zagorski, M.G., Carey, P.R., and Anderson, V.E. (2006). Secondary structure of alpha-synuclein oligomers: characterization by raman and atomic force microscopy. J. Mol. Biol. *355*, 63-71.

Arias-Carrion, O., Stamelou, M., Murillo-Rodriguez, E., Menendez-Gonzalez, M., and Poppel, E. (2010). Dopaminergic reward system: a short integrative review. Int. Arch. Med. *3*, 24.

Arndt, S., Unger, P., Wacker, E., Shimizu, T., Heinlin, J., Li, Y.F., Thomas, H.M., Morfill, G.E., Zimmermann, J.L., Bosserhoff, A.K., *et al.* (2013). Cold atmospheric plasma (CAP) changes gene expression of key molecules of the wound healing machinery and improves wound healing in vitro and in vivo. PLoS One *8*, e79325.

Ayton, S., and Lei, P. (2014). Nigral iron elevation is an invariable feature of Parkinson's disease and is a sufficient cause of neurodegeneration. Biomed. Res. Int. *2014*, 581256.

Bamberger, M.E., Harris, M.E., McDonald, D.R., Husemann, J., and Landreth, G.E. (2003). A cell surface receptor complex for fibrillar beta-amyloid mediates microglial activation. J. Neurosci. *23*, 2665-2674.

Ban, N., Nissen, P., Hansen, J., Capel, M., Moore, P.B., and Steitz, T.A. (1999). Placement of protein and RNA structures into a 5 A-resolution map of the 50S ribosomal subunit. Nature *400*, 841-847.

Barekzi, N., and Laroussi, M. (2012). Dose-dependent killing of leukemia cells by low-temperature plasma. J. Phys. D: Appl. Phys. *45*, 422002.

Bartels, T., Choi, J.G., and Selkoe, D.J. (2011). alpha-Synuclein occurs physiologically as a helically folded tetramer that resists aggregation. Nature *477*, 107-110.

Battistuzzi, G., Borsari, M., and Sola, M. (2001). Redox properties of cytochrome c. Antioxid. Redox Signal *3*, 279-291.

Bellucci, A., Collo, G., Sarnico, I., Battistin, L., Missale, C., and Spano, P. (2008). Alpha-synuclein aggregation and cell death triggered by energy deprivation and dopamine overload are counteracted by D2/D3 receptor activation. J. Neurochem. *106*, 560-577.

Bellucci, A., Navarria, L., Zaltieri, M., Missale, C., and Spano, P. (2012). alpha-Synuclein synaptic pathology and its implications in the development of novel therapeutic approaches to cure Parkinson's disease. Brain Res. *1432*, 95-113.

Benaroudj, N., Zwickl, P., Seemuller, E., Baumeister, W., and Goldberg, A.L. (2003). ATP hydrolysis by the proteasome regulatory complex PAN serves multiple functions in protein degradation. Molec. Cell *11*, 69-78.

Bertoncini, C.W., Jung, Y.S., Fernandez, C.O., Hoyer, W., Griesinger, C., Jovin, T.M., and Zweckstetter, M. (2005). Release of long-range tertiary interactions potentiates aggregation of natively unstructured alpha-synuclein. Proc. Natl. Acad. Sci. USA *102*, 1430-1435.

Beyer, K., Ispierto, L., Latorre, P., Tolosa, E., and Ariza, A. (2011). Alpha- and beta-synuclein expression in Parkinson disease with and without dementia. J. Neurol. Sci. *310*, 112-117.

Biasini, M., Bienert, S., Waterhouse, A., Arnold, K., Studer, G., Schmidt, T., Kiefer, F., Cassarino, T.G., Bertoni, M., Bordoli, L., *et al.* (2014). SWISS-MODEL: modelling protein tertiary and quaternary structure using evolutionary information. Nucleic Acids Res., epub ahead of print.

Binolfi, A., Rasia, R.M., Bertoncini, C.W., Ceolin, M., Zweckstetter, M., Griesinger, C., Jovin, T.M., and Fernandez, C.O. (2006). Interaction of alpha-synuclein with divalent

metal ions reveals key differences: a link between structure, binding specificity and fibrillation enhancement. J. Am. Chem. Soc. *128*, 9893-9901.

Bisaglia, M., Mammi, S., and Bubacco, L. (2009). Structural insights on physiological functions and pathological effects of alpha-synuclein. FASEB J. *23*, 329-340.

Bleecker, M.L. (1988). Parkinsonism: a clinical marker of exposure to neurotoxins. Neurotoxicol. Teratol. *10*, 475-478.

Bocca, B., Alimonti, A., Senofonte, O., Pino, A., Violante, N., Petrucci, F., Sancesario, G., and Forte, G. (2006). Metal changes in CSF and peripheral compartments of parkinsonian patients. J. Neurol. Sci. *248*, 23-30.

Boden, G. (2008). Obesity and Free Fatty Acids. Endocrin. Metab. Clin. *37*, 635-646.

Bonifati, V., Rizzu, P., Squitieri, F., Krieger, E., Vanacore, N., van Swieten, J.C., Brice, A., van Duijn, C.M., Oostra, B., Meco, G., *et al.* (2003). DJ-1(PARK7), a novel gene for autosomal recessive, early onset parkinsonism. Neurol. Sci. *24*, 159-160.

Borghi, R., Marchese, R., Negro, A., Marinelli, L., Forloni, G., Zaccheo, D., Abbruzzese, G., and Tabaton, M. (2000). Full length alpha-synuclein is present in cerebrospinal fluid from Parkinson's disease and normal subjects. Neurosci. Lett. *287*, 65-67.

Bousset, L., Pieri, L., Ruiz-Arlandis, G., Gath, J., Jensen, P.H., Habenstein, B., Madiona, K., Olieric, V., Bockmann, A., Meier, B.H., *et al.* (2013). Structural and functional characterization of two alpha-synuclein strains. Nat. Commun. *4*, 2575.

Braga, C.A., Follmer, C., Palhano, F.L., Khattar, E., Freitas, M.S., Romao, L., Di Giovanni, S., Lashuel, H.A., Silva, J.L., and Foguel, D. (2011). The anti-Parkinsonian drug selegiline delays the nucleation phase of alpha-synuclein aggregation leading to the formation of nontoxic species. J. Mol. Biol. *405*, 254-273.

Breydo, L., Wu, J.W., and Uversky, V.N. (2012). alpha-Synuclein misfolding and Parkinson's disease. BBA-Molec. Basis Dis. *1822*, 261-285.

Brockwell, D.J., Smith, D.A., and Radford, S.E. (2000). Protein folding mechanisms: new methods and emerging ideas. Curr. Opin. Struct. Biol. *10*, 16-25.

Bross, P., Andresen, S. B., Corydon,J.T., and Gregersen, N. (2011). Protein Misfolding and Degradation in Genetic Disease. In: Encyclopedia of Life Sciences (ELS). John Wiley &Sons, Ltd: Chichester *DOI: 10.1002/9780470015902.a0006016.pub2*, 1-8.

Brun, P., Brun, P., Vono, M., Venier, P., Tarricone, E., Deligianni, V., Martines, E., Zuin, M., Spagnolo, S., Cavazzana, R., *et al.* (2012). Disinfection of ocular cells and tissues by atmospheric-pressure cold plasma. PLoS One *7*, e33245.

Burchell, V.S., Nelson, D.E., Sanchez-Martinez, A., Delgado-Camprubi, M., Ivatt, R.M., Pogson, J.H., Randle, S.J., Wray, S., Lewis, P.A., Houlden, H., *et al.* (2013). The Parkinson's disease-linked proteins Fbxo7 and Parkin interact to mediate mitophagy. Nat. Neurosci. *16*, 1257-1265.

Burre, J., Sharma, M., Tsetsenis, T., Buchman, V., Etherton, M.R., and Sudhof, T.C. (2010). alpha-Synuclein Promotes SNARE-Complex Assembly in Vivo and in Vitro. Science *329*, 1663-1667.

Cattaneo, E., Rigamonti, D., Goffredo, D., Zuccato, C., Squitieri, F., and Sipione, S. (2001). Loss of normal huntingtin function: new developments in Huntington's disease research. Trends Neurosci. *24*, 182-188.

Chadchankar, H., Ihalainen, J., Tanila, H., and Yavich, L. (2011). Decreased reuptake of dopamine in the dorsal striatum in the absence of alpha-synuclein. Brain Res. *1382*, 37-44.

Chamberlain, A.K., MacPhee, C.E., Zurdo, J., Morozova-Roche, L.A., Hill, H.A., Dobson, C.M., and Davis, J.J. (2000). Ultrastructural organization of amyloid fibrils by atomic force microscopy. Biophys. J. *79*, 3282-3293.

Chatani, E., Lee, Y.H., Yagi, H., Yoshimura, Y., Naiki, H., and Goto, Y. (2009). Ultrasonication-dependent production and breakdown lead to minimum-sized amyloid fibrils. Proc. Natl. Acad. Sci. USA *106*, 11119-11124.

Chaudhuri, T.K., and Gupta, P. (2005). Factors governing the substrate recognition by GroEL chaperone: a sequence correlation approach. Cell Stress Chaperon. *10*, 24-36.

Chen, B., Retzlaff, M., Roos, T., and Frydman, J. (2011). Cellular Strategies of Protein Quality Control. CSH Perspect. Biol. *3*, a004374.

Chen, X., de Silva, H.A., Pettenati, M.J., Rao, P.N., St George-Hyslop, P., Roses, A.D., Xia, Y., Horsburgh, K., Ueda, K., and Saitoh, T. (1995). The human NACP/alpha-synuclein gene: chromosome assignment to 4q21.3-q22 and TaqI RFLP analysis. Genomics *26*, 425-427.

Chen, Y.H., Yang, J.T., and Martinez, H.M. (1972). Determination of the secondary structures of proteins by circular dichroism and optical rotatory dispersion. Biochemistry *11*, 4120-4131.

Cherny, I., Rockah, L., and Gazit, E. (2005). The YoeB toxin is a folded protein that forms a physical complex with the unfolded YefM antitoxin. J. Biol. Chem. *280*, 30063-30072.

Cheung, M.S., Garcia, A.E., and Onuchic, J.N. (2002). Protein folding mediated by solvation: water expulsion and formation of the hydrophobic core occur after the structural collapse. Proc. Natl. Acad. Sci. USA *99*, 685-690.

Chiti, F., and Dobson, C.M. (2006). Protein misfolding, functional amyloid, and human disease. Annu. Rev. Biochem. *75*, 333-366.

Chiti, F., Webster, P., Taddei, N., Clark, A., Stefani, M., Ramponi, G., and Dobson, C.M. (1999). Designing conditions for in vitro formation of amyloid protofilaments and fibrils. Proc. Natl. Acad. Sci. USA *96*, 3590-3594.

Choubey, V., Safiulina, D., Vaarmann, A., Cagalinec, M., Wareski, P., Kuum, M., Zharkovsky, A., and Kaasik, A. (2011). Mutant A53T alpha-Synuclein Induces Neuronal Death by Increasing Mitochondrial Autophagy. J. Biol. Chem. *286*, 10814-10824.

Chu, Y., and Kordower, J.H. (2007). Age-associated increases of alpha-synuclein in monkeys and humans are associated with nigrostriatal dopamine depletion: Is this the target for Parkinson's disease? Neurobiol. Dis. *25*, 134-149.

Ciechanover, A., and Brundin, P. (2003). The ubiquitin proteasome system in neurodegenerative diseases: sometimes the chicken, sometimes the egg. Neuron *40*, 427-446.

Ciechanover, A., Orian, A., and Schwartz, A.L. (2000). Ubiquitin-mediated proteolysis: biological regulation via destruction. Bioessays *22*, 442-451.

Clore, G.M., and Gronenborn, A.M. (1998). Determining the structures of large proteins and protein complexes by NMR. Trends Biotechnol. *16*, 22-34.

Collins, J.C., and Greene, L.H. (2012). Biophysical analysis of the transition of an all alpha-helical Greek-key protein into amyloid fibrils composed of beta-sheet structure. Protein Pept. Lett. *19*, 982-990.

Collins, J.C., and Greene, L.H. (2014). Conversion of α-helical Proteins into an Alternative β-amyloid Conformation. In Bio-nanoimaging Protein Misfolding and Aggregation, V. Uversky, Y. Lyubchenko, ed. (Elsevier Inc.), pp. 492-499.

Colton, C.A., Fagni, L., and Gilbert, D. (1989). The Action of Hydrogen-Peroxide on Paired Pulse and Long-Term Potentiation in the Hippocampus. Free Radical Bio. Med. *7*, 3-8.

Conway, K.A., Harper, J.D., and Lansbury, P.T. (1998). Accelerated in vitro fibril formation by a mutant alpha-synuclein linked to early-onset Parkinson disease. Nat. Med. *4*, 1318-1320.

Conway, K.A., Harper, J.D., and Lansbury, P.T., Jr. (2000). Fibrils formed in vitro from alpha-synuclein and two mutant forms linked to Parkinson's disease are typical amyloid. Biochemistry *39*, 2552-2563.

Cuervo, A.M., Wong, E.S., and Martinez-Vicente, M. (2010). Protein degradation, aggregation, and misfolding. Mov. Disord. *25 Suppl 1*, S49-54.

Daggett, V., and Fersht, A.R. (2003). Is there a unifying mechanism for protein folding? Trends Biochem. Sci. *28*, 18-25.

Dahiya, V., and Chaudhuri, T.K. (2014). Chaperones GroEL/GroES accelerate the refolding of a multidomain protein through modulating on-pathway intermediates. J. Biol. Chem. *289*, 286-298.

Danzer, K.M., Krebs, S.K., Wolff, M., Birk, G., and Hengerer, B. (2009). Seeding induced by alpha-synuclein oligomers provides evidence for spreading of alpha-synuclein pathology. J. Neurochem. *111*, 192-203.

Darios, F., Corti, O., Lucking, C.B., Hampe, C., Muriel, M.P., Abbas, N., Gu, W.J., Hirsch, E.C., Rooney, T., Ruberg, M., *et al.* (2003). Parkin prevents mitochondrial swelling and cytochrome c release in mitochondria-dependent cell death. Hum. Mol. Genet. *12*, 517-526.

Davies, P., Moualla, D., and Brown, D.R. (2011). Alpha-synuclein is a cellular ferrireductase. PLoS One *6*, e15814.

De Franceschi, G., Frare, E., Pivato, M., Relini, A., Penco, A., Greggio, E., Bubacco, L., Fontana, A., and de Laureto, P.P. (2011). Structural and morphological characterization of aggregated species of alpha-synuclein induced by docosahexaenoic acid. J. Biol. Chem. *286*, 22262-22274.

De Los Rios, P., and Barducci, A. (2014). Hsp70 chaperones are non-equilibrium machines that achieve ultra-affinity by energy consumption. eLife *3*, e02218.

Dereeper, A., Guignon, V., Blanc, G., Audic, S., Buffet, S., Chevenet, F., Dufayard, J.F., Guindon, S., Lefort, V., Lescot, M., *et al.* (2008). Phylogeny.fr: robust phylogenetic analysis for the non-specialist. Nucleic Acids Res. *36*, W465-469.

Desplats, P., Lee, H.J., Bae, E.J., Patrick, C., Rockenstein, E., Crews, L., Spencer, B., Masliah, E., and Lee, S.J. (2009). Inclusion formation and neuronal cell death through neuron-to-neuron transmission of alpha-synuclein. Proc. Natl. Acad. Sci. USA *106*, 13010-13015.

Dettmer, U., Newman, A.J., Luth, E.S., Bartels, T., and Selkoe, D. (2013). In Vivo Cross-linking Reveals Principally Oligomeric Forms of alpha-Synuclein and beta-Synuclein in Neurons and Non-neural Cells. J. Biol. Chem. *288*, 6371-6385.

Dikic, I., Wakatsuki, S., and Walters, K.J. (2009). Ubiquitin-binding domains - from structures to functions. Nat. Rev. Mol. Cell Biol. *10*, 659-671.

Dikiy, I., and Eliezer, D. (2014). N-terminal acetylation stabilizes N-terminal helicity in lipid- and micelle-bound alpha-synuclein and increases its affinity for physiological membranes. J. Biol. Chem. *289*, 3652-3665.

Dill, K.A., and Chan, H.S. (1997). From Levinthal to pathways to funnels. Nat. Struct. Biol. *4*, 10-19.

Dinner, A.R., Sali, A., Smith, L.J., Dobson, C.M., and Karplus, M. (2000). Understanding protein folding via free-energy surfaces from theory and experiment. Trends Biochem. Sci. *25*, 331-339.

Dobson, C.M. (1999). Protein misfolding, evolution and disease. Trends Biochem. Sci. *24*, 329-332.

Dobson, C.M. (2001). The structural basis of protein folding and its links with human disease. Philos. Trans. R. Soc. Lond. B: Biol. Sci. *356*, 133-145.

Dobson, C.M. (2003). Protein folding and misfolding. Nature *426*, 884-890.

Dobson, C.M. (2004). Principles of protein folding, misfolding and aggregation. Semin. Cell. Dev. Biol. *15*, 3-16.

Dudzik, C.G., Walter, E.D., Abrams, B.S., Jurica, M.S., and Millhauser, G.L. (2013). Coordination of copper to the membrane-bound form of alpha-synuclein. Biochemistry *52*, 53-60.

Dufty, B.M., Warner, L.R., Hou, S.T., Jiang, S.X., Gomez-Isla, T., Leenhouts, K.M., Oxford, J.T., Feany, M.B., Masliah, E., and Rohn, T.T. (2007). Calpain-cleavage of alpha-synuclein: connecting proteolytic processing to disease-linked aggregation. Am. J. Pathol. *170*, 1725-1738.

Dunker, A.K., Brown, C.J., Lawson, J.D., Iakoucheva, L.M., and Obradovic, Z. (2002). Intrinsic disorder and protein function. Biochemistry *41*, 6573-6582.

Dunker, A.K., Lawson, J.D., Brown, C.J., Williams, R.M., Romero, P., Oh, J.S., Oldfield, C.J., Campen, A.M., Ratliff, C.M., Hipps, K.W., *et al.* (2001). Intrinsically disordered protein. J. Mol. Graph Model *19*, 26-59.

Edgar, R.C. (2004). MUSCLE: multiple sequence alignment with high accuracy and high throughput. Nucleic Acids Res. *32*, 1792-1797.

Elbaz, A., and Moisan, F. (2008). Update in the epidemiology of Parkinson's disease. Curr. Opin. Neurol. *21*, 454-460.

Ellis, C.E., Schwartzberg, P.L., Grider, T.L., Fink, D.W., and Nussbaum, R.L. (2001). Alpha-synuclein is phosphorylated by members of the Src family of protein-tyrosine kinases. J. Biol. Chem. *276*, 3879-3884.

Falquet, L., Pagni, M., Bucher, P., Hulo, N., Sigrist, C.J.A., Hofmann, K., and Bairoch, A. (2002). The PROSITE database, its status in 2002. Nucleic Acids Res. *30*, 235-238.

Fasshauer, D., Otto, H., Eliason, W.K., Jahn, R., and Brunger, A.T. (1997). Structural changes are associated with soluble N-ethylmaleimide-sensitive fusion protein attachment protein receptor complex formation. J. Biol. Chem. *272*, 28036-28041.

Fauvet, B., Mbefo, M.K., Fares, M.B., Desobry, C., Michael, S., Ardah, M.T., Tsika, E., Coune, P., Prudent, M., Lion, N., *et al.* (2012). Alpha-synuclein in central nervous system and from erythrocytes, mammalian cells, and Escherichia coli exists predominantly as disordered monomer. J. Biol. Chem. *287*, 15345-15364.

Fersht, A.R. (1995). Mapping the structures of transition states and intermediates in folding: delineation of pathways at high resolution. Philos. Trans. R. Soc. Lond. B: Biol. Sci. *348*, 11-15.

Fersht, A.R. (2000). Transition-state structure as a unifying basis in protein-folding mechanisms: contact order, chain topology, stability, and the extended nucleus mechanism. Proc. Natl. Acad. Sci. USA *97*, 1525-1529.

Fink, A.L. (1999). Chaperone-mediated protein folding. Physiol. Rev. *79*, 425-449.

Forte, G., Alimonti, A., Violante, N., Di Gregorio, M., Senofonte, O., Petrucci, F., Sancesario, G., and Bocca, B. (2005). Calcium, copper, iron, magnesium, silicon and zinc content of hair in Parkinson's disease. J. Trace Elem. Med. Biol. *19*, 195-201.

Fowler, D.M., and Kelly, J.W. (2012). Functional amyloidogenesis and cytotoxicity-insights into biology and pathology. PLoS Biol. *10*, e1001459.

Fowler, D.M., Koulov, A.V., Balch, W.E., and Kelly, J.W. (2007). Functional amyloid-from bacteria to humans. Trends Biochem. Sci. *32*, 217-224.

Fujita, M., Sugama, S., Sekiyama, K., Sekigawa, A., Tsukui, T., Nakai, M., Waragai, M., Takenouchi, T., Takamatsu, Y., Wei, J., *et al.* (2010). A beta-synuclein mutation linked to dementia produces neurodegeneration when expressed in mouse brain. Nat. Commun. *1*, 110.

Fujiwara, H., Hasegawa, M., Dohmae, N., Kawashima, A., Masliah, E., Goldberg, M.S., Shen, J., Takio, K., and Iwatsubo, T. (2002). Alpha-synuclein is phosphorylated in synucleinopathy lesions. Nat. Cell Biol. *4*, 160-164.

Fuxreiter, M., Simon, I., Friedrich, P., and Tompa, P. (2004). Preformed structural elements feature in partner recognition by intrinsically unstructured proteins. J. Mol. Biol. *338*, 1015-1026.

Gaikwad, S., Larionov, S., Wang, Y., Dannenberg, H., Matozaki, T., Monsonego, A., Thal, D.R., and Neumann, H. (2009). Signal regulatory protein-beta1: a microglial modulator of phagocytosis in Alzheimer's disease. Am. J. Pathol. *175*, 2528-2539.

Garrett, R.H., and Grisham, C.M. (2013). Proteins: Secondary, Tertiary, and Quaternary Strucure, 4th edn (Boston, MA: Brooks/Cole, Cengage Learning), pp. 134-158.

Gebbink, M.F., Claessen, D., Bouma, B., Dijkhuizen, L., and Wosten, H.A. (2005). Amyloids--a functional coat for microorganisms. Nat. Rev. Microbiol. *3*, 333-341.

George, J.M. (2002). The synucleins. Genome Biol. *3*, reviews3002.3001-3002.3006.

Giasson, B.I., Murray, I.V., Trojanowski, J.Q., and Lee, V.M. (2001). A hydrophobic stretch of 12 amino acid residues in the middle of alpha-synuclein is essential for filament assembly. J. Biol. Chem. *276*, 2380-2386.

Giehm, L., Svergun, D.I., Otzen, D.E., and Vestergaard, B. (2011). Low-resolution structure of a vesicle disrupting α-synuclein oligomer that accumulates during fibrillation. Proc. Natl. Acad. Sci. USA *108*, 3246-3251.

Gitler, A.D., Chesi, A., Geddie, M.L., Strathearn, K.E., Hamamichi, S., Hill, K.J., Caldwell, K.A., Caldwell, G.A., Cooper, A.A., Rochet, J.C., *et al.* (2009). alpha-Synuclein is part of a diverse and highly conserved interaction network that includes PARK9 and manganese toxicity. Nat. Genet. *41*, 308-315.

Glaser, C.B., Yamin, G., Uversky, V.N., and Fink, A.L. (2005). Methionine oxidation, alpha-synuclein and Parkinson's disease. BBA: Prot. Proteomics *1703*, 157-169.

Glenner, G.G., and Wong, C.W. (1984). Alzheimer's disease: initial report of the purification and characterization of a novel cerebrovascular amyloid protein. Biochem. Biophys. Res. Commun. *120*, 885-890.

Glickman, M.H., and Ciechanover, A. (2002). The ubiquitin-proteasome proteolytic pathway: destruction for the sake of construction. Physiol. Rev. *82*, 373-428.

Goldberg, A.L. (2003). Protein degradation and protection against misfolded or damaged proteins. Nature *426*, 895-899.

Gorell, J.M., Rybicki, B.A., Cole Johnson, C., and Peterson, E.L. (1999). Occupational metal exposures and the risk of Parkinson's disease. Neuroepidemiology *18*, 303-308.

Gosavi, N., Lee, H.J., Lee, J.S., Patel, S., and Lee, S.J. (2002). Golgi fragmentation occurs in the cells with prefibrillar alpha-synuclein aggregates and precedes the formation of fibrillar inclusion. J. Biol. Chem. *277*, 48984-48992.

Goyal, K., Walton, L.J., and Tunnacliffe, A. (2005). LEA proteins prevent protein aggregation due to water stress. Biochem. J. *388*, 151-157.

Greene, L.H., and Grant, T.M. (2012). Protein folding by 'levels of separation': a hypothesis. FEBS Lett. *586*, 962-966.

Greene, L.H., Hamada, D., Eyles, S.J., and Brew, K. (2003). Conserved signature proposed for folding in the lipocalin superfamily. FEBS Lett. *553*, 39-44.

Greene, L.H., and Higman, V.A. (2003). Uncovering network systems within protein structures. J. Mol. Biol. *334*, 781-791.

Greenfield, N.J. (2006). Using circular dichroism spectra to estimate protein secondary structure. Nat. Protoc. *1*, 2876-2890.

Grundke-Iqbal, I., Iqbal, K., Quinlan, M., Tung, Y.C., Zaidi, M.S., and Wisniewski, H.M. (1986). Microtubule-associated protein tau. A component of Alzheimer paired helical filaments. J. Biol. Chem. *261*, 6084-6089.

Gruschus, J.M., Yap, T.L., Pistolesi, S., Maltsev, A.S., and Lee, J.C. (2013). NMR structure of calmodulin complexed to an N-terminally acetylated alpha-synuclein peptide. Biochemistry *52*, 3436-3445.

Gurry, T., Ullman, O., Fisher, C.K., Perovic, I., Pochapsky, T., and Stultz, C.M. (2013). The dynamic structure of alpha-synuclein multimers. J. Am. Chem. Soc. *135*, 3865-3872.

Haass, C., Kaether, C., Thinakaran, G., and Sisodia, S. (2012). Trafficking and proteolytic processing of APP. CSH Perspect. Med. *2*, a006270.

Haigis, M.C., and Yankner, B.A. (2010). The aging stress response. Mol. Cell *40*, 333-344.

Hamodrakas, S.J., Hoenger, A., and Iconomidou, V.A. (2004). Amyloid fibrillogenesis of silkmoth chorion protein peptide-analogues via a liquid-crystalline intermediate phase. J. Struct. Biol. *145*, 226-235.

Harada, R., Kobayashi, N., Kim, J., Nakamura, C., Han, S.W., Ikebukuro, K., and Sode, K. (2009). The effect of amino acid substitution in the imperfect repeat sequences of alpha-synuclein on fibrillation. BBA-Mol. Basis Dis. *1792*, 998-1003.

Hardesty, B., Tsalkova, T., and Kramer, G. (1999). Co-translational folding. Curr. Opin. Struct. Biol. *9*, 111-114.

Harper, J.D., and Lansbury, P.T., Jr. (1997). Models of amyloid seeding in Alzheimer's disease and scrapie: mechanistic truths and physiological consequences of the time-dependent solubility of amyloid proteins. Annu. Rev. Biochem. *66*, 385-407.

Hartl, F.U. (2011). Chaperone-assisted protein folding: the path to discovery from a personal perspective. Nat. Med. *17*, 1206-1210.

Hartl, F.U., and Hayer-Hartl, M. (2002). Molecular chaperones in the cytosol: from nascent chain to folded protein. Science *295*, 1852-1858.

Hartl, F.U., and Martin, J. (1995). Molecular chaperones in cellular protein folding. Curr. Opin. Struct. Biol. *5*, 92-102.

Hasegawa, T. (2010). Tyrosinase-expressing neuronal cell line as in vitro model of Parkinson's disease. Int J. Mol. Sci. *11*, 1082-1089.

Hashimoto, M., Rockenstein, E., Mante, M., Crews, L., Bar-On, P., Gage, F.H., Marr, R., and Masliah, E. (2004). An antiaggregation gene therapy strategy for Lewy body disease utilizing beta-synuclein lentivirus in a transgenic model. Gene Ther. *11*, 1713-1723.

Hashimoto, T., Nishi, K., Nagasao, J., Tsuji, S., and Oyanagi, K. (2008). Magnesium exerts both preventive and ameliorating effects in an in vitro rat Parkinson disease model involving 1-methyl-4-phenylpyridinium (MPP+) toxicity in dopaminergic neurons. Brain Res. *1197*, 143-151.

Hayton, J., Polesel-Maris, J., Demadrille, R., Brun, M., Thoyer, F., Lubin, C., Cousty, J., and Grevin, B. (2010). Atomic force microscopy imaging using a tip-on-chip: opening the door to integrated near field nanotools. Rev. Sci. Instrum. *81*, 093707.

Heinlin, J., Morfill, G., Landthaler, M., Stolz, W., Isbary, G., Zimmermann, J.L., Shimizu, T., and Karrer, S. (2010). Plasma medicine: possible applications in dermatology. J. Dtsch. Dermatol. Ges. *8*, 968-976.

Hilbich, C., Kisters-Woike, B., Reed, J., Masters, C.L., and Beyreuther, K. (1992). Substitutions of hydrophobic amino acids reduce the amyloidogenicity of Alzheimer's disease beta A4 peptides. J. Mol. Biol. *228*, 460-473.

Hodara, R., Norris, E.H., Giasson, B.I., Mishizen-Eberz, A.J., Lynch, D.R., Lee, V.M., and Ischiropoulos, H. (2004). Functional consequences of alpha-synuclein tyrosine nitration: diminished binding to lipid vesicles and increased fibril formation. J. Biol. Chem. *279*, 47746-47753.

Hong, D.P., Han, S., Fink, A.L., and Uversky, V.N. (2011). Characterization of the non-fibrillar alpha-synuclein oligomers. Protein Pept. Lett. *18*, 230-240.

Hoyer, W., Antony, T., Cherny, D., Heim, G., Jovin, T.M., and Subramaniam, V. (2002). Dependence of alpha-synuclein aggregate morphology on solution conditions. J. Molec. Biol. *322*, 383-393.

Hsu, J.C.C., Chen, E.H.L., Snoeberger, R.C., Luh, F.Y., Lim, T.S., Hsu, C.P., and Chen, R.P.Y. (2013). Thioflavin T and Its Photoirradiative Derivatives: Exploring Their Spectroscopic Properties in the Absence and Presence of Amyloid Fibrils. J. Phys. Chem. B *117*, 3459-3468.

Huberts, D.H., and van der Klei, I.J. (2010). Moonlighting proteins: An intriguing mode of multitasking. BBA-Mol. Cell Res. *1803*, 1038-1042.

Isbary, G., Morfill, G., Schmidt, H.U., Georgi, M., Ramrath, K., Heinlin, J., Karrer, S., Landthaler, M., Shimizu, T., Steffes, B., *et al.* (2010). A first prospective randomized controlled trial to decrease bacterial load using cold atmospheric argon plasma on chronic wounds in patients. Br. J. Dermatol. *163*, 78-82.

Israeli, E., and Sharon, R. (2009). Beta-synuclein occurs in vivo in lipid-associated oligomers and forms hetero-oligomers with alpha-synuclein. J. Neurochem. *108*, 465-474.

Jackson, S.E. (1998). How do small single-domain proteins fold? Fold. Des. *3*, R81-91.

Jackson, S.E., and Fersht, A.R. (1991). Folding of chymotrypsin inhibitor 2. 1. Evidence for a two-state transition. Biochemistry *30*, 10428-10435.

Jain, N., Bhasne, K., Hemaswasthi, M., and Mukhopadhyay, S. (2013). Structural and dynamical insights into the membrane-bound alpha-synuclein. PLoS One *8*, e83752.

Jannasch, H.W., Wirsen, C.O., Nelson, D.C., and Robertson, L.A. (1985). Thiomicrospira-Crunogena Sp-Nov, a Colorless, Sulfur-Oxidizing Bacterium from a Deep-Sea Hydrothermal Vent. Int. J. Syst. Bacteriol. *35*, 422-424.

Jenco, J.M., Rawlingson, A., Daniels, B., and Morris, A.J. (1998). Regulation of phospholipase D2: Selective inhibition of mammalian phospholipase D isoenzymes by alpha- and beta-synucleins. Biochemistry *37*, 4901-4909.

Jensen, E. (2013). Types of Imaging, Part 3: Atomic Force Microscopy. Anat. Rec. *296*, 179-183.

Kaltenbach, L.S., Romero, E., Becklin, R.R., Chettier, R., Bell, R., Phansalkar, A., Strand, A., Torcassi, C., Savage, J., Hurlburt, A., *et al.* (2007). Huntingtin interacting proteins are genetic modifiers of neurodegeneration. PLoS Genet. *3*, e82.

Kang, L., Janowska, M.K., Moriarty, G.M., and Baum, J. (2013). Mechanistic insight into the relationship between N-terminal acetylation of alpha-synuclein and fibril formation rates by NMR and fluorescence. PLoS One *8*, e75018.

Kang, L., Moriarty, G.M., Woods, L.A., Ashcroft, A.E., Radford, S.E., and Baum, J. (2012). N-terminal acetylation of alpha-synuclein induces increased transient helical propensity and decreased aggregation rates in the intrinsically disordered monomer. Protein Sci *21*, 911-917.

Karakas, E., Munyanyi, A., Greene, L., and Laroussi, M. (2010). Destruction of alpha-synuclein based amyloid fibrils by a low temperature plasma jet. Appl. Phys. Lett. *97*, 143702.

Karnchanatat, A., Petsom, A., Angvanich, P.S., PiapukieW, J., Whalley, A.J.S., Reynoldsc, C.D., Gadd, G.M., and Sihanonth, P. (2008). A novel thermostable endoglucanase from the wood-decaying fungus Daldinia eschschokii (Ehrenb.: Fr.) Rehm. Enzyme Microb. Tech. *42*, 404-413.

Karplus, M., and Weaver, D.L. (1994). Protein folding dynamics: the diffusion-collision model and experimental data. Protein Sci. *3*, 650-668.

Kasuga, K., Tokutake, T., Ishikawa, A., Uchiyama, T., Tokuda, T., Onodera, O., Nishizawa, M., and Ikeuchi, T. (2010). Differential levels of alpha-synuclein, beta-amyloid42 and tau in CSF between patients with dementia with Lewy bodies and Alzheimer's disease. J. Neurol. Neurosurg. Psychiatry *81*, 608-610.

Keidar, M., Shashurin, A., Volotskova, O., Stepp, M.A., Srinivasan, P., Sandler, A., and Trink, B. (2013). Cold atmospheric plasma in cancer therapy. Phys. Plasmas *20*.

Kelly, J.W. (1998). The alternative conformations of amyloidogenic proteins and their multi-step assembly pathways. Curr. Opin. Struct. Biol. *8*, 101-106.

Kelly, S.M., Jess, T.J., and Price, N.C. (2005). How to study proteins by circular dichroism. Biochim. Biophys. Acta *1751*, 119-139.

Kelly, S.M., and Price, N.C. (2000). The Use of Circular Dichroism in the Investigation of Protein Structure and Function. Curr. Protein Pept. Sci. *1*, 349-384.

Khurana, R., Coleman, C., Ionescu-Zanetti, C., Carter, S.A., Krishna, V., Grover, R.K., Roy, R., and Singh, S. (2005). Mechanism of thioflavin T binding to amyloid fibrils. J. Struct. Biol. *151*, 229-238.

Kim, J., Harada, R., Kobayashi, M., Kobayashi, N., and Sode, K. (2010). The inhibitory effect of pyrroloquinoline quinone on the amyloid formation and cytotoxicity of truncated alpha-synuclein. Mol. Neurodegener. *5*, 20.

Kim, P.S., and Baldwin, R.L. (1982). Specific intermediates in the folding reactions of small proteins and the mechanism of protein folding. Annu. Rev. Biochem. *51*, 459-489.

Kim, R., Kim, K.K., Yokota, H., and Kim, S.H. (1998). Small heat shock protein of Methanococcus jannaschii, a hyperthermophile. Proc. Natl. Acad. Sci. USA *95*, 9129-9133.

Kim, Y.E., Hipp, M.S., Bracher, A., Hayer-Hartl, M., and Hartl, F.U. (2013). Molecular chaperone functions in protein folding and proteostasis. Annu. Rev. Biochem. *82*, 323-355.

Kinch, L.N., and Grishin, N.V. (2002). Evolution of protein structures and functions. Curr. Opin. Struct. Biol. *12*, 400-408.

Kisselev, A.F., Akopian, T.N., Woo, K.M., and Goldberg, A.L. (1999). The sizes of peptides generated from protein by mammalian 26 and 20 S proteasomes - Implications for understanding the degradative mechanism and antigen presentation. J. Biol. Chem. *274*, 3363-3371.

Kleppe, R., Toska, K., and Haavik, J. (2001). Interaction of phosphorylated tyrosine hydroxylase with 14-3-3 proteins: evidence for a phosphoserine 40-dependent association. J. Neurochem. *77*, 1097-1107.

Kong, M.G., Kroesen, G., Morfill, G., Nosenko, T., Shimizu, T., van Dijk, J., and Zimmermann, J.L. (2009). Plasma medicine: an introductory review. New J. Phys. *11*, 115012.

Kopito, R.R. (2000). Aggresomes, inclusion bodies and protein aggregation. Trends Cell Biol. *10*, 524-530.

Kordower, J.H., Chu, Y., Hauser, R.A., Olanow, C.W., and Freeman, T.B. (2008). Transplanted dopaminergic neurons develop PD pathologic changes: a second case report. Mov. Disord. *23*, 2303-2306.

Kottyan, L.C., Woo, J.G., Keddache, M., Banach, W., Crimmins, N.A., Dolan, L.M., and Martin, L.J. (2012). Novel variations in the adiponectin gene (ADIPOQ) may affect distribution of oligomeric complexes. SpringerPlus *1*, 66.

Kranenburg, O., Bouma, B., Kroon-Batenburg, L.M., Reijerkerk, A., Wu, Y.P., Voest, E.E., and Gebbink, M.F. (2002). Tissue-type plasminogen activator is a multiligand cross-beta structure receptor. Curr. Biol. *12*, 1833-1839.

Kruger, R., Kuhn, W., Muller, T., Woitalla, D., Graeber, M., Kosel, S., Przuntek, H., Epplen, J.T., Schols, L., and Riess, O. (1998). Ala30Pro mutation in the gene encoding alpha-synuclein in Parkinson's disease. Nat. Genet. *18*, 106-108.

Kumar, S., Sarkar, A., and Sundar, D. (2009). Controlling aggregation propensity in A53T mutant of alpha-synuclein causing Parkinson's disease. Biochem. Biophys. Res. Commun. *387*, 305-309.

Kuznetsov, I.B., and Rackovsky, S. (2003). On the properties and sequence context of structurally ambivalent fragments in proteins. Protein Sci. *12*, 2420-2433.

Lambert, S.J., Nicholson, J.M., Chantalat, L., Reid, A.J., Donovan, M.J., and Baldwin, J.P. (1999). Purification of histone core octamers and 2.15 A X-ray analysis of crystals in KCl/phosphate. Acta Crystallogr. D Biol. Crystallogr. *55*, 1048-1051.

Laroussi, M. (2009). Low-Temperature Plasmas for Medicine? IEEE Trans. Plasma Sci. *37*, 714-725.

Laroussi, M., and Lu, X. (2005). Room-temperature atmospheric pressure plasma plume for biomedical applications. Appl. Phys. Lett. *87*, 113902.

Larsen, K., Hedegaard, C., Bertelsen, M.F., and Bendixen, C. (2009). Threonine 53 in α-synuclein is conserved in long-living non-primate animals. Biochem. Biophys. Res. Commun 387, 602-605.

Lashuel, H.A., Petre, B.M., Wall, J., Simon, M., Nowak, R.J., Walz, T., and Lansbury, P.T. (2002). Alpha-synuclein, especially the Parkinson's disease-associated mutants, forms pore-like annular and tubular protofibrils. J. Mol. Biol. *322*, 1089-1102.

Lavedan, C. (1998). The synuclein family. Genome Res. *8*, 871-880.

Leal, R.B., Sim, A.T., Goncalves, C.A., and Dunkley, P.R. (2002). Tyrosine hydroxylase dephosphorylation by protein phosphatase 2A in bovine adrenal chromaffin cells. Neurochem. Res. *27*, 207-213.

Lee, S.J., Lim, H.S., Masliah, E., and Lee, H.J. (2011). Protein aggregate spreading in neurodegenerative diseases: problems and perspectives. Neurosci. Res. *70*, 339-348.

Lemkau, L.R., Comellas, G., Lee, S.W., Rikardsen, L.K., Woods, W.S., George, J.M., and Rienstra, C.M. (2013). Site-specific perturbations of alpha-synuclein fibril structure by the Parkinson's disease associated mutations A53T and E46K. PLoS One *8*, e49750.

Lesage, S., Anheim, M., Letournel, F., Bousset, L., Honore, A., Rozas, N., Pieri, L., Madiona, K., Durr, A., Melki, R., *et al.* (2013). G51D alpha-Synuclein mutation causes a novel Parkinsonian-pyramidal syndrome. Ann. Neurol. *73*, 459-471.

Levinthal, C. (1968). Are There Pathways for Protein Folding. J. Chim. Phys. *65*, 44.

Lewis, K.A., Su, Y., Jou, O., Ritchie, C., Foong, C., Hynan, L.S., White, C.L., 3rd, Thomas, P.J., and Hatanpaa, K.J. (2010). Abnormal neurites containing C-terminally

truncated alpha-synuclein are present in Alzheimer's disease without conventional Lewy body pathology. Am. J. Pathol. *177*, 3037-3050.

Li, J., Uversky, V.N., and Fink, A.L. (2001). Effect of familial Parkinson's disease point mutations A30P and A53T on the structural properties, aggregation, and fibrillation of human alpha-synuclein. Chem. Biol. *11*, 1513-1521.

Li, J., Zhu, M., Rajamani, S., Uversky, V.N., and Fink, A.L. (2004). Rifampicin inhibits alpha-synuclein fibrillation and disaggregates fibrils. Chem. Biol. *11*, 1513-1521.

Li, W.X., West, N., Colla, E., Pletnikova, O., Troncoso, J.C., Marsh, L., Dawson, T.M., Jakala, P., Hartmann, T., Price, D.L., *et al.* (2005). Aggregation promoting C-terminal truncation of alpha-synuclein is a normal cellular process and is enhanced by the familial Parkinson's disease-linked mutations. Proc. Natl. Acad. Sci. USA *102*, 2162-2167.

Lin, M.C., Mirzabekov, T., and Kagan, B.L. (1997). Channel formation by a neurotoxic prion protein fragment. J. Biol. Chem. *272*, 44-47.

Linding, R., Russell, R.B., Neduva, V., and Gibson, T.J. (2003). GlobPlot: exploring protein sequences for globularity and disorder. Nucleic Acids Research *31*, 3701-3708.

Linding, R., Schymkowitz, J., Rousseau, F., Diella, F., and Serrano, L. (2004). A comparative study of the relationship between protein structure and beta-aggregation in globular and intrinsically disordered proteins. J. Mol. Biol. *342*, 345-353.

Lipman, D.J., and Pearson, W.R. (1985). Rapid and sensitive protein similarity searches. Science *227*, 1435-1441.

Liu, C.W., Giasson, B.I., Lewis, K.A., Lee, V.M., Demartino, G.N., and Thomas, P.J. (2005). A precipitating role for truncated alpha-synuclein and the proteasome in alpha-synuclein aggregation: implications for pathogenesis of Parkinson disease. J Biol Chem *280*, 22670-22678.

Lo Bianco, C., Ridet, J.L., Schneider, B.L., Deglon, N., and Aebischer, P. (2002). alpha-Synucleinopathy and selective dopaminergic neuron loss in a rat lentiviral-based model of Parkinson's disease. Proc. Natl. Acad. Sci. USA *99*, 10813-10818.

Lopez De La Paz, M., Goldie, K., Zurdo, J., Lacroix, E., Dobson, C.M., Hoenger, A., and Serrano, L. (2002). De novo designed peptide-based amyloid fibrils. Proc. Natl. Acad. Sci. USA *99*, 16052-16057.

Lou, H., Montoya, S.E., Alerte, T.N., Wang, J., Wu, J., Peng, X., Hong, C.S., Friedrich, E.E., Mader, S.A., Pedersen, C.J., *et al.* (2010). Serine 129 phosphorylation reduces the ability of alpha-synuclein to regulate tyrosine hydroxylase and protein phosphatase 2A in vitro and in vivo. J. Biol. Chem. *285*, 17648-17661.

Louis-Jeune, C., Andrade-Navarro, M.A., and Perez-Iratxeta, C. (2011). Prediction of protein secondary structure from circular dichroism using theoretically derived spectra. Proteins *80*, 375-380.

Lowe, R., Pountney, D.L., Jensen, P.H., Gai, W.P., and Voelcker, N.H. (2004). Calcium(II) selectively induces alpha-synuclein annular oligomers via interaction with the C-terminal domain. Protein Sci. *13*, 3245-3252.

Lucchini, R.G., Martin, C.J., and Doney, B.C. (2009). From manganism to manganese-induced parkinsonism: a conceptual model based on the evolution of exposure. Neuromolecular Med. *11*, 311-321.

Ma, G., Zhang, H., Guo, J., Zeng, X., Hu, X., and Hao, W. (2014). Assessment of the Inhibitory Effect of Rifampicin on Amyloid Formation of Hen Egg White Lysozyme: Thioflavin T Fluorescence Assay versus FTIR Difference Spectroscopy. J. Spectrosc. *2014*, Article ID 285806.

Magadum, S., Banerjee, U., Murugan, P., Gangapur, D., and Ravikesavan, R. (2013). Gene duplication as a major force in evolution. J. Genet. *92*, 155-161.

Mak, S.K., McCormack, A.L., Langston, J.W., Kordower, J.H., and Di Monte, D.A. (2009). Decreased alpha-synuclein expression in the aging mouse substantia nigra. Exp. Neurol. *220*, 359-365.

Malkov, S.N., Zivkovic, M.V., Beljanski, M.V., Stojanovic, S.D., and Zaric, S.D. (2009). A reexamination of correlations of amino acids with particular secondary structures. Protein J. *28*, 74-86.

Mandelkow, E.M., and Mandelkow, E. (2012). Biochemistry and cell biology of tau protein in neurofibrillary degeneration. CSH Perspect. Med. *2*, a006247.

Mannige, R.V., Brooks, C.L., and Shakhnovich, E.I. (2012). A universal trend among proteomes indicates an oily last common ancestor. PLoS Comput.Biol. *8*, e1002839.

Maroteaux, L., Campanelli, J.T., and Scheller, R.H. (1988). Synuclein: a neuron-specific protein localized to the nucleus and presynaptic nerve terminal. J. Neurosci. *8*, 2804-2815.

Martin, J.B. (1999). Molecular basis of the neurodegenerative disorders. N. Engl. J. Med. *340*, 1970-1980.

Mattson, M.P. (2000). Apoptosis in neurodegenerative disorders. Nat. Rev. Mol. Cell Biol. *1*, 120-129.

McClellan, A.J., and Frydman, J. (2001). Molecular chaperones and the art of recognizing a lost cause. Nat. Cell Biol. *3*, E51-53.

McCormack, A.L., Mak, S.K., and Di Monte, D.A. (2012). Increased alpha-synuclein phosphorylation and nitration in the aging primate substantia nigra. Cell Death Dis. *3*, e315.

McLean, J.R., Hallett, P.J., Cooper, O., Stanley, M., and Isacson, O. (2012). Transcript expression levels of full-length alpha-synuclein and its three alternatively spliced variants in Parkinson's disease brain regions and in a transgenic mouse model of alpha-synuclein overexpression. Mol. Cell Neurosci. *49*, 230-239.

McWilliam, H., Li, W., Uludag, M., Squizzato, S., Park, Y.M., Buso, N., Cowley, A.P., and Lopez, R. (2013). Analysis Tool Web Services from the EMBL-EBI. Nucleic Acids Res. *41*, W597-600.

Mericam-Bourdet, N., Laroussi, M., Begum, A., and Karakas, E. (2009). Experimental investigations of plasma bullets. J. Phys. D: Appl. Phys. *42*, 055207.

Meyer, E. (1992). Atomic Force Microscopy. Prog. Surf. Sci. *41*, 3-49.

Miao, Y., Nichols, S.E., and McCammon, J.A. (2014). Free energy landscape of G-protein coupled receptors, explored by accelerated molecular dynamics. Phys. Chem. Chem. Phys. *16*, 6398-6406.

Migliore, L., and Coppede, F. (2009). Genetics, environmental factors and the emerging role of epigenetics in neurodegenerative diseases. Mutat. Res. *667*, 82-97.

Mijaljica, D., Prescott, M., and Devenish, R.J. (2010). Autophagy in disease. Methods Mol. Biol. *648*, 79-92.

Misra, N.N., Pankaj, S.K., Walsh, T., O'Regan, F., Bourke, P., and Cullen, P.J. (2014). In-package nonthermal plasma degradation of pesticides on fresh produce. J. Hazard Mater. *271C*, 33-40.

Mosharov, E.V., Larsen, K.E., Kanter, E., Phillips, K.A., Wilson, K., Schmitz, Y., Krantz, D.E., Kobayashi, K., Edwards, R.H., and Sulzer, D. (2009). Interplay between cytosolic dopamine, calcium, and alpha-synuclein causes selective death of substantia nigra neurons. Neuron *62*, 218-229.
Mounsey, R.B., and Teismann, P. (2010). Mitochondrial dysfunction in Parkinson's disease: pathogenesis and neuroprotection. Parkinsons Dis. *2011*, 617472.

Mounsey, R.B., and Teismann, P. (2012). Chelators in the treatment of iron accumulation in Parkinson's disease. Int. J. Cell Biol. *2012*, 983245.

Murakami, K., Murata, N., Noda, Y., Tahara, S., Kaneko, T., Kinoshita, N., Hatsuta, H., Murayama, S., Barnham, K.J., Irie, K., *et al.* (2011). SOD1 (Copper/Zinc Superoxide Dismutase) Deficiency Drives Amyloid beta Protein Oligomerization and Memory Loss in Mouse Model of Alzheimer Disease. J. Biol. Chem. *286*, 44557-44568.

Murphy, M.P. (2009). How mitochondria produce reactive oxygen species. Biochem J. *417*, 1-13.

Narkiewicz, J., Giachin, G., and Legname, G. (2014). In vitro aggregation assays for the characterization of alpha-synuclein prion-like properties. Prion *8*, 19-32.

Nelson, D.L., and Cox, M.M. (2013). Principles of Biochemistry, 6th edn (New York, NY.: W. H. Freeman and Company), pp. 141-142.

Niemira, B.A. (2012). Cold plasma decontamination of foods. Annu. Rev. Food Sci. Technol. *3*, 125-142.

Nilsson, M.R. (2004). Techniques to study amyloid fibril formation in vitro. Methods *34*, 151-160.

Nolting, B., and Andert, K. (2000). Mechanism of protein folding. Proteins *41*, 288-298.

Norouzi, P., Faridbod, F., Rashedi, H., and Ganjali, M.R. (2010). Flow Injection Glutamate Biosensor Based on Carbon Nanotubes and Pt-Nanoparticles Using FFT Continuous Cyclic Voltammetry. Int. J. Electrochem. Sci. *5*, 1713-1725.

Norris, E.H., Giasson, B.I., Hodara, R., Xu, S., Trojanowski, J.Q., Ischiropoulos, H., and Lee, V.M. (2005). Reversible inhibition of alpha-synuclein fibrillization by dopaminochrome-mediated conformational alterations. J. Biol. Chem. *280*, 21212-21219.

Oaks, A.W., Frankfurt, M., Finkelstein, D.I., and Sidhu, A. (2013). Age-dependent effects of A53T alpha-synuclein on behavior and dopaminergic function. PLoS One *8*, e60378.

Obsilova, V., Nedbalkova, E., Silhan, J., Boura, E., Herman, P., Vecer, J., Sulc, M., Teisinger, J., Dyda, F., and Obsil, T. (2008). The 14-3-3 protein affects the conformation of the regulatory domain of human tyrosine hydroxylase. Biochemistry *47*, 1768-1777.

Ohi, M., Li, Y., Cheng, Y., and Walz, T. (2004). Negative Staining and Image Classification - Powerful Tools in Modern Electron Microscopy. Biol. Proced. Online *6*, 23-34.

Ohtake, H., Limprasert, P., Fan, Y., Onodera, O., Kakita, A., Takahashi, H., Bonner, L.T., Tsuang, D.W., Murray, I.V., Lee, V.M., *et al.* (2004). Beta-synuclein gene alterations in dementia with Lewy bodies. Neurology *63*, 805-811.

Olzmann, J.A., Li, L., and Chin, L.S. (2008). Aggresome formation and neurodegenerative diseases: therapeutic implications. Curr. Med. Chem. *15*, 47-60.

Oueslati, A., Fournier, M., and Lashuel, H.A. (2010). Role of post-translational modifications in modulating the structure, function and toxicity of alpha-synuclein: implications for Parkinson's disease pathogenesis and therapies. Prog. Brain Res. *183*, 115-145.

Oueslati, A., Paleologou, K.E., Schneider, B.L., Aebischer, P., and Lashuel, H.A. (2012). Mimicking phosphorylation at serine 87 inhibits the aggregation of human alpha-synuclein and protects against its toxicity in a rat model of Parkinson's disease. J. Neurosci. *32*, 1536-1544.

Oyanagi, K., Kawakami, E., Kikuchi-Horie, K., Ohara, K., Ogata, K., Takahama, S., Wada, M., Kihira, T., and Yasui, M. (2006). Magnesium deficiency over generations in rats with special references to the pathogenesis of the Parkinsonism-dementia complex and amyotrophic lateral sclerosis of Guam. Neuropathology *26*, 115-128.

Ozawa, D., Yagi, H., Ban, T., Kameda, A., Kawakami, T., Naiki, H., and Goto, Y. (2009). Destruction of Amyloid Fibrils of a beta(2)-Microglobulin Fragment by Laser Beam Irradiation. J. Biol. Chem. *284*, 1009-1017.

Paleologou, K.E., Oueslati, A., Shakked, G., Rospigliosi, C.C., Kim, H.Y., Lamberto, G.R., Fernandez, C.O., Schmid, A., Chegini, F., Gai, W.P., *et al.* (2010). Phosphorylation at S87 is enhanced in synucleinopathies, inhibits alpha-synuclein oligomerization, and influences synuclein-membrane interactions. J. Neurosci. *30*, 3184-3198.

Pan, T., Kondo, S., Le, W., and Jankovic, J. (2008). The role of autophagy-lysosome pathway in neurodegeneration associated with Parkinson's disease. Brain *131*, 1969-1978.

Pankaj, S.K., Bueno-Ferrer, C., Misra, N.N., Milosavljevic, V., O'Donnell, C.P., Bourke, P., Keener, K.M., and Cullen, P.J. (2014). Applications of cold plasma technology in food packaging. Trends Food Sci. Tech. *35*, 5-17.

Parihar, M.S., Parihar, A., Fujita, M., Hashimoto, M., and Ghafourifar, P. (2008). Mitochondrial association of alpha-synuclein causes oxidative stress. Cell. Mol. Life Sci. *65*, 1272-1284.

Park, J.Y., and Lansbury, P.T., Jr. (2003). Beta-synuclein inhibits formation of alpha-synuclein protofibrils: a possible therapeutic strategy against Parkinson's disease. Biochemistry *42*, 3696-3700.

Park, S.M., Jung, H.Y., Chung, K.C., Rhim, H., Park, J.H., and Kim, J. (2002). Stress-induced aggregation profiles of GST-alpha-synuclein fusion proteins: role of the C-terminal acidic tail of alpha-synuclein in protein thermosolubility and stability. Biochemistry *41*, 4137-4146.

Pearlman, S.M., Serber, Z., and Ferrell, J.E., Jr. (2011). A mechanism for the evolution of phosphorylation sites. Cell *147*, 934-946.

Peng, X., Tehranian, R., Dietrich, P., Stefanis, L., and Perez, R.G. (2005). Alpha-synuclein activation of protein phosphatase 2A reduces tyrosine hydroxylase phosphorylation in dopaminergic cells. J. Cell Sci. *118*, 3523-3530.

Pereira, J.H., Chen, Z.W., McAndrew, R.P., Sapra, R., Chhabra, S.R., Sale, K.L., Simmons, B.A., and Adams, P.D. (2010). Biochemical characterization and crystal structure of endoglucanase Cel5A from the hyperthermophilic Thermotoga maritima. J. Struct. Biol. *172*, 372-379.

Perez, R.G., Waymire, J.C., Lin, E., Liu, J.J., Guo, F., and Zigmond, M.J. (2002). A role for alpha-synuclein in the regulation of dopamine biosynthesis. J. Neurosci. *22*, 3090-3099.

Perrin, R.J., Woods, W.S., Clayton, D.F., and George, J.M. (2001). Exposure to long chain polyunsaturated fatty acids triggers rapid multimerization of synucleins. J. Biol. Chem. *276*, 41958-41962.

Petkova, A.T., Yau, W.M., and Tycko, R. (2006). Experimental constraints on quaternary structure in Alzheimer's beta-amyloid fibrils. Biochemistry *45*, 498-512.

Polverini, E., Fasano, A., Zito, F., Riccio, P., and Cavatorta, P. (1999). Conformation of bovine myelin basic protein purified with bound lipids. Eur. Biophys. J. *28*, 351-355.

Polymeropoulos, M.H., Lavedan, C., Leroy, E., Ide, S.E., Dehejia, A., Dutra, A., Pike, B., Root, H., Rubenstein, J., Boyer, R., *et al.* (1997). Mutation in the alpha-synuclein gene identified in families with Parkinson's disease. Science *276*, 2045-2047.

Pountney, D.L., Voelcker, N.H., and Gai, W.P. (2005). Annular alpha-synuclein oligomers are potentially toxic agents in alpha-synucleinopathy. Hypothesis. Neurotox. Res. *7*, 59-67.

Pronin, A.N., Morris, A.J., Surguchov, A., and Benovic, J.L. (2000). Synucleins are a novel class of substrates for G protein-coupled receptor kinases. J. Biol. Chem. *275*, 26515-26522.

Radford, S.E. (2000). Protein folding: progress made and promises ahead. Trends Biochem. Sci. *25*, 611-618.

Rajamani, D., Thiel, S., Vajda, S., and Camacho, C.J. (2004). Anchor residues in protein-protein interactions. Proc. Natl. Acad. Sci. USA *101*, 11287-11292.

Ramakrishnan, V., Finch, J.T., Graziano, V., Lee, P.L., and Sweet, R.M. (1993). Crystal structure of globular domain of histone H5 and its implications for nucleosome binding. Nature *362*, 219-223.

Rao, J.N., Jao, C.C., Hegde, B.G., Langen, R., and Ulmer, T.S. (2010). A combinatorial NMR and EPR approach for evaluating the structural ensemble of partially folded proteins. J. Am. Chem. Soc. *132*, 8657-8668.

Rapoport, S.I. (2008). Arachidonic Acid and the Brain. J. Nutri. *138*, 2515-2520.

Redfern, O.C., Dessailly, B.H., Dallman, T.J., Sillitoe, I., and Orengo, C.A. (2009). FLORA: a novel method to predict protein function from structure in diverse superfamilies. PLoS Comput. Biol. *5*, e1000485.

Rekas, A., Ahn, K.J., Kim, J., and Carver, J.A. (2012). The chaperone activity of alpha-synuclein: Utilizing deletion mutants to map its interaction with target proteins. Proteins *80*, 1316-1325.

Rivers, R.C., Kumita, J.R., Tartaglia, G.G., Dedmon, M.M., Pawar, A., Vendruscolo, M., Dobson, C.M., and Christodoulou, J. (2008). Molecular determinants of the aggregation behavior of alpha- and beta-synuclein. Protein Sci. *17*, 887-898.

Rodrigues, J.V., Henriques, B.J., Lucas, T.G., and Gomes, C.M. (2012). Cofactors and metabolites as protein folding helpers in metabolic diseases. Curr. Top. Med. Chem. *12*, 2546-2559.

Ross, C.A., and Pickart, C.M. (2004). The ubiquitin-proteasome pathway in Parkinson's disease and other neurodegenerative diseases. Trends Cell Biol. *14*, 703-711.

Ross, C.A., and Poirier, M.A. (2004). Protein aggregation and neurodegenerative disease. Nat. Med. *10 Suppl*, S10-17.

Rowe, N. (1996). The pictorial guide to the living primates. (Pogonias Press, East Hampton, NY.).

Sakamoto, N., Kotre, A.M., and Savageau, M.A. (1975). Glutamate dehydrogenase from Escherichia coli: purification and properties. J. Bacteriol. *124*, 775-783.

Sanchez-Romero, I., Ariza, A., Wilson, K.S., Skjot, M., Vind, J., De Maria, L., Skov, L.K., and Sanchez-Ruiz, J.M. (2013). Mechanism of protein kinetic stabilization by engineered disulfide crosslinks. PLoS One *8*, e70013.

Sandgren, M., Shaw, A., Ropp, T.H., Bott, S.W.R., Cameron, A.D., Stahlberg, J., Mitchinson, C., and Jones, T.A. (2001). The X-ray crystal structure of the Trichoderma reesei family 12 endoglucanase 3, Cel12A, at 1.9 angstrom resolution. J. Mol. Biol. *308*, 295-310.

Santner, A., and Uversky, V.N. (2010). Metalloproteomics and metal toxicology of alpha-synuclein. Metallomics *2*, 378-392.

Saric, T., Graef, C.I., and Goldberg, A.L. (2004). Pathway for degradation of peptides generated by proteasomes - A key role for thimet oligopeptidase and other metallopeptidases. J. Biol. Chem. *279*, 46723-46732.

Sato, H., Arawaka, S., Hara, S., Fukushima, S., Koga, K., Koyama, S., and Kato, T. (2011). Authentically phosphorylated alpha-synuclein at Ser129 accelerates neurodegeneration in a rat model of familial Parkinson's disease. J. Neurosci. *31*, 16884-16894.

Schapira, A.H.V. (2007). Mitochondrial dysfunction in Parkinson's disease. Cell Death Differ. *14*, 1261-1266.

Schapira, A.H.V. (2008). Mitochondria in the aetiology and pathogenesis of Parkinson's disease. Lancet Neurol. *7*, 97-109.

Schlesinger, M.J., Ryan, C., Chi, M.M., Carter, J.G., Pusateri, M.E., and Lowry, O.H. (1997). Metabolite changes associated with heat shocked avian fibroblast mitochondria. Cell Stress Chaperones *2*, 25-30.

Schonichen, A., Webb, B.A., Jacobson, M.P., and Barber, D.L. (2013). Considering Protonation as a Posttranslational Modification Regulating Protein Structure and Function. Annu. Rev. Biophys. *42*, 289-314.

Schultz, C.P. (2000). Illuminating folding intermediates. Nat. Struct. Biol. *7*, 7-10.

Schulz-Schaeffer, W.J. (2010). The synaptic pathology of alpha-synuclein aggregation in dementia with Lewy bodies, Parkinson's disease and Parkinson's disease dementia. Acta Neuropathol. *120*, 131-143.

Serpell, L.C., Berriman, J., Jakes, R., Goedert, M., and Crowther, R.A. (2000). Fiber diffraction of synthetic alpha-synuclein filaments shows amyloid-like cross-beta conformation. Proc. Natl. Acad. Sci. USA *97*, 4897-4902.

Shaiu, W.L., Hu, T., and Hsieh, T.S. (1999). The hydrophilic, protease-sensitive terminal domains of eucaryotic DNA topoisomerases have essential intracellular functions. Pac. Symp. Biocomput., 578-589.

Shaltiel-Karyo, R., Frenkel-Pinter, M., Egoz-Matia, N., Frydman-Marom, A., Shalev, D.E., Segal, D., and Gazit, E. (2010). Inhibiting alpha-synuclein oligomerization by stable cell-penetrating beta-synuclein fragments recovers phenotype of Parkinson's disease model flies. PLoS One *5*, e13863.

Sherman, M.Y., and Goldberg, A.L. (2001). Cellular defenses against unfolded proteins: a cell biologist thinks about neurodegenerative diseases. Neuron *29*, 15-32.

Shi, J.J., Zhong, F.C., Zhang, J., Liu, D.W., and Kong, M.G. (2008). A hypersonic plasma bullet train traveling in an atmospheric dielectric-barrier discharge jet. Phys. Plasmas *15*, 013504.

Sidhu, A., Wersinger, C., and Vernier, P. (2004a). alpha-Synuclein regulation of the dopaminergic transporter: a possible role in the pathogenesis of Parkinson's disease. FEBS Lett. *565*, 1-5.

Sidhu, A., Wersinger, C., and Vernier, P. (2004b). Does alpha-synuclein modulate dopaminergic synaptic content and tone at the synapse? FASEB J. *18*, 637-647.

Simola, N., Pinna, A., and Fenu, S. (2010). Pharmacological therapy of Parkinson's disease: current options and new avenues. Recent Pat CNS Drug Discov. *5*, 221-238.

Simon, D.J., Weimer, R.M., McLaughlin, T., Kallop, D., Stanger, K., Yang, J., O'Leary, D.D., Hannoush, R.N., and Tessier-Lavigne, M. (2012). A caspase cascade regulating developmental axon degeneration. J. Neurosci. *32*, 17540-17553.

Siso, S., Hanzlicek, D., Fluehmann, G., Kathmann, I., Tomek, A., Papa, V., and Vandevelde, M. (2006). Neurodegenerative diseases in domestic animals: a comparative review. Vet. J. *171*, 20-38.

Slauch, J.M. (2011). How does the oxidative burst of macrophages kill bacteria? Still an open question. Mol. Microbiol. *80*, 580-583.

Smyth, M.S., and Martin, J.H.J. (2000). X-Ray crystallography. J. Clin. Pathol.-Mol. Pathol. *53*, 8-14.

Sode, K., Ochiai, S., Kobayashi, N., and Usuzaka, E. (2007). Effect of reparation of repeat sequences in the human alpha-synuclein on fibrillation ability. Int. J. Biol. Sci. *3*, 1-7.

Sokollek, S.J., Hertel, C., and Hammes, W.P. (1998). Description of Acetobacter oboediens sp. nov. and Acetobacter pomorum sp. nov., two new species isolated from industrial vinegar fermentations. Int. J. Syst. Bacteriol. *48*, 935-940.

Soto, C. (2003). Unfolding the role of protein misfolding in neurodegenerative diseases. Nat Rev Neurosci *4*, 49-60.

Spillantini, M.G., Divane, A., and Goedert, M. (1995). Assignment of human alpha-synuclein (SNCA) and beta-synuclein (SNCB) genes to chromosomes 4q21 and 5q35. Genomics *27*, 379-381.

Spillantini, M.G., Schmidt, M.L., Lee, V.M., Trojanowski, J.Q., Jakes, R., and Goedert, M. (1997). Alpha-synuclein in Lewy bodies. Nature *388*, 839-840.

Sreerama, N., and Woody, R.W. (2004). Computation and analysis of protein circular dichroism spectra. Methods Enzymol. *383*, 318-351.

Srinivasan, S. (2012). A Current Perspective on Membrane Protein Folding. Biochem. Anal. Biochem. *1: e123. doi:10.4172/2161-1009.1000e123.*

Stewart, L., Ireton, G.C., and Champoux, J.J. (1996). The domain organization of human topoisomerase I. J. Biol. Chem. *271*, 7602-7608.

Sultana, R., Perluigi, M., and Butterfield, D.A. (2006). Protein oxidation and lipid peroxidation in brain of subjects with Alzheimer's disease: insights into mechanism of neurodegeneration from redox proteomics. Antioxid. Redox Signal *8*, 2021-2037.

Sunde, M., and Blake, C. (1997). The structure of amyloid fibrils by electron microscopy and X-ray diffraction. Adv. Protein Chem. *50*, 123-159.

Sung, Y.H., and Eliezer, D. (2006). Secondary structure and dynamics of micelle bound beta- and gamma-synuclein. Protein Sci. *15*, 1162-1174.

Sung, Y.H., and Eliezer, D. (2007). Residual structure, backbone dynamics, and interactions within the synuclein family. J. Mol. Biol. *372*, 689-707.

Suzuki, Y. (2014). Emerging novel concept of chaperone therapies for protein misfolding diseases. Proc. Jpn. Acad. Ser. B: Phys. Biol. Sci. *90*, 145-162.

Sweers, K.K.M., Segers-Nolten, I.M.J., Bennink, M.L., and Subramaniam, V. (2012). Structural model for alpha-synuclein fibrils derived from high resolution imaging and nanomechanical studies using atomic force microscopy. Soft Matter *8*, 7215-7222.
Takalo, M., Salminen, A., Soininen, H., Hiltunen, M., and Haapasalo, A. (2013). Protein aggregation and degradation mechanisms in neurodegenerative diseases. Am. J. Neurodegener. Dis. *2*, 1-14.

Tarawneh, R., and Galvin, J.E. (2010). Potential future neuroprotective therapies for neurodegenerative disorders and stroke. Clin. Geriatr. Med. *26*, 125-147.

Timmermeyer, N., Gerlach, T., Guempel, C., Knoche, J., Pfann, J.F., Schliessmann, D., and Michiels, N.K. (2010). The function of copulatory plugs in Caenorhabditis remanei: hints for female benefits. Front. Zool. *7*, 28.

Timsit, Y., Acosta, Z., Allemand, F., Chiaruttini, C., and Springer, M. (2009). The role of disordered ribosomal protein extensions in the early steps of eubacterial 50 S ribosomal subunit assembly. Int. J. Mol. Sci. *10*, 817-834.

Tinsley, R.B., Kotschet, K., Modesto, D., Ng, H., Wang, Y., Nagley, P., Shaw, G., and Horne, M.K. (2010). Sensitive and specific detection of alpha-synuclein in human plasma. J. Neurosci. Res. *88*, 2693-2700.

Todd, A.E., Orengo, C.A., and Thornton, J.M. (2001). Evolution of function in protein superfamilies, from a structural perspective. J. Mol. Biol. *307*, 1113-1143.

Tokuda, T., Qureshi, M.M., Ardah, M.T., Varghese, S., Shehab, S.A., Kasai, T., Ishigami, N., Tamaoka, A., Nakagawa, M., and El-Agnaf, O.M. (2010). Detection of elevated levels of alpha-synuclein oligomers in CSF from patients with Parkinson disease. Neurology *75*, 1766-1772.

Tokuda, T., Salem, S.A., Allsop, D., Mizuno, T., Nakagawa, M., Qureshi, M.M., Locascio, J.J., Schlossmacher, M.G., and El-Agnaf, O.M. (2006). Decreased alpha-synuclein in cerebrospinal fluid of aged individuals and subjects with Parkinson's disease. Biochem. Biophys. Res. Commun. *349*, 162-166.

Tompa, P. (2002). Intrinsically unstructured proteins. Trends Biochem. Sci. *27*, 527-533.

Tompa, P. (2005). The interplay between structure and function in intrinsically unstructured proteins. FEBS Lett. *579*, 3346-3354.

Tompa, P., Szasz, C., and Buday, L. (2005). Structural disorder throws new light on moonlighting. Trends Biochem. Sci. *30*, 484-489.

Trexler, A.J., and Rhoades, E. (2012). N-Terminal acetylation is critical for forming alpha-helical oligomer of alpha-synuclein. Protein Sci. *21*, 601-605.

Turner, B.J., Atkin, J.D., Farg, M.A., Zang, D.W., Rembach, A., Lopes, E.C., Patch, J.D., Hill, A.F., and Cheema, S.S. (2005). Impaired extracellular secretion of mutant superoxide dismutase 1 associates with neurotoxicity in familial amyotrophic lateral sclerosis. J. Neurosci. *25*, 108-117.

Tycko, R., and Wickner, R.B. (2013). Molecular structures of amyloid and prion fibrils: consensus versus controversy. Acc. Chem. Res. *46*, 1487-1496.

Ulmer, T.S., Bax, A., Cole, N.B., and Nussbaum, R.L. (2005). Structure and dynamics of micelle-bound human alpha-synuclein. J. Biol. Chem. *280*, 9595-9603.

Uversky, V.N., Gillespie, J.R., and Fink, A.L. (2000). Why are "natively unfolded" proteins unstructured under physiologic conditions? Proteins *41*, 415-427.

Uversky, V.N., Gillespie, J.R., Millett, I.S., Khodyakova, A.V., Vasiliev, A.M., Chernovskaya, T.V., Vasilenko, R.N., Kozovskaya, G.D., Dolgikh, D.A., Fink, A.L., *et al.* (1999). Natively unfolded human prothymosin alpha adopts partially folded collapsed conformation at acidic pH. Biochemistry *38*, 15009-15016.

Uversky, V.N., Li, J., and Fink, A.L. (2001a). Evidence for a partially folded intermediate in alpha-synuclein fibril formation. J. Biol. Chem. *276*, 10737-10744.

Uversky, V.N., Li, J., and Fink, A.L. (2001b). Metal-triggered structural transformations, aggregation, and fibrillation of human alpha-synuclein. A possible molecular NK between Parkinson's disease and heavy metal exposure. J. Biol. Chem. *276*, 44284-44296.

Uversky, V.N., Li, J., Souillac, P., Millett, I.S., Doniach, S., Jakes, R., Goedert, M., and Fink, A.L. (2002). Biophysical properties of the synucleins and their propensities to fibrillate: inhibition of alpha-synuclein assembly by beta- and gamma-synucleins. J. Biol. Chem. *277*, 11970-11978.

Vabulas, R.M., Raychaudhuri, S., Hayer-Hartl, M., and Hartl, F.U. (2010). Protein Folding in the Cytoplasm and the Heat Shock Response. CSH Perspect. Biol *2*, a004390.

Valastyan, J.S., and Lindquist, S. (2014). Mechanisms of protein-folding diseases at a glance. Dis. Model Mech. *7*, 9-14.

Valente, E.M., Salvi, S., Ialongo, T., Marongiu, R., Elia, A.E., Caputo, V., Romito, L., Albanese, A., Dallapiccola, B., and Bentivoglio, A.R. (2004). PINK1 mutations are associated with sporadic early-onset parkinsonism. Ann. Neurol. *56*, 336-341.

Valentini, G., M. Maggi, A. L. Pey (2013). Protein Stability, folding and misfolding in human PGK1 Deficiency. Biomolecules *3*, 1030-1052

van Rooijen, B.D., Claessens, M.M., and Subramaniam, V. (2010). Membrane Permeabilization by Oligomeric alpha-Synuclein: In Search of the Mechanism. PLoS One *5*, e14292.

Vendruscolo, M., Paci, E., Dobson, C.M., and Karplus, M. (2001). Three key residues form a critical contact network in a protein folding transition state. Nature *409*, 641-645.

Vigneswara, V., Cass, S., Wayne, D., Bolt, E.L., Ray, D.E., and Carter, W.G. (2013). Molecular ageing of alpha- and Beta-synucleins: protein damage and repair mechanisms. PLoS One *8*, e61442.

Voges, D., Zwickl, P., and Baumeister, W. (1999). The 26S proteasome: A molecular machine designed for controlled proteolysis. Annu. Rev. Biochem. *68*, 1015-1068.

Wakeman, D.R., Dodiya, H.B., and Kordower, J.H. (2011). Cell transplantation and gene therapy in Parkinson's disease. Mt. Sinai J. Med. *78*, 126-158.

Walsh, D.M., Hartley, D.M., Kusumoto, Y., Fezoui, Y., Condron, M.M., Lomakin, A., Benedek, G.B., Selkoe, D.J., and Teplow, D.B. (1999). Amyloid beta-protein fibrillogenesis. Structure and biological activity of protofibrillar intermediates. J. Biol. Chem. *274*, 25945-25952.

Walsh, D.M., Lomakin, A., Benedek, G.B., Condron, M.M., and Teplow, D.B. (1997). Amyloid beta-protein fibrillogenesis. Detection of a protofibrillar intermediate. J. Biol. Chem. *272*, 22364-22372.

Walters, B.T., Mayne, L., Hinshaw, J.R., Sosnick, T.R., and Englander, S.W. (2013). Folding of a large protein at high structural resolution. Proc. Natl. Acad. Sci. USA *110*, 18898-18903.

Wan, O.W., and Chung, K.K. (2012). The role of alpha-synuclein oligomerization and aggregation in cellular and animal models of Parkinson's disease. PLoS One *7*, e38545.

Wang, J.T., Medress, Z.A., and Barres, B.A. (2012). Axon degeneration: molecular mechanisms of a self-destruction pathway. J. Cell Biol. *196*, 7-18.

Wang, W., Perovic, I., Chittuluru, J., Kaganovich, A., Nguyen, L.T., Liao, J., Auclair, J.R., Johnson, D., Landeru, A., Simorellis, A.K., *et al.* (2011). A soluble alpha-synuclein construct forms a dynamic tetramer. Proc. Natl. Acad. Sci. USA *108*, 17797-17802.

Wang, Z.L. (2000). Transmission electron microscopy of shape-controlled nanocrystals and their assemblies. J. Phys. Chem. B *104*, 1153-1175.

Weinkam, P., Zimmermann, J., Romesberg, F.E., and Wolynes, P.G. (2010). The folding energy landscape and free energy excitations of cytochrome c. Acc. Chem. Res. *43*, 652-660.

Wersinger, C., Banta, M., and Sidhu, A. (2004). Comparative analyses of alpha-synuclein expression levels in rat brain tissues and transfected cells. Neurosci. Lett. *358*, 95-98.

Wersinger, C., Prou, D., Vernier, P., and Sidhu, A. (2003). Modulation of dopamine transporter function by alpha-synuclein is altered by impairment of cell adhesion and by induction of oxidative stress. FASEB J. *17*, 2151-2153.

Westermark, P., Benson, M.D., Buxbaum, J.N., Cohen, A.S., Frangione, B., Ikeda, S., Masters, C.L., Merlini, G., Saraiva, M.J., and Sipe, J.D. (2007). A primer of amyloid nomenclature. Amyloid *14*, 179-183.

Westermark, P., Wilander, E., and Johnson, K.H. (1987). Islet amyloid polypeptide. Lancet *2*, 623.

Whitmore, L., and Wallace, B.A. (2008). Protein secondary structure analyses from circular dichroism spectroscopy: Methods and reference databases. Biopolymers *89*, 392-400.

Wietek, J., Haralampiev, I., Amoussouvi, A., Herrmann, A., and Stockl, M. (2013). Membrane bound alpha-synuclein is fully embedded in the lipid bilayer while segments with higher flexibility remain. FEBS Lett. *587*, 2572-2577.

Williams, R.M., Obradovi, Z., Mathura, V., Braun, W., Garner, E.C., Young, J., Takayama, S., Brown, C.J., and Dunker, A.K. (2001). The protein non-folding problem: amino acid determinants of intrinsic order and disorder. Pac. Symp. Biocomput. *6*, 89-100.

Williamson, M.P. (1994). The structure and function of proline-rich regions in proteins. Biochem J. *297 (Pt 2)*, 249-260.

Wiltzius, J.J.W., Sievers, S.A., Sawaya, M.R., and Eisenberg, D. (2009). Atomic structures of IAPP (amylin) fusions suggest a mechanism for fibrillation and the role of insulin in the process. Protein Sci. *18*, 1521-1530.

Wolfe, L.S., Calabrese, M.F., Nath, A., Blaho, D.V., Miranker, A.D., and Xiong, Y. (2010). Protein-induced photophysical changes to the amyloid indicator dye thioflavin T. Proc. Natl. Acad. Sci. USA *107*, 16863-16868.

Wolynes, P.G. (1997). Folding funnels and energy landscapes of larger proteins within the capillarity approximation. Proc. Natl. Acad. Sci. USA *94*, 6170-6175.

Woodside, M.T., and Block, S.M. (2014). Reconstructing folding energy landscapes by single-molecule force spectroscopy. Annu. Rev. Biophys. *43*, 19-39.

Wootton, J.C. (1994). Sequences with Unusual Amino-Acid Compositions. Curr. Opin. Struct. Biol. *4*, 413-421.

Wright, M.H., Heal, W.P., Mann, D.J., and Tate, E.W. (2010). Protein myristoylation in health and disease. J. Chem. Biol. *3*, 19-35.
Wright, P.E., and Dyson, H.J. (1999). Intrinsically unstructured proteins: re-assessing the protein structure-function paradigm. J. Mol. Biol. *293*, 321-331.

Wu, C.K. (2011). Parkinson's disease with dementia, lewy-body disorders and alpha-synuclein: recent advances and a case report. Acta Neurol. Taiwan *20*, 4-14.

Xue, W.F., Hellewell, A.L., Gosal, W.S., Homans, S.W., Hewitt, E.W., and Radford, S.E. (2009). Fibril fragmentation enhances amyloid cytotoxicity. J. Biol. Chem. *284*, 34272-34282.

Yagi, H., Ozawa, D., Sakurai, K., Kawakami, T., Kuyama, H., Nishimura, O., Shimanouchi, T., Kuboi, R., Naiki, H., and Goto, Y. (2010). Laser-induced propagation and destruction of amyloid beta fibrils. J. Biol. Chem. *285*, 19660-19667.

Yamin, G., Glaser, C.B., Uversky, V.N., and Fink, A.L. (2003). Certain metals trigger fibrillation of methionine-oxidized alpha-synuclein. J. Biol. Chem. *278*, 27630-27635.

Yamin, G., Munishkina, L.A., Karymov, M.A., Lyubchenko, Y.L., Uversky, V.N., and Fink, A.L. (2005). Forcing nonamyloidogenic beta-synuclein to fibrillate. Biochemistry *44*, 9096-9107.

Yoshida, H., Craxton, M., Jakes, R., Zibaee, S., Tavare, R., Fraser, G., Serpell, L.C., Davletov, B., Crowther, R.A., and Goedert, M. (2006). Synuclein proteins of the pufferfish Fugu rubripes: sequences and functional characterization. Biochemistry *45*, 2599-2607.

Yuan, J., and Zhao, Y. (2013). Evolutionary aspects of the synuclein super-family and sub-families based on large-scale phylogenetic and group-discrimination analysis. Biochem. Biophys. Res. Commun. *441*, 308-317.

Yusupov, M.M., Yusupova, G.Z., Baucom, A., Lieberman, K., Earnest, T.N., Cate, J.H.D., and Noller, H.F. (2001). Crystal structure of the ribosome at 5.5 angstrom resolution. Science *292*, 883-896.

Zarranz, J.J., Alegre, J., Gomez-Esteban, J.C., Lezcano, E., Ros, R., Ampuero, I., Vidal, L., Hoenicka, J., Rodriguez, O., Atares, B., *et al.* (2004). The new mutation, E46K, of alpha-synuclein causes Parkinson and Lewy body dementia. Ann. Neurol. *55*, 164-173.

Zhang, J.Z. (2003). Evolution by gene duplication: an update. Trends Ecol. Evol. *18*, 292-298.

Zhang, W., Wang, T., Pei, Z., Miller, D.S., Wu, X., Block, M.L., Wilson, B., Zhou, Y., Hong, J.S., and Zhang, J. (2005). Aggregated alpha-synuclein activates microglia: a process leading to disease progression in Parkinson's disease. FASEB J. *19*, 533-542.

Zhao, L., and Koopman, P. (2012). SRY protein function in sex determination: thinking outside the box. Chromosome Res. *20*, 153-162.

Zhao, M., Cascio, D., Sawaya, M.R., and Eisenberg, D. (2011). Structures of segments of alpha-synuclein fused to maltose-binding protein suggest intermediate states during amyloid formation. Protein Sci. *20*, 996-1004.

Zhou, W.B., Long, C.M., Reaney, S.H., Di Monte, D.A., Fink, A.L., and Uversky, V.N. (2010). Methionine oxidation stabilizes non-toxic oligomers of alpha-synuclein through strengthening the auto-inhibitory intra-molecular long-range interactions. BBA-Mol. Basis. Dis. *1802*, 322-330.

Zimprich, A., Biskup, S., Leitner, P., Lichtner, P., Farrer, M., Lincoln, S., Kachergus, J., Hulihan, M., Uitti, R.J., Calne, D.B., *et al.* (2004). Mutations in LRRK2 cause autosomal-dominant parkinsonism with pleomorphic pathology. Neuron *44*, 601-607.

Ziuzina, D., Patil, S., Cullen, P.J., Keener, K.M., and Bourke, P. (2013). Atmospheric cold plasma inactivation of Escherichia coli in liquid media inside a sealed package. J. Appl. Microbiol. *114*, 778-787.

Zuo, P.J., Qu, W., Cooper, R.N., Goyer, R.A., Diwan, B.A., and Waalkes, M.P. (2009). Potential Role of alpha-Synuclein and Metallothionein in Lead-Induced Inclusion Body Formation. Toxicol. Sci. *111*, 100-108.

APPENDIX A

CALIBRATION OF G-75 SEPHADEX SIZE EXCLUSION COLUMN WITH PROTEIN STANDARDS BLUE DEXTRAN, OVALBUMIN, ALBUMIN AND RIBONUCLEASE

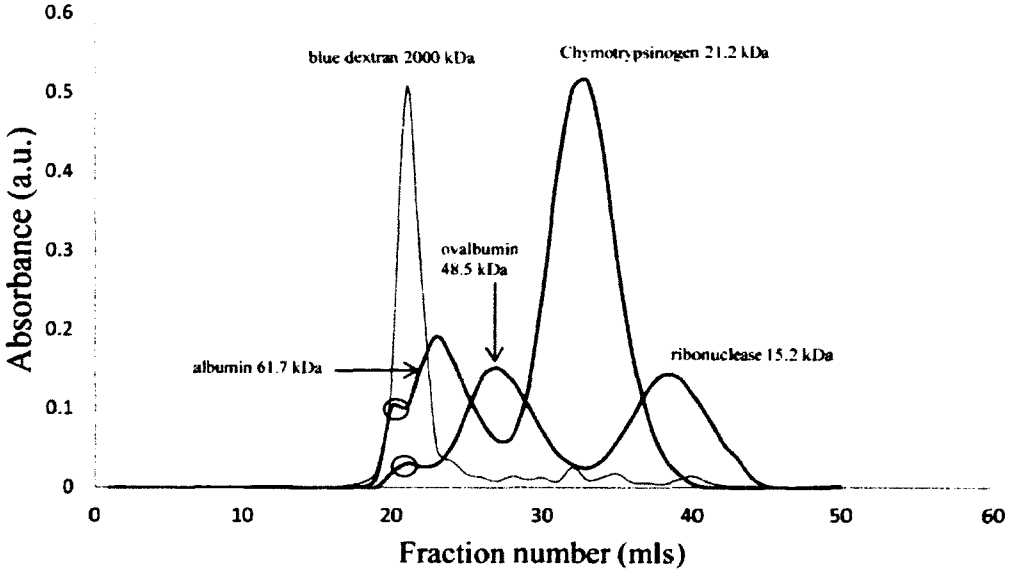

Figure A. Calibration of the G-75 size exclusion column.

Absorbance of the protein standards were determined by UV spectrophotometer at 280 nm. Absorbance on the Y-axis was plotted against fractions on the X-axis. The volume of each fraction is 5 mls. The void volume of our column is 105. The blue dextran elutes at fraction 21.The shoulder molecules (red circles) are dimer species of the albumin (61.7 kDa) and ovalbumin (48.5 kDa).The dimers species under conditions of our column elute in the void volume. The G-75 column cannot separate the blue dextran from albumin since they elute to the same fraction 20.

APPENDIX B

SITES FOR PROTEIN MODIFICATION IN THE SYNUCLEINS

Protein	Myristoylation		Casein kinase phosphorylation		Tyrosine kinase phosphorylation	
Endoglucanase	3-8	GAaaTD	212-215	TlsD		
	76-81	GTchAW				
	87-92	GTnkAW				
	109-114	GSrkAW				
	120-125	GSekAW				
	131-136	GTnAW				
	142-147	GTekTW				
	175-180	GSrkAW				
	197-202	GTenAA				
CRE-DUR-1	176-181	GCaySQ	39-42	TgaE	410-417	KegaEaaY
	401-406	GAaeGY	58-61	TqtD		
	412-417	GAeaAY	68-71	SaeE		
	423-428	GActAV	334-337	TglE		
	466-471	GGaeAA	426-429	TavE		
			452-455	SmhD		
			459-462	SagD		
Marsupial	14-19	GVvgAV	54-57	SvaE	32-39	KtkEgvmY
	24-5-30	GVteAA	81-84	TveE		
	261-266	GlmsGA	148-151	SprE		
			220-223	Spre		
Cytochrome c	21-26	GAllAA	45-48	StsE		
	128-133	GChgAS	56-59	TtqE		
			74-77	SveE		
			81-84	SagE		
			92-95	SanE		
			96-99	TtkD		
			118-121	SgqE		
			159-162	SgkE		
			178-181	SdaE		
α-Synuclein	7-12	GLskAK	54-57	TvaE	32-39	KtkEgvlY
	14-19	GVvaAA				
	25-30	GVaeAA				
	47-52	GVvhGV				
	68-73	GAvvTG				
	86-91	GSiaAA				
β-Synuclein	7-12	GLsmAK	54-57	SvaE	32-39	KtkEgvlY
	14-19	GVvaAA	118-121	SveD		
	25-30	GVteAA				
	47-52	GVvqGV				
	68-73	GAvfSG				
	75-80	GNiaAA				
γ-Synuclein	14-19	GVvgAV	54-57	SvaE	32-39	KtkEgvmY
	25-30	GVteAA	81-84	TveE		
			124-127	SggD		

Table 1. Protein Modification Sites.

Myristic acid is added to specific conserved glycines in both synucleins and the disparate proteins. Phosphate groups are also added to specific conserved threonine, serine, or tyrosine residues to both the synucleins and the disparate proteins.

APPENDIX C

LIST OF FIGURES WITH PERMISSIONS OBTAINED FROM PUBLISHERS

Figure 3	Figure 16
Figure 4	Figure 17
Figure 5	Figure 18
Figure 6	Figure 21
Figure 7	Figure 22
Figure 8	Figure 23
Figure 9	Figure 24
Figure 10	Figure 35
Figure 11	Figure 55
Figure 13	Figure 60

Electronic copies of the permissions are on file and maintained on the ODU Department of Chemistry and Biochemistry K-drive as a permanent record.

VITA

Department of Chemistry and Biochemistry, Old Dominion University, 4541 Hampton Boulevard, Norfolk, VA, 23529, USA

EDUCATION

2014 Ph.D. in Biomedical Sciences with a Biochemistry Track, Old Dominion University, Norfolk, Virginia

1981 M.S. in Clinical Chemistry, Old Dominion University, Norfolk, Virginia

1980 B.S. in Medical Technology, Old Dominion University, Norfolk, Virginia

1978 B.A with a major in Chemistry, Hampton Institute, Hampton, Virginia

PUBLICATIONS

1) E. Karakas, A. Munyanyi, L. Greene and M. Laroussi (2010) Destruction of α-synuclein based amyloid fibrils by a low temperature plasma jet. *Appl. Phys. Lett.* 97: 143702.

2) P.A. Pleban, A. Munyanyi and J. Beachum (1982) Determination of selenium concentration and glutathione peroxidase activity in plasma and erythrocytes. *Clin. Chem.* 28: 311-6.

PRESENTATIONS

1) 91st Virginia Academy of Science, Virginia Tech, Blacksburg, VA (May 2013). A. Munyanyi, J. Bedford and L.H Greene, The synuclein family shares sequence identity with a marsupial protein, endoglucanase from *Acetobacter pomorum* and cytochrome c from *vibrio cholera*: A computational analysis of the synuclein proteins.

2) 90th Virginia Academy of Science, Norfolk State University, VA (May 2012). A. Munyanyi, J. Bedford and L.H. Greene, β-synuclein forms a helical tetramer.